frontiers | Research Topics

Advances in the management of lung cancer: from the bench to the bedside and back

Edited by
Vincenzo Pio Di Noia and Alessandro Leonetti

Coordinated by
Francesca Fusco

Published in
Frontiers in Medicine

ISSN 1664-8714
ISBN 978-2-8325-6660-2
DOI 10.3389/978-2-8325-6660-2

Generative AI statement
Any alternative text (Alt text) provided alongside figures in the articles in this ebook has been generated by Frontiers with the support of artificial intelligence and reasonable efforts have been made to ensure accuracy, including review by the authors wherever possible. If you identify any issues, please contact us.

About Frontiers

Frontiers is more than just an open access publisher of scholarly articles: it is a pioneering approach to the world of academia, radically improving the way scholarly research is managed. The grand vision of Frontiers is a world where all people have an equal opportunity to seek, share and generate knowledge. Frontiers provides immediate and permanent online open access to all its publications, but this alone is not enough to realize our grand goals.

Frontiers journal series

The Frontiers journal series is a multi-tier and interdisciplinary set of open-access, online journals, promising a paradigm shift from the current review, selection and dissemination processes in academic publishing. All Frontiers journals are driven by researchers for researchers; therefore, they constitute a service to the scholarly community. At the same time, the *Frontiers journal series* operates on a revolutionary invention, the tiered publishing system, initially addressing specific communities of scholars, and gradually climbing up to broader public understanding, thus serving the interests of the lay society, too.

Dedication to quality

Each Frontiers article is a landmark of the highest quality, thanks to genuinely collaborative interactions between authors and review editors, who include some of the world's best academicians. Research must be certified by peers before entering a stream of knowledge that may eventually reach the public - and shape society; therefore, Frontiers only applies the most rigorous and unbiased reviews. Frontiers revolutionizes research publishing by freely delivering the most outstanding research, evaluated with no bias from both the academic and social point of view. By applying the most advanced information technologies, Frontiers is catapulting scholarly publishing into a new generation.

What are Frontiers Research Topics?

Frontiers Research Topics are very popular trademarks of the *Frontiers journals series*: they are collections of at least ten articles, all centered on a particular subject. With their unique mix of varied contributions from Original Research to Review Articles, Frontiers Research Topics unify the most influential researchers, the latest key findings and historical advances in a hot research area.

Find out more on how to host your own Frontiers Research Topic or contribute to one as an author by contacting the Frontiers editorial office: frontiersin.org/about/contact

Advances in the management of lung cancer: from the bench to the bedside and back

Topic editors
Vincenzo Pio Di Noia — IRCCS Istituto Nazionale Tumori Regina Elena, Italy
Alessandro Leonetti — University Hospital of Parma, Italy

Topic coordinator
Francesca Fusco — IRCCS Istituto Nazionale Tumori Regina Elena, Italy

Citation
Di Noia, V. P., Leonetti, A., Fusco, F., eds. (2025). *Advances in the management of lung cancer: from the bench to the bedside and back*. Lausanne: Frontiers Media SA. doi: 10.3389/978-2-8325-6660-2

Table of contents

frontiers | Frontiers in Medicine

TYPE Original Research
PUBLISHED 07 August 2024
DOI 10.3389/fmed.2024.1449537

OPEN ACCESS

EDITED BY
Alessandro Leonetti,
University Hospital of Parma, Italy

REVIEWED BY
Milena Man,
University of Medicine and Pharmacy Iuliu Hatieganu, Romania
Savvas Lampridis,
Imperial College London, United Kingdom

*CORRESPONDENCE
Eun Hye Lee
✉ hieunhye@yuhs.ac

RECEIVED 15 June 2024
ACCEPTED 29 July 2024
PUBLISHED 07 August 2024

CITATION
Kwak SH, Kim KY, Choi JS, Kim MC, Seol CH, Kim SR and Lee EH (2024) Impact of AI-assisted CXR analysis in detecting incidental lung nodules and lung cancers in non-respiratory outpatient clinics. *Front. Med.* 11:1449537. doi: 10.3389/fmed.2024.1449537

Impact of AI-assisted CXR analysis in detecting incidental lung nodules and lung cancers in non-respiratory outpatient clinics

Se Hyun Kwak[1], Kyeong Yeon Kim[1], Ji Soo Choi[1], Min Chul Kim[1], Chang Hwan Seol[1], Sung Ryeol Kim[1] and Eun Hye Lee[1,2]*

[1]Division of Pulmonology, Allergy and Critical Care Medicine, Department of Internal Medicine, Yongin Severance Hospital, Yonsei University College of Medicine, Yongin-si, Republic of Korea, [2]Center for Digital Health, Yongin Severance Hospital, Yonsei University College of Medicine, Yongin-si, Gyeonggi-do, Republic of Korea

Purpose: The use of artificial intelligence (AI) for chest X-ray (CXR) analysis is becoming increasingly prevalent in medical environments. This study aimed to determine whether AI in CXR can unexpectedly detect lung nodule detection and influence patient diagnosis and management in non-respiratory outpatient clinics.

Methods: In this retrospective study, patients over 18 years of age, who underwent CXR at Yongin Severance Hospital outpatient clinics between March 2021 and January 2023 and were identified to have lung nodules through AI software, were included. Commercially available AI-based lesion detection software (Lunit INSIGHT CXR) was used to detect lung nodules.

Results: Out Of 56,802 radiographic procedures, 40,191 were from non-respiratory departments, with AI detecting lung nodules in 1,754 cases (4.4%). Excluding 139 patients with known lung lesions, 1,615 patients were included in the final analysis. Out of these, 30.7% (495/1,615) underwent respiratory consultation and 31.7% underwent chest CT scans (512/1,615). As a result of the CT scans, 71.5% (366 cases) were found to have true nodules. Among these, the final diagnoses included 36 lung cancers (7.0%, 36/512), 141 lung nodules requiring follow-up (27.5%, 141/512), 114 active pulmonary infections (22.3%, 114/512), and 75 old inflammatory sequelae (14.6%, 75/512). The mean AI nodule score for lung cancer was significantly higher than that for other nodules (56.72 vs. 33.44, $p < 0.001$). Additionally, active pulmonary infection had a higher consolidation score, and old inflammatory sequelae had the highest fibrosis score, demonstrating differences in the AI analysis among the final diagnosis groups.

Conclusion: This study indicates that AI-detected incidental nodule abnormalities on CXR in non-respiratory outpatient clinics result in a substantial number of clinically significant diagnoses, emphasizing AI's role in detecting lung nodules and need for further evaluation and specialist consultation for proper diagnosis and management.

KEYWORDS

artificial intelligence, X-rays, lung neoplasms, lung nodule, detection

1 Introduction

Recent advancements in artificial intelligence (AI) have led to the widespread integration of various AI technologies in healthcare settings. Among these, AI applications for interpreting chest X-rays (CXRs) have been increasingly utilized (1–4). CXRs are fundamental diagnostic tools that are routinely used in primary care and referral hospitals because of their accessibility and ease of use. They are commonly used for patients with respiratory symptoms and as part of routine outpatient and inpatient examinations, preoperative assessments, and emergency room visits. Several previous studies have demonstrated the benefits of AI in detecting malignant lung nodules on CXRs (5, 6). Despite the widespread use of CXRs in clinical settings, obtaining immediate radiological interpretations remains challenging, particularly in outpatient and emergency environments. This limitation has driven the increased use of AI as an instant screening tool, helping bridge the gap between image acquisition and diagnosis (7–9).

Among the AI-detected CXR abnormalities, those accompanied by respiratory symptoms, such as pneumothorax and acute respiratory infections, are easier to detect based on the patient's symptoms. In contrast, incidental lung nodules, which often present without respiratory symptoms, are particularly challenging for identification and accurate diagnosis. These nodules can lead to missed lung cancer and delayed diagnosis (10–12), eventually affecting patient outcomes. Therefore, the discovery of an appropriate diagnostic approach for incidental lung nodules is crucial for patient prognosis. Although the role of AI in enhancing diagnostic accuracy is well-documented (13–15), there is a lack of research on the actual diagnostic approaches and interventions implemented for patients with abnormalities identified by AI in real-world clinical settings. Therefore, it is essential to understand how AI-flagged abnormalities in CXRs influence diagnostic processes and treatment interventions in real-world healthcare settings.

This study aimed to investigate the diagnostic processes and clinical outcomes of patients with AI-detected lung nodule abnormalities on CXR in non-respiratory outpatient clinics and to explore the clinical significance of these AI abnormalities in patient care.

2 Material and methods

2.1 Patients and clinical data

Patients (≥ 18 years old) who underwent CXR at the outpatient clinic between March 2021 and January 2023 at Yongin Severance Hospital were retrospectively reviewed (Figure 1). The hospital implemented AI software for all CXR performed, providing immediate reports of abnormal findings at the time the CXRs were performed. Among them, we included patients with lung nodules detected on CXR by AI in the outpatient clinic after excluding those related to the lung abnormalities department (pulmonology, thoracic surgery, and oncology), and health check-up center. In cases where a patient underwent multiple CXR, we used the first CXR as the subject of analysis. The medical records of the patients' diagnostic workup, whether chest computed tomography (CT) was performed, final diagnosis, and diagnosis of lung cancer were reviewed. Lung cancer stage was assessed according to the 8th edition of the TNM classification (16). The research protocol was approved by the Institutional Review Board (IRB) of Yongin Severance Hospital (IRB No. 9-2024-0087). The requirement for informed consent was waived because of the retrospective nature of the study.

2.2 AI-based CXR analysis

Commercially available AI-based lesion detection software (Lunit INSIGHT for Chest Radiography, version 3.1.2; Lunit Inc., Republic of Korea) has been used for all CXRs in our hospital since March 2021. The software can detect eight different lesion types (nodule, consolidation, pneumothorax, pneumoperitoneum, fibrosis, atelectasis, cardiomegaly, and pleural effusion). Lesion location was displayed in the chest radiographs by a grayscale contour map when the abnormality score (probability of an abnormal lesion existing) was above the preset operating point of 15% (17, 18). The radiograph classification and nodule detection performances are reported to have an area under the curve (AUC) in the range of 0.92–0.99 (19). The earlier version detects the nodule only, whereas INSIGHT CXR 3 is equipped with an extended list of detectable abnormalities including lung nodule, consolidation, and pneumothorax with an accuracy of 97–99% (20). The analyzed AI results were automatically attached to the original CXR image as a secondary file, allowing the attending physician to immediately check the results. We extracted each abnormality score and lesion type from the AI server by uploading digital imaging and communications in medicine (DICOM) images of the CXR to the server.

2.3 Classification of true lung nodules

For patients with AI nodule score of 15% or higher on CXR, the actual number of nodules was analyzed only in those who underwent chest CT within 3 months after CXR was performed. An actual nodule in the lesion detected as a nodule by AI on chest CT was defined as a true nodule; if there was no actual nodule on chest CT, it was defined as a false nodule. The final diagnoses of the nodules were classified into the following four categories: (1) patients ultimately diagnosed with lung cancer; (2) nodules that exist but are not confirmed as lung cancer and require follow-up; (3) active pulmonary infections such as pneumonia, pulmonary tuberculosis (TB), and nontuberculous mycobacteria (NTM); and (4) old inflammatory sequelae. Old inflammatory sequelae are characterized by the presence of calcified nodules, pleural thickening, fibrosis, volume loss, and parenchymal bands. The presence of nodules on chest CT was determined based on the official interpretation by radiologists, and the final diagnosis was verified through a review of the images by two pulmonologists, SHK and EHL, with 5 and 8 years of experience, respectively. Medical records for diagnostic work-up and final diagnosis were reviewed until April 2023 and 3 months after the last CXR was performed.

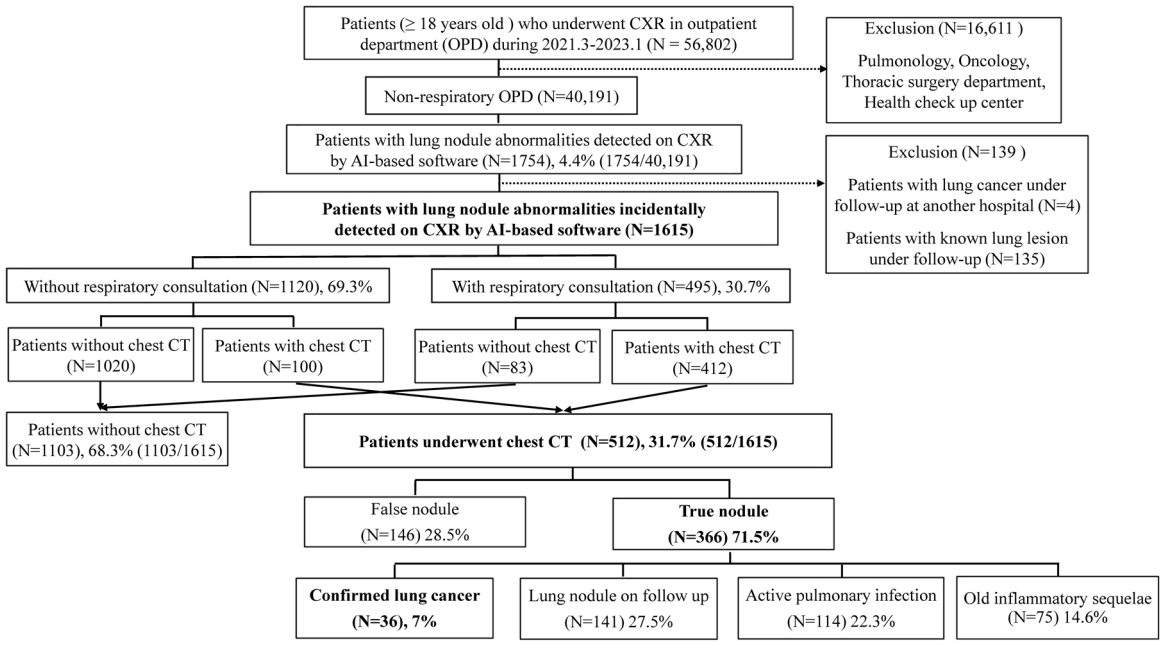

FIGURE 1
Flowchart of study patient enrollment. AI, artificial intelligence; CXR, chest radiograph; CT, computed tomography.

2.4 Statistical analysis

Statistical analyses were performed using R program (version 4.4.0, Foundation for Statistical Computing, Vienna, Austria; packages: survival, rms, compareC, and pec). Values are presented as mean with standard deviation (SD) or median with interquartile range (IQR). The ggplot2 library facilitated the generation of plots to compare the AI abnormality scores between true and false nodules across the final diagnosis groups. The mean difference was compared using *t*-test, and a p-value < 0.05 was considered significant for all analyses.

3 Results

3.1 Study patients

Between March 2021 and January 2023, a total of 56,802 patients (≥ 18 years old) underwent CXR in the outpatient department (OPD) (Figure 1). After excluding pulmonology, oncology, thoracic surgery department, health-up center, 40,191 patients with CXR were analyzed. Among these patients, 1,754 (4.4%) had lung nodule abnormalities detected on CXR by AI software (Figure 1). A total of 1,615 patients were included in the final analysis after excluding 135 patients with known lung lesions and 4 patients who were being followed up for lung cancer at another hospital. Out of these, 30.7% (495/1,615) underwent respiratory consultation and 69.3% (1,120/1,615) did not undergo respiratory consultation. Among the 495 patients who underwent respiratory consultation, 412 performed additional chest CT, and 100 out of 1,120 patients who did not undergo respiratory consultation also performed chest CT within 3 months of CXR, making a total of 512 patients (31.7%, 512/1,615). Out of 512 patients with chest CT, 146 patients (28.5%) were considered false positives because the nodule was not actually present on chest CT. The remaining 366 patients (71.5%) had actual nodules discovered on chest CT, and 36 patients, which is 7% of all patients who underwent chest CT, were ultimately diagnosed with lung cancer. Additionally, 141 patients (27.5%) were classified as having lung nodules requiring follow-up; 114 patients (22.3%) had pulmonary infections such as pneumonia, pulmonary TB, and NTM; and the remaining 75 patients (14.6%) had old inflammatory sequelae (Figure 1). Table 1 presents the characteristics of each diagnostic group. Compared to the group ultimately diagnosed with lung cancer (A), the old inflammatory sequelae group (D) had a significantly higher history of old TBc. Additionally, the nodule size and AI nodule score in group A were significantly higher than those in the other groups ($p < 0.001$, all). Figure 2 shows examples of patients who underwent chest CT after suspected lung nodules were detected on CXR by AI.

3.2 Difference in AI lung nodule score between groups during diagnostic work-up

Figure 3 shows the differences in the lung nodule AI scores between each group during the lung nodule diagnostic workup process. Among all patients with abnormal lung nodule scores on CXR, the mean AI lung nodule score was significantly higher in the group of patients who underwent chest CT than in those who did not (Figure 3A, mean 30.3 vs. 33.9, $p < 0.001$). In addition, among the patients who underwent chest CT, the mean AI nodule score of the true nodule group was significantly higher

TABLE 1 The characteristics of the 512 patients who underwent chest CT.

Characteristic	A Lung cancer (*n* = 36)	B Other lung nodules (*n* = 141)	C Pulmonary infection (*n* = 114)	D Old inflammatory sequelae (*n* = 75)	E False nodule (*n* = 146)	*P*-value A vs. B	A vs. C	A vs. D	A vs. E
Age, year, IQR	74.5 (69.2–83.2)	75 (66–81)	73 (63.2–80.8)	68 (60.5–76)	71.5 (60–80)	0.572	0.41	0.019	0.109
Sex, male, *n* (%)	24 (66.7)	81 (57.4)	69 (60.5)	33 (44)	70 (49.7)	0.415	0.642	0.042	0.068
Ever smoker, *n* (%)	15 (41.7)	52 (36.9)	32 (28.1)	21 (28.0)	40 (27.4)	0.737	0.184	0.221	0.142
Comorbidity, *n* (%)									
HTN	24 (66.7)	79 (56.0)	59 (51.8)	45 (60.0)	82 (56.2)	0.334	0.169	0.639	0.339
DM	14 (38.9)	42 (29.8)	43 (37.7)	21 (28.0)	39 (26.7)	0.397	1.0	0.348	0.217
Old Tbc	5 (13.9)	17 (12.1)	13 (11.4)	36 (48.0)	13 (8.9)	0.989	0.916	0.001	0.558
Nodule characteristics*									
GGO/subsolid	7 (19.4)	36 (25.5)	51 (44.7)	0	–	0.588	0.001	< 0.001	–
Solid	29 (80.6)	105 (74.5)	53 (46.5)	0	–				
Calcification/fibrotic scar	0		10 (8.77)	75 (100)	–				
Nodule size*									
≤ 1 cm	0	106 (75.2)	111 (97.4)	71 (94.7)	–	< 0.001	< 0.001	< 0.001	–
> 1 cm, ≤ 2 cm	7 (19.4)	20 (14.2)	0	1 (1.3)	–				
> 2 cm, ≤ 3 cm	9 (25)	8 (5.7)	1 (0.9)	2 (2.7)	–				
> 3 cm	20 (55.6)	7 (4.9)	2 (1.8)	1 (1.3)	–				
AI abnormality score, mean ± SD									
Nodule	56.7 ± 29.7	34.5 ± 21.9	28.1 ± 15.3	36 ± 21.9	29.4 ± 20.6	< 0.001	< 0.001	< 0.001	< 0.001
Consolidation	30.3 ± 35.8	23.9 ± 30.7	57.2 ± 33.8	19.8 ± 26.0	38.0 ± 36.1	0.331	< 0.001	0.121	0.255
Fibrosis	21.9 ± 23.9	23.1 ± 28.7	31.4 ± 32.0	41.0 ± 34.8	23.3 ± 31.1	0.792	0.059	0.001	0.767
Atelectasis	7.21 ± 10.6	9.55 ± 16.7	14.0 ± 19.4	10.1 ± 17.1	14.5 ± 21.9	0.302	0.009	0.285	0.005
Pleural effusion	21.8 ± 33.6	10.8 ± 23.5	22.7 ± 34.7	13.7 ± 26.1	18.0 ± 32.6	0.069	0.895	0.206	0.539

*For multiple nodules, characteristics of the nodule with the maximal size. Values are presented as medians with interquartile ranges (IQR) or numbers with percentages. IQR, interquartile range; SD, standard deviation; HTN, hypertension; DM, diabetes; Tbc, tuberculosis; GGO, ground glass opacity.

10.3389/fmed.2024.1449537

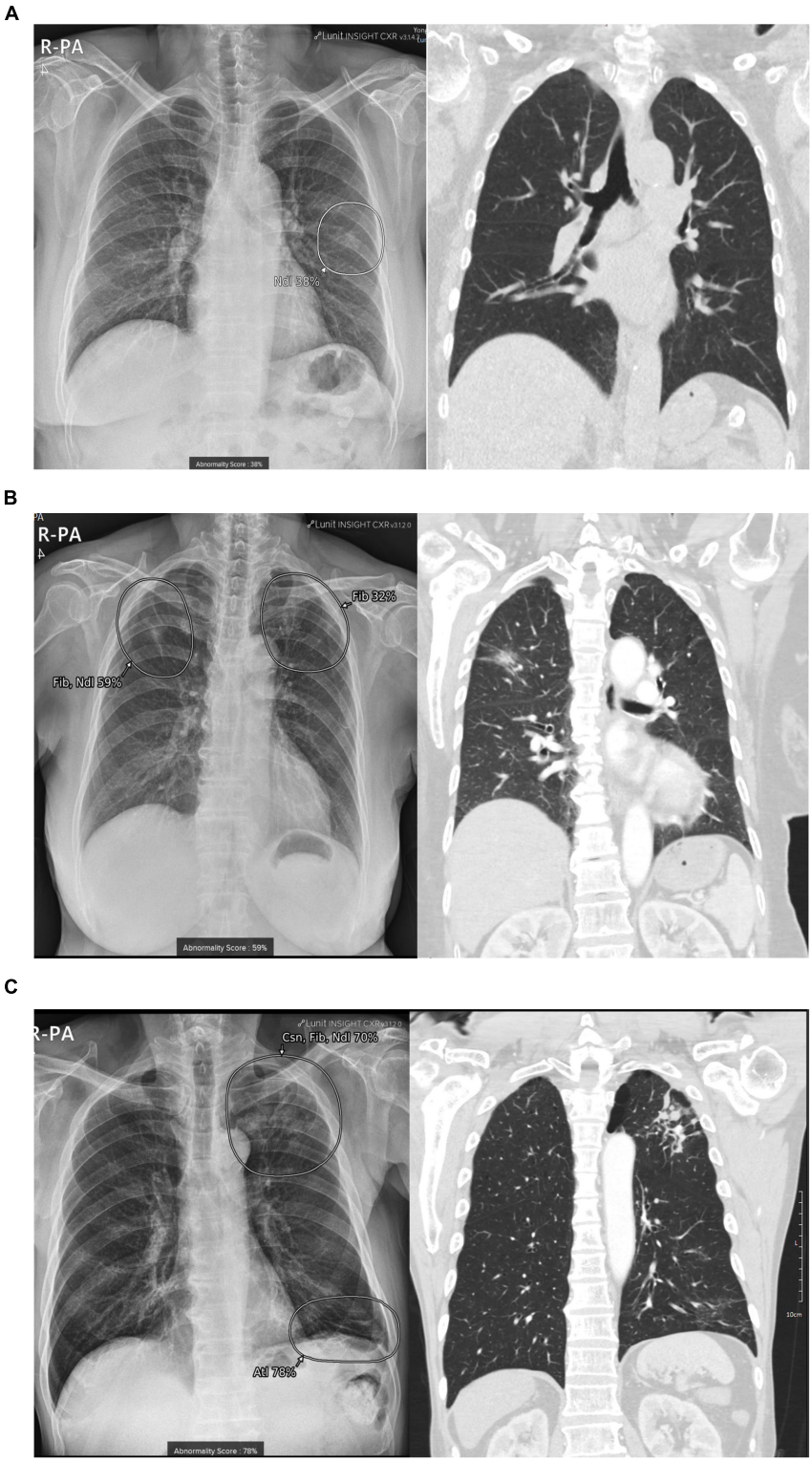

FIGURE 2
Examples of patient cases. **(A)** False-positive nodule detected on CXR by AI: A 75-year-old man underwent a CXR examination at the cardiology outpatient clinic, which suggested a nodule in the left middle lung field (AI nodule score: 38%). Subsequent chest CT revealed no significant abnormalities, and the nodule was identified as a rib or a vascular shadow. **(B)** True-positive nodule detected on CXR by AI, lung cancer: A 71-year-old woman underwent a preoperative examination for spinal surgery, which suggested fibrosis combined with a nodule in the right upper lung field. A subsequent chest CT scan revealed an approximately 3 cm part-solid nodule. The final pathological diagnosis after surgery confirmed stage IA adenocarcinoma (Nodule score: 59%; Fibrosis score: 26%). **(C)** True-positive nodule detected on CXR by AI and acute pulmonary infection: A 75-year-old female patient underwent CXR at the gastroenterology outpatient clinic, where AI suggested combined findings of consolidation, fibrosis, and a nodule in the left upper lung field. Subsequent chest CT revealed multiple centrilobular nodules, and a sputum test was performed to diagnose active pulmonary TB (AI Nodule score, 54%; consolidation score, 24%; fibrosis score, 70%). AI, artificial intelligence; CXR, chest radiograph; Ndl, nodule; Csn, consolidation; Fib, fibrosis.

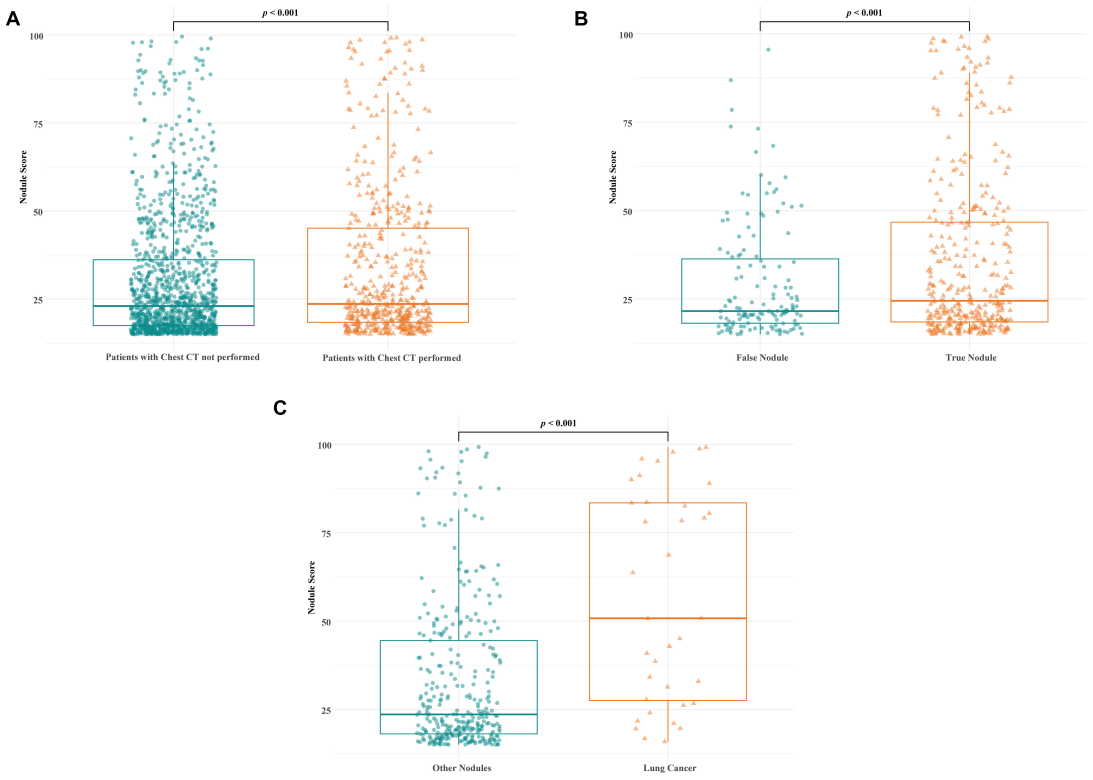

FIGURE 3
Comparison of AI nodule scores on CXR among each group during the diagnostic workup process. **(A)** The mean AI lung nodule score was significantly higher in the group of patients who underwent chest CT than in those who did not [**(A)**, mean 30.3 vs. 33.9, $p < 0.001$]. **(B)** Among the patients who underwent CT, the mean AI nodule score was significantly higher in the true nodule group than in the false nodule group (mean 29.4 vs. 35.7, $p < 0.001$). **(C)** Among the patients with true nodules, the mean AI nodule score was significantly higher in those diagnosed with lung cancer than in those diagnosed with other conditions (mean 33.4 vs. 56.7, $p < 0.001$).

than that of the false nodule group (Figure 3B, mean 29.4 vs. 35.7, $p < 0.001$). Additionally, the AI nodule scores of the 36 patients ultimately diagnosed with lung cancer showed significantly higher mean values than those of patients diagnosed with other nodules (Figure 3C, mean 33.4 vs. 56.7, $p < 0.001$).

3.3 Difference in AI score between different final diagnosis groups

Figure 4 shows the results of the comparison of AI scores on CXR among the three groups diagnosed with active pulmonary infection ($n = 114$), lung cancer ($n = 36$), and old inflammatory sequelae ($n = 75$). Depending on the patient's final diagnosis, nodules, consolidation, and fibrosis may coexist; however, the nodule abnormality score was statistically higher in lung cancer patients than in the active pulmonary infection ($p < 0.001$) and old inflammatory sequelae patients ($p < 0.001$) (Figure 4A, mean 28.1 vs. 56.7 vs. 36.0). In the case of the mean consolidation score, active pulmonary infection was statistically higher than lung cancer ($p < 0.001$) and old inflammatory sequelae ($p < 0.001$) (Figure 4B, mean 57.2 vs. 30.3 vs. 19.8). Finally, in the case of AI fibrosis scores, the old inflammatory sequelae group showed a statistically higher mean level than lung cancer ($p = 0.001$); however, there was no statistically significant difference from active pulmonary infection (0.057) (Figure 4C, mean 31.4 vs. 21.9 vs. 41.0).

3.4 Characteristics of patients diagnosed with lung cancer

Table 2 shows the baseline characteristics of the 36 patients ultimately diagnosed with lung cancer. The median age was 74.5 years, and 66.7% of patients were male. Approximately 55.5% of patients had confirmed adenocarcinoma, and 3 patients were diagnosed with lung cancer via a multidisciplinary approach without pathologic confirmation. Overall, 33.3% of the total patients were finally confirmed as stage I, and surgical treatment was performed in 36.1% of the total patients. Regarding the AI abnormality score, the nodule score showed the highest mean value; however, the mean values of consolidation, fibrosis, and pleural effusion also showed abnormal values > 15%, indicating that they can be accompanied by abnormal findings other than nodules (Table 1).

4 Discussion

In this study, we investigated the clinical processes of incidental lung nodules detected on CXR in a non-respiratory outpatient setting. The results showed that despite the detection of lung nodule abnormalities by AI, only 30.7% of patients underwent respiratory consultation and chest CT was performed in 31.7% of the cases.

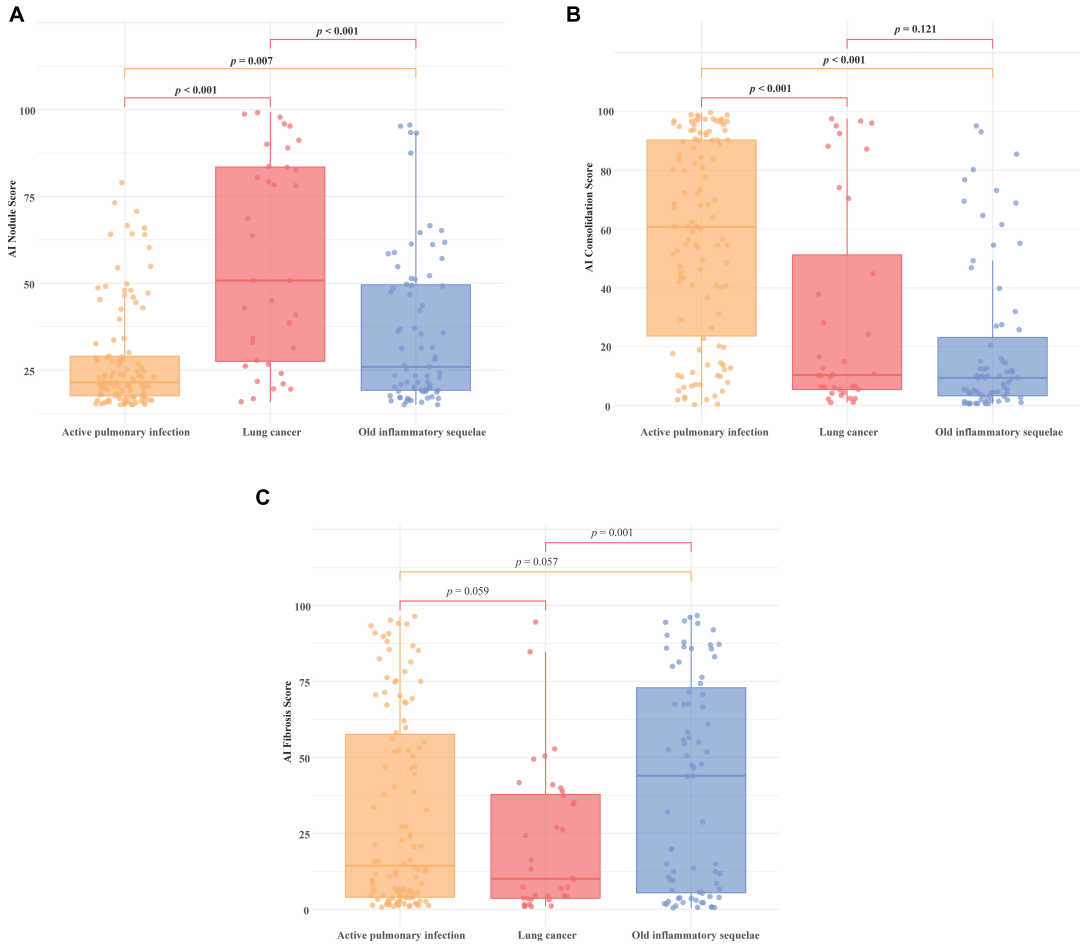

FIGURE 4
Comparison of AI nodule, consolidation, and fibrosis scores by final diagnosis group. Comparison of AI scores on CXR among the three groups diagnosed with active pulmonary infection (n = 114), lung cancer (n = 36), and old inflammatory sequelae (n = 75). The AI scores for **(A)** nodule, **(B)** consolidation, and **(C)** fibrosis are shown for each group. **(A)** The mean nodule score was significantly higher in lung cancer patients than in the active pulmonary infection ($p < 0.001$) and old inflammatory sequelae groups ($p < 0.001$) (mean 28.1 vs. 56.7 vs. 36.0, respectively). **(B)** The mean consolidation score of active pulmonary infection was statistically higher than lung cancer ($p < 0.001$) and old inflammation sequelae ($p < 0.001$), respectively (mean 57.2 vs. 30.3 vs. 19.8). **(C)** Fibrosis score: The old inflammatory sequelae group showed a statistically higher mean fibrosis score than lung cancer ($p = 0.001$), and there was no statistical difference between the active pulmonary infection and old inflammatory sequelae group ($p = 0.057$) (mean 31.4 vs. 21.9 vs. 41.0).

Among the patients who underwent further chest CT workup, 71.5% were found to have true nodules and 7% were diagnosed with incidental lung cancer. Additionally, among the 512 patients who underwent chest CT after showing abnormal nodule scores on CXR by AI, 291 patients (56.8%) required additional follow-up or therapeutic intervention (36 lung cancer, 141 lung nodules requiring follow-up, 114 active pulmonary infections, Figure 1).

Lung cancer remains the leading cause of cancer-related mortality worldwide (21), with the highest incidence among men and fifth among women in Korea (22, 23). Despite advancements in diagnostic technology, the role of chest radiography in the early detection of lung cancer remains unclear. Currently, low-dose chest CT scans are recommended for early detection; however, their application is mostly confined to high-risk groups (24, 25). This limitation is particularly concerning for lung cancer screening in women, who account for one-third of all lung cancer cases and for the increasing number of lung cancers in nonsmokers. Recent large-scale studies conducted in Korea have highlighted the potential benefits of chest radiography in identifying early stage lung cancer (26). These studies have shown a significant rate of early stage lung cancer detection in patients who underwent chest radiography prior to their diagnosis. Notably, women who participated in chest X-ray screenings exhibited about a 10% reduction in mortality rate, suggesting a critical need for further research into the effectiveness of chest X-rays in detecting pulmonary nodules and lung cancer (26). Considering that the incidence of lung cancer in large-scale RCTs targeting high-risk groups is less than 1% (24, 25), the finding that 7% of patients who underwent chest CT based on AI-detected lung nodule abnormalities on CXR performed in non-respiratory departments were diagnosed with lung cancer was notably high. Furthermore, among the 512 patients who underwent chest CT based on AI findings, not only was lung cancer detected, but 56.8% showed clinically significant results, including lung nodules requiring follow-up and pulmonary infections such as TB, pneumonia, and NTM. This underscores the importance of a further workup

TABLE 2 Characteristics of 36 patients diagnosed with lung cancer.

	Total (n = 36)
Age, year, IQR	74.5 (39.25–83.25)
Sex, male, n (%)	24 (66.7)
Subtype, n (%)	
Adenocarcinoma	20 (55.5)
Squamous cell carcinoma	8 (22.2)
SCLC	5 (13.8)
Not confirmed (radiologic diagnosis)	3 (8.3)
Pathologic stage, n (%)	
I	12 (33.3)
II	3 (8.3)
III	5 (13.8)
IV	16 (44.4)
Treatment	
Surgery	13 (36.1)
SBRT	5 (13.8)
CCRT	2 (5.5)
Chemotherapy	13 (36.1)
Palliative care only	3 (8.3)

Values are presented as medians with interquartile ranges (IQR) or numbers with percentages. IQR, interquartile range; SCLC, small cell lung cancer; SBRT, stereotactic body radiotherapy; CCRT, concurrent chemoradiotherapy.

for CXR nodule abnormalities. This demonstrates the clinical effectiveness of the AI CXR nodule software.

While AI abnormal findings on CXR cannot by themselves provide a definitive diagnosis, they can serve as a basis for further workup, such as chest CT scans or respiratory consultations. This facilitates the detection of respiratory diseases and lung cancer that might otherwise be missed in asymptomatic patients, especially in non-respiratory department. However, in our study, 28.5% of patients who underwent chest CT were found to have false positive nodules, raising concerns about the potential risk of overexposure to unnecessary tests. The AI's ability to assign abnormality scores is crucial in early detection and decision-making, potentially improving patient outcomes. However, the potential for false positives and subsequent excessive testing must be carefully managed. Additional research to evaluation of the cost-effectiveness analysis of the actual implementation of AI CXR and explore ways to reduce false positives is necessary.

On the other hand, 68.3% of the patients with AI-detected lung nodule score abnormalities on CXR did not undergo additional workup. Although AI is predominantly used in medical environments, physicians who are not specialists in the relevant field may not fully understand the abnormalities detected by AI. In the case of CXR, the understanding of AI-detected abnormalities may be limited among physicians who are not radiologists or specialists in respiratory or thoracic medicine. Therefore, even if AI abnormalities are detected, there may be instances in which non-radiologists or non-respiratory specialists may not recognize these abnormalities owing to a lack of understanding of the software. In our institution, there are no alert alarms or critical value reports (CVR) for CXR abnormalities directed at attending physicians. Therefore, it is difficult to determine whether non-respiratory physicians are aware of AI-detected abnormalities. Although there have been numerous studies on the diagnostic accuracy of AI-detected abnormalities and the efficiency of AI in reducing radiologists' reading time and effort (27–29), studies on how AI-detected abnormal nodule findings in clinical settings influence physicians' diagnostic processes are rare. Our study differs from previous research by examining how diagnostic workups are conducted in clinical settings when AI detects abnormal nodule findings. In our study, a large proportion of patients with AI-detected abnormal nodules did not receive further workup, highlighting the necessity of establishing proper diagnostic processes. This includes providing AI education to attending physicians, implementing the alert alarm system for AI-detected abnormalities, and ensuring appropriate referrals to specialists.

This study had several limitations. Firstly, as a retrospective study conducted at a single institution, it is challenging to generalize the findings. Additionally, for a large proportion of patients who did not receive further workup, it is difficult to determine the exact reasons, and we lack information on the patients' demographic characteristics that might have influenced the decision for additional workup. Additionally, the study did not include a normal control group, making it difficult to assess the AI's performance and accuracy. Despite its limitations, this study is valuable as it investigates how commercially approved AI software for CXR nodule abnormalities is applied in clinical practice and provides insights into the diagnostic process and outcomes.

In conclusion, this study indicated that AI-detected incidental nodule abnormalities on CXR in non-respiratory outpatient clinics lead to a substantial number of clinically significant diagnoses, including lung cancer and respiratory infections, highlighting the potential role of AI in identifying abnormal lung nodules. When AI detects nodule abnormalities on CXR, clinical attention and further evaluation, such as specialist consultation and additional diagnostic workup, are necessary to ensure proper diagnosis and management. Moreover, to effectively connect AI-detected abnormalities to patient diagnostic strategies, the integration of alert signals into AI systems may be necessary.

Data availability statement

The original contributions presented in this study are included in the article/supplementary material, further inquiries can be directed to the corresponding author.

Ethics statement

The studies involving humans were approved by the Institutional Review Board of Yongin Severance Hospital. The studies were conducted in accordance with the local legislation and institutional requirements. The ethics committee/institutional review board waived the requirement of written informed consent for participation from the participants or the participants' legal guardians/next of kin because of the retrospective nature of the

study and the use of anonymized clinical data. Written informed consent was not obtained from the individual(s) for the publication of any potentially identifiable images or data included in this article because the requirement for informed consent was waived by the IRB of Yongin Severance Hospital because of the retrospective nature of the study and the use of anonymized clinical data.

Author contributions

SHK: Formal analysis, Writing – original draft. KK: Data curation, Formal analysis, Writing – review & editing. JC: Writing – review & editing. MK: Writing – review & editing. CS: Writing – review & editing. SRK: Writing – review & editing. EL: Conceptualization, Data curation, Formal analysis, Funding acquisition, Writing – original draft, Writing – review & editing.

Funding

The authors declare that financial support was received for the research, authorship, and/or publication of this article. This study was supported by the National Research Foundation of Korea (NRF) grant funded by the Korean Government (MSIT) (RS-2022-00166711). The funders had no role in the study design, data collection and analysis, decision to publish, or manuscript preparation.

Acknowledgments

We thank Dr. Hyun Joo Shin for providing resources for AI analysis and Seok-Jae Heo for statistical consultation.

Conflict of interest

The authors declare that the research was conducted in the absence of any commercial or financial relationships that could be construed as a potential conflict of interest.

Publisher's note

References

1. Nam J, Hwang E, Kim J, Park N, Lee E, Kim H, et al. AI improves nodule detection on chest radiographs in a health screening population: A randomized controlled trial. *Radiology.* (2023) 307:e221894. doi: 10.1148/radiol.221894

2. Ueda D, Yamamoto A, Shimazaki A, Walston S, Matsumoto T, Izumi N, et al. Artificial intelligence-supported lung cancer detection by multi-institutional readers with multi-vendor chest radiographs: A retrospective clinical validation study. *BMC Cancer.* (2021) 21:1120. doi: 10.1186/s12885-021-08847-9

3. Armato S III. Deep learning demonstrates potential for lung cancer detection in chest radiography. *Radiology.* (2020) 297:697–8. doi: 10.1148/radiol.2020203538

4. Yoo H, Kim K, Singh R, Digumarthy S, Kalra M. Validation of a deep learning algorithm for the detection of malignant pulmonary nodules in chest radiographs. *JAMA Netw Open.* (2020) 3:e2017135. doi: 10.1001/jamanetworkopen.2020.17135

5. Kwak S, Kim E, Kim M, Lee E, Shin H. Incidentally found resectable lung cancer with the usage of artificial intelligence on chest radiographs. *PLoS One.* (2023) 18:e0281690. doi: 10.1371/journal.pone.0281690

6. Hwang S, Shin H, Kim E, Lee E, Lee M. Clinical outcomes and actual consequence of lung nodules incidentally detected on chest radiographs by artificial intelligence. *Sci Rep.* (2023) 13:19732. doi: 10.1038/s41598-023-47194-6

7. Jang S, Song H, Shin Y, Kim J, Kim J, Lee K, et al. Deep learning-based automatic detection algorithm for reducing overlooked lung cancers on chest radiographs. *Radiology.* (2020) 296:652–61. doi: 10.1148/radiol.2020200165

8. Hong W, Hwang E, Lee J, Park J, Goo J, Park C. Deep learning for detecting pneumothorax on chest radiographs after needle biopsy: Clinical implementation. *Radiology.* (2022) 303:433–41. doi: 10.1148/radiol.211706

9. Hwang E, Nam J, Lim W, Park S, Jeong Y, Kang J, et al. Deep learning for chest radiograph diagnosis in the emergency department. *Radiology.* (2019) 293:573–80. doi: 10.1148/radiol.2019191225

10. Quekel L, Kessels A, Goei R, van Engelshoven J. Miss rate of lung cancer on the chest radiograph in clinical practice. *Chest.* (1999) 115:720–4. doi: 10.1378/chest.115.3.720

11. Nam J, Hwang E, Kim D, Yoo S, Choi H, Goo J, et al. Undetected lung cancer at posteroanterior chest radiography: Potential role of a deep learning-based detection algorithm. *Radiol Cardiothorac Imaging.* (2020) 2:e190222. doi: 10.1148/ryct.2020190222

12. Bradley S, Bhartia B, Callister M, Hamilton W, Hatton N, Kennedy M, et al. Chest X-ray sensitivity and lung cancer outcomes: A retrospective observational study. *Br J Gen Pract.* (2021) 71:e862–8. doi: 10.3399/bjgp.2020.1099

13. Yoo H, Lee S, Arru C, Doda Khera R, Singh R, Siebert S, et al. AI-based improvement in lung cancer detection on chest radiographs: Results of a multi-reader study in NLST dataset. *Eur Radiol.* (2021) 31:9664–74. doi: 10.1007/s00330-021-08074-7

14. Lee S, Yim J, Kwak N, Lee Y, Lee J, Lee J, et al. Deep learning to determine the activity of pulmonary tuberculosis on chest radiographs. *Radiology.* (2021) 301:435–42. doi: 10.1148/radiol.2021210063

15. Shin H, Kim M, Son N, Han K, Kim E, Kim Y, et al. Clinical implication and prognostic value of artificial-intelligence-based results of chest radiographs for assessing clinical outcomes of COVID-19 patients. *Diagnostics (Basel).* (2023) 13:2090. doi: 10.3390/diagnostics13122090

16. Goldstraw P, Chansky K, Crowley J, Rami-Porta R, Asamura H, Eberhardt W, et al. The IASLC lung cancer staging project: Proposals for revision of the TNM stage groupings in the forthcoming (Eighth) edition of the TNM classification for lung cancer. *J Thorac Oncol.* (2016) 11:39–51. doi: 10.1016/j.jtho.2015.09.009

17. Hwang E, Goo J, Yoon S, Beck K, Seo J, Choi B, et al. Use of artificial intelligence-based software as medical devices for chest radiography: A position paper from the Korean society of thoracic radiology. *Korean J Radiol.* (2021) 22:1743–8. doi: 10.3348/kjr.2021.0544

18. Lee S, Shin H, Kim S, Kim E. Successful implementation of an artificial intelligence-based computer-aided detection system for chest radiography in daily clinical practice. *Korean J Radiol.* (2022) 23:847–52. doi: 10.3348/kjr.2022.0193

19. Nam J, Park S, Hwang E, Lee J, Jin K, Lim K, et al. Development and validation of deep learning-based automatic detection algorithm for malignant pulmonary nodules on chest radiographs. *Radiology.* (2019) 290:218–28. doi: 10.1148/radiol.2018180237

20. Ahn J, Ebrahimian S, McDermott S, Lee S, Naccarato L, Di Capua J, et al. Association of artificial intelligence-aided chest radiograph interpretation with reader performance and efficiency. *JAMA Netw Open.* (2022) 5:e2229289. doi: 10.1001/jamanetworkopen.2022.29289

21. WHO. *WHO fact sheet–cancer*. Geneva: WHO (2021).

22. Kim M, Kim S, Lee M, Eom J. Recent advances in adjuvant therapy for non-small-cell lung cancer. *Tuberc Respir Dis (Seoul).* (2024) 87:31–9. doi: 10.4046/trd.2023.0085

23. Park H, Lee S, Chang Y. Recent advances in diagnostic technologies in lung cancer. *Korean J Intern Med.* (2020) 35:257–68. doi: 10.3904/kjim.2020.030

24. Aberle D, Adams A, Berg C, Black W, Clapp J, Fagerstrom R, et al. Reduced lung-cancer mortality with low-dose computed tomographic screening. *N Engl J Med.* (2011) 365:395–409. doi: 10.1056/NEJMoa1102873

25. de Koning H, van der Aalst C, de Jong P, Scholten E, Nackaerts K, Heuvelmans M, et al. reduced lung-cancer mortality with volume CT screening in a randomized trial. *N Engl J Med.* (2020) 382:503–13. doi: 10.1056/NEJMoa1911793

26. Koo H, Choi C, Park S, Lee H, Oh D, Ji W, et al. Chest radiography surveillance for lung cancer: Results from a national health insurance database in South Korea. *Lung Cancer.* (2019) 128:120–6. doi: 10.1016/j.lungcan.2018.12.024

27. Lee J, Sun H, Park S, Kim H, Hwang E, Goo J, et al. Performance of a deep learning algorithm compared with radiologic interpretation for lung cancer detection on chest radiographs in a health screening population. *Radiology.* (2020) 297:687–96. doi: 10.1148/radiol.2020201240

28. Shin H, Han K, Ryu L, Kim E. The impact of artificial intelligence on the reading times of radiologists for chest radiographs. *NPJ Digit Med.* (2023) 6:82. doi: 10.1038/s41746-023-00829-4

29. Lee J, Hong H, Nam G, Hwang E, Park C. Effect of human-AI interaction on detection of malignant lung nodules on chest radiographs. *Radiology.* (2023) 307:e222976. doi: 10.1148/radiol.222976

frontiers | Frontiers in Medicine

TYPE Original Research
PUBLISHED 12 August 2024
DOI 10.3389/fmed.2024.1450711

OPEN ACCESS

EDITED BY
Alessandro Leonetti,
University Hospital of Parma, Italy

REVIEWED BY
Luigi Ventura,
Sheffield Teaching Hospital NHS Foundation Trust, United Kingdom
Giovanni Bocchialini,
University Hospital of Parma, Italy

*CORRESPONDENCE
Yingjun Wei
✉ 349646070@163.com
Qing Wang
✉ pillawang@163.com

†These authors have contributed equally to this work

RECEIVED 18 June 2024
ACCEPTED 22 July 2024
PUBLISHED 12 August 2024

CITATION
Niu C, Lin H, Zhang Z, Wang Q and Wei Y (2024) Impact of pulmonary rehabilitation on exercise capacity, health-related quality of life, and cardiopulmonary function in lung surgery patients: a retrospective propensity score-matched analysis.
Front. Med. 11:1450711.
doi: 10.3389/fmed.2024.1450711

Impact of pulmonary rehabilitation on exercise capacity, health-related quality of life, and cardiopulmonary function in lung surgery patients: a retrospective propensity score-matched analysis

Chunlai Niu[1†], Huan Lin[2†], Zinan Zhang[1†], Qing Wang[3*] and Yingjun Wei[1*]

[1]Department of Respiratory and Critical Care Rehabilitation, Shanghai Second Rehabilitation Hospital, Shanghai, China, [2]Department of Respiratory and Critical Care Medicine, The First Affiliated Hospital of Naval Medical University, Shanghai, China, [3]Department of Thoracic Surgery, Shanghai Chest Hospital, School of Medicine, Shanghai Jiao Tong University, Shanghai, China

Background: Pulmonary rehabilitation is considered beneficial for patients undergoing lung surgery, yet its specific impacts on exercise capacity, health-related quality of life (HRQL), and cardiopulmonary function require further elucidation. This study aimed to evaluate the effect of PR on these outcomes in patients undergoing lung surgery using a retrospective propensity score-matched analysis.

Methods: We retrospectively analyzed 420 patients with non-small cell lung cancer (NSCLC) who underwent lung surgery from January 2022 to May 2024. Among these, 84 patients received PR while 336 did not (control group). Propensity score matching (PSM) at a 1:1 ratio yielded 46 patients in each group. Baseline characteristics, spirometry, cardiopulmonary exercise testing, respiratory muscle strength, HRQL, and muscle measurements were assessed pre-and post-surgery.

Results: Before PSM, significant differences existed between groups, with the PR group being older and having different pulmonary function baselines. After PSM, groups were well-balanced. Postoperatively, the PR group showed significant improvements in FEV1/FVC (64.17% vs. 50.87%, $p < 0.001$), FEV1 (2.31 L/min vs. 1.75 L/min, $p < 0.001$), and predicted FVC percentage (88.75% vs. 68.30%, $p < 0.001$). Cardiovascular responses showed a lower CI during exercise in the PR group post-PSM (6.24 L/min/m^2 vs. 7.87 L/min/m^2, $p < 0.001$). In terms of exercise capacity, the PR group had higher maximal WR percentage (104.76% vs. 90.00%, $p = 0.017$) and peak VO2 (1150.70 mL/min vs. 1004.74 mL/min, $p = 0.009$). PR also resulted in less leg soreness and lower total CAT scores postoperatively. Muscle measurements indicated significantly smaller reductions in ΔHU_{ESMCSA} and percentage change in the PR group.

Conclusion: Pulmonary rehabilitation significantly enhances exercise capacity, HRQL, and cardiopulmonary function in patients undergoing lung surgery. It also mitigates postoperative muscle loss, underscoring its importance in the postoperative management of lung surgery patients.

KEYWORDS

pulmonary rehabilitation, lung surgery, exercise capacity, health-related quality of life, cardiopulmonary function

Introduction

Lung cancer remains one of the leading causes of cancer-related morbidity and mortality worldwide, with non-small cell lung cancer (NSCLC) accounting for approximately 85% of cases (1). Surgical resection is a primary treatment modality for early-stage NSCLC, but it is often associated with significant postoperative complications and a decline in pulmonary function and exercise capacity (2). Pulmonary rehabilitation has emerged as an effective intervention to mitigate these adverse outcomes by improving respiratory muscle strength, exercise capacity, and overall quality of life in patients with chronic lung diseases (3, 4).

PR programs, which typically include exercise training, education, and psychological support, have been shown to be beneficial in various chronic respiratory conditions, including chronic obstructive pulmonary disease (COPD) and interstitial lung disease (ILD) (5, 6). These programs aim to enhance the functional status and reduce the symptom burden of patients through a multidisciplinary approach (7). In the context of lung cancer, PR is increasingly recognized for its potential to improve preoperative and postoperative outcomes, thereby enhancing recovery and reducing healthcare utilization (8, 9).

Despite the recognized benefits of PR in chronic lung diseases, its role in the perioperative management of lung cancer patients undergoing surgical resection is less well-defined. Studies have suggested that PR can improve preoperative pulmonary function and reduce postoperative complications, but comprehensive data, particularly from propensity score-matched analyses, are limited (2, 10). Given the heterogeneity in patient populations and PR program designs, there is a need for robust evidence to guide clinical practice in this setting (11).

This retrospective propensity score-matched analysis aims to evaluate the effects of PR on exercise capacity, health-related quality of life (HRQL), and cardiopulmonary function in patients undergoing lung cancer surgery. By comparing outcomes between patients who received PR and those who did not, this study seeks to provide a clearer understanding of the clinical benefits of PR in this patient population.

Materials and methods

Study design and patient selection

This study was a retrospective analysis of patients diagnosed with non-small cell lung cancer (NSCLC) who underwent lung cancer surgery from January 2022 to May 2024. A total of 632 patients were initially identified from the medical records of Shanghai Chest Hospital. Patients were eligible if they had histologically confirmed NSCLC, underwent VATS/minimally invasive surgery, were aged 18 years or older. Exclusion criteria included patients with missing data in their medical records, severe orthopedic or neurological impairments that precluded participation in exercise testing or pulmonary rehabilitation, significant changes in tumor size or evidence of metastasis indicating disease progression, and those who experienced severe postoperative complications. Patients with severe postoperative complications were excluded from the study to maintain a homogenous study population and to avoid confounding factors that could skew the results. Patients under the age of 18 were also excluded.

After excluding 126 patients with missing data, 10 patients with severe complications, and 2 patients under the age of 18, a total of 420 patients were eligible for further analysis. Among these, 84 patients received pulmonary rehabilitation (PR), while 336 did not (control group, CTRL). To minimize selection bias and balance baseline characteristics between the groups, propensity score matching (PSM) was employed. Patients were matched at a 1:1 ratio, resulting in 46 patients in each group. This matching process ensured comparable baseline demographics and clinical characteristics between the PR and control groups. Data analysis included baseline characteristics, spirometry, cardiopulmonary exercise testing, respiratory muscle strength, health-related quality of life (HRQL), and muscle measurements. The flowchart in Figure 1 illustrates the patient selection and grouping process.

Ethical statement

This study was conducted in accordance with the ethical standards laid down in the Declaration of Helsinki and its subsequent amendments. The study protocol was reviewed and approved by the Ethics Committee of Shanghai Second Rehabilitation Hospital. Given the retrospective nature of the study, the requirement for informed consent was waived. However, confidentiality and privacy of the patient data were strictly maintained throughout the study. All data were anonymized prior to analysis to ensure patient confidentiality. The study aimed to provide insights that could improve clinical practice and patient outcomes, adhering to ethical principles of beneficence and non-maleficence.

Pulmonary rehabilitation program

Pulmonary rehabilitation included a combination of exercise and education programs (2, 12), aligned with the Enhanced Recovery After Surgery (ERAS) protocol. The exercise sessions were held one to three times weekly, lasting 30–40 min each. Educational sessions were repeatedly conducted in the outpatient clinic and the exercise therapy room. The exercise regimen comprised aerobic activities (such as walking, bicycle ergometer, treadmill, and arm ergometer), strength training (focused on upper-limb exercises), flexibility exercises, and inspiratory muscle training. Educational components included guidance on smoking cessation, breathing techniques (pursed-lip, diaphragmatic, and segmental breathing), and secretion removal

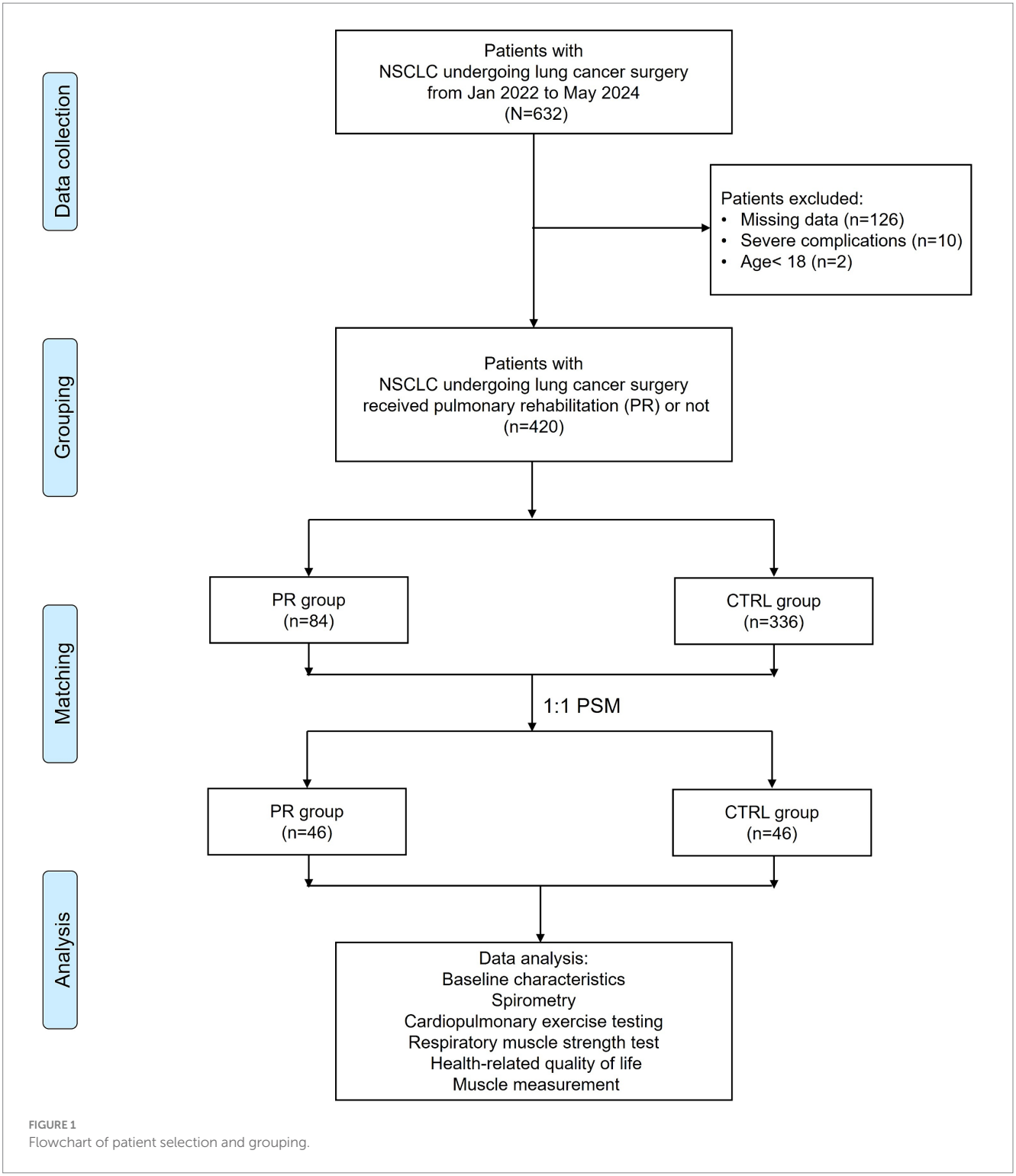

FIGURE 1
Flowchart of patient selection and grouping.

methods (coughing exercises, huffing, assisted coughing, and postural drainage). Exercise intensity for patients was tailored based on metabolic equivalent, peak oxygen consumption, and heart rate.

Patients participated in pulmonary rehabilitation at least once or twice before surgery. Postoperatively, their condition was reassessed 2–3 weeks after the operation, and rehabilitation was resumed. To support ongoing home-based rehabilitation, patients were provided with educational materials such as pamphlets, notes, and posters.

Postoperative reassessment

Postoperative reassessment of the patients was conducted 2–3 weeks after surgery to evaluate their recovery and readiness to resume pulmonary rehabilitation. During this reassessment period, all mentioned tests and measurements were performed, including spirometry, cardiopulmonary exercise testing, and respiratory muscle strength measurements. These comprehensive assessments

were crucial in determining the patient's postoperative status and tailoring the subsequent rehabilitation program to their specific needs. The spirometry tests measured forced expiratory volume in 1 s (FEV1) and forced vital capacity (FVC), while the cardiopulmonary exercise tests evaluated parameters such as peak oxygen uptake (VO2), work rate (WR), and other cardiovascular responses. Respiratory muscle strength was assessed using maximum inspiratory pressure (MIP) and maximum expiratory pressure (MEP).

Pulmonary function testing

Pulmonary function was assessed using spirometry (Medical Graphics Corp., St. Paul, MN, United States) following the guidelines of the American Thoracic Society (ATS). Parameters measured included FEV1, FVC, and the FEV1/FVC ratio.

Cardiopulmonary exercise testing

CPET was performed using a bicycle ergometer (Lode Corival, Groningen, Netherlands) with an incremental protocol. Key variables measured included VO2, carbon dioxide output (VCO2), tidal volume (VT), and RF. HR, BP, and SpO2 were monitored simultaneously. Anaerobic threshold (AT) was determined using the V-slope method, and work efficiency (WE) was calculated by linear regression analysis of the VO2 to WR ratio. Oxygen pulse (O2P) was determined by dividing VO2 by HR, and the ventilatory equivalent (VEQ) was calculated as the ratio of VCO2 to minute ventilation (VE) at nadir during CPET.

Respiratory muscle strength testing

MIP and MEP were measured using a respiratory pressure meter (Micro Medical Corp., England). MIP was measured after the patient exhaled to residual volume, followed by a rapid and forceful maximal inspiration. MEP was measured after the patient inhaled to total lung capacity, followed by maximal effort exhalation.

Cardiac performance assessment

Cardiac performance, including stroke volume index (SVI) and cardiac index (CI), was measured using Physioflow (Manatec Biomedical, Poissy, France), a non-invasive hemodynamic monitoring device that uses thoracic impedance cardiography. Electrodes placed on the thorax assessed changes in impedance caused by pulsatile blood flow.

Health-related quality of life assessment

HRQL was assessed using the Chronic Obstructive Pulmonary Disease Assessment Test (CAT), which comprises eight items evaluating symptoms such as cough, phlegm, chest tightness, breathlessness, limited activities, confidence in leaving home, sleeplessness, and energy levels. Each item is scored from 0 to 5, with higher scores indicating more severe symptoms.

Muscle measurement

As previously described, we focused on and measured three muscles: the pectoralis, thoracic erector spinae, and lumbar erector spinae (12). We selected the erector spinae muscles at the first lumbar level for three reasons: prior studies have analyzed COPD patients using CT-based measurements of the pectoralis and thoracic erector spinae muscles, but these may be less accurate in patients who underwent lung surgery due to potential damage. Routine chest CT scans include images only up to the first lumbar level. Additionally, research on lung cancer patients suggested that the first lumbar erector spinae muscle provides a better prognosis than the pectoralis muscle.

We used the Hounsfield unit (HU) average value within the patient's erector spinae muscle area on CT images to assess muscle mass, defining it as "HU_{ESMcsa}". First, to mitigate image quality variations due to patient size and scanning protocol, we denoised all chest CT images using commercial software. The HU_{ESMcsa} was then manually calculated by an experienced clinician and two researchers using in-house software that semi-automatically measures muscle and fat indices and calculates the HU range. Each measurement was performed twice per person to ensure accuracy and repeatability.

The process involved selecting the region of interest (ROI) within the erector spinae muscle area on CT images. Using in-house developed software, we manually calibrated the HU intensity range for muscle and adipose tissue. The HU dividing points were set to −30 at 120 kVp based on previous studies. Average intensity HU values were measured and validated against standard literature to account for variations in scanning protocols.

We applied a modified flood fill technique to precisely delineate the ROI, avoiding boundary edge areas that might include inhomogeneous intensity. This method allowed us to calculate the muscle and adipose tissue distribution, determining muscle density or "muscle index" by interpreting the mixture of muscle and fat within the selected ROI.

Statistical analysis

Statistical analyses were performed using SPSS version 24.0 (SPSS Inc., Chicago, IL, United States). Continuous variables are presented as the mean ± standard deviation, while categorical variables are shown as counts and percentages. The Student's *t*-test was employed for comparisons of continuous variables. Categorical variables were compared using the chi-square test or, when the expected number of events was fewer than five, the Fisher exact test. A *p*-value of less than 0.05 was considered statistically significant.

Pulmonary rehabilitation is generally recommended for patients with compromised lung function before undergoing lung surgery. This resulted in differences in baseline characteristics and pulmonary function between the two groups. To address these disparities, propensity score matching was used. Propensity scores were determined for each patient via multivariable logistic regression, considering covariates such as age, sex, height, weight, FEV1 (%), DLCO (%), comorbidities, cancer-related treatment (including neoadjuvant

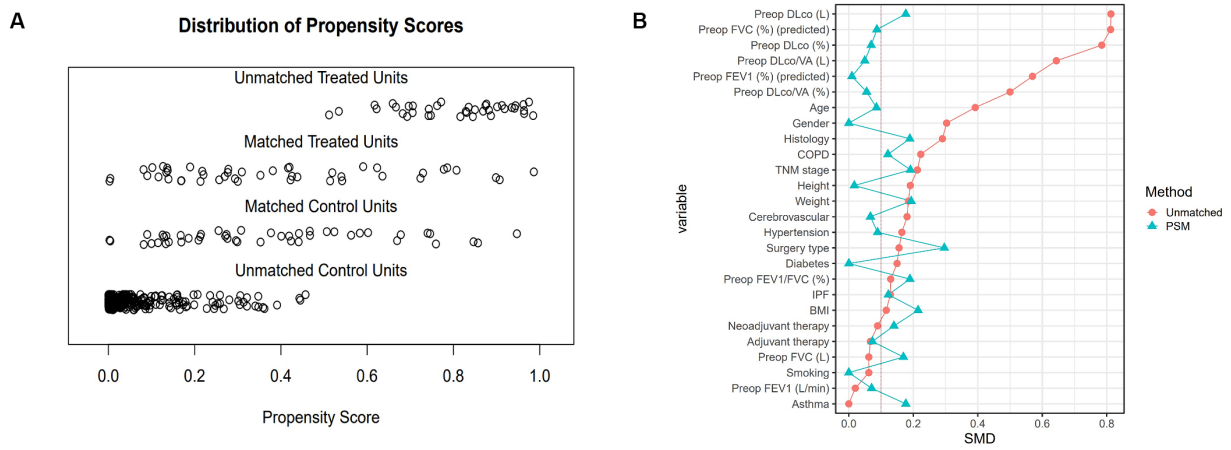

FIGURE 2
Distribution of propensity scores and standardized mean differences before and after PSM. **(A)** Propensity score distribution showing unmatched treated units, matched treated units, matched control units, and unmatched control units. After matching, the propensity scores of treated and control units align more closely, indicating improved balance. **(B)** Standardized mean differences (SMD) for each variable before and after PSM. Red dots represent the SMDs before matching, and blue triangles represent the SMDs after matching. The reduction in SMDs post-matching indicates successful balancing of the baseline characteristics between the PR and CTRL groups. PSM, propensity score matching; PR, pulmonary rehabilitation; CTRL, control; SMD, standardized mean difference; Preop, preoperative; FEV1, forced expiratory volume in 1 second; FVC, forced vital capacity; DLco, diffusing capacity of the lungs for carbon monoxide; VA, alveolar volume; COPD, chronic obstructive pulmonary disease; IPF, idiopathic pulmonary fibrosis; BMI, body mass index.

chemotherapy and neoadjuvant concurrent chemoradiotherapy), surgery type, and operation site. The nearest-neighbor method was utilized for 1:1 matching to ensure the most comparable propensity scores, and the effect size of the standardized mean difference (d) was calculated to evaluate the appropriateness of the propensity score matching (Figure 2).

Results

Baseline demographic and clinical characteristics

Before PSM, significant differences were observed between the PR and CTRL groups in several baseline characteristics. The mean age was higher in the PR group (57.29 vs. 51.92 years, $p = 0.001$, SMD = 0.392). The gender distribution also differed, with fewer females in the PR group (25.0% vs. 39.0%, $p = 0.024$, SMD = 0.303). There were no significant differences in height, weight, BMI, smoking status, COPD, asthma, IPF, hypertension, diabetes, cerebrovascular history, histological subtypes, TNM stages, neoadjuvant and adjuvant therapies, or surgery types between the groups before matching (Table 1).

After PSM, the baseline characteristics between the PR and CTRL groups were well-balanced with no significant differences in age (56.17 vs. 54.98 years, $p = 0.682$, SMD = 0.086) and identical gender distribution (28.3% female in both groups). Other variables such as height, weight, BMI, smoking status, COPD, asthma, IPF, hypertension, diabetes, cerebrovascular history, histological subtypes, TNM stages, neoadjuvant and adjuvant therapies, and surgery types also showed no significant differences post-matching, indicating successful balancing between the groups (Figure 3).

Preoperative pulmonary function test results

Before PSM, significant differences were observed between the PR and CTRL groups in several preoperative pulmonary function test variables. The PR group had a lower predicted FEV1 percentage (79.51% vs. 89.49%, $p < 0.001$, SMD = 0.57) and a lower predicted FVC percentage (84.26% vs. 96.23%, $p < 0.001$, SMD = 0.812). The diffusing capacity of the lungs for carbon monoxide (DLco) was also significantly lower in the PR group both in absolute terms (14.24 L vs. 17.54 L, $p < 0.001$, SMD = 0.813) and as a percentage of predicted values (75.10% vs. 86.16%, $p < 0.001$, SMD = 0.785). Similarly, DLco per alveolar volume (DLco/VA) was lower in the PR group in both absolute values (3.21 L vs. 3.77 L, $p < 0.001$, SMD = 0.644) and percentage of predicted values (82.85% vs. 89.94%, $p < 0.001$, SMD = 0.5). The relatively lower FEV1 and FVC in the PR group can be attributed to the fact that we administered PR to patients with poorer respiratory conditions, aiming to improve their preoperative status. Despite these initial differences, the PSM provided well-balanced cohorts for subsequent analysis (Table 2).

After PSM, the PR and CTRL groups were well-balanced with no significant differences in any preoperative pulmonary function test variables. FEV1/FVC percentage (62.65% vs. 64.53%, $p = 0.366$, SMD = 0.19), absolute FEV1 (2.30 L vs. 2.25 L, $p = 0.735$, SMD = 0.071), and predicted FEV1 percentage (81.82% vs. 81.65%, $p = 0.963$, SMD = 0.01) were similar between groups. Likewise, FVC (3.75 L vs. 3.55 L, $p = 0.419$, SMD = 0.169) and predicted FVC percentage (88.32% vs. 87.22%, $p = 0.678$, SMD = 0.087) showed no significant differences. DLco values, both absolute (14.52 L vs. 15.19 L, $p = 0.399$, SMD = 0.177) and predicted percentage (78.94% vs. 78.05%, $p = 0.74$, SMD = 0.069), as well as DLco/VA values in absolute terms (3.49 L vs. 3.53 L, $p = 0.813$, SMD = 0.049) and predicted percentage (83.15% vs. 83.97%, $p = 0.791$, SMD = 0.055), were balanced post-matching.

10.3389/fmed.2024.1450711

TABLE 1 Comparison of baseline characteristics and demographics between PR and CTRL groups pre-and post-propensity score matching.

Variables	Level	Before PSM				After PSM			
		CTRL group (n = 336)	PR group (n = 84)	p value	SMD	CTRL group (n = 46)	PR group (n = 46)	p value	SMD
Age (y)		51.92 (13.43)	57.29 (13.94)	0.001	0.392	54.98 (14.23)	56.17 (13.65)	0.682	0.086
Gender (%)	Female	131 (39.0)	21 (25.0)	0.024	0.303	13 (28.3)	13 (28.3)	1	<0.001
	Male	205 (61.0)	63 (75.0)			33 (71.7)	33 (71.7)		
Height		170.07 (9.10)	171.75 (8.49)	0.126	0.191	172.28 (9.01)	172.13 (8.74)	0.935	0.017
Weight		70.62 (13.53)	73.06 (12.79)	0.137	0.185	75.22 (14.33)	72.52 (13.53)	0.356	0.193
BMI		24.50 (3.73)	24.94 (3.76)	0.341	0.116	25.46 (4.19)	24.61 (3.71)	0.306	0.215
Smoking (%)	Current smoker	27 (8.0)	8 (9.5)	0.875	0.062	4 (8.7)	4 (8.7)	1	<0.001
	Ex-smoker	119 (35.4)	28 (33.3)			14 (30.4)	14 (30.4)		
	Never-smoker	190 (56.5)	48 (57.1)			28 (60.9)	28 (60.9)		
COPD (%)	No	259 (77.1)	72 (85.7)	0.114	0.223	38 (82.6)	40 (87.0)	0.772	0.121
	Yes	77 (22.9)	12 (14.3)			8 (17.4)	6 (13.0)		
Asthma (%)	No	328 (97.6)	82 (97.6)	1	<0.001	42 (91.3)	44 (95.7)	0.673	0.177
	Yes	8 (2.4)	2 (2.4)			4 (8.7)	2 (4.3)		
IPF (%)	No	328 (97.6)	80 (95.2)	0.421	0.129	45 (97.8)	44 (95.7)	1	0.123
	Yes	8 (2.4)	4 (4.8)			1 (2.2)	2 (4.3)		
Hypertension (%)	No	215 (64.0)	47 (56.0)	0.217	0.165	29 (63.0)	27 (58.7)	0.831	0.089
	Yes	121 (36.0)	37 (44.0)			17 (37.0)	19 (41.3)		
Diabetes (%)	No	283 (84.2)	75 (89.3)	0.319	0.15	40 (87.0)	40 (87.0)	1	<0.001
	Yes	53 (15.8)	9 (10.7)			6 (13.0)	6 (13.0)		
Cerebrovascular (%)	No	304 (90.5)	71 (84.5)	0.167	0.181	41 (89.1)	40 (87.0)	1	0.067
	Yes	32 (9.5)	13 (15.5)			5 (10.9)	6 (13.0)		
Histology (%)	Adenocarcinoma	156 (46.4)	51 (60.7)	0.063	0.29	21 (45.7)	25 (54.3)	0.665	0.189
	Others	84 (25.0)	16 (19.0)			12 (26.1)	9 (19.6)		
	Squamous cell carcinoma	96 (28.6)	17 (20.2)			13 (28.3)	12 (26.1)		
TNM stage (%)	I	100 (29.8)	20 (23.8)	0.37	0.213	14 (30.4)	14 (30.4)	0.841	0.191
	II	140 (41.7)	32 (38.1)			17 (37.0)	17 (37.0)		
	III	83 (24.7)	27 (32.1)			11 (23.9)	13 (28.3)		
	IV	13 (3.9)	5 (6.0)			4 (8.7)	2 (4.3)		
Neoadjuvant therapy (%)	No	298 (88.7)	72 (85.7)	0.572	0.089	40 (87.0)	42 (91.3)	0.738	0.14
	Yes	38 (11.3)	12 (14.3)			6 (13.0)	4 (8.7)		
Adjuvant therapy (%)	No	303 (90.2)	74 (88.1)	0.717	0.067	42 (91.3)	41 (89.1)	1	0.073
	Yes	33 (9.8)	10 (11.9)			4 (8.7)	5 (10.9)		
Surgery type (%)	Lobectomy	132 (39.3)	32 (38.1)	0.645	0.156	20 (43.5)	20 (43.5)	0.578	0.296
	Pneumonectomy	9 (2.7)	2 (2.4)			1 (2.2)	0 (0.0)		
	Segmentectomy	86 (25.6)	27 (32.1)			14 (30.4)	11 (23.9)		
	Wedge resection	109 (32.4)	23 (27.4)			11 (23.9)	15 (32.6)		

PSM, propensity score matching; CTRL, control; PR, pulmonary rehabilitation; SMD, standardized mean difference; COPD, chronic obstructive pulmonary disease; IPF, idiopathic pulmonary fibrosis; TNM, tumor, node, metastasis; y, years; BMI, body mass index.

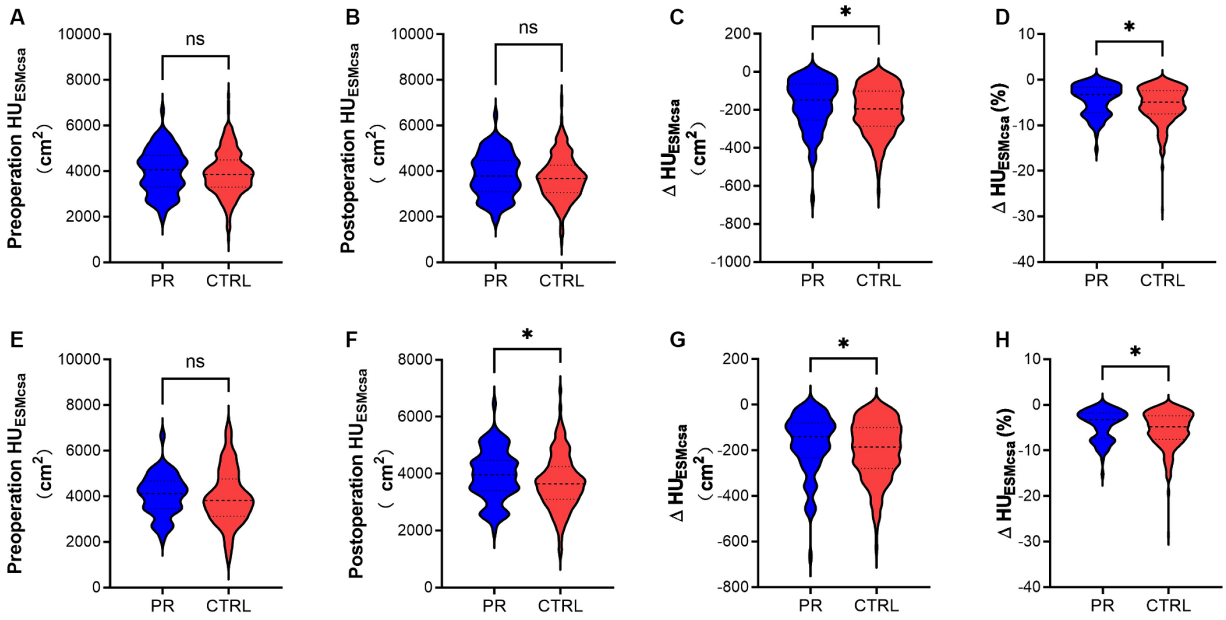

FIGURE 3
Changes in HUESMCSA of the PR and CTRL groups before **(A–D)** and after PSM (E-H). **(A,E)** Show preoperative HUESMCSA (cm^2) in the PR and CTRL groups with no significant difference (ns). **(B,F)** Display postoperative HUESMCSA (cm^2), with a significant difference in **(F)** (*). **(C,G)** Illustrate the change in HUESMCSA (ΔHUESMCSA) (cm^2) between preoperative and postoperative measurements, showing significant differences in both (*). **(D,H)** Depict the percentage change in HUESMCSA (ΔHUESMCSA %) between preoperative and postoperative measurements, also indicating significant differences (*). * Indicates $p < 0.05$. ns indicates no significant difference. Data are presented as violin plots, with each plot displaying the distribution, median, and quartiles of the data. HUESMCSA, Hounsfield unit erector spinae muscle cross-sectional area; PR, pulmonary rehabilitation; CTRL, control; PSM, propensity score matching.

TABLE 2 **Preoperative pulmonary function test results for PR and CTRL groups before and after propensity score matching.**

Variables	Before PSM				After PSM			
	CTRL group (*n* = 336)	PR group (*n* = 84)	*p* value	SMD	CTRL group (*n* = 46)	PR group (*n* = 46)	*p* value	SMD
FEV1/FVC (%)	64.38 (9.53)	63.11 (10.07)	0.279	0.13	64.53 (9.26)	62.65 (10.53)	0.366	0.19
FEV1 (L/min)	2.21 (0.62)	2.22 (0.63)	0.869	0.02	2.25 (0.67)	2.30 (0.62)	0.735	0.071
FEV1 (%) (predicted)	89.49 (20.04)	79.51 (14.56)	<0.001	0.57	81.65 (20.19)	81.82 (13.24)	0.963	0.01
FVC (L)	3.51 (1.15)	3.58 (1.14)	0.612	0.062	3.55 (1.15)	3.75 (1.16)	0.419	0.169
FVC (%) (predicted)	96.23 (15.00)	84.26 (14.49)	<0.001	0.812	87.22 (12.70)	88.32 (12.70)	0.678	0.087
DLco (L)	17.54 (4.85)	14.24 (3.05)	<0.001	0.813	15.19 (4.39)	14.52 (3.07)	0.399	0.177
DLco (%)	86.16 (14.42)	75.10 (13.77)	<0.001	0.785	78.05 (13.78)	78.94 (11.70)	0.74	0.069
DLco/VA (L)	3.77 (0.92)	3.21 (0.81)	<0.001	0.644	3.53 (0.87)	3.49 (0.60)	0.813	0.049
DLco/VA (%)	89.94 (14.70)	82.85 (13.62)	<0.001	0.5	83.97 (15.97)	83.15 (13.22)	0.791	0.055

PSM, propensity score matching; CTRL, control; PR, pulmonary rehabilitation; SMD, standardized mean difference; Preop, preoperative; FEV1, forced expiratory volume in 1 second; FVC, forced vital capacity; DLco, diffusing capacity of the lungs for carbon monoxide; VA, alveolar volume.

Exercise capacity, peak exercise symptoms, and HRQL

Before PSM, the PR group demonstrated significantly higher maximal WR in watts (86.24 vs. 78.01, $p = 0.01$, SMD = 0.331) and as a percentage (105.33% vs. 92.88%, $p = 0.001$, SMD = 0.421). Similarly, peak oxygen uptake (VO2) in mL/min was significantly higher in the PR group (1180.96 vs. 1014.37, $p < 0.001$, SMD = 0.622) and as a percentage (83.71% vs. 78.61%, $p = 0.011$, SMD = 0.313). The PR group also reported less leg soreness during exercise (3.42 vs. 4.13, $p < 0.001$, SMD = 0.474) and a lower total CAT score (9.80 vs. 12.40, $p < 0.001$, SMD = 0.574). There were no significant differences in dyspnea during exercise ($p = 0.115$), cough, phlegm, chest tightness, limited activities, confidence in leaving home, sleeplessness, and lack of energy (Table 3).

TABLE 3 Exercise capacity, peak exercise symptoms, and HRQL in PR and CTRL groups before and after propensity score matching.

Variables	Before PSM				After PSM			
	CTRL group (n = 336)	PR group (n = 84)	p value	SMD	CTRL group (n = 46)	PR group (n = 46)	p value	SMD
Maximal WR (watt)	78.01 (26.60)	86.24 (22.98)	0.01	0.331	73.33 (30.12)	81.67 (19.58)	0.119	0.328
Maximal WR (%)	92.88 (28.84)	105.33 (30.35)	0.001	0.421	90.00 (29.94)	104.76 (28.23)	0.017	0.507
Peak VO2 (mL/min)	1014.37 (255.51)	1180.96 (279.94)	<0.001	0.622	1004.74 (252.51)	1150.70 (269.62)	0.009	0.559
Peak VO2 (%)	78.61 (16.54)	83.71 (16.07)	0.011	0.313	78.04 (18.24)	82.46 (15.86)	0.219	0.258
Leg soreness during exercise	4.13 (1.47)	3.42 (1.49)	<0.001	0.474	4.15 (1.43)	3.33 (1.46)	0.007	0.572
Dyspnea during exercise	4.50 (1.75)	4.16 (2.01)	0.115	0.184	4.14 (1.90)	4.28 (1.97)	0.727	0.073
Total CAT score	12.40 (5.38)	9.80 (3.48)	<0.001	0.574	13.18 (5.55)	10.17 (3.96)	0.003	0.627
Cough	2.01 (0.10)	2.01 (0.11)	0.807	0.029	2.00 (0.10)	2.02 (0.10)	0.349	0.196
Phlegm	1.40 (0.10)	1.40 (0.09)	0.921	0.013	1.40 (0.12)	1.40 (0.08)	1	<0.001
Chest tightness	1.80 (0.10)	1.80 (0.10)	0.553	0.073	1.78 (0.09)	1.81 (0.09)	0.226	0.254
Breathlessness	1.90 (0.10)	1.51 (0.11)	<0.001	3.599	1.90 (0.11)	1.52 (0.10)	<0.001	3.78
Limited activities	0.94 (0.62)	0.79 (0.63)	0.05	0.238	0.90 (0.52)	0.77 (0.60)	0.269	0.232
Confidence in leaving home	0.89 (0.53)	0.69 (0.38)	0.001	0.43	0.91 (0.61)	0.71 (0.36)	0.054	0.407
Sleeplessness	1.66 (0.91)	1.31 (0.83)	0.001	0.401	1.70 (0.75)	1.34 (0.83)	0.032	0.455
Lack of energy	1.41 (0.92)	1.25 (0.83)	0.147	0.182	1.42 (0.91)	1.20 (0.87)	0.245	0.244

PSM, propensity score matching; CTRL, control; PR, pulmonary rehabilitation; SMD, standardized mean difference; WR, work rate; VO2, oxygen uptake; CAT, chronic obstructive pulmonary disease assessment test.

After PSM, the PR group continued to show significant improvements in several parameters. The maximal WR percentage remained higher (104.76% vs. 90.00%, $p = 0.017$, SMD = 0.507), and peak VO2 in mL/min (1150.70 vs. 1004.74, $p = 0.009$, SMD = 0.559) was significantly better in the PR group. Leg soreness during exercise was significantly lower (3.33 vs. 4.15, $p = 0.007$, SMD = 0.572), and the total CAT score was reduced (10.17 vs. 13.18, $p = 0.003$, SMD = 0.627). Breathlessness showed a marked improvement in the PR group both before ($p < 0.001$) and after PSM ($p < 0.001$). Other variables such as dyspnea during exercise, cough, phlegm, chest tightness, limited activities, confidence in leaving home, sleeplessness, and lack of energy did not show significant differences between the groups post-matching, indicating a good balance in these aspects.

Postoperative pulmonary function test results

Before PSM, the PR group exhibited significantly better postoperative pulmonary function compared to the CTRL group. This included higher FEV1/FVC percentage (63.27% vs. 50.96%, $p < 0.001$, SMD = 0.904), FEV1 in liters per minute (2.25 vs. 1.74, $p < 0.001$, SMD = 0.705), and predicted FEV1 percentage (81.02% vs. 70.68%, $p < 0.001$, SMD = 0.489). Similarly, the PR group had higher FVC in liters (3.75 vs. 2.80, $p < 0.001$, SMD = 0.762) and predicted FVC percentage (84.32% vs. 76.10%, $p < 0.001$, SMD = 0.393). While the DLco in absolute terms was not significantly different ($p = 0.077$), the predicted DLco percentage was higher in the PR group (75.02% vs. 68.44%, $p = 0.001$, SMD = 0.383). DLco/VA was lower in the PR group both in absolute values (2.53 vs. 2.97, $p < 0.001$, SMD = 0.545) and as a percentage of predicted values (63.60% vs. 71.22%, $p < 0.001$, SMD = 0.517) (Table 4).

After PSM, the PR group continued to show significantly better postoperative pulmonary function results. The differences in FEV1/FVC percentage (64.17% vs. 50.87%, $p < 0.001$, SMD = 0.906), FEV1 in liters per minute (2.31 vs. 1.75, $p < 0.001$, SMD = 0.806), predicted FEV1 percentage (84.45% vs. 64.32%, $p < 0.001$, SMD = 0.997), FVC in liters (3.92 vs. 2.79, $p < 0.001$, SMD = 0.968), and predicted FVC percentage (88.75% vs. 68.30%, $p < 0.001$, SMD = 1.036) remained statistically significant. Additionally, DLco in both absolute terms (15.50 vs. 11.90, $p < 0.001$, SMD = 0.863) and predicted percentage (78.66% vs. 60.46%, $p < 0.001$, SMD = 1.175) showed significant improvement in the PR group. No significant differences were found in DLco/VA values post-matching. There were no significant differences in MIP, MEP, resting VT, RF, or SpO2 at rest or during exercise between the groups post-matching, indicating balanced postoperative characteristics.

Postoperative cardiovascular responses to exercise

Before PSM, there were significant differences between the PR and CTRL groups in certain cardiovascular responses to exercise. The PR

TABLE 4 Postoperative pulmonary function test data at rest and during exercise for PR and CTRL groups before and after propensity score matching.

Variables	Before PSM				After PSM			
	CTRL group (n = 336)	PR group (n = 84)	p value	SMD	CTRL group (n = 46)	PR group (n = 46)	p value	SMD
FEV1/FVC (%)	50.96 (10.60)	63.27 (16.08)	<0.001	0.904	50.87 (10.32)	64.17 (18.01)	<0.001	0.906
FEV1 (L/min)	1.74 (0.57)	2.25 (0.86)	<0.001	0.705	1.75 (0.57)	2.31 (0.80)	<0.001	0.806
FEV1 (%) (postdicted)	70.68 (20.50)	81.02 (21.73)	<0.001	0.489	64.32 (18.52)	84.45 (21.73)	<0.001	0.997
FVC (L)	2.80 (1.07)	3.75 (1.40)	<0.001	0.762	2.79 (0.98)	3.92 (1.32)	<0.001	0.968
FVC (%) (postdicted)	76.10 (17.64)	84.32 (23.77)	<0.001	0.393	68.30 (15.02)	88.75 (23.55)	<0.001	1.036
DLco (L)	13.87 (4.56)	14.85 (4.53)	0.077	0.217	11.90 (3.69)	15.50 (4.59)	<0.001	0.863
DLco (%)	68.44 (15.33)	75.02 (18.82)	0.001	0.383	60.46 (14.44)	78.66 (16.47)	<0.001	1.175
DLco/VA (L)	2.97 (0.86)	2.53 (0.74)	<0.001	0.545	2.72 (0.80)	2.75 (0.59)	0.871	0.034
DLco/VA (%)	71.22 (16.17)	63.60 (13.17)	<0.001	0.517	65.53 (15.59)	64.33 (12.94)	0.69	0.083
MIP (cmH20)	74.57 (25.60)	78.01 (24.52)	0.268	0.137	76.41 (24.77)	77.53 (25.61)	0.831	0.045
MEP (cmH2O)	112.26 (31.58)	110.39 (30.48)	0.625	0.06	106.72 (35.49)	108.82 (29.56)	0.758	0.064
VT (mL) (at rest)	501.88 (145.42)	501.19 (142.23)	0.969	0.005	459.35 (137.48)	529.57 (133.43)	0.015	0.518
VT (mL) (during exercise)	1108.84 (315.15)	1245.95 (304.78)	<0.001	0.442	1190.00 (286.21)	1260.65 (308.08)	0.258	0.238
RF (breaths/min) (at rest)	19.66 (4.92)	20.10 (5.06)	0.475	0.087	19.74 (5.20)	20.15 (5.55)	0.714	0.077
RF (breaths/min) (during exercise)	34.60 (6.10)	35.73 (5.58)	0.126	0.192	33.83 (6.07)	35.33 (5.85)	0.231	0.252
SpO2 (%) (at rest)	94.09 (2.63)	93.56 (2.72)	0.102	0.198	93.91 (2.86)	93.76 (2.68)	0.793	0.055
SpO2 (%) (during exercise)	93.08 (2.69)	92.50 (2.82)	0.081	0.211	92.89 (2.73)	92.65 (2.85)	0.682	0.086

PSM, propensity score matching; CTRL, control; PR, pulmonary rehabilitation; SMD, standardized mean difference; FEV1, forced expiratory volume in 1 second; FVC, forced vital capacity; DLco, diffusing capacity of the lungs for carbon monoxide; VA, alveolar volume; MIP, maximum inspiratory pressure; MEP, maximum expiratory pressure; VT, tidal volume; RF, respiratory frequency.

group had a lower CI during exercise (6.41 vs. 7.71 L/min/m^2, $p < 0.001$, SMD = 0.681) and higher oxygen pulse (O2P) (9.23 vs. 8.48 mL/beat, $p = 0.001$, SMD = 0.393). SVI at rest and during exercise, CI at rest, WE, AT, HR and mean BP during exercise showed no significant differences before matching (Table 5).

After PSM, the PR group continued to show a significantly lower CI during exercise (6.24 vs. 7.87 L/min/m^2, $p < 0.001$, SMD = 0.869). No significant differences were observed in other variables, including SVI at rest ($p = 0.311$) and during exercise ($p = 0.25$), CI at rest ($p = 0.215$), O2P ($p = 0.176$), WE ($p = 0.643$), AT ($p = 0.35$), HR during exercise ($p = 0.084$), and mean BP during exercise ($p = 0.251$). This indicates a good balance between the PR and CTRL groups in terms of postoperative cardiovascular responses after matching.

Muscle measurements and changes post-surgery

In our analysis of muscle measurements, we found no significant differences between the PR and CTRL groups in preoperative and postoperative muscle cross-sectional area (CSA) in HU_{ESMCSA}. However, when examining the changes post-surgery, the PR group experienced significantly smaller reductions in both absolute HU_{ESMCSA} values and percentage changes compared to the CTRL group. Specifically, the PR group showed less decline in ΔHU_{ESMCSA} and percentage change in two different muscle groups, indicating that pulmonary rehabilitation was effective in mitigating muscle loss post-surgery. These findings highlight the potential benefits of PR in preserving muscle mass in lung surgery patients.

Discussion

Our study demonstrated significant improvements in exercise capacity, HRQL, and cardiopulmonary function in patients with NSCLC who underwent pulmonary rehabilitation. Notably, the PR group showed higher values in FEV1/FVC, FEV1, predicted FVC percentage, and maximal WR percentage post-surgery. Furthermore, patients in the PR group exhibited better cardiovascular responses, including a lower CI during exercise and higher peak oxygen uptake (VO2). Muscle measurements indicated significantly smaller reductions in ΔHU_{ESMCSA}, highlighting the role of PR in mitigating postoperative muscle loss. These findings underline the effectiveness of PR in enhancing

TABLE 5 Postoperative cardiovascular responses to exercise in PR and CTRL groups.

Variables	Before PSM				After PSM			
	CTRL group (n = 336)	PR group (n = 84)	p value	SMD	CTRL group (n = 46)	PR group (n = 46)	p value	SMD
SVI (ml/min/m^2) (at rest)	41.98 (10.16)	42.67 (9.74)	0.575	0.069	44.51 (10.30)	42.42 (9.34)	0.311	0.212
SVI (ml/min/m^2) (during exercise)	54.40 (14.34)	50.83 (17.57)	0.052	0.223	55.42 (13.52)	51.71 (17.07)	0.25	0.241
CI (L/min/m^2) (at rest)	3.44 (0.67)	3.39 (0.58)	0.478	0.091	3.46 (0.62)	3.30 (0.58)	0.215	0.26
CI (L/min/m^2) (during exercise)	7.71 (1.91)	6.41 (1.92)	<0.001	0.681	7.87 (1.83)	6.24 (1.90)	<0.001	0.869
O2P (mL/beat)	8.48 (1.86)	9.23 (1.94)	0.001	0.393	8.51 (1.52)	8.99 (1.87)	0.176	0.285
WE (mL/min/W)	9.02 (1.93)	9.15 (2.06)	0.569	0.068	8.58 (1.87)	8.77 (2.03)	0.643	0.097
AT (mL/min)	679.64 (138.62)	705.83 (155.61)	0.132	0.178	669.78 (150.13)	699.78 (155.84)	0.35	0.196
HR (beats/min) (during exercise)	131.19 (20.88)	127.69 (16.86)	0.155	0.185	132.26 (19.38)	125.98 (14.81)	0.084	0.364
Mean BP (mmHg) (during exercise)	108.99 (14.78)	107.12 (13.85)	0.294	0.131	112.22 (15.06)	108.63 (14.72)	0.251	0.241

PSM, propensity score matching; CTRL, control; PR, pulmonary rehabilitation; SMD, standardized mean difference; SVI, stroke volume index; CI, cardiac index; O2P, oxygen pulse; WE, work efficiency; AT, anaerobic threshold; HR, heart rate; BP, blood pressure.

postoperative recovery and overall physical function in lung cancer patients. The relationship between PR and the ERAS protocol is complementary, with each addressing different aspects of patient care. PR focuses on respiratory and physical rehabilitation, improving muscle strength, exercise capacity, and quality of life. ERAS encompasses broader perioperative care, including pain management, nutritional support, and early mobilization, to enhance recovery and reduce hospital stay. Together, they offer a comprehensive strategy to optimize patient outcomes and reduce complications, highlighting the importance of incorporating both protocols in managing lung surgery patients (13).

The improvements in exercise capacity and cardiopulmonary function observed in our study align with previous research highlighting the benefits of PR in patients with chronic respiratory diseases (14–16). Huang et al. reported that PR significantly improved exercise capacity, HRQL, and cardiopulmonary function in lung cancer patients, with increased peak VO2 and WR, reduced exertional symptoms, and enhanced respiratory muscle strength (17). Our findings are consistent with these results, indicating that PR can lead to substantial enhancements in physical performance and quality of life for lung cancer patients undergoing surgery. Pulmonary function parameters, such as FEV1/FVC ratio and FVC, showed significant improvement in the PR group, corroborating the results of previous studies on the positive effects of PR on lung function. Wang et al. (10) conducted a meta-analysis that demonstrated PR's efficacy in improving postoperative clinical status in patients with lung cancer and COPD, showing enhanced pulmonary function and reduced postoperative complications. PR is known to reduce the risk of postoperative complications, although this aspect was not initially discussed in our paper. PR improves respiratory muscle strength, enhances exercise capacity, and promotes overall recovery, which can collectively reduce the incidence of postoperative complications. Similarly, our study revealed significant improvements in FEV1 and FVC percentages, suggesting that PR can effectively enhance lung function and aid in postoperative recovery.

The cardiovascular benefits of PR observed in our study, including improved CI and O2P during exercise, further emphasize the comprehensive impact of PR on patients' overall health. Exercise training, a core component of PR, has been shown to improve cardiac function and enhance oxygen delivery to tissues, contributing to better exercise performance and reduced symptoms (18–20). Our findings align with this evidence, demonstrating that PR not only benefits respiratory function but also significantly improves cardiovascular performance, which is crucial for enhancing overall physical capacity and quality of life in lung cancer patients (21–23).

Our study also highlighted the importance of PR in mitigating muscle loss post-surgery. The PR group experienced significantly smaller reductions in ΔHU_{ESMCSA} compared to the CTRL group, indicating that PR helps preserve muscle mass during the postoperative period. This finding is consistent with research by Illini et al. (24), who reported that PR effectively preserves muscle mass and improves physical function in lung cancer patients following surgery. The preservation of muscle mass is crucial for maintaining physical strength and function, reducing the risk of complications, and enhancing the overall recovery process (25–27).

Despite the significant findings, our study has several limitations. First, the sample size is relatively small, and the single-center design may introduce selection bias. Future multicenter studies with larger sample sizes are necessary to validate our findings. Second, Our study included patients with relatively better baseline pulmonary function

compared to typical rehabilitation cohorts. This selection bias is inherent due to the retrospective nature of our study and the inclusion criteria we applied. Specifically, patients were chosen based on their ability to participate in the rehabilitation program and to minimize the impact of severe comorbidities, which resulted in higher baseline FEV1 and DLCO values. This criterion ensured that the participants could safely engage in the intensive exercise components of the pulmonary rehabilitation program. Consequently, the outcomes observed in this study may not fully represent the broader population of lung surgery patients, particularly those with more compromised pulmonary function. This limitation highlights the need for further prospective studies to evaluate the effects of pulmonary rehabilitation in a more diverse and representative patient population, including those with more severe baseline pulmonary impairments. Additionally, the relatively short follow-up period of 12 weeks may not be sufficient to determine the long-term effects of PR. Longer follow-up studies are required to confirm the sustained benefits of PR. Finally, all patients in this study had NSCLC, and the results may not be generalizable to patients with small cell lung cancer (SCLC), who may have different treatment responses and prognoses. Another limitation of our study is the type of surgical procedure performed. Specifically, 32% of the patients underwent a wedge resection, a non-anatomical resection with debated oncological benefits. This decision was based on clinical judgment regarding the tumor's location, size, and the patient's health status. While necessary for some patients, this introduces variability that may affect the generalizability of our findings.

Conclusion

In summary, our study underscores the significant benefits of PR in improving exercise capacity, HRQL, and cardiopulmonary function in lung cancer patients. PR also plays a vital role in preserving muscle mass post-surgery, contributing to better physical function and recovery. These findings highlight the importance of incorporating PR into the standard care of lung cancer patients undergoing surgery to enhance their overall health outcomes and quality of life.

Data availability statement

The raw data supporting the conclusions of this article will be made available by the authors, without undue reservation.

Ethics statement

The studies involving humans were approved by the Ethics Committee of Shanghai Second Rehabilitation Hospital. The studies were conducted in accordance with the local legislation and institutional requirements. The ethics committee/institutional review board waived the requirement of written informed consent for participation from the participants or the participants' legal guardians/next of kin because Given the retrospective nature of the study, the requirement for informed consent was waived.

Author contributions

CN: Conceptualization, Formal analysis, Investigation, Methodology, Visualization, Writing – original draft. HL: Formal analysis, Methodology, Validation, Writing – review & editing. ZZ: Data curation, Formal analysis, Methodology, Writing – review & editing. QW: Conceptualization, Data curation, Resources, Visualization, Writing – review & editing. YW: Project administration, Supervision, Validation, Writing – review & editing.

Funding

The author(s) declare that no financial support was received for the research, authorship, and/or publication of this article.

Conflict of interest

The authors declare that the research was conducted in the absence of any commercial or financial relationships that could be construed as a potential conflict of interest.

Publisher's note

References

1. Siegel RL, Miller KD, Wagle NS, Jemal A. Cancer statistics, 2023. *CA Cancer J Clin*. (2023) 73:17–48. doi: 10.3322/caac.21763

2. Bradley A, Marshall A, Stonehewer L, Reaper L, Parker K, Bevan-Smith E, et al. Pulmonary rehabilitation programme for patients undergoing curative lung cancer surgery. *Eur J Cardiothorac Surg*. (2013) 44:E266–e271. doi: 10.1093/ejcts/ezt381

3. Holland AE, Cox NS, Houchen-Wolloff L, Rochester CL, Garvey C, ZuWallack R, et al. Defining modern pulmonary rehabilitation an official American Thoracic Society workshop report. *Ann Am Thorac Soc*. (2021) 18:E12–29. doi: 10.1513/AnnalsATS.202102-146ST

4. Pehlivan E, Balci A, Kiliç L. Can functional inoperability in lung cancer patients be changed by pulmonary rehabilitation? *Turk Gogus Kalp Damar Cerrahisi Derg*. (2019) 27:212–8. doi: 10.5606/tgkdc.dergisi.2019.16474

5. Wouters EFM, Posthuma R, Koopman M, Liu WY, Sillen MJ, Hajian B, et al. An update on pulmonary rehabilitation techniques for patients with chronic obstructive pulmonary disease. *Expert Rev Respir Med*. (2020) 14:149–61. doi: 10.1080/17476348.2020.1700796

6. Benzo R, Wigle D, Novotny P, Wetzstein M, Nichols F, Shen RK, et al. Preoperative pulmonary rehabilitation before lung cancer resection: results from two randomized studies. *Lung Cancer*. (2011) 74:441–5. doi: 10.1016/j.lungcan.2011.05.011

7. Spruit MA, Singh SJ, Garvey C, ZuWallack R, Nici L, Rochester C, et al. An official American Thoracic Society/European Respiratory Society statement: key concepts and advances in pulmonary rehabilitation. *Am J Respir Crit Care Med*. (2013) 188:E13–64. doi: 10.1164/rccm.201309-1634ST

8. Vagvolgyi A, Rozgonyi Z, Kerti M, Agathou G, Vadasz P, Varga J. Effectiveness of pulmonary rehabilitation and correlations in between functional parameters, extent of thoracic surgery and severity of post-operative complications: randomized clinical trial. *J Thorac Dis*. (2018) 10:3519. doi: 10.21037/jtd.2018.05.202

9. Del Bianco N, Borsati A, Toniolo L, Ciurnielli C, Belluomini L, Insolda J, et al. What is the role of physical exercise in the era of cancer prehabilitation? A systematic review. Critical reviews in oncology. *Hematology*. (2024) 198:104350. doi: 10.1016/j.critrevonc.2024.104350

10. Wang L, Yu M, Ma Y, Tian R, Wang X. Effect of pulmonary rehabilitation on postoperative clinical status in patients with lung Cancer and chronic obstructive pulmonary disease: a systematic review and meta-analysis. *Evid Based Complement Alternat Med*. (2022) 2022:1–9. doi: 10.1155/2022/4133237

11. Mao X, Ni Y, Niu Y, Jiang L. The clinical value of pulmonary rehabilitation in reducing postoperative complications and mortality of lung Cancer resection: a systematic review and meta-analysis. *Front Surg*. (2021) 8:685485. doi: 10.3389/fsurg.2021.685485

12. Choi J, Yang Z, Lee J, Lee JH, Kim HK, Yong HS, et al. Usefulness of pulmonary rehabilitation in non-small cell lung Cancer patients based on pulmonary function tests and muscle analysis using computed tomography images. *Cancer Res Treat*. (2022) 54:793–802. doi: 10.4143/crt.2021.769

13. Zheng Y, Mao M, Li F, Wang L, Zhang X, Zhang X, et al. Effects of enhanced recovery after surgery plus pulmonary rehabilitation on complications after video-assisted lung cancer surgery: a multicentre randomised controlled trial. *Thorax*. (2023) 78:574–86. doi: 10.1136/thoraxjnl-2021-218183

14. Dowman L, Hill CJ, Holland AE. Pulmonary rehabilitation for interstitial lung disease. *Cochrane Database Syst Rev*. (2014) 10:CD006322. doi: 10.1002/14651858.CD006322.pub3

15. Al Moamary MS, Aloriny H, Al-Hajjaj MS. Pulmonary rehabilitation: a regional perspective evidenced-based review. *Ann Thorac Med*. (2014) 9:3–7. doi: 10.4103/1817-1737.124408

16. Bamonti PM, Boyle JT, Goodwin CL, Wan ES, Silberbogen AK, Finer EB, et al. Predictors of outpatient pulmonary rehabilitation uptake, adherence, completion, and treatment response among male US veterans with chronic obstructive pulmonary disease. *Arch Phys Med Rehabil*. (2022) 103:1113. doi: 10.1016/j.apmr.2021.10.021

17. Huang CY, Hsieh MS, Hsieh PC, Wu YK, Yang MC, Huang SY, et al. Pulmonary rehabilitation improves exercise capacity, health-related quality of life, and cardiopulmonary function in patients with non-small cell lung cancer. *BMC Cancer*. (2024) 24:211. doi: 10.1186/s12885-024-11977-5

18. Farsani MK, Sourani M. The effect of a 10-week aerobic exercise on cardiac function among overweight female breast cancer survivors; a randomized clinical trial. *Immunopathol Persa*. (2023) 9:15220. doi: 10.34172/ipp.2023.15220

19. Bellmann B, Lin T, Greissinger K, Rottner L, Rillig A, Zimmerling S. The beneficial effects of cardiac rehabilitation. *Cardiol Ther*. (2020) 9:35–44. doi: 10.1007/s40119-020-00164-9

20. Troosters T, Gayan-Ramirez G, Pitta F, Gosselin N, Gosselink R, Decramer M. Exercise training for COPD: physiological basis and results. *Rev Mal Respir*. (2004) 21:319–27. doi: 10.1016/S0761-8425(04)71289-9

21. Takei R, Matsuda T, Fukihara J, Sasano H, Yamano Y, Yokoyama T, et al. Changes in patient-reported outcomes in patients with non-idiopathic pulmonary fibrosis fibrotic interstitial lung disease and progressive pulmonary fibrosis. *Front Med*. (2023) 10:10. doi: 10.3389/fmed.2023.1067149

22. Morishita S, Hamaue Y, Fukushima T, Tanaka T, Fu JB, Nakano J. Effect of exercise on mortality and recurrence in patients with Cancer: A systematic review and meta-analysis. *Integr Cancer Ther*. (2020) 19:153473542091746. doi: 10.1177/1534735420917462

23. Chiu K-L, Hsieh P-C, Wu C-W, Tzeng IS, Wu Y-K, Lan C-C. Exercise training increases respiratory muscle strength and exercise capacity in patients with chronic obstructive pulmonary disease and respiratory muscle weakness. *Heart Lung*. (2020) 49:556–63. doi: 10.1016/j.hrtlng.2020.03.005

24. Illini O, Valipour A, Gattinger D, Petrovic M, Fabikan H, Hochmair MJ, et al. Effectiveness of outpatient pulmonary rehabilitation in patients with surgically resected lung Cancer: A retrospective real-world analysis. *Cancers*. (2022) 14:3479. doi: 10.3390/cancers14143479

25. Hagiyama A, Sugimoto S, Tanaka S, Matsubara K, Miyoshi K, Katayama Y, et al. Impact of changes in skeletal muscle mass and quality during the waiting time on outcomes of lung transplantation. *Clin Transpl*. (2024) 38:e15169. doi: 10.1111/ctr.15169

26. Zou RH, Nouraie SM, Karoleski C, Zhang Y, Sciurba FC, Forman DE, et al. Incident low muscle mass is associated with greater lung disease and lower circulating leptin in a tobacco-exposed longitudinal cohort. *Respir Res*. (2023) 24:224. doi: 10.1186/s12931-023-02521-3

27. Montes-Ibarra M, Orsso CE, Limon-Miro AT, Gonzalez MC, Marzetti E, Landi F, et al. Prevalence and clinical implications of abnormal body composition phenotypes in patients with COVID-19: a systematic review. *Am J Clin Nutr*. (2023) 117:1288–305. doi: 10.1016/j.ajcnut.2023.04.003

Glossary

PR	Pulmonary Rehabilitation
HRQL	Health-Related Quality of Life
NSCLC	Non-Small Cell Lung Cancer
PSM	Propensity Score Matching
CTRL	Control
FEV1	Forced Expiratory Volume in 1 Second
FVC	Forced Vital Capacity
CI	Cardiac Index
WR	Work Rate
VO2	Oxygen Uptake
ΔHU_{ESMCSA}	Change in Hounsfield Unit Erector Spinae Muscle Cross-Sectional Area
COPD	Chronic Obstructive Pulmonary Disease
ILD	Interstitial Lung Disease
ATS	American Thoracic Society
CAT	Chronic Obstructive Pulmonary Disease Assessment Test
CPET	Cardiopulmonary Exercise Testing
VCO2	Carbon Dioxide Output
VT	Tidal Volume
RF	Respiratory Frequency
BP	Blood Pressure
AT	Anaerobic Threshold
WE	Work Efficiency
O2P	Oxygen Pulse
VEQ	Ventilatory Equivalent
MIP	Maximum Inspiratory Pressure
MEP	Maximum Expiratory Pressure
SVI	Stroke Volume Index
ROI	Region of Interest
HU	Hounsfield Unit
DLco	Diffusing Capacity of the Lungs for Carbon Monoxide
VA	Alveolar Volume
IPF	Idiopathic Pulmonary Fibrosis
BMI	Body Mass Index
SD	Standard Deviation
SpO2	Arterial Oxygen Saturation
SMD	Standardized Mean Difference
Preop	Preoperative
ERAS	Enhanced Recovery After Surgery

frontiers | Frontiers in Oncology

TYPE Original Research
PUBLISHED 19 September 2024
DOI 10.3389/fonc.2024.1403344

OPEN ACCESS

EDITED BY
Vincenzo Pio Di Noia,
IRCCS Istituto Nazionale Tumori Regina Elena, Italy

REVIEWED BY
Abhishek Tyagi,
Wake Forest University, United States
Yingcheng Charles Wu,
Fudan University, China

*CORRESPONDENCE
Tianlu Wang
wangtianlu126@126.com
Yingqiu Song
syq18900917411@163.com

†These authors have contributed equally to this work

RECEIVED 15 April 2024
ACCEPTED 26 August 2024
PUBLISHED 19 September 2024

CITATION
Zhang X, Zeng W, Yan X, Wang Z, Xu K, Li M, Wang T and Song Y (2024) Association between smoking status and the prognosis of brain metastasis in patients with non-small cell lung cancer.
Front. Oncol. 14:1403344.
doi: 10.3389/fonc.2024.1403344

Association between smoking status and the prognosis of brain metastasis in patients with non-small cell lung cancer

Xiaofang Zhang[1†], Weilin Zeng[1†], Xingyu Yan[2], Zheng Wang[3], Ke Xu[4], Mo Li[4], Tianlu Wang[1*] and Yingqiu Song[1*]

[1]Department of Radiotherapy, Cancer Hospital of China Medical University, Liaoning Cancer Hospital & Institute, Cancer Hospital of Dalian University of Technology, Shenyang, Liaoning, China, [2]The First Clinical College of China Medical University, Shenyang, Liaoning, China, [3]Department of Cerebral Surgery, Cancer Hospital of China Medical University, Liaoning Cancer Hospital & Institute, Cancer Hospital of Dalian University of Technology, Shenyang, Liaoning, China, [4]Department of Thoracic Surgery, Cancer Hospital of China Medical University, Liaoning Cancer Hospital & Institute, Cancer Hospital of Dalian University of Technology, Shenyang, Liaoning, China

Objective: This study aimed to explore the relationship between smoking status and the interval to brain metastasis in patients with non-small cell lung cancer (NSCLC) and its impact on survival time after brain metastasis.

Methods: Data were collected from patients with NSCLC with brain metastases who were treated at our centre between January 2005 and December 2017. Clinical indices such as clinicopathological features and smoking status were recorded, and patients were followed up until 1 September 2022. Based on our inclusion and exclusion criteria, 461 patients were analysed and matched using 1:1 propensity score matching. Three balanced groups were formed: non-smoking (n = 113), smoking cessation (n = 113), and smoking (n = 113). The interval to brain metastasis and overall survival were compared between the groups.

Results: There was a statistically significant difference in the interval to brain metastasis between the non-smoking and smoking cessation groups (p = 0.001), as well as between the non-smoking and smoking groups (p < 0.001). However, the difference between the smoking cessation and smoking groups was not statistically significant (p = 0.106). Multivariate and univariate analyses identified smoking status, clinical stage, lung cancer surgery, chemotherapy, and chest radiotherapy as independent predictors of the interval to brain metastasis. Additionally, the multivariate analysis showed that smoking status, driver gene mutations, and chest radiotherapy independently influenced survival after brain metastasis.

Conclusion: Smoking status in patients with NSCLC affects the interval to brain metastasis and survival after brain metastasis.

KEYWORDS

smoking status, non-small cell lung cancer, brain metastasis, interval time, survival time

Abbreviations: NSCLC, non-small cell lung cancer; BMs, brain metastases; iPFS, intracranial progression-free survival; OS, overall survival; KPS, Karnofsky performance status; PSM, propensity score matching.

1 Introduction

Lung cancer is the most common malignancy and a leading cause of cancer-related death worldwide (1), with non-small cell lung cancer (NSCLC) and small cell lung cancer accounting for approximately 85% and 15% of cases, respectively. Approximately 57% of patients with NSCLC have distant metastases at diagnosis, and approximately 20% have brain metastases (BMs) (2, 3). BMs from lung cancer constitute over 50% of all BMs (4). Due to the blood–brain barrier and specific physiological features, treatment strategies for patients with NSCLC-induced BMs are limited, resulting in poor prognosis (5) and a median survival of 4–7 months for untreated patients (6). However, with advances in tumour treatment and diagnostic techniques, patients with NSCLC-induced BMs have shown a median survival of approximately 16 months after treatment (7). This improvement also correlates with increased intracranial progression-free survival and overall survival (OS) (8).

The incidence of BMs is significantly higher in smokers than in non-smokers among patients with NSCLC, indicating a potentially shorter survival (9, 10). A systematic evaluation and meta-analysis of over 10,000 patients with lung cancer across 21 articles published between 1980 and 2021 quantified the impact of smoking cessation at or around the time of diagnosis or during treatment on survival. The results showed that quitting smoking significantly improved the OS in patients with lung cancer, with a particularly greater benefit observed in those with NSCLC (11). Parsons et al. (12) investigated the prognostic impact of smoking cessation on lung cancer by constructing life tables of patients who had quit smoking for several decades. Data obtained from multiple databases indicated that quitting smoking after an early lung cancer diagnosis improved prognosis. The 5-year survival rate for 65-year-old patients with early-stage NSCLC who continued to smoke was 33%, compared to 70% for those who quit (12).

Several studies have confirmed the negative impact of smoking on survival in patients with lung cancer; however, several questions have been raised. Does smoking cessation provide a survival benefit for patients with NSCLC by preventing BM development? How do the interval to BMs and survival after BMs differ among non-smokers, those who quit smoking after diagnosis, and those who continue to smoke after diagnosis? Convincing evidence is urgently needed to answer these questions.

This study aimed to assess the impact of different smoking statuses —never smokers, those who quit smoking after diagnosis, and those who continued to smoke after diagnosis—on the occurrence of BMs and survival after BMs. We retrospectively analysed the timing and prognosis of BMs in patients with NSCLC by identifying the study population, collecting clinical data from a large sample, conducting follow-up observations, obtaining patient survival information, and employing various statistical methods to draw conclusions.

2 Materials and methods

2.1 Data extraction

This retrospective study included clinical data from patients with NSCLC-induced BMs treated at the Cancer Hospital of China Medical University between January 2005 and December 2017. Patient data at the time of NSCLC diagnosis were collected from the hospital information system, including age, sex, Karnofsky performance status score, smoking status, pathological type, lymph node metastasis, lung cancer site, clinical stage (according to the eighth edition of the TNM staging system published by the International Association for the Study of Lung Cancer), treatment regimen, and treatment-related adverse effects.

2.2 Study population

Inclusion criteria were as follows: age ≥ 18 years; a clear pathological NSCLC diagnosis; data regarding the time to diagnosis (via bronchoscopy, lung puncture biopsy, biopsy of metastases, or surgical biopsy); a pathological diagnosis of squamous lung cancer or adenocarcinoma; imaging results (e.g. head-enhanced magnetic resonance imaging and/or pathology) confirming NSCLC BMs; and complete baseline information. Exclusion criteria were as follows: no pathological diagnosis or an unclear pathological type; presence of other primary tumours; incomplete case information; incomplete treatment plan or treatment; unspecified smoking status; and loss to follow-up. Overall, 461 patients were evaluated in the study. All cases were collected before December 2017, and no patients were receiving immunotherapy.

2.3 Follow-up visits

The interval to BMs in NSCLC was defined as the period from the date of NSCLC diagnosis to the date of BM diagnosis. The OS for patients with BMs in NSCLC was defined as the period from the date of BM diagnosis to the date of death or the last effective follow-up (the last follow-up cut-off date was 1 September 2022).

2.4 Smoking status

Patients were divided into three groups according to their smoking status: non-smoking, smoking cessation, and smoking. According to a study published in the *Journal of Thoracic Oncology* in 2022, 'quitters' were defined as individuals who had quit smoking upon or within 3 months after NSCLC diagnosis (11). According to the definition of smoking status by the World Health Organization, the smoking group included individuals who had smoked over 100 cigarettes (including hand-rolled cigarettes, cigars, and cigarillos) in their lifetime and had smoked within 28 d of the evaluation. The smoking cessation group included individuals who had smoked over 100 cigarettes in their lifetime but had not smoked within 28 d of the evaluation. The non-smoking group included individuals who had not smoked more than 100 cigarettes in their lifetime and were currently non-smokers.

2.5 Statistical analysis

IBM SPSS (Version 26.0; IBM Corp., Armonk, NY, USA) and R (Version 3.6.3) were used for statistical analyses and visualisation.

Two-way comparisons between groups were conducted using 1:1 propensity score matching (PSM) with SPSS software to reduce the effects of bias and confounding variables. The matching variables included sex, T-stage, concurrently diagnosed BMs, and a matching tolerance of 0.1. Optimal performance was achieved by non-relaxation sampling with a randomised case order and a random seed number of six.

Cardinality tests were conducted using the base R package to analyse baseline characteristics before and after PSM. Prognostic correlations were assessed using the Cox proportional hazards regression model with the survival package for R (Version 3.2–10). Survival curves were plotted using the Survminer package for R (Version 0.4.9), and survival data analysis was conducted using the survival package (Version 3.2–10).

3 Results

3.1 Baseline patient characteristics

This study included 566 patients with NSCLC-induced BMs who were first diagnosed at the Cancer Hospital of China Medical University between March 2005 and December 2017. In total, 105 patients were excluded for the following reasons: 19 patients had an unclear pathological diagnosis, 11 had pathological types other than lung adenocarcinoma or squamous lung cancer, 23 were lost to follow-up, 27 had incomplete clinical data, and 25 had unknown smoking status. Ultimately, 461 cases were included in the study. Of these, 164 were non-smokers, 150 were quitters and 147 were current smokers. Using 1:1 PSM, 113 cases each of non-smokers, quitters, and smokers were matched to achieve balance between the groups. The case enrolment process is shown in Figure 1.

Table 1 shows the baseline information of the cases enrolled after PSM. A comparison of each factor among the non-smoking, smoking cessation, and smoking groups revealed no statistical differences between the three groups. To ensure that confounding factors were balanced between each pair of groups, Supplementary Tables S2, S3, and S4 present the baseline results of the two-way comparisons between groups after PSM, with no statistical differences in any of the factors between the groups. Univariate and multivariate analysis results of the entire population, baseline results of before/after PSM are shown in Supplementary Table S1-S8.

3.2 Analysis of factors influencing the time to the development of brain metastases in NSCLC

Figure 2 shows the impact of smoking status on the time to development of BMs in NSCLC. The log-rank test revealed a statistical difference between the non-smoking, smoking cessation, and smoking groups ($\chi^2 = 23.46$, $p < 0.001$). Comparisons between groups showed that the interval to BMs in NSCLC was longer in the non-smoking group than in the smoking cessation group ($\chi^2 = 12.05$, HR = 1.56 (1.19–2.05), $p = 0.001$). The interval was also longer in the smoking cessation group than in the smoking group ($\chi^2 = 20.91$, HR = 1.78 (1.35–2.34), $p < 0.001$). However, there was no significant difference in the interval to BMs between the non-smoking and smoking groups ($\chi^2 = 2.62$, HR = 1.23 (0.94–1.60), $p = 0.106$).

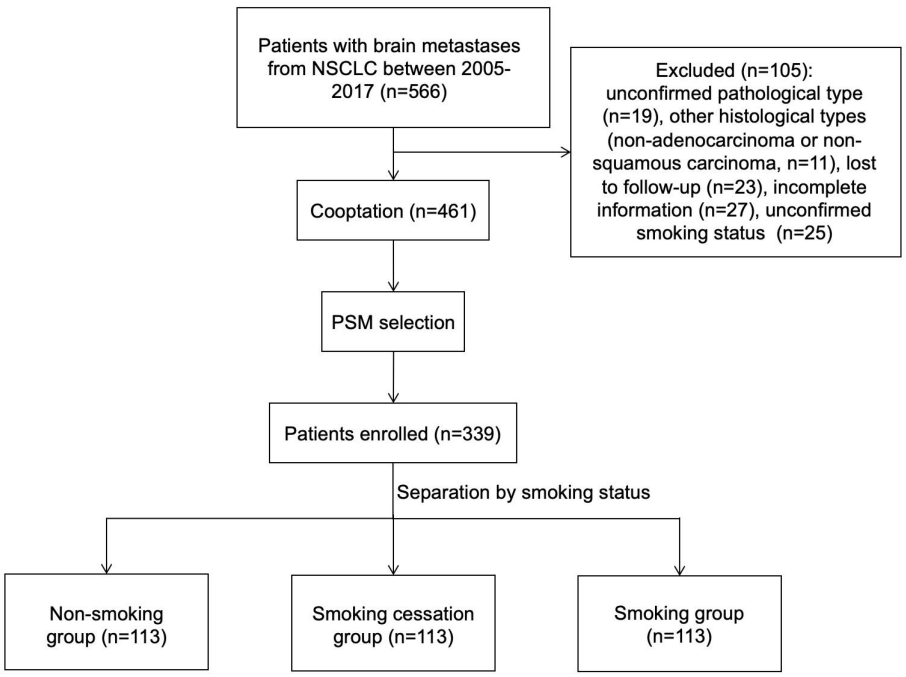

FIGURE 1
Flow chart for group entry. NSCLC: non-small cell lung cancer.

10.3389/fonc.2024.1403344

TABLE 1 Baseline characteristics of patients with BM at the diagnosis of NSCLC after PSM.

Characteristics	Total (n = 461)	Non-smoking (n = 164)	Smoking cessation (n = 150)	Smoking (n = 147)	χ^2	*p*-value
Age					0.69	0.710
< 60 years	202	68 (20.1)	70 (20.6)	64 (18.9)		
≥ 60 years	137	45 (13.3)	43 (12.7)	49 (14.5)		
Sex					1.80	0.407
Female	176	64 (18.9)	58 (17.1)	54 (15.9)		
Male	163	49 (14.5)	55 (16.2)	59 (17.4)		
KPS score					0.70	0.706
≥ 90	131	43 (12.7)	47 (13.9)	41 (12.1)		
< 90	208	70 (20.6)	66 (19.5)	72 (21.2)		
Pathological pattern					4.68	0.096
Squamous carcinoma	52	13 (3.8)	24 (7.1)	15 (4.4)		
Adenocarcinoma	287	100 (29.5)	89 (26.3)	98 (28.9)		
Lymph node metastasis					2.37	0.305
No	84	33 (9.7)	28 (8.3)	23 (6.8)		
Yes	255	80 (23.6)	85 (25.1)	90 (26.5)		
Position					0.36	0.834
Peripheral	249	85 (25.1)	81 (23.9)	83 (24.5)		
Central	90	28 (8.3)	32 (9.4)	30 (8.8)		
T classification					0.17	0.916
T1-2	209	71 (20.9)	68 (20.1)	70 (20.6)		
T3-4	130	42 (12.4)	45 (13.3)	43 (12.7)		
N classification					0.47	0.791
N0-1	134	45 (13.3)	42 (12.4)	47 (13.9)		
N2-3	205	68 (20.1)	71 (20.9)	66 (19.5)		
Clinical Stage					0	1.000
I/II/III	129	43 (12.7)	43 (12.7)	43 (12.7)		
IV	210	70 (20.6)	70 (20.6)	70 (20.6)		
Concurrent diagnosis of brain metastases					2.84	0.242
No	244	86 (25.4)	83 (24.5)	75 (22.1)		
Yes	95	27 (8.0)	30 (8.8)	38 (11.2)		
Oncogenic driver mutations					5.15	0.525
Negative	265	86 (25.4)	85 (25.1)	94 (27.7)		
Positive						
EGFR	65	25 (7.4)	23 (6.8)	17 (5.0)		
ALK	8	2 (0.6)	4 (1.2)	2 (0.6)		
KRAS	1	0 (0.0)	1 (0.3)	0 (0.0)		

(Continued)

TABLE 1 Continued

Characteristics	Total (n = 461)	Non-smoking (n = 164)	Smoking cessation (n = 150)	Smoking (n = 147)	χ^2	*p*-value
Surgery					0	1.000
No	261	87 (25.7)	87 (25.7)	87 (25.7)		
Yes	78	26 (7.7)	26 (7.7)	26 (7.7)		
Chemotherapy					2.87	0.238
No	236	72 (21.2)	81 (23.9)	83 (24.5)		
Yes	103	41 (12.1)	32 (9.4)	30 (8.8)		
Thoracic Radiotherapy					0.72	0.698
No	75	23 (6.8)	24 (7.1)	28 (8.3)		
Yes	264	90 (26.5)	89 (26.3)	85 (25.1)		

3.3 Analysis of factors influencing survival after brain metastases from NSCLC

Figure 3 illustrates the effect of smoking status on survival time following the development of BMs. The log-rank test indicated a significant difference in survival between the non-smoking, smoking cessation, and smoking groups (χ^2 = 45.78, p < 0.001). Comparative analysis using the log-rank test showed that the non-smoking group had a longer survival time after NSCLC BMs than the smoking cessation group, with more non-smokers surviving beyond 60 months. In contrast, survival in the smoking cessation group was more concentrated within 30 months (χ^2 = 9.18, HR = 1.49 (1.13–1.95), p = 0.002). The smoking cessation group had longer survival than the smoking group (χ^2 = 35.89, HR = 2.17 (1.63–2.89), p < 0.001). Additionally, the non-smoking group had longer survival than the smoking group (χ^2 = 16.15, HR = 1.70 (1.29–2.23), p < 0.001.

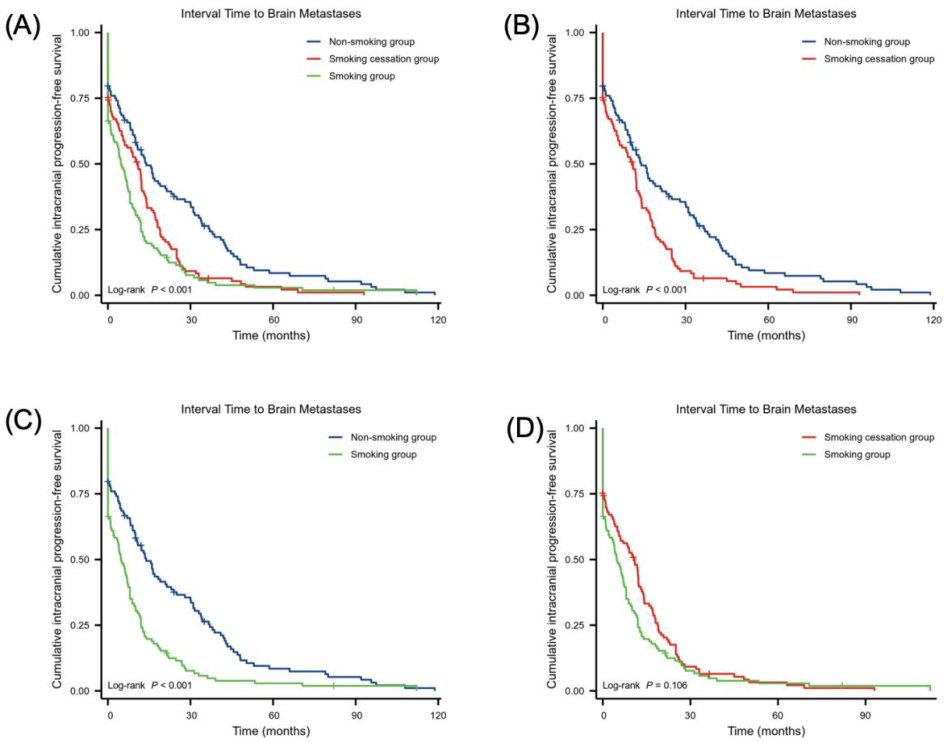

FIGURE 2
Relationship between smoking status and the interval to BMs in NSCLC. **(A–D)** smoking group (n = 113), non-smoking group (n = 113) and smoking cessation group (n = 113). Statistical analysis was conducted using the log-rank test.

4 Discussion

To assess the impact of smoking cessation on survival in patients with lung cancer, researchers analysed a cohort of patients with cancer who smoked. Using the Cancer Genome Atlas database, they found that smoking cessation was a protective factor for OS in patients with squamous lung cancer, indicating that patients who quit smoking might have longer survival (13). Additionally, Heberg (14) analysed data from 7841 individuals who smoked at the time of lung cancer diagnosis and found a significantly lower mortality risk in those who quit smoking compared to those who continued smoking.

Comparisons of the physical status at 6 and 12 months after lung cancer diagnosis among patients with NSCLC who did and did not quit smoking showed that patients who quit smoking maintained a better physical status (15). One investigator prospectively studied patients with NSCLC recruited between 2007 and 2016 and followed them annually until 2020. The median OS of patients who quit smoking was 21.6 months higher compared to patients who continued smoking. Patients who quit smoking had higher 5-year OS and progression-free survival rates than those who continued to smoke, with smoking cessation linked to a reduced risk of all-cause mortality, cancer-specific mortality, and disease progression (16). Reviews of the relationship between smoking cessation and OS and relapse-free survival among 543 patients with early-stage NSCLC revealed that the hazard ratio decreased with increasing duration of smoking cessation compared to current smokers. Thus, smoking cessation was associated with improved survival in patients with early-stage NSCLC, with longer cessation durations correlating with better survival outcomes (17).

Regarding the effect of smoking on lung cancer–induced BMs, we identified seven relevant articles through a literature search. A retrospective analysis of patient data from these articles revealed that BM incidence was significantly higher in smokers compared to non-smokers, and the progression-free survival and OS of patients with BMs were shorter in smokers (Supplementary Table S9). These findings are consistent with our study results.

Studies have shown that smoking is associated with the rapid progression of BMs in patients with lung cancer. This occurs through inflammatory signalling pathways, squamous epithelial chemotaxis–related genes, and glycolysis, leading to oxidative stress and other responses (18). Research indicates that metabolism plays an important role in tumour immunity and that the metabolic phenotype of primary tumour cells differs from that of metastatic tumour cells, making metabolic therapies targeting primary tumours potentially less effective against metastasis (19). Additionally, high metabolic activation was found in MRC1 + CCL18 + M2 macrophages at metastatic sites, and effective neoadjuvant chemotherapy can slow this metabolic activation (20). It has also been reported that neutrophils have complex functions and may play opposite roles in different cancer types, with the neutrophils driving the metastatic niche playing an important role (21). Notably, some

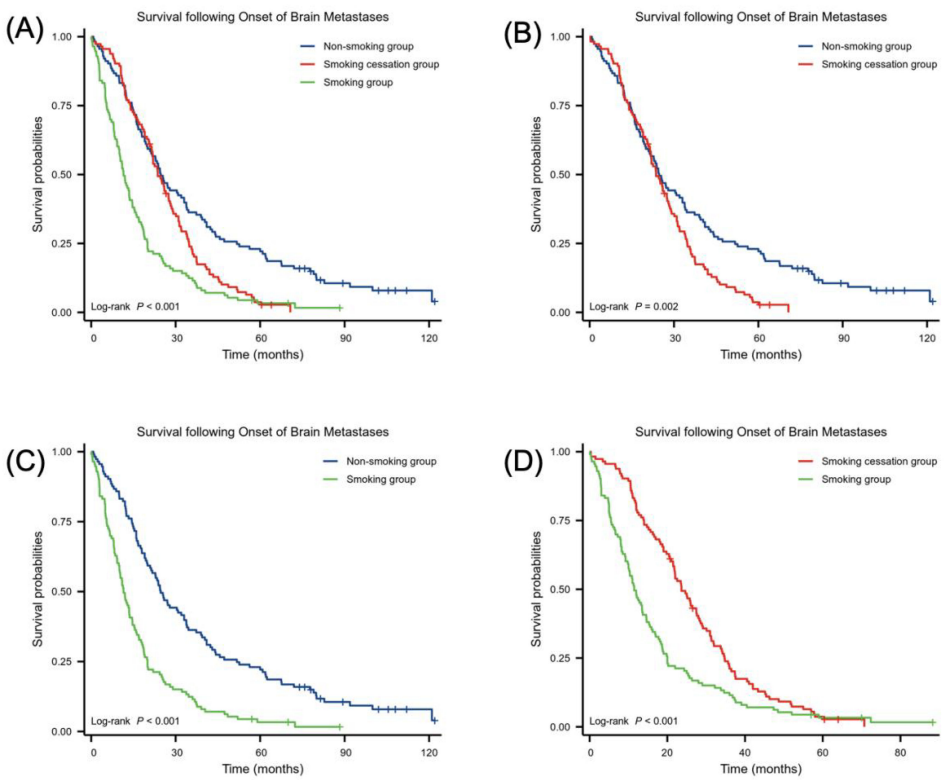

FIGURE 3
Relationship between smoking status and survival following BM onset. Number of samples in **(A–D)** smoking group (n = 113), non-smoking group (n = 113) and smoking cessation group (n = 113). Statistical analysis was conducted using the log-rank test.

studies have demonstrated the ability of nicotine to alter immune cell status, playing a crucial role in the mechanism of BM from lung cancer. Currently, the effects of nicotine on microglia and neutrophils in the brain are the most extensively studied. Specifically, long-term chronic exposure to nicotine in the brain's pre-metastatic niche causes significant aggregation of N2-neutrophils through the STAT3 pathway. These aggregated N2-neutrophils secrete miR-4466, which promotes the BM of metastatic lung cancer cells through the SKI/SOX2/CPT1A axis (22). Prolonged nicotine exposure also leads to a substantial increase in microglia in the brain, shifting them toward the M2 phenotype. Additionally, M2-microglia enhance IGF-1 and CCL20 secretion and increase SIRPα expression. IGF-1 and CCL20 promote tumour progression, while SIRPα interacts with CD47 expressed on tumour cells to inhibit microglial phagocytosis. This process suppresses the innate immune function of microglia and promotes lung cancer BM. Notably, nicotine enhances this effect (23).

As is shown in Figure 4, nicotine promotes tumour growth by activating nicotinic acetylcholine (nACh) receptors in tumour cells. These receptors are expressed in microglia, with the α4β2 receptor being the most abundant nACh receptor in the brain and the main mediator of nicotine dependence (24). Nicotine enhances α7-nACh receptor expression and promotes the M2-type polarisation of microglia by disrupting EGFR signalling and STAT3 pathways, thus promoting cancer cell progression and metastasis. This suggests that nicotine can reprogram the brain tumour microenvironment to promote tumour progression by activating its receptors (25).

Additionally, nicotine in tobacco causes a sharp increase in intracellular reactive oxygen species, which remain at moderate levels during sustained exposure. This abnormal elevation of reactive oxygen species induces the endoplasmic reticulum stress response and activates the unfolded protein response by upregulating binding immunoglobulin protein expression and increasing the phosphorylation level of PERK. Furthermore, prolonged nicotine exposure affects the activation of the p53 protein by sodium arsenite. When p53 is inhibited or damaged, sustained nicotine exposure causes lung epithelial cells to form colonies on soft agar, exhibiting oncogenic properties (26). Researchers from the United States have resolved the cellular heterogeneity of human respiratory epithelial tissue at the single-cell level and comparatively analysed the effects of smoking on individual cell compositions and their intrinsic functions. Their evaluation of the respiratory epithelium found that inflammatory signalling pathways, squamous epithelial chemotaxis–related genes, and glycolysis were significantly upregulated in smokers, while innate immunity and antigen delivery were downregulated. Specifically, pathways significantly upregulated in the mature ciliated cells of smokers included apoptosis regulation, the NOTCH pathway, and the oxidative stress response. Conversely, the expression of genes related to the electron transport chain and lysosomes decreased in mixed-ciliated cells (27).

As is shown in Figure 5, Zhou et al. (28) demonstrated that tobacco smoke induces PD-L1 expression in lung epithelial cells through the aromatic hydrocarbon receptor (AhR), enabling the cells to evade T-cell killing and promote tumourigenesis. They also showed that AhR could predict a patient's response to immunotherapy and be an attractive therapeutic target. Kheradmand et al. (29) found that long-term inhalation of nanoscale carbon black ultrafine particles (15–75 nm) led to mitochondrial damage and metabolic reprogramming of lung macrophages. This reprogramming increases lactate secretion and

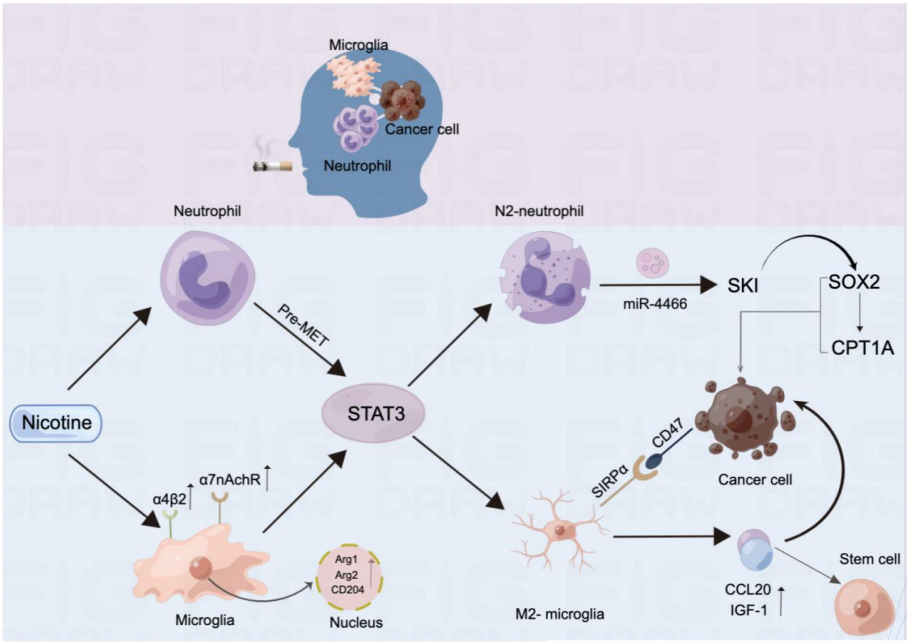

FIGURE 4
Mechanism by which nicotine promotes BM in lung cancer and alters immune cell infiltration in the brain.

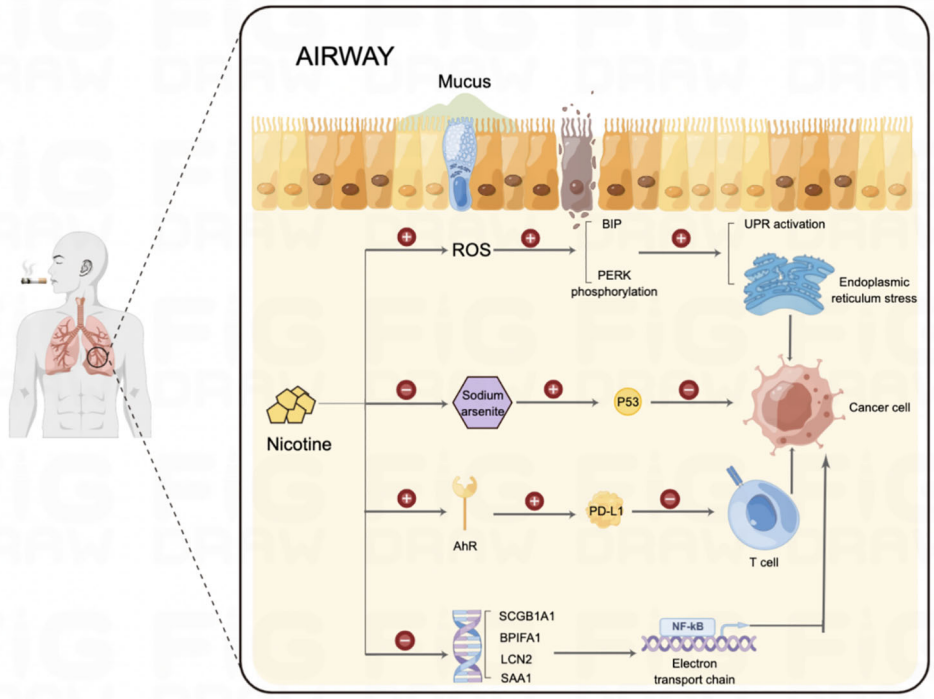

FIGURE 5
Effects of nicotine on the pulmonary microenvironment.

forms an immunosuppressive microenvironment, ultimately contributing to lung cancer development and metastasis. Huang et al. (30) collected proximal bronchial basal cells from 14 non-smokers and 19 smokers, conducting genome-wide somatic mutation profiling using single-cell multiple displacement amplification. The results showed that the number of mutations in lung cells increased linearly with the years of smoking. However, the increase in cell mutations ceased after 23 years of exposure to smoking factors. This cessation may be related to the body's enhanced ability to repair DNA damage or detoxify cigarette smoke after long-term exposure.

This study provides clinical evidence that the interval length and prognosis of BMs in patients with NSCLC are significantly associated with smoking status. To eliminate the effects of confounding factors, we equalised baseline differences using PSM. Non-smokers and patients with NSCLC who managed to quit and remain abstinent after diagnosis benefited from clinical care, supporting early smoking cessation as an essential part of lung cancer management and indicating the need for adequate support.

5 Conclusion

Smoking status is an independent factor influencing the interval between the onset of BM and prognosis after BM in patients with NSCLC. The median interval lengths for the occurrence of BMs in the non-smoking, smoking cessation, and smoking groups were 12, 10, and 6 months, respectively, with significant differences in the statistical analysis. Independent factors affecting the interval length of BM occurrence in NSCLC included smoking status, clinical stage, lung cancer surgery, chemotherapy, and chest radiotherapy.

The median survival times after BM in the non-smoking, smoking cessation, and smoking groups were 25, 24, and 11 months, respectively, with significant differences in the statistical analysis.

Data availability statement

The original contributions presented in the study are included in the article/Supplementary Material. Further inquiries can be directed to the corresponding authors.

Ethics statement

The studies involving humans were approved by Medical Ethics Committee of Liaoning Cancer Hospital and the number is 2020X0102. The studies were conducted in accordance with the local legislation and institutional requirements. The participants provided their written informed consent to participate in this study.

Author contributions

XZ: Formal analysis, Writing – original draft, Writing – review & editing. WZ: Formal analysis, Writing – original draft, Writing – review & editing. XY: Software, Writing – review & editing. ZW:

Validation, Writing – review & editing. KX: Validation, Writing – review & editing. ML: Visualization, Writing – review & editing. TW: Data curation, Funding acquisition, Project administration, Resources, Writing – review & editing. YS: Funding acquisition, Project administration, Writing – review & editing.

Funding

The author(s) declare financial support was received for the research, authorship, and/or publication of this article. This work is supported by the Fundamental Research Funds for the Central Universities (LD2023032, LD2023011, LD202221), Ministry of Science and Technology of the Peoples Republic of China [G2023127016L].

Acknowledgments

We would like to thank all patients and their families for their active cooperation and all hospital staff for their assistance in the study.

Conflict of interest

The authors declare that the research was conducted in the absence of any commercial or financial relationships that could be construed as a potential conflict of interest.

Publisher's note

Supplementary material

The Supplementary Material for this article can be found online at: https://www.frontiersin.org/articles/10.3389/fonc.2024.1403344/full#supplementary-material

References

1. Bray F, Ferlay J, Soerjomataram I, Siegel RL, Torre LA, Jemal A. Global cancer statistics 2018: GLOBOCAN estimates of incidence and mortality worldwide for 36 cancers in 185 countries. *CA: A Cancer J Clin*. (2018) 68:394–424. doi: 10.3322/caac.21492

2. Siegel RL, Miller KD, Jemal A. Cancer statistics, 2019. *CA: A Cancer J Clin*. (2019) 69:7–34. doi: 10.3322/caac.21551

3. Sinha R, Sage W, Watts C. The evolving clinical management of cerebral metastases. *Eur J Surg Oncol (EJSO)*. (2017) 43:1173–85. doi: 10.1016/j.ejso.2016.10.006

4. Halperin EC, Brady LW, Wazer DE, Perez CA. *Perez & Brady's principles and practice of radiation oncology*. Philadelphia: Lippincott Williams & Wilkins (2013).

5. Sperduto PW, Kased N, Roberge D, Xu Z, Shanley R, Luo X, et al. Summary report on the graded prognostic assessment: an accurate and facile diagnosis-specific tool to estimate survival for patients with brain metastases. *J Clin Oncol*. (2012) 30:419. doi: 10.1200/JCO.2011.38.0527

6. Ali A, Goffin JR, Arnold A, Ellis PM. Survival of patients with non-small-cell lung cancer after a diagnosis of brain metastases. *Curr Oncol*. (2013) 20:300–6. doi: 10.3747/co.20.1481

7. Lin X, DeAngelis LM. Treatment of brain metastases. *J Clin Oncol*. (2015) 33:3475. doi: 10.1200/JCO.2015.60.9503

8. Smith DR, Bian Y, Wu CC, Saraf A, Tai CH, Nanda T, et al. Natural history, clinical course and predictors of interval time from initial diagnosis to development of subsequent NSCLC brain metastases. *J Neuro-Oncol*. (2019) 143:145–55. doi: 10.1007/s11060-019-03149-4

9. Rivera GA, Wakelee H. Lung cancer in never smokers. *Lung Cancer Personalized Med*. (2016) 893:43–57. doi: 10.1007/978-3-319-24223-1_3

10. Sung H, Ferlay J, Siegel RL, Laversanne M, Soerjomataram I, Jemal A, et al. Global cancer statistics 2020: GLOBOCAN estimates of incidence and mortality worldwide for 36 cancers in 185 countries. *CA: A Cancer J Clin*. (2021) 71:209–49. doi: 10.3322/caac.21660

11. Caini S, Del Riccio M, Vettori V, Scotti V, Martinoli C, Raimondi S, et al. Quitting smoking at or around diagnosis improves the overall survival of lung cancer patients: A systematic review and meta-analysis. *J Thorac Oncol*. (2022) 17(5):623–36. doi: 10.1016/j.jtho.2021.12.005

12. Parsons A, Daley A, Begh R, Aveyard P. Influence of smoking cessation after diagnosis of early stage lung cancer on prognosis: systematic review of observational studies with meta-analysis. *BMJ*. (2010) 340:b5569. doi: 10.1136/bmj.b5569

13. Yang S, Liu T, Liang G. The benefits of smoking cessation on survival in cancer patients by integrative analysis of multi-omics data. *Mol Oncol*. (2020) 14:2069–80. doi: 10.1002/1878-0261.12755

14. Heberg J, Simonsen MK, Thomsen T, Zoffmann V, Danielsen AK. Smoking cessation prolongs survival in female cancer survivors-the Danish nurse cohort. *Eur J Oncol Nurs*. (2020) 47:101796. doi: 10.1016/j.ejon.2020.101796

15. Baser S, Shannon VR, Eapen GA, Jimenez CA, Onn A, Lin E, et al. Smoking cessation after diagnosis of lung cancer is associated with a beneficial effect on performance status. *Chest*. (2006) 130:1784–90. doi: 10.1016/S0012-3692(15)50902-1

16. Sheikh M, Mukeriya A, Shangina O, Brennan P, Zaridze D. Postdiagnosis smoking cessation and reduced risk for lung cancer progression and mortality: a prospective cohort study. *Ann Internal Med*. (2021) 174:1232–9. doi: 10.7326/M21-0252

17. Zhou W, Heist RS, Liu G, Park S, Neuberg DS, Asomaning K, et al. Smoking cessation before diagnosis and survival in early stage non-small cell lung cancer patients. *Lung Cancer*. (2006) 53:375–80. doi: 10.1016/j.lungcan.2006.05.017

18. Shenker RF, McTyre ER, Ruiz J, et al. The Effects of smoking status and smoking history on patients with brain metastases from lung cancer. *Cancer Med*. (2017) 6:944–52. doi: 10.1002/cam4.1058

19. Wu Y, Zou Q, Jiang P, Gao Q. Tumor-host cometabolism collaborates to shape cancer immunity. *Cancer Discovery*. (2024) 14:653–7. doi: 10.1158/2159-8290.CD-23-1509

20. Wu Y, Yang S, Ma J, Chen Z, Song G, Rao D, et al. Spatiotemporal immune landscape of colorectal cancer liver metastasis at single-cell level. *Cancer Discovery*. (2022) 12:134–53. doi: 10.1158/2159-8290.CD-21-0316

21. Wu Y, Ma J, Yang X, Nan F, Zhang T, Ji S, et al. Neutrophil profiling illuminates anti-tumor antigen-presenting potency. *Cell*. (2024) 187:1422–1439.e24. doi: 10.1016/j.cell.2024.02.005

22. Tyagi A, Wu SY, Sharma S, Wu K, Zhao D, Deshpande R, et al. Exosomal miR-4466 from nicotine-activated neutrophils promotes tumor cell stemness and metabolism in lung cancer metastasis. *Oncogene*. (2022) 41:3079–92. doi: 10.1038/s41388-022-02322-w

23. Wu SY, Xing F, Sharma S, Wu K, Tyagi A, Liu Y, et al. Nicotine promotes brain metastasis by polarizing microglia and suppressing innate immune function. *J Exp Med*. (2020) 217(8):e20191131. doi: 10.1084/jem.20191131

24. Mazzaferro S, Bermudez I, Sine SM. [amp]]alpha;4β2 nicotinic acetylcholine receptors: relationships between subunit stoichiometry and function at the single channel level. *J Biol Chem*. (2017) 292:2729–40. doi: 10.1074/jbc.M116.764183

25. Wang ML, Hsu YF, Liu CH, Kuo YL, Chen YC, Yeh YC, et al. Low-dose nicotine activates EGFR signaling via α5-nAChR and promotes lung adenocarcinoma progression. *Int J Mol Sci*. (2020) 21:6829. doi: 10.3390/ijms21186829

26. Zhang Q, Ganapathy S, Avraham H, Nishioka T, Chen C. Nicotine exposure potentiates lung tumorigenesis by perturbing cellular surveillance. *Br J Cancer*. (2020) 122:904–11. doi: 10.1038/s41416-020-0730-0

27. Goldfarbmuren KC, Jackson ND, Sajuthi SP, Dyjack N, Li KS, Rios CL, et al. Dissecting the cellular specificity of smoking effects and reconstructing lineages in the human airway epithelium. *Nat Commun*. (2020) 11:1–21. doi: 10.1038/s41467-020-16239-z

28. Wang GZ, Zhang L, Zhao XC, Gao SH, Qu LW, Yu H, et al. The Aryl hydrocarbon receptor mediates tobacco-induced PD-L1 expression and is associated with response to immunotherapy. *Nat Commun*. (2019) 10:1–13. doi: 10.1038/s41467-019-08887-7

29. Chang CY, You R, Armstrong D, Bandi A, Cheng YT, Burkhardt PM, et al. Chronic exposure to carbon black ultrafine particles reprograms macrophage metabolism and accelerates lung cancer. *Sci Adv*. (2022) 8:eabq0615. doi: 10.1126/sciadv.abq0615

30. Huang Z, Sun S, Lee M, Maslov AY, Shi M, Waldman S, et al. Single-cell analysis of somatic mutations in human bronchial epithelial cells in relation to aging and smoking. *Nat Genet*. (2020) 54:492–8. doi: 10.1038/s41588-022-01035-w

frontiers | Frontiers in Medicine

TYPE Original Research
PUBLISHED 08 October 2024
DOI 10.3389/fmed.2024.1484327

OPEN ACCESS

EDITED BY
Vincenzo Pio Di Noia,
IRCCS Istituto Nazionale Tumori Regina Elena, Italy

REVIEWED BY
Erdal Tekin,
Atatürk University, Türkiye
Yunhuan Liu,
Tongji University, China

*CORRESPONDENCE
Haibo Shen
✉ chest001shb@sina.com

RECEIVED 21 August 2024
ACCEPTED 23 September 2024
PUBLISHED 08 October 2024

CITATION
Hua Q, Liu S, Shen L, Yang Z and Shen H (2024) The safety and efficacy of additional chest tube placement in patients with prolonged air leaks after pulmonary resection: a propensity score-matched analysis. *Front. Med.* 11:1484327. doi: 10.3389/fmed.2024.1484327

The safety and efficacy of additional chest tube placement in patients with prolonged air leaks after pulmonary resection: a propensity score-matched analysis

Qingwang Hua, Suyue Liu, Lu Shen, Zhenhua Yang and Haibo Shen*

Department of Thoracic Surgery, Ningbo No.2 Hospital, Ningbo, China

Background: This study evaluates the symptomatic management of prolonged pleural air leaks following pulmonary resection, assesses the efficacy and safety of chest tube placement, and introduces experiences with high-positioned chest tube insertion.

Methods: We retrospectively reviewed 84 patients with prolonged pleural air leaks after lung surgery at Ningbo No.2 Hospital from January 2022 to December 2023. These patients were divided into a conservative treatment group (Group A, $n = 64$) and a chest tube placement group (Group B, $n = 20$). The propensity score matching method was applied to balance confounders between the two groups, resulting in 12 matched pairs. The study compared the time to chest tube removal, average hospital stays time, postoperative drainage volume, and facial visual analog pain score between the two groups.

Results: The average hospital stays and chest tube removal time of patients in group B were significantly lower than those of patients in group A (8.00 ± 1.12 vs. 9.75 ± 1.60 days, $P = 0.003$, 6.92 ± 1.08 vs. 8.58 ± 1.67 days, $P = 0.005$, respectively). However, the mean facial visual analog pain score in group B was higher than that in group A (1.58 ± 0.58 vs. 1.00 ± 0.01, $P = 0.020$). There were no significant differences between the two groups in terms of postoperative drainage volume.

Conclusions: For patients with prolonged air leaks, additional chest tube placement postoperatively significantly reduces both hospitals stay duration and chest tube indwelling time compared to conservative treatment. This method may be a potential treatment measure for prolonged air leak in selected patients.

KEYWORDS

air leak, chest drains, postoperative, pulmonary surgery, tube

Introduction

Non-small cell lung cancer (NSCLC) has emerged as a predominant malignancy with significant morbidity and mortality rates globally (1). In China, the incidence and prevalence of NSCLC have been steadily rising, posing a substantial public health challenge (2). The increasing burden of NSCLC underscores the necessity for effective surgical

interventions and postoperative care strategies to enhance patient outcomes and mitigate the adverse effects associated with this condition.

The surgical treatment of NSCLC has advanced rapidly, with video-assisted thoracoscopic surgery (VATS) now being the predominant approach (3). Despite its minimally invasive nature and quicker recovery times, uniportal VATS is also frequently accompanied by various postoperative complications, which remain a focal point of clinical research aimed at improving surgical outcomes (4). Among these complications, prolonged air leak (PAL) being one of the most common issues, stand out due to its impact on patient recovery (5–7). PAL is characterized by the inability to remove the chest tube postoperatively, resulting in extended hospital stays, which contradicts the principles of enhanced recovery after surgery (ERAS) (8).

The etiology of PAL is multifactorial, and its management focuses on promoting rapid lung re-expansion and effective drainage of the residual pleural space. Conventional conservative treatments for PAL include external negative pressure drainage, pleurodesis, and endoscopic treatments, etc. However, these approaches are often ineffective and costly in certain situations and fail to significantly reduce hospital stay, which may increase morbidity and mortality after lung resection and hinder the recovery process (9).

In this study, we conducted a retrospective analysis to evaluate the effectiveness of bedside chest tube placement in patients with prolonged air leaks following pulmonary resection. Our findings suggest that this intervention can substantially enhance lung re-expansion and reduce hospital stay durations, offering a more efficacious and inexpensive approach compared to traditional conservative treatments. This investigation highlights the importance of re-evaluating current PAL management protocols and emphasizes the potential benefits of incorporating timely chest tube placement into postoperative care strategies.

Methods

Patient inclusion and exclusion criteria

A retrospective analysis was conducted on patients who underwent video-assisted thoracoscopic surgery (VATS) for lung cancer at our institution (Department of Thoracic Surgery, Ningbo No.2 Hospital) from January 01 2022 to December 31 2023. Inclusion criteria were as follows: (I) All patients underwent preoperative enhanced chest CT scans to determine clinical staging, and the surgeries were all VATS procedures. Intraoperative frozen section analysis was conducted by pathology experts to confirm a pathological diagnosis of non-small cell lung cancer; (II) All patients' baseline vital conditions were thoroughly evaluated preoperatively to ensure they could tolerate lung cancer surgery; (III) No cardiovascular or cerebrovascular infarcts occurred within 3 months prior to surgery; (IV) Normal coagulation function with no use of anticoagulants in the 2 weeks preceding surgery. (V) Prolonged air leak while Chest tube indwelling for more than 5 days.

Exclusion criteria were as follows: (I) Multi-lesion resection in different lobes or Sleeve bronchial resection; (II) VATS converted to thoracotomy patients. (III) Prior ipsilateral lung surgery; (IV) Neoadjuvant therapy patients; (V) Pathological diagnosis was small cell lung cancer; (VI) Postoperative bronchoscopy revealed bronchopleural fistula. The flow chart for inclusion and exclusion of patients as Figure 1. This study was conducted in accordance with the Helsinki Declaration (revised in 2013). The study was approved by ethics board of Ningbo No.2 Hospital and informed consent was obtained for each patient.

Grouping criteria and chest tube insertion/removal criteria

When the air leak lasted for more than 5 days, we defined the patient as having PAL (10). We divided these PAL patients into group A and group B according to whether the patients had another chest tube inserted. If the patients had another chest tube inserted, they belonged to group B. Otherwise, they belonged to group A. The conservative treatment group (Group A) received extracorporeal negative pressure drainage (-8-−10 cm H_2O) and pleurodesis, such as intrathoracic injection of diluted povidone-iodine or 50% glucose solution, autologous blood pleurodesis. This treatment should be considered first for patients with PLA. In general, patients in group A presented with simple air leak without other clinical symptoms. Their chest x-ray usually shows a pneumothorax volume of $<$30%. While for the chest tube placement group (Group B), we inserted another chest tube in the pleural cavity. The chest tube was placed in the following situations: (I) pneumothorax volume $\geq$30% after conservative treatment; (II) pneumothorax with extensive subcutaneous emphysema (Figure 2a); (III) the grade of air leak does not decrease after conservative treatment. The drainage status of all chest tubes will be included in the observation regardless of group A or group B. If there is no air leakage within 24 h and the total amount of light limpid fluid drainage in 24 h is $\leq$300 mL, the chest tube removal should be considered.

Surgical information and follow-up indicators

All patients underwent uniportal VATS procedure and were performed by the same surgical team. All patients received standardized pulmonary resection and mediastinal lymphadenectomy according to the Chinese Medical Association guidelines for the clinical diagnosis and treatment of lung cancer (edition 2018). The incision hole was located at the anterior axillary line of the 4th or 5th interspace for pulmonary resection (including lobectomy and Sub-lobar resection) and lymphadenectomy with a length of 3–4 cm. Generally, the 4th interspace for right lobes and the 5th interspace for left lobes. At the end of surgery, the conventional chest tube (24 Fr, 8.00 mm in diameter) was used. The chest tube was inserted from the incision straight to the top of the chest through the anterior mediastinum pathway, which was connected to water-seal bottles without negative pressure. After the operations, we collected the postoperative thoracic drainage volume, the average VAS

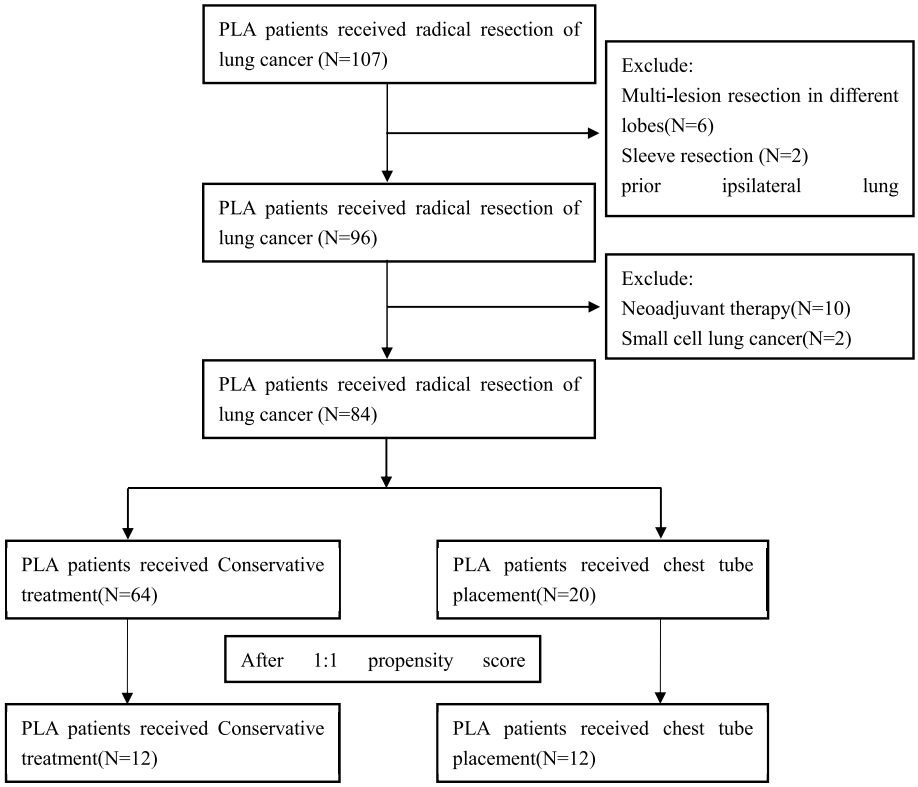

FIGURE 1
Flow chart for inclusion and exclusion of patients.

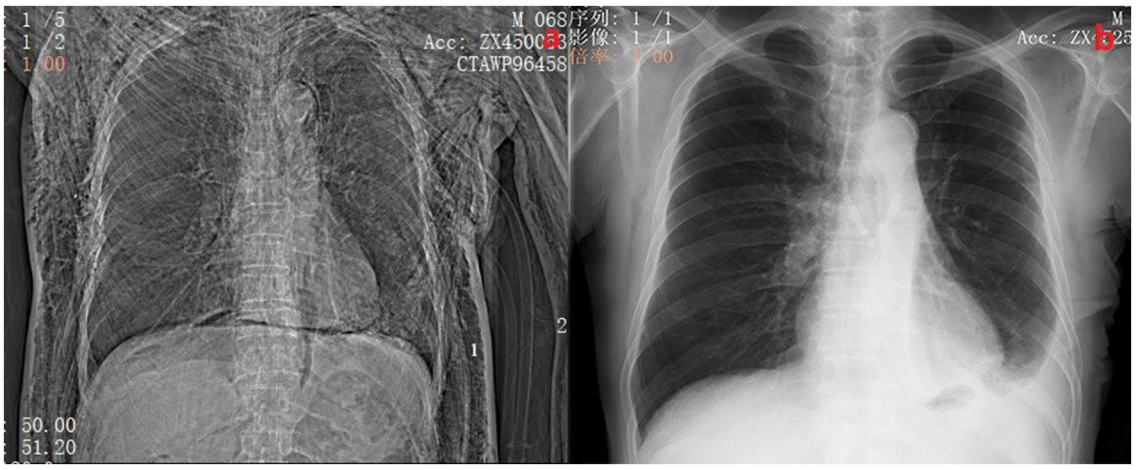

FIGURE 2
(A) Shows a patient with postoperative pneumothorax and subcutaneous emphysema with 2 chest tubes inserted. The side marked with 1 is the chest tube placed during surgery, and the side marked with 2 is the chest tube placed at the bedside. **(B)** Shows a chest X-ray of the same patient 2 weeks after discharge.

pain scores in incisions, average hospital stay time, chest tube removal time during the perioperative period, levels of serum CRP and pulmonary complications during hospitalization. If the chest X-ray or CT shows that the residual lung re-expansion and without obvious inflammation (Reference the levels of serum C-reactive protein (CRP) and bodies' temperature), and the patient with no obvious complaints of discomfort, then the patient was acceptable criteria for discharge (Figure 2b). 2 weeks after discharge, the incision sutures were removed and chest X-rays were reviewed. A follow-up chest CT scan was also performed 1 month after discharge to ensure the patient's recovery.

High position chest tube insertion procedure

The chest tubes were performed by the same person. Generally, we placed the chest tube with a needle (PAHSCO, 28 Fr with 9.33 mm in diameter, Figure 4) in the "triangle of safety," which was inserted straight to the top of the chest cavity through the anterior mediastinum pathway, the key points of simple procedures: (a) Usually, the patient lies in a reclining position on the bed with the arms abducted, identify the "triangle of safety:" the center of the axilla, the lateral aspect of musculus latissimus dorsi, and the lateral pectoralis major at the line of the nipple. (b) An incision approximately with 1–2 cm was made at the 3th intercostal space at the lateral edge of the pectoralis major muscle nearby the anterior axillary line through the "triangle of safety," as like red cross mark b-2. The b-1 red cross mark is the first chest tube which was placed after surgery. (c) Muscle tissue is then dissected using a blunt instrument e.g., a set of arterial forceps, creating a canal to the parietal pleura which is then breached for access to the pleural cavity. A hiss of air, or ooze of blood may present at this point. (d) The pleural cavity is explored using a finger, assessing for the position of the lung and any adhesions. The resulting tube remains open to allow enough air to enter the chest cavity. In the case of artificial pneumothorax, the chest tube is inserted into the chest cavity under the guidance of needle. Be careful not to puncture the lung or other tissues to avoid secondary damage. In our experience, the tube with the side hole is usually placed in the top of the chest cavity at a scale of 12–14 cm [Figure 3 (11)]. Moreover, the tube was connected to water-seal bottles with negative pressure.

Data collection and statistical methods

All patients' data were collected from hospital charts or databases. SPSS 26.0 software was used to analyze the data (IBM SPSS Statistics, USA). Continuous variables were presented as means ± standard deviation or medians (range), and the comparison between the two groups was performed using the *t*-test. Categorical variables were presented as counts or rates and A chi squared test or Fisher s exact test was used to compare dichotomous variables. The Mann-Whitney *U*-test is used for statistical analysis of rank data. The balance of measured variables between groups after propensity score-matching was analyzed using a paired *t*-test for continuous measures and the McNemar test for categorical variables. Propensity score matching was used to mitigate discrepancies in the characteristics of the study cohort that may influence our outcomes. Cases were matched **1:1** with a caliper size of 0.02. Variables used for matching were age, gender, smoking history, COPD, FEV1, FEV1%, and the operation style. A P-value < 0.05 was considered statistically significant.

Result

A total of 84 patients were enrolled in the study (Figure 1). Patients were classified into the conservative treatment group (Group A, $n = 64$) and the chest tube placement group (Group B, $n = 20$) according to the different treatment methods. After calculating the propensity scores (ratio = 1:1), 12 pairs were matched. Table 1 shows the patient demographic and clinical data before and after propensity score matching. The basic line of patients who undergoing chest tube placement were quite similar compared to those in the conservative treatment group except for the age, gender, COPD and pTNM stage ($P < 0.05$) before PSM matching (Table 1). After propensity score-matching, both groups were well-matched in theses parameters. Baseline characteristics of the matched patients were listed in Table 2. The mean operation time was 101.67 ± 11.46 min in group A and 98.33 ± 5.29 min in group B ($P = 0.386$). The mean Thoracic drainage volume in group A is less than that in group B (544.58 ± 242.44 ml vs. 897.50 ± 266.53 ml, $P = 0.660$), but without statistical differences, also as the parameter of Blood loss ($P = 0.104$), Pleural adhesion ($P = 0.453$) and the Serum C-reactive protein before discharge (39.80 ± 22.95 vs. 53.29 ± 28.23 mg/L, $P = 0.660$). The Average hospital stay and the Chest tube removal time in group A is significantly longer than those patients in group B (9.75 ± 1.60 vs. 8.00 ± 1.12 days, $P = 0.003$, 8.58 ± 1.67 vs. 6.92 ± 1.08 days, $P = 0.005$, respectively). However, the mean facial visual analog pain score in group A was lower than that in group B, which also indicated a significant difference (1.00 ± 0.01 vs. 1.58 ± 0.58, $P = 0.020$).

Discussion

VATS is currently considered the primary treatment modality for early-stage NSCLC (3). With advancements in technology, uniportal VATS has become the mainstream surgical technique due to its advantages of minimal invasiveness, rapid recovery, and less pain. Most importantly, compared with conventional thoracoscopic surgery, the oncological prognosis is almost the same (12). However, postoperative complications remain unchanged, with PAL continuing to be one of the most common postoperative complications in thoracic surgery, clinically manifested as pneumothorax. PAL has numerous adverse effects on patients, significantly prolonging the duration of chest tube drainage and hospitalization (9, 13). It can also lead to severe complications such as extensive subcutaneous emphysema, respiratory distress, pulmonary infection, wound infection, and empyema, thereby increasing the psychological and economic burden on patients and contradicting the principles of ERAS.

There are numerous factors contributing to the occurrence of PAL, with alveolar air leakage due to visceral pleural rupture from surgical trauma being the primary cause. Rivera et al. demonstrated that surgical factors can influence the occurrence of PAL (13). In most cases, PAL results from the dissection of visceral pleural adhesions or the presence of incomplete development of pulmonary fissures (14, 15). For our cases, several challenges are presented by the uniportal VATS approach with PAL: Firstly, uniportal VATS makes it difficult to separate adhesions at the base of the thoracic cavity and around the operative uniport, increasing the likelihood of visceral pleural damage and air leakage. Secondly, the incomplete development of pulmonary fissures or unclear anatomical structures of the lung parenchyma led to substantial visceral pleural damage, further increasing the risk of air leakage. Lastly, the common practice is not creating a separate chest tube insertion incision after uniportal VATS. Usually, we placed

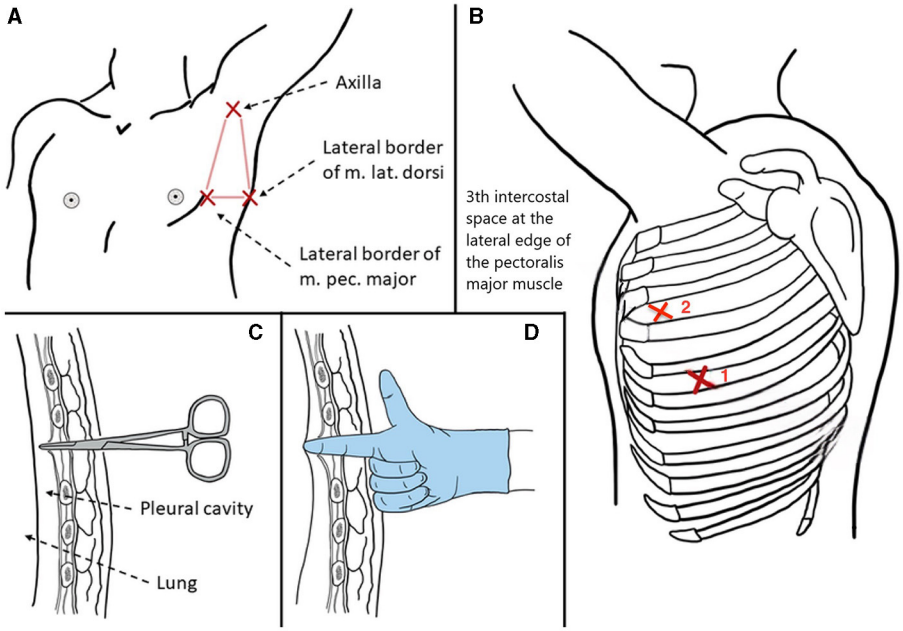

FIGURE 3
The high position chest tube insertion procedure.

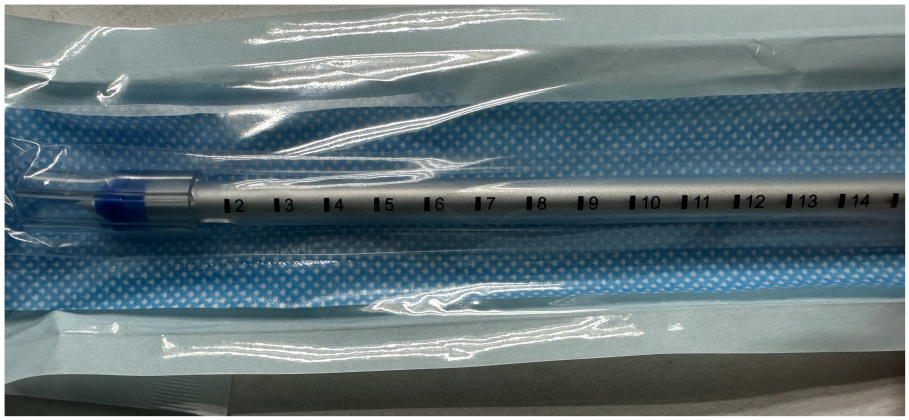

FIGURE 4
The chest tube with a needle.

the tube in a higher placement because of the original incision. Thus, the tube is insufficient for draining air and fluid from the lower thoracic cavity, thereby contributing to poor drainage. To address this issue, we retrospectively evaluated this specific surgical approach, comparing outcomes before and after the chest tube placement. To obtain more reliable comparisons, we employed the Propensity Score Matching (PSM) method to balance key variables and mitigate selection bias between the groups.

The chest tube plays a crucial role in managing postoperative PAL (16, 17). Regarding chest tube management, the majority of experts in previous literature advocate for single-tube placement as the first choice. You et al. thinks that compared with double chest drains, single chest drain has its advantages and safety for pulmonary lobectomy (18). However, our observations have led us to identify three phenomena: Firstly, a higher incidence of postoperative PLA following lobectomy, possibly due to the larger residual pleural cavity; Secondly, PLA patients with subcutaneous emphysema generally have poor lung quality, and the original chest tube cannot provide sufficient air drainage. Extra air can penetrate the muscles of the wound and form subcutaneous emphysema. This phenomenon usually requires additional catheterization because a single chest tube is not enough to meet their clinical needs. Finally, the positioning of a single chest tube may not align with the ideal location to some patients, leading to suboptimal drainage of the upper thoracic cavity. This misalignment may be due to changes in chest tube positioning during wound closure, body position changes, or postoperatively expanded lung tissue compressing and displacing the chest tube. For all these cases, another chest tube may need to be placed to increase effective drainage (19). We reviewed previous cases and traditional

TABLE 1 Demographics and clinical data before PSM and after PSM.

Variables	Before PSM			After PSM		
	Conservative treatment group *N* (%) (*n* = 64)	Chest tube group *N* (%) (*n* = 20)	*P*-value	Conservative treatment group *N* (%) (*n* = 12)	Chest tube group *N* (%) (*n* = 12)	*P*-value
Age (years old)	61.69 ± 12.24	67.90 ± 7.67	0.036	64.83 ± 7.17	67.92 ± 9.61	0.249
Gender			0.005			1.000
Male	25 (39.1)	15 (75.0)		7 (58.3)	7 (58.3)	
Female	39 (60.9)	5 (25.0)		5 (41.7)	5 (41.7)	
Past history						
Smoking	27 (42.2)	12 (60.0)	0.163	7 (58.3)	7 (58.3)	1.000
Hypertension	36 (56.3)	16 (80.0)	0.056	8 (66.7)	9 (75)	1.000
Diabetes	10 (15.6)	6 (30.0)	0.153	1 (8.3)	2 (16.7)	1.000
COPD	4 (6.3)	9 (45.0)	0.000	4 (33.3)	4 (33.3)	1.000
FEV1	2.47 ± 0.62	2.72 ± 0.51	0.078	2.48 ± 0.59	2.51 ± 0.54	0.882
FEV1%	81.26 ± 5.44	80.15 ± 4.62	0.410	79.83 ± 3.56	80.00 ± 4.95	0.913
MDL (cm)	2.00 ± 0.86	2.64 ± 1.31	0.053	2.12 ± 0.99	2.32 ± 1.23	0.640
Lesion site			0.178			0.539
Left upper lobe	18 (28.1)	5 (25.0)		5 (41.7)	4 (33.3)	
Left lower lobe	13 (20.3)	2 (10.0)		2 (16.7)	2 (16.7)	
Right upper lobe	18 (28.1)	9 (45.0)		4 (33.3)	4 (33.3)	
Right middle lobe	4 (6.2)	0		0	0	
Right lower lobe	11 (17.2)	4 (20.0)		1 (8.3)	2 (16.7)	
Pathological type			0.097			0.574
SQC	12 (18.8)	9 (45.0)		4 (33.3)	5 (41.7)	
ADC	49 (76.6)	11 (55)		7 (58.3)	7 (58.3)	
Others	3 (4.7)	0		1 (8.3)	0	
Operation style			1.000			1.000
Lobectomy	55 (85.9)	17 (85.0)		10 (83.3)	10 (83.3)	
Sublobar resection	9 (14.1)	3 (15.0)		2 (16.7)	2 (16.7)	
Pathological stage			0.008			0.871
IA	44 (68.8)	9 (45.0)		7 (58.3)	7 (58.3)	
IB	11 (17.2)	1 (5.0)		2 (16.7)	1 (8.3)	
IIA	2 (3.1)	1 (5.0)		0	1 (8.3)	
IIB	3 (4.7)	1 (5.0)		1 (8.3)	0	
IIIA	4 (6.3)	8 (40.0)		2 (16.7)	3 (25.0)	

COPD, Chronic obstructive pulmonary disease; MDL, Maximum diameter of lesion; SQC, Squamous carcinoma; ADC, Adenocarcinoma.

textbooks and found that double chest tubes may be beneficial for these patients.

The choice of treatment modality for PLA primarily depends on its efficacy and feasibility. Our standard approach for treating most cases of PLA involves thoracic negative pressure suction and pleurodesis with agents such as diluted povidone-iodine, autologous blood, or 50% glucose solution (20–22). Most cases can solve with these methods. According to our experience, we need to keep the patient completely supine in bed when we perform this type of chemical pleurodesis. Inject the drug through the chest tube and instruct the patient to cough to expel the remaining air in the chest, and make the highest point of the chest tube higher than the patient's chest plane, ensure the air can flow out and the fluid can be fully retained in the chest. This method promotes adhesions in the roof of the pleural cavity. We do not recommend Trendelenburg position as it may cause symptoms such as dizziness or hypotension etc. Other methods such as the use of digital chest drainage systems have also been reported in other literature.

TABLE 2 Perioperative outcome between the two matched groups.

Variables	Conservative treatment group *N* (%) ($n = 12$)	Chest tube group *N* (%) ($n = 12$)	*P*-value
Operation time (min)	101.67 ± 11.46	98.33 ± 5.29	0.386
Blood loss (mL)	53.33 ± 8.87	63.33 ± 14.35	0.104
Pleural adhesion	6 (50.0)	3 (25.0)	0.453
Average hospital stay time (d)	9.75 ± 1.60	8.00 ± 1.12	0.003
Chest tube removal time (d)	8.58 ± 1.67	6.92 ± 1.08	0.005
Thoracic drainage volume (mL)	844.58 ± 242.44	897.50 ± 266.53	0.660
Visual analog scale (VAS)	1.00 ± 0.01	1.58 ± 0.58	0.020
Serum C-reactive protein (mg/L)	39.80 ± 22.95	53.29 ± 28.23	0.299

Comacchio et al. believe that the use of digital drainage systems can remove chest drains earlier than traditional systems (23). Bao et al. deems that discharge patient' chest tube management can be accomplished in selected patients without a major increase in morbidity or mortality (24). However, these methods cannot be implemented in primary hospitals due to technical feasibility.

Chest tube placement is more appropriate for patients with significantly larger residual cavities, incomplete lung re-expansion with subcutaneous emphysema, and prolapsed chest tubes (25). These patients share common clinical characteristics, including inadequate air drainage and failure of the visceral and parietal pleura to adhere, resulting in persistent pneumothorax. In our clinical practice, we usually take chest X-rays routinely on the 1st and 3rd day after VATS surgery. For the situations mentioned above (25), including situations I and II, we will perform extracorporeal negative pressure drainage. If the situation does not improve, we will immediately insert the chest tube because in these cases, a single chest tube is not sufficient to remove the excess gas. While for situation III (the grade air leak does not decrease after conservative treatment), we decide whether to intubate based on the degree of air leak after conservative treatment of the patient. Typically, we start conservative management on the 3rd postoperative day for patients with air leak. Pleural adhesion agents such as diluted povidone-iodine are injected intrathoracically once a day for two consecutive times. If the air leak does not decrease, we will insert the chest tube decisively. Patients who require chest tube placement have grade II or III air leaks, because grade I air leaks will almost always improve after conservative treatment.

We must carefully consider the appropriateness of chest tube placement because of the inherent risks of this action. Remember, conservative treatment is always the first choice for patients with PLA because it is less invasive and has lower risks. In most cases of group B, postoperative lungs are not fully collapsed, and improper handling may cause secondary harm to the patient, leading to various short-term complications, including increased pain, pulmonary contusion, hemothorax, arrhythmias such as atrial fibrillation, and even the need for secondary repair surgery (26). In our experience, seven patients experienced minor complications. The prevalence of increased pain was the most frequently observed finding, aligning with the results of our study (1.58 ± 0.58 vs. 1.00 ± 0.01, $P = 0.020$). Four patients received additional analgesic drugs. Another patient had atrial fibrillation after placement that was controlled by antiarrhythmic therapy. One patient had little thoracic hemorrhagic exudation after the operation, which was promptly treated with hemostatic drugs. The final patient experienced lung damage due to a puncture caused by the needle, which exacerbated the air leak, and received a secondary surgical intervention. In order to avoid the occurrence of the above complications, we have returned to the traditional double chest tube placement method in recent surgeries for patients with poor lung quality. Our experience with chest tube placement has yielded several insights, and the procedural steps are illustrated in the accompanying (Figure 4). The primary technical points involve creating an artificial pneumothorax and utilizing the needle to guide the placement of the chest tube at a high thoracic position. For surgeons with limited experience, we advocate for more stringent preoperative assessment and more cautious intraoperative decision-making as essential factors to ensure the safety of this challenging procedure.

Our study indicates that although chest tube repositioning may temporarily increase patient discomfort and burden, it remains a simple and safe technique. It is also much less cost-effective than endoscopic treatment (27, 28). After matching patients in the early stages, compared to the conservative treatment group, chest tube repositioning significantly reduced hospitalization time and financial burden. In terms of short-term outcomes, there was no significant increase in thoracic drainage volume (844.58 ± 242.44 vs. 897.50 ± 266.53 ml, $P = 0.660$), patients showed lung recovery well without infection before discharge (Serum C-reactive protein: 39.80 ± 22.95 vs. 53.29 ± 28.23 mg/L, $P = 0.299$), and there were no records of readmission at 1 month postoperatively.

The limitations of our study are evident. Due to the retrospective nature of the study and the relatively small sample size, selection bias is inevitable. Additionally, given the limited sample size, the long-term outcomes remain to be further reviewed. Future studies with larger sample sizes or prospective randomized controlled study are necessary to validate the potential benefits of additional chest tube placement.

Conclusion

Based on our study, additional chest tube placement appears to be safe and effective and may serve as a suitable alternative

in selected patients with prolong air leaks. Our findings must be confirmed by large-sample, prospective randomized controlled studies.

Data availability statement

The original contributions presented in the study are included in the article/supplementary material, further inquiries can be directed to the corresponding author.

Ethics statement

The study was approved by Ethics Board of Ningbo No.2 Hospital and informed consent was obtained for each patient. The studies were conducted in accordance with the local legislation and institutional requirements. The participants provided their written informed consent to participate in this study.

Author contributions

QH: Writing – original draft, Writing – review & editing. SL: Software, Writing – review & editing. LS: Supervision, Writing – review & editing. ZY: Supervision, Writing – review & editing. HS: Conceptualization, Funding acquisition, Writing – review & editing.

Funding

The author(s) declare financial support was received for the research, authorship, and/or publication of this article. This study was supported by the Research Foundation of Ningbo No. 2 Hospital, Ningbo, China (2023HMKY34).

Conflict of interest

The authors declare that the research was conducted in the absence of any commercial or financial relationships that could be construed as a potential conflict of interest.

Publisher's note

References

1. Bray F, Laversanne M, Sung H, Ferlay J, Siegel RL, Soerjomataram I, et al. Global cancer statistics 2022: GLOBOCAN estimates of incidence and mortality worldwide for 36 cancers in 185 countries. *CA Cancer J Clin.* (2024) 74:229–63. doi: 10.3322/caac.21834

2. Zheng RS, Chen R, Han BF, Wang SM, Li L, Sun KX, et al. Cancer incidence and mortality in China, 2022. *Zhonghua Zhong Liu Za Zhi.* (2024) 46:221–31. doi: 10.3760/cma.j.cn112152-20240119-00035

3. Yang HX, Woo KM, Sima CS, Bains MS, Adusumilli PS, Huang J, et al. Long-term survival based on the surgical approach to lobectomy for clinical stage I nonsmall cell lung cancer: comparison of robotic, video-assisted thoracic surgery, and thoracotomy lobectomy. *Ann Surg.* (2017) 265:431–7. doi: 10.1097/SLA.0000000000001708

4. Scarci M, Gonzalez-Rivas D, Schmidt J, Bedetti B. Management of intraoperative difficulties during uniportal video-assisted thoracoscopic surgery. *Thorac Surg Clin.* (2017) 27:339–46. doi: 10.1016/j.thorsurg.2017.06.002

5. Ponholzer F, Ng C, Maier H, Lucciarini P, Öfner D, Augustin F. Risk factors, complications and costs of prolonged air leak after video-assisted thoracoscopic surgery for primary lung cancer. *J Thorac Dis.* (2023) 15:866–77. doi: 10.21037/jtd-21-2011

6. Lapidot M, Levy Faber D, Bueno R. Prolonged air leak after lung surgery-prevalent complication without a perfect solution. *J Thorac Dis.* (2023) 15:5285–6. doi: 10.21037/jtd-23-1180

7. Hoeijmakers F, Hartemink KJ, Verhagen AF, Steup WH, Marra E, Röell WFB, et al. Variation in incidence, prevention and treatment of persistent air leak after lung cancer surgery. *Eur J Cardiothorac Surg.* (2021) 61:110–7. doi: 10.1093/ejcts/ezab376

8. Bertolaccini L, Brunelli A. Devising the guidelines: the techniques of uniportal video-assisted thoracic surgery-postoperative management and enhanced recovery after surgery. *J Thorac Dis.* (2019) 11:S2069–72. doi: 10.21037/jtd.2019.01.62

9. Attaar A, Luketich JD, Schuchert MJ, Winger DG, Sarkaria IS, Nason KS. Prolonged air leak after pulmonary resection increases risk of noncardiac complications, readmission, and delayed hospital discharge: a propensity score-adjusted analysis. *Ann Surg.* (2021) 273:163–72. doi: 10.1097/SLA.0000000000003191

10. Seder CW, Basu S, Ramsay T, Rocco G, Blackmon S, Liptay MJ, et al. A prolonged air leak score for lung cancer resection: an analysis of the society of thoracic surgeons general thoracic surgery database. *Ann Thorac Surg.* (2019) 108:1478–83. doi: 10.1016/j.athoracsur.2019.05.069

11. Mohrsen S, McMahon N, Corfield A, McKee S. Complications associated with pre-hospital open thoracostomies: a rapid review. *Scand J Trauma Resusc Emerg Med.* (2021) 29:166. doi: 10.1186/s13049-021-00976-1

12. Shen Y, Wang H, Feng M, Xi Y, Tan L, Wang Q. Single- versus multiple-port thoracoscopic lobectomy for lung cancer: a propensity-matched study. *Eur J Cardiothorac Surg.* (2016) 49(Suppl.1):i48–53. doi: 10.1093/ejcts/ezv358

13. Rivera C, Bernard A, Falcoz P-E, Thomas P, Schmidt A, Bénard S, et al. Characterization and prediction of prolonged air leak after pulmonary resection: a nationwide study setting up the index of prolonged air leak. *Ann Thorac Surg.* (2011) 92:1062–8. doi: 10.1016/j.athoracsur.2011.04.033

14. Stamenovic D, Bostanci K, Messerschmidt A, Jahn T, Schneider T. Fissureless fissure-last video-assisted thoracoscopic lobectomy for all lung lobes: a better alternative to decrease the incidence of prolonged air leak? *Eur J Cardiothorac Surg.* (2016) 50:118–23. doi: 10.1093/ejcts/ezv455

15. Aprile V, Bacchin D, Calabrò F, Korasidis S, Mastromarino MG, Ambrogi MC, et al. Intraoperative prevention and conservative management of postoperative prolonged air leak after lung resection: a systematic review. *J Thorac Dis.* (2023) 15:878–92. doi: 10.21037/jtd-22-736

16. Yan S, Wang X, Wang Y, Lv C, Wang Y, Wang J, et al. Intermittent chest tube clamping may shorten chest tube drainage and postoperative hospital stay after lung cancer surgery: a propensity score matching analysis. *J Thorac Dis.* (2017) 9:5061–7. doi: 10.21037/jtd.2017.11.08

17. Deng B, Qian K, Zhou J-H, Tan Q-Y, Wang R-W. Optimization of chest tube management to expedite rehabilitation of lung cancer patients after video-assisted thoracic surgery: a meta-analysis and systematic review. *World J Surg.* (2017) 41:2039–45. doi: 10.1007/s00268-017-3975-x

18. You J, Zhang H, Li W, Dai N, Zheng Z. Single versus double chest drains after pulmonary lobectomy: a systematic review and meta-analysis. *World J Surg Oncol.* (2020) 18:175. doi: 10.1186/s12957-020-01945-1

19. Tanaka M, Sagawa M, Usuda K, Machida Y, Ueno M, Motono N, et al. Postoperative drainage with one chest tube is appropriate for pulmonary lobectomy: a randomized trial. *Tohoku J Exp Med.* (2014) 232:55–61. doi: 10.1620/tjem.232.55

20. Park JB, Lee SA, Lee WS, Kim YH, Hwang JJ. The management of chemical pleurodesis with viscum album in patients with persistent air leakage. *J Thorac Dis.* (2018) 10:371–6. doi: 10.21037/jtd.2017.12.67

21. Chaari Z, Hentati A, Ayed AB, Abid W, Frikha I. Effectiveness and safety of povidone iodine for prolonged lung air-leak after lung surgery. *Asian Cardiovasc Thorac Ann.* (2022) 30:314–20. doi: 10.1177/02184923211067637

22. Hugen N, Hekma EJ, Claessens NJM, Smit HJM, Reijnen MMPJ. Efficacy of an autologous blood patch for prolonged air leak: a systematic review. *Ann Thorac Surg.* (2022) 114:1064–71. doi: 10.1016/j.athoracsur.2021.05.047

23. Comacchio G, Marulli G, Mendogni P, Andriolo LG, Guerrera F, Brascia D, et al. Comparison between electronic and traditional chest drainage systems: a multicenter randomized study. *Ann Thorac Surg.* (2023) 116:104–9. doi: 10.1016/j.athoracsur.2023.02.057

24. Bao F, Dimitrovska NT, Hu S, Chu X, Li W. Safety of early discharge with a chest tube after pulmonary segmentectomy. *Eur J Cardiothorac Surg.* (2020) 58:613–8. doi: 10.1093/ejcts/ezaa097

25. Satoh Y. Management of chest drainage tubes after lung surgery. *Gen Thorac Cardiovasc Surg.* (2016) 64:305–8. doi: 10.1007/s11748-016-0646-z

26. Anderson D, Chen SA, Godoy LA, Brown LM, Cooke DT. Comprehensive review of chest tube management: a review. *J Am Med Assoc Surg.* (2022) 157:269–74. doi: 10.1001/jamasurg.2021.7050

27. Abu-Hijleh M, Styrvoky K, Anand V, Woll F, Yarmus L, Machuzak MS, et al. Intrabronchial valves for air leaks after lobectomy, segmentectomy, and lung volume reduction surgery. *Lung.* (2019) 197:627–33. doi: 10.1007/s00408-019-00268-7

28. Konagaya K, Yamamoto H, Nishida T, Morita T, Suda T, Isogai J, et al. Negative-pressure wound therapy to treat thoracic empyema with COVID-19-related persistent air leaks: a case report. *Front Med.* (2022) 9:970239. doi: 10.3389/fmed.2022.970239

frontiers | Frontiers in Medicine

TYPE Original Research
PUBLISHED 14 October 2024
DOI 10.3389/fmed.2024.1400049

OPEN ACCESS

EDITED BY
Vincenzo Pio Di Noia,
IRCCS Istituto Nazionale Tumori Regina Elena, Italy

REVIEWED BY
Vinit Nalawade,
Duke University Health System, United States
Lucia Mangone,
IRCCS Local Health Authority of Reggio Emilia, Italy

*CORRESPONDENCE
Ki Young Son
✉ mdsky75@gmail.com

RECEIVED 12 March 2024
ACCEPTED 27 August 2024
PUBLISHED 14 October 2024

CITATION
Huh Y, Kim H-R, Kim HJ and Son KY (2024) Risk score model for predicting mortality among patients with lung cancer.
Front. Med. 11:1400049.
doi: 10.3389/fmed.2024.1400049

Risk score model for predicting mortality among patients with lung cancer

Youn Huh[1], Hae-Rim Kim[2], Hwa Jung Kim[3] and Ki Young Son[4]*

[1]Department of Family Medicine, Uijeongbu Eulji Medical Center, Eulji University, Gyeonggi-do, Republic of Korea, [2]College of Natural Science, School of Statistics, University of Seoul, Seoul, Republic of Korea, [3]Department of Preventive Medicine and Clinical Epidemiology and Biostatics, Asan Medical Center, University of Ulsan College of Medicine, Seoul, Republic of Korea, [4]Department of Family Medicine, Asan Medical Center, University of Ulsan College of Medicine, Seoul, Republic of Korea

Background: To develop an accurate mortality risk predictive model among patients with lung cancer.

Methods: The development cohort included 96,255 patients with lung cancer aged ≥19 years, who underwent a Korean National Health Insurance Service health check-up from 2005 to 2015. The validation cohort consisted of 18,432 patients (≥19 years) with lung cancer from another region. The outcome was all-cause mortality between January 1, 2005, and December 31, 2020.

Results: Approximately 60.5% of the development cohort died within a median follow-up period of 2.32 (0.72–5.00) years. Risk score was highest in participants aged ≥65 years, followed by those who underwent treatment, had a history of emergency room visits, and were current smokers. Participants treated by surgery had the lowest risk score, followed by combined surgery and chemotherapy, combined surgery and radiation therapy, women, and regular exercisers. The C statistic in the development and validation cohorts was 0.78 (95% confidence interval, 0.77–0.78) and 0.81 (95% confidence interval, 0.78–0.84), respectively.

Conclusion: Advanced age, lung cancer stage, and treatment type were strong risk factors of mortality in lung cancer patients, while being a woman and exercise were preventive factors. These will aid in the prediction of mortality and management of lung cancer patients.

KEYWORDS

lung cancer, mortality, risk score, development cohort, validation cohort

Introduction

Lung cancer resulted in 2.2 million new cases and was the second most common cancer in 2020 worldwide (1). In the United States, approximately 118,000 new cases of lung cancer were estimated in 2022, and this malignancy was the second most common after prostate cancer in men and breast cancer in women (2). In Korea, the age-standardized incidence rate of lung cancer was 27.6 per 100,000, and lung cancer was the fourth most common type of cancer (3). Despite improvements in lung cancer treatments, the survival rate of lung cancer is lower than that of any other cancer (4). For example, the 5-year survival rate in Korea from 2014 to 2018 was 32% for lung cancer, despite being 66% for all cancers except thyroid (3).

This figure was higher than that in the United States or United Kingdom, which was likely related to health insurance system in Korea (5). Moreover, a previous study found that risk factors of mortality among adults with lung cancer included advanced age, male sex, treatment with radiotherapy, organ failure, infection, and admission to the intensive care unit (6).

Methods for assessing risk can be useful in identifying and selecting which patients will attend additional healthcare facilities, be at high risk of mortality, and experience decreased body function (7–9). Risk stratification models not only help quickly detect and manage patients with a poor prognosis, such as hospitalization or mortality, but also prevent low-risk patients from becoming high-risk and improve the health status in moderate-risk patients (10).

Because lung cancer is such a prevalent disease worldwide, the management of this malignancy is vital. However, studies on the risk factors and risk score for lung cancer-related mortality are insufficient. Therefore, we aimed to create a mortality risk score model using a combination of mortality risk factors based on nationwide Korean cohort data. In addition, the validity of our model was tested using data from a cohort of patients with lung cancer from another region in Korea.

Methods

Study participants

We used data from the Korean National Health Insurance System (KNHIS), which represents Koreans. The KNHIS was instituted in 2000 as the only national health insurance system in South Korea and covers more than 97% of the Korean population. The KNHIS database was created for use by public health researchers and policy makers. Therefore, it retains extensive medical data, including demographic characteristics, health check-up data, disease diagnosis codes, treatments, and procedures based on medical claims according to the International Classification of Diseases 10th Revision (ICD-10) codes for the South Korean population. The KNHIS data have been utilized by qualified researchers submitting a study plan approved by official review committees since 2015.

Using this database, we initially identified 228,258 individuals diagnosed with lung cancer (ICD-10 codes C33 and C34) who underwent a national health check-up offered by the KNHIS from January 1, 2005, to December 31, 2015. We selected patients from Seoul as the development cohort and those from Busan and Gyeongsangnam-do as the validation cohort. There were no inherent differences in standard of care or quality of care between the development and validation cohorts, as they were supervised by the Health Insurance Review and Assessment Service. However, because the number of medical institutions and medical staff were concentrated in the two cohorts, which are big cities, our study defined the largest city in Korea as the development cohort and the next largest local region as the validation cohort. Those who lived in other regions ($n = 66,337$), individuals aged <19 years ($n = 100$), and those with missing data for any of the study variables ($n = 47,134$) were excluded. Finally, 114,687 individuals (96,255 in the development cohort and 18,432 in the validation cohort) were eligible for the study.

This study adhered to the principles of the Declaration of Helsinki and was approved by the Institutional Review Board of Uijeongbu Eulji Medical Center (IRB No: UEMC 2021–08-022). The requirement for informed consent was waived by the Institutional Review Board of Uijeongbu Eulji Medical Center due to the use of anonymized and de-identified data.

Main outcome of study

The outcome of our study was all-cause mortality between January 1, 2005, and December 31, 2020.

Covariates

The KNHIS database includes accurate demographic characteristics and lifestyle data, which were evaluated using standardized, self-administered questionnaires. The lowest 20% of the income range of the participants was classified as low income, and the remaining incomes were classified as non-low income. Smoking status was classified into two groups: non-smoker and current smoker. Individuals who consumed any alcohol on a weekly basis were classified as alcohol drinkers, and those who did not were classified as non-drinkers. Regular physical activity was defined as follows: moderate-intensity exercise, such as light walking for at least 5 days per week or high-intensity exercise, such as tennis for at least 3 days per week. Health examinations were conducted by qualified medical staff and included anthropometric and laboratory measurements. Anthropometric parameters included height, body weight, and waist circumference (WC), which were evaluated using standard protocols and equipment. The height of the participants was measured to the nearest 0.1 cm using a stadiometer. Body weight was measured to the nearest 0.1 kg on a balance scale, with the participants wearing only undergarments. The body mass index (BMI) was calculated by dividing the body weight (kg) by the height squared (m^2). According to the definition of obesity by the Korean Society for the Study of Obesity, BMI was divided into three groups as follows: < 18.5, 18.5–24.9, and $\geq 25\,kg/m^2$. Blood pressure was checked while the participants sat and had rested for at least 5 min. After overnight fasting, the participants underwent laboratory tests, including serum glucose and total cholesterol.

Chronic diseases were identified according to health examination results and medical claims for disease diagnoses and medication prescriptions. Chronic diseases were defined by the Office of the Assistant Secretary for Health before the diagnosis of lung cancer (11). A total of 20 chronic diseases were identified.

The type of treatment for lung cancer was divided into eight groups: none, chemotherapy, surgery, radiation, surgery and chemotherapy, surgery and radiation, chemotherapy and radiation, and surgery combined with chemotherapy and radiation. Emergency room visits were identified according to whether the participants visited the emergency room within 1 year of death or the last follow-up period.

Statistical analysis

We performed all analyses using the SAS software (version 9.4; SAS Institute, Cary, NC, United States). We identified mortality risk

factors by multivariate Cox proportional hazards analysis and calculated points proportional to the regression coefficient values to approximate scores. Model 1 was not adjusted, while Model 2 was adjusted for covariables with a *p*-value <0.05 in Model 1. A risk score was calculated for each individual, and the scores were classified as low-, moderate-, and high-risk for mortality. The optimal cut off were selected by calculating maximized log likelihood. The cutoff values of the risk groups were 7 points and 11 points. Risk scores for the validation cohort were calculated using the same method as that of the development cohort. For validation, we created a receiver operating characteristic (ROC) curve for the development and validation cohorts.

Kaplan–Meier survival curves for patients in each of the three risk groups were generated to show the risk of mortality for both the development and validation cohorts. The predictive accuracy of the risk scoring system was evaluated using the C statistic and by estimating the difference between the mortality probability of the high- and low-risk groups within 1 and 5 years.

Results

Baseline characteristics

Table 1 shows the baseline characteristics of the 114,687 eligible participants with lung cancer. Among them, the proportion of men was 69.1% ($n = 79,242$). The median follow-up period was 2.32 (0.72–5.00) years. The mean age was 66.1 ± 10.9 years, and men tended to be older than women ($p < 0.001$). Men were more likely than women to be current smokers, alcohol drinkers, and perform regular exercise ($p < 0.001$). Additionally, low income was slightly more common among women than men. Moreover, women had a slightly higher mean BMI and total cholesterol than men. In contrast, the mean systolic and diastolic blood pressure were higher in men than women ($p < 0.001$). The proportion of participants who did not undergo treatment for lung cancer was the highest among the treatment types for both men and women. In men, no treatment was followed by radiation therapy, surgery, and combined chemotherapy and radiation therapy. In women, no treatment was followed by surgery, combined chemotherapy and radiation therapy, and radiation therapy. The proportion of participants with ≥5 chronic diseases was >50% among both men and women, but higher in women ($p < 0.001$). Finally, men were more likely to visit the emergency room than women ($p < 0.001$).

TABLE 1 Baseline characteristics of study participants.

	Total	Sex		P-value
		Men	Women	
Sex (men)	79,242 (69.1%)			
Age (years)	66.1 ± 10.9	66.8 ± 10.3	64.7 ± 11.9	<0.001
Current smoker	33,161 (28.9%)	31,263 (39.5%)	1898 (5.4%)	<0.001
Alcohol drinker	22,942 (20.0%)	21,831 (27.6%)	1,111 (3.1%)	<0.001
Regular exercise	42,507 (37.1%)	30,230 (38.2%)	12,277 (34.6%)	<0.001
Income (low)	20,600 (18.0%)	13,798 (17.4%)	6,802 (19.2%)	<0.001
BMI (kg/m²)	23.3 ± 3.2	23.2 ± 3.1	23.7 ± 3.3	<0.001
Type of treatment				
None	43,762 (38.2%)	30,752 (38.8%)	13,010 (36.7%)	<0.001
Chemotherapy	9,062 (7.9%)	5,434 (6.9%)	3,628 (10.2%)	
Surgery	17,234 (15.0%)	11,100 (14.0%)	6,134 (17.3%)	
Radiation	18,628 (16.2%)	15,265 (19.3%)	3,363 (9.5%)	
Surgery + chemotherapy	2,456 (2.1%)	1,333 (1.7%)	1,123 (3.2%)	
Surgery + radiation	5,393 (4.7%)	4,285 (5.4%)	1,108 (3.1%)	
Chemotherapy + radiation	13,940 (12.2%)	8,587 (10.8%)	5,353 (15.1%)	
Surgery + chemotherapy + radiation	4,212 (3.7%)	2,486 (3.1%)	1,726 (4.9%)	
Number of chronic diseases				
0	2,664 (2.3%)	1,975 (2.5%)	689 (1.9%)	<0.001
1	7,039 (6.1%)	5,296 (6.7%)	1,743 (4.9%)	
2	11,073 (9.7%)	8,192 (10.3%)	2,881 (8.1%)	
3	13,865 (12.1%)	10,184 (12.9%)	3,681 (10.4%)	
4	15,378 (13.4%)	11,017 (13.9%)	4,361 (12.3%)	
≥5	64,668 (56.4%)	42,578 (53.7%)	22,090 (62.3%)	
Emergency room visit (Yes)	34,616 (30.2%)	24,842 (31.4%)	9,774 (27.6%)	<0.001

All values are presented as the number (percentage) or mean ± standard deviation (SD).

Risk analysis and risk scoring system in the development cohort

Table 2 shows the mortality risk analysis and risk scores of the development cohort. Approximately 60.5% ($n = 58,241$) of the development cohort had died within a median follow-up period of 2.32 years. The mortality risk of women was lower than that of men [HR (95% CI) 0.72 (0.71–0.74)]. The risk in those aged ≥65 years and 45–64 years was 2.32 (2.19–2.45) and 1.30 (1.23–1.38) times greater than that in those aged 19–44 years, respectively. Current smokers had a 35% higher risk of mortality than non-smokers [1.35 (1.33–1.38)]. Additionally, alcohol drinkers had an 8% higher risk of mortality compared to non-drinkers [1.08 (1.06–1.10)]. Patients that participated in regular exercise [0.85 (0.83–0.86)] had a decreased risk of mortality compared to non-exercisers, while low income patients [1.07 (1.05–1.09)] had an increased risk of mortality compared to patients at other income levels. Obese participants had the lowest risk

TABLE 2 Multivariate cox proportional hazards analysis of the development cohort.

Covariates		*N*	Mortality	IR[a]	HR (95% CI)					
					Model 1[b]	*p*- value	Model 2[c]	*p*- value	B regression coefficient	Point
Sex	Men	65,816	43,374 (65.9%)	25.6	1 (Ref.)		1 (Ref.)		1(Ref.)	
	Women	30,439	14,867 (48.8%)	14.5	0.60 (0.59–0.61)	<0.001	0.72 (0.71–0.74)	<0.001	−0.0965	−5
Age	19–44	3,538	1,408 (39.8%)	10.6	1 (Ref.)		1 (Ref.)		1(Ref.)	
	45–64	37,428	17,887 (47.8%)	14.0	1.29 (1.22–1.36)	<0.001	1.30 (1.23–1.38)	<0.001	0.0753	4
	≥65	55,289	38,946 (70.4%)	29.6	2.55 (2.41–2.69)	<0.001	2.32 (2.19–2.45)	<0.001	0.2667	15
Smoking status	Non	69,916	39,110 (55.9%)	18.4	1 (Ref.)		1 (Ref.)		1(Ref.)	
	Current	26,339	19,131 (72.6%)	32.1	1.63 (1.60–1.66)	<0.001	1.35 (1.33–1.38)	<0.001	0.088	5
Alcohol consumption	No	77,386	45,401 (58.7%)	20.1	1 (Ref.)		1 (Ref.)		1(Ref.)	
	Yes	18,869	12,840 (68.1%)	27.5	1.31 (1.28–1.33)	<0.001	1.08 (1.06–1.10)	<0.001	0.0226	1
Exercise	Non	60,011	38,093 (63.5%)	23.5	1 (Ref.)		1 (Ref.)		1(Ref.)	
	Regular	36,244	20,148 (55.6%)	18.3	0.80 (0.79–0.82)	<0.001	0.85 (0.83–0.86)	<0.001	−0.0539	−3
Income	Others	79,417	47,632 (60.0%)	21.0	1 (Ref.)		1 (Ref.)		1(Ref.)	
	Low	16,838	10,609 (63.0%)	23.1	1.09 (1.07–1.11)	<0.001	1.07 (1.05–1.09)	<0.001	0.0221	1
BMI (kg/m^2)	<18.5	4,672	3,369 (72.1%)	31.4	1.37 (1.32–1.42)	<0.001	1.16 (1.12–1.21)	<0.001	0.0588	3
	18.5–25	62,828	38,580 (61.4%)	22.0	1 (Ref.)		1 (Ref.)		1(Ref.)	
	≥25	28,755	16,292 (56.7%)	18.9	0.87 (0.85–0.89)	<0.001	0.90 (0.89–0.92)	<0.001	−0.0349	−2
Treatment	None	33,927	21,485 (63.3%)	26.4	1 (Ref.)		1 (Ref.)		1(Ref.)	
	Chemotherapy	7,652	6,262 (81.8%)	36.8	1.24 (1.21–1.28)	<0.001	1.24 (1.21–1.28)	<0.001	0.2067	11
	Surgery	15,381	2,525 (16.4%)	3.7	0.15 (0.14–0.16)	<0.001	0.16 (0.16–0.17)	<0.001	−0.3975	−22
	Radiation	16,092	13,086 (81.3%)	42.3	1.43 (1.40–1.46)	<0.001	1.25 (1.22–1.28)	<0.001	0.1585	9
	Surgery + chemotherapy	2,136	770 (36.1%)	8.5	0.34 (0.31–0.36)	<0.001	0.36 (0.34–0.39)	<0.001	−0.2082	−12
	Surgery + radiation	4,863	2,199 (45.2%)	12.3	0.48 (0.46–0.50)	<0.001	0.45 (0.43–0.47)	<0.001	−0.1589	−9
	Chemotherapy + radiation	12,358	10,177 (82.4%)	32.3	1.09 (1.07–1.12)	<0.001	1.20 (1.17–1.23)	<0.001	0.2484	14
	Surgery + chemotherapy + radiation	3,846	1,737 (45.2%)	11.1	0.43 (0.41–0.46)	<0.001	0.49 (0.46–0.51)	<0.001	−0.1037	−6
Number of chronic diseases	0	2,273	1,014 (44.6%)	12.6	1 (Ref.)		1 (Ref.)		1 (Ref.)	
	1	5,940	3,011 (50.7%)	15.3	1.20 (1.11–1.28)	<0.001	1.07 (1.00–1.15)	0.1	0.0181	1
	2	9,203	5,013 (54.5%)	17.5	1.34 (1.26–1.44)	<0.001	1.13 (1.05–1.21)	0	0.0297	2
	3	11,614	6,680 (57.5%)	19.3	1.48 (1.38–1.58)	<0.001	1.18 (1.11–1.26)	<0.001	0.0408	2
	4	12,820	7,509 (58.6%)	20.1	1.53 (1.43–1.64)	<0.001	1.20 (1.12–1.28)	<0.001	0.0444	2
	≥5	54,405	35,014 (64.4%)	24.3	1.81 (1.70–1.93)	<0.001	1.30 (1.22–1.39)	<0.001	0.0716	4
Emergency room visit	No	65,683	35,307 (53.8%)	17.9	1 (Ref.)		1 (Ref.)		1(Ref.)	
	Yes	30,572	22,934 (75.0%)	30.7	1.56 (1.54–1.59)	<0.001	1.28 (1.26–1.31)	<0.001	0.1303	7

HR, hazard ratio; IR, incidence rate. [a]Incidence per 1,000 person-years. [b]Model 1 was not adjusted. [c]Model 1 was not adjusted.

of mortality [0.90 (0.89–0.92)], while underweight participants had the highest risk of mortality according to BMI (1.16 [1.12–1.21]). Participants treated by chemotherapy [1.24 (1.21–1.28)], radiation therapy [1.25 (1.22–1.28)], and chemotherapy combined with radiation therapy [1.20 (1.17–1.23)], had a higher risk of mortality than those who did not undergo treatment. As the number of chronic diseases increased, the risk of mortality increased. Finally, patients who visited the emergency room had a higher risk of mortality than those who did not [1.35 (1.33–1.38)].

In the risk scoring system, participants aged ≥65 years had the highest risk score (15 points), followed by those that underwent combined chemotherapy and radiation therapy (14 points), chemotherapy (11 points), and radiation therapy (9 points), those with a history of emergency room visits (7 points), and current

smokers (5 points). Participants aged 45–64 years and those with ≥5 chronic diseases each scored 4 points. Additionally, participants treated by surgery had the lowest risk score (−22 points), followed by those treated by surgery combined with chemotherapy (−12 points), participants treated by surgery combined with radiation therapy (−9 points), those that underwent surgery combined with chemotherapy and radiation therapy (−6 points), women (−5 points), regular exercisers (−3 points), and those with a BMI ≥25 kg/m^2 (−2 points).

Validation of the risk scoring system in lung cancer

Figure 1 presents the ROC curves for the development and validation cohorts. The area under the curve was 0.82 in the development cohort and 0.80 in the validation cohort. These values show the high discriminative ability of our risk scoring model. Table 3 presents the risk of mortality at 1, 3, and 5 years in the development and validation cohorts according to the mortality risk category. Among both cohorts, as the risk category increased, the percentage of the risk of mortality increased in all time periods. The C statistics in the development and validation cohorts were 0.78 (0.77–0.78) and 0.81 (0.78–0.84), respectively. As shown in the Kaplan–Meier survival curves according to risk category, the survival rate decreased as the follow-up period increased, and the slope of the graph became steeper from the low-risk to high-risk group (Figure 2).

Discussion

Our study showed the risk and preventive factors for mortality and developed a risk scoring system for mortality among patients with lung cancer. We also performed external validation of our system using nationwide cohort data in Korea. Advanced age, some types of treatment, and emergency room visits were the strongest risk factors of mortality, while other types of treatment, being female, regular exercise, and obesity were preventive factors of mortality. According to the external validation methods, our risk scoring system accurately predicted the mortality risk of Korean patients with lung cancer.

Our study showed that 10 variables were associated with the risk of mortality in patients with lung cancer. In Thailand, among 17,687 patients with lung cancer that had been admitted to the intensive care unit, the risk of 1-year mortality was increased by 3 and 22%, respectively, in those aged 65–74 years and ≥75 years compared to those aged 18–64 years.[5] Other studies have estimated that the elderly tend to treat and investigate potential illnesses less than younger people because physicians and patients are often less adherent to guidelines in this population (12). Consistent with other risk assessment studies (13, 14), an emergency room visit increased the risk of mortality because it occurred due to general weakness, exacerbation of chronic diseases and lung cancer, and infection. Moreover, current smokers had an independently increased risk of mortality, perhaps because smoking decreases the lung function and lung volume and can worsen chronic diseases (15). In addition, smoking is the strongest risk factor of lung cancer and is associated with cardiovascular and other pulmonary diseases (16). In another study, the hazard ratio of moderate and severe comorbidity ranged from 1.04 to 1.78 compared to no and mild comorbidity among lung cancer patients (17). Cancer patients with severe comorbidity were associated with an increased risk morbidity (18). Finally, individuals with many chronic diseases experience a decreased quality of life, greater use of medical facilities, and decreased physical activity (19, 20).

According to previous studies, the mortality risk of lung cancer differs depending on the type of anticancer treatment (6, 21, 22). Because the lung cancer stage and biopsy were not included in the KNHIS database, we analyzed the type of anticancer treatment. The mortality risk was lowest when patients were treated by surgery, which is consistent with another study (6). Similarly, surgery has been found to be among the best treatment strategies for non-small cell lung cancer stage IA to IIB and limited-stage small cell lung cancer (23). Therefore, patients treated by surgery had a lower mortality risk because they were in the early stages of disease. On the other hand, advanced lung cancer patients tended to undergo chemotherapy (23).

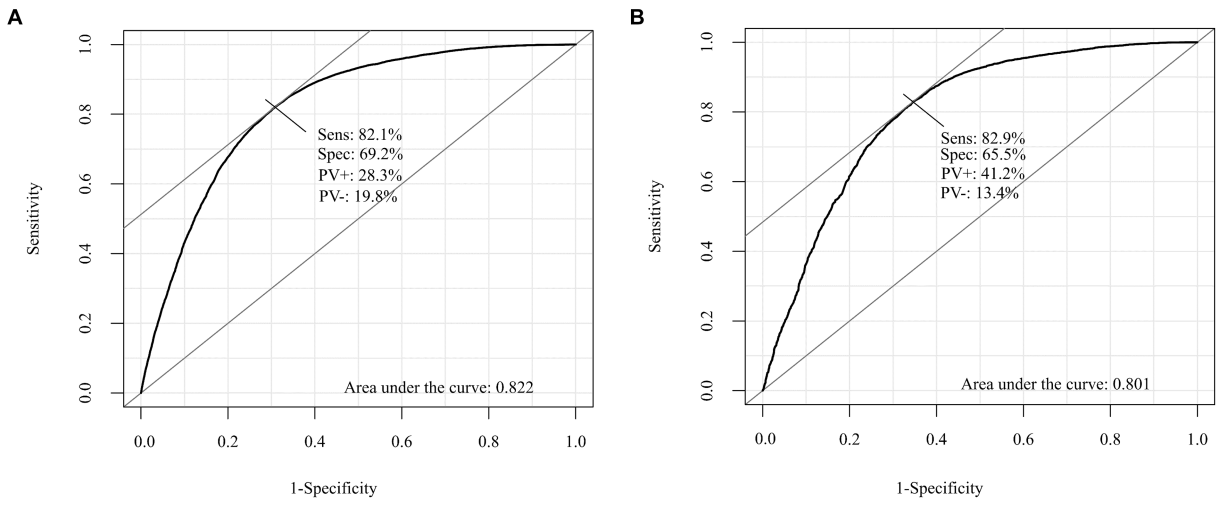

FIGURE 1
Receiver operating characteristic (ROC) curve for the development and validation cohorts. **(A)** The development cohorts. **(B)** The validation cohorts.

TABLE 3 Risk of mortality at one, three, and 5 years in the development and validation cohorts.

Risk category	Development cohort (Seoul)				Validation cohort (Busan and Gyeongsangnam-do)			
		Percentage of mortalities (95% CI)						
		At 5 years	At 1 year	At 3 years		At 5 years	At 1 year	At 3 years
Low	14,176 (14.7%)	11 (10–12)	3 (2–4)	8 (7–9)	1,536 (8.3%)	17 (10–24)	5 (4–7)	12 (8–16)
Intermediate	17,961 (18.7%)	35 (33–36)	13 (11–15)	26 (25–28)	2,426 (13.2%)	40 (36–44)	19 (15–23)	33 (29–37)
High	64,118 (66.6%)	78 (77–79)	40 (39–41)	69 (68–70)	14,470 (78.5%)	84 (83–86)	52 (50–54)	78 (75–81)
		Difference in probability of mortality[a]			Difference in probability of mortality[a]			
		0.67	0.37	0.61		0.67	0.47	0.66
C statistic[b] (95% CI)		0.78 (0.77–0.78)				0.81 (0.78–0.84)		

[a]The difference in the probability of mortality between the high- and low-risk groups was calculated as (Phigh-Plow)/100. [b]The C statistic for the overall score is presented.

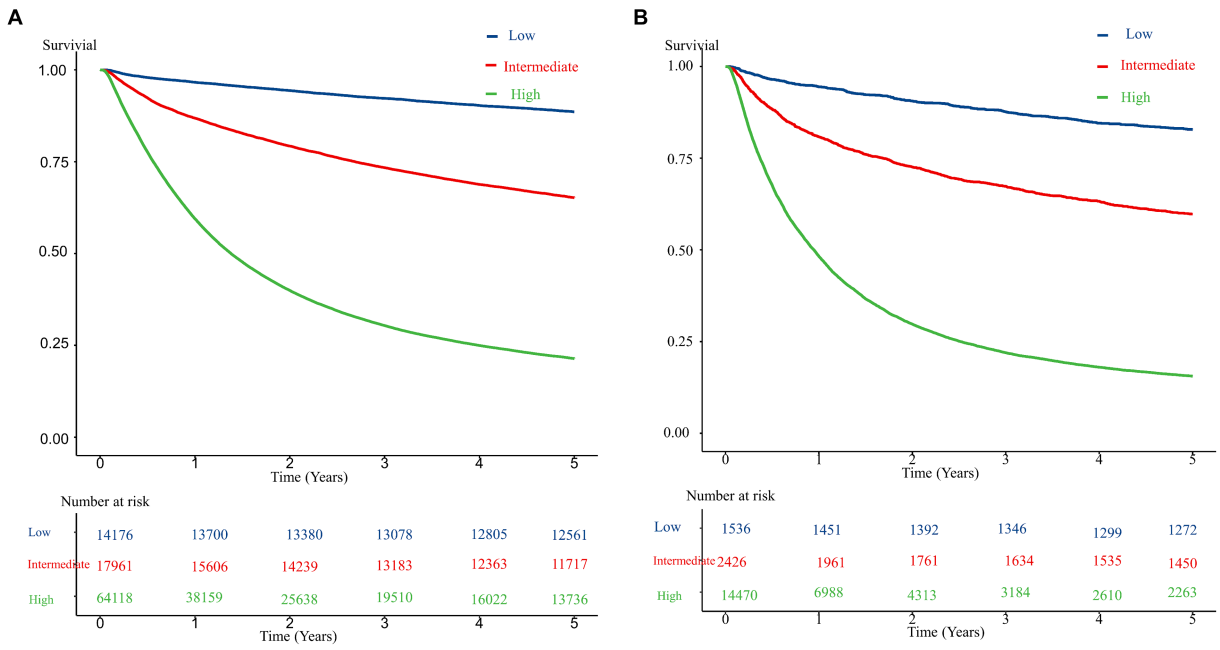

FIGURE 2
Kaplan–Meier survival curve for the development and validation cohorts according to risk level. **(A)** The development cohorts. **(B)** The validation cohorts.

A meta-analysis showed that high BMI decreased mortality risk in patients with lung cancer. Specifically, a BMI increase of 5 kg/m^2 decreased the mortality risk by 12% (24). Consistent with those results, our study found that underweight patients experienced an increased mortality risk, while those with obesity had a decreased mortality risk.

Being a woman and regular exercise were the main preventive factors of lung cancer-related mortality. Unlike the pattern in other countries, in Korea, the prevalence of lung cancer among men was much higher than that among women (3) because of the significant difference between smoking habits in men and women (25). Previous studies have shown that screening tests (26) and healthy smoking- and alcohol-related behaviors (27) affect cancer-related mortality among men and women. Furthermore, among 38,000 American men, high- and moderate-intensity exercise resulted in a 57 and 52% lower mortality risk than low-intensity exercise, because exercise may improve immune function and systemic inflammation, decrease oxidative stress, and improve pulmonary function (28).

Risk stratification using our risk scoring model could identify at-risk patients and decrease the risk of mortality. Because our model provides comprehensive risk assessment including BMI, income, health behavior, and healthcare use, it can be used for managing the treatment of patients with lung cancer. We used multivariate analysis

to confirm the risk factors of lung cancer. In addition, our risk scoring model was validated using an independent external cohort.

Despite the advantages of our study, it had some limitation. First, the KNHIS database is used for prescription purposes, and chronic diseases might be over-diagnosed or under-diagnosed if the diagnosis codes were unclear. In addition, the KNHIS did not include the stage and biopsy results of lung cancer, which is the most important prognostic factor of cancer; therefore, it was adjusted by the type of treatment. In addition, because we did not used cancer registration data, the exact incidence rate and primary cancer status cannot be unclear. Third, although we considered many confounders that could affect mortality among patients with lung cancer, we did not include confounders that were not included in the KNHIS, such as the care provider and pulmonary function. Finally, because the present study was conducted on the population of only one country, we were unable to establish a completely different validation cohort from the development cohort. Despite the limitations, we identified risk and preventive factors of mortality among patients with lung cancer and validated our risk scoring system using an external validation cohort. Therefore, this study could be helpful in identifying patients' likelihood of survival.

In conclusion, we developed a risk scoring system to predict the risk of mortality among patients with lung cancer. Advanced age, cancer stage, and some types of anticancer treatment were strong risk factors of mortality in patients with lung cancer. In contrast, being female, some types of anticancer treatment, and exercise were preventive factors of mortality in patients with lung cancer. These results will aid clinicians in predicting the risk of mortality and appropriately managing lung cancer patients.

Data availability statement

The data analyzed in this study is subject to the following licenses/restrictions: the dataset analyzed in the present study is available from the corresponding author upon reasonable request. Requests to access these datasets should be directed to KS, mdsky75@gmail.com.

Ethics statement

This study adhered to the principles of the Declaration of Helsinki and was approved by the Institutional Review Board of Uijeongbu Eulji Medical Center (IRB no. UEMC 2021–08-022). The requirement for informed consent was waived by the Institutional Review Board of Uijeongbu Eulji Medical Center due to the use of anonymized and de-identified data.

Author contributions

YH: Conceptualization, Data curation, Investigation, Methodology, Writing – original draft. H-RK: Data curation, Formal analysis, Methodology, Writing – review & editing. HK: Conceptualization, Investigation, Writing – review & editing. KS: Conceptualization, Data curation, Methodology, Supervision, Validation, Visualization, Writing – original draft, Writing – review & editing.

Funding

The author(s) declare that financial support was received for the research, authorship, and/or publication of this article. This study was supported by a National Research Foundation of Korea (NRF) grant funded by the Korean government (MSIT) (No. NRF-2021R1G1A1091986) (YH).

Acknowledgments

We would like to thank the Korean National Health Insurance Corporation and all the participants of the study.

Conflict of interest

The authors declare that the research was conducted in the absence of any commercial or financial relationships that could be construed as a potential conflict of interest.

Publisher's note

References

1. Sung H, Ferlay J, Siegel RL, Laversanne M, Soerjomataram I, Jemal A, et al. Global cancer statistics 2020: GLOBOCAN estimates of incidence and mortality worldwide for 36 cancers in 185 countries. *CA Cancer J Clin*. (2021) 71:209–49. doi: 10.3322/caac.21660

2. Siegel RL, Miller KD, Fuchs HE, Jemal A. Cancer statistics, 2022. *CA Cancer J Clin*. (2022) 72:7–33. doi: 10.3322/caac.21708

3. Hong S, Won YJ, Lee JJ, Jung KW, Kong HJ, Im JS, et al. Cancer statistics in Korea: incidence, mortality, survival, and prevalence in 2018. *Cancer Res Treat*. (2021) 53:301–15. doi: 10.4143/crt.2021.291

4. Bunn PA, Shepherd FA, Sandler A, le Chevalier T, Belani CP, Kosmidis PA, et al. Ongoing and future trials of biologic therapies in lung cancer. *Lung Cancer*. (2003) 41:175–86. doi: 10.1016/S0169-5002(03)00161-2

5. Allemani C, Matsuda T, Di Carlo V, Harewood R, Matz M, Nikšić M, et al. Global surveillance of trends in cancer survival 2000-14 (CONCORD-3): analysis of individual records for 37,513,025 patients diagnosed with one of 18 cancers from 322 population-based registries in 71 countries. *Lancet*. (2019) 391:1023–75. doi: 10.1016/S0140-6736(17)33326-3

6. Lai CC, Ho CH, Chen CM, Chiang SR, Chao CM, Liu WL, et al. Risk factors and mortality of adults with lung cancer admitted to the intensive care unit. *J Thorac Dis*. (2018) 10:4118–26. doi: 10.21037/jtd.2018.06.165

7. Lemke KW, Weiner JP, Clark JM. Development and validation of a model for predicting inpatient hospitalization. *Med Care*. (2012) 50:131–9. doi: 10.1097/MLR.0b013e3182353ceb

8. Lewis G, Vaithianathan R, Wright L, Brice MR, Lovell P, Rankin S, et al. Integrating care for high-risk patients in England using the virtual ward model: lessons in the process of care integration from three case sites. *Int J Integr Care*. (2013) 13:e406. doi: 10.5334/ijic.1150

9. Arce RS, De Ormijana AS, Orueta JF, Gagnon MP, Nuño-Solinís R. A qualitative study on clinicians' perceptions about the implementation of a population risk stratification tool in primary care practice of the Basque health service. *BMC Fam Pract*. (2014) 15:1–10. doi: 10.1186/1471-2296-15-150

10. Wennberg D, Dixon J, Billings J. Combined predictive model–final report. London: King's Fund (2006).

11. Goodman RA, Posner SF, Huang ES, Parekh AK, Koh HK. Defining and measuring chronic conditions: imperatives for research, policy, program, and practice. *Prev Chronic Dis*. (2014) 10:120239. doi: 10.5888/pcd10.120239

12. Bandini M, Marchioni M, Pompe RS, Tian Z, Martel T, Chun FK, et al. The effect of age on cancer-specific mortality in patients with small renal masses: a population-based analysis. *Can Urol Assoc J*. (2018) 12:E325–30. doi: 10.5489/cuaj.4854

13. Doñate-Martínez A, Ferrer JG, Rigla FR. Application of screening tools to detect risk of hospital readmission in elderly patients in Valencian healthcare system (VHS)(Spain). *Arch Gerontol Geriatr*. (2014) 59:408–14. doi: 10.1016/j.archger.2014.06.004

14. Dhalla IA, O'Brien T, Morra D, Thorpe KE, Wong BM, Mehta R, et al. Effect of a postdischarge virtual ward on readmission or death for high-risk patients: a randomized clinical trial. *JAMA*. (2014) 312:1305–12. doi: 10.1001/jama.2014.11492

15. Lee SJ, Lee J, Park YS, Lee CH, Lee SM, Yim JJ, et al. Impact of smoking on mortality of patients with non-small cell lung cancer. *Thorac Cancer*. (2014) 5:43–9. doi: 10.1111/1759-7714.12051

16. Piccirillo JF, Tierney RM, Costas I, Grove L, Spitznagel EL Jr. Prognostic importance of comorbidity in a hospital-based cancer registry. *JAMA*. (2004) 291:2441–7. doi: 10.1001/jama.291.20.2441

17. Read WL, Tierney RM, Page NC, Costas I, Govindan R, Spitznagel ELJ, et al. Differential prognostic impact of comorbidity. *J Clin Oncol*. (2004) 22:3099–103. doi: 10.1200/JCO.2004.08.040

18. Soares M, Salluh JI, Ferreira CG, Luiz RR, Spector N, Rocco JR. Impact of two different comorbidity measures on the 6-month mortality of critically ill cancer patients. *Intensive Care Med*. (2005) 31:408–15. doi: 10.1007/s00134-005-2554-z

19. Van Oostrom SH, Picavet HS, de Bruin SR, Stirbu I, Korevaar JC, Schellevis FG, et al. Multimorbidity of chronic diseases and health care utilization in general practice. *BMC Fam Pract*. (2014) 15:1–9. doi: 10.1186/1471-2296-15-61

20. Lehnert T, Heider D, Leicht H, Heinrich S, Corrieri S, Luppa M, et al. Health care utilization and costs of elderly persons with multiple chronic conditions. *Med Care Res Rev*. (2011) 68:387–420. doi: 10.1177/1077558711399580

21. Soares M, Darmon M, Salluh JIF, Ferreira CG, Thiéry G, Schlemmer B, et al. Prognosis of lung cancer patients with life-threatening complications. *Chest*. (2007) 131:840–6. doi: 10.1378/chest.06-2244

22. Chang Y, Huh JW, Hong SB, Lee DH, Suh C, Kim SW, et al. Outcomes and prognostic factors of patients with lung cancer and pneumonia-induced respiratory failure in a medical intensive care unit: a single-center study. *J Critic Care*. (2014) 29:414–9. doi: 10.1016/j.jcrc.2014.01.005

23. Sase K, Fujisaka Y, Shoji M, Mukai M. Cardiovascular complications associated with contemporary lung Cancer treatments. *Curr Treat Options in Oncol*. (2021) 22:1–19. doi: 10.1007/s11864-021-00869-6

24. Wang J, Xu H, Zhou S, Wang D, Zhu L, Hou J, et al. Body mass index and mortality in lung cancer patients: a systematic review and meta-analysis. *Eur J Clin Nutr*. (2018) 72:4–17. doi: 10.1038/ejcn.2017.70

25. Huh Y, Han K, Choi MJ, Kim JH, Kim SM, Nam GE. Association of smoking status with the risk of type 2 diabetes among young adults: a nationwide cohort study in South Korea. *Nicotine Tob Res*. (2022) 24:1234–40. doi: 10.1093/ntr/ntac044

26. Moss S, Mathews C, Day TJ, Smith S, Seaman HE, Snowball J, et al. Increased uptake and improved outcomes of bowel cancer screening with a faecal immunochemical test: results from a pilot study within the national screening programme in England. *Gut*. (2016) 66:1631–44. doi: 10.1136/gutjnl-2015-310691

27. Boyle T, Fritschi L, Platell C, Heyworth J. Lifestyle factors associated with survival after colorectal cancer diagnosis. *Br J Cancer*. (2013) 109:814–22. doi: 10.1038/bjc.2013.310

28. Sui X, Lee DC, Matthews CE, Adams SA, Hébert JR, Church TS, et al. The influence of cardiorespiratory fitness on lung cancer mortality. *Med Sci Sports Exerc*. (2010) 42:872–8. doi: 10.1249/MSS.0b013e3181c47b65

frontiers | Frontiers in Oncology

TYPE Original Research
PUBLISHED 06 November 2024
DOI 10.3389/fonc.2024.1441025

OPEN ACCESS

EDITED BY
Alessandro Leonetti,
University Hospital of Parma, Italy

REVIEWED BY
Lorenzo Belluomini,
University of Verona, Italy
Jing Zhao,
Zhejiang University, China

*CORRESPONDENCE
Kaihua Lu
lukaihua@njmu.edu.cn
Meiqi Shi
shimeiqi1963@163.com

†These authors have contributed equally to this work

RECEIVED 30 May 2024
ACCEPTED 16 September 2024
PUBLISHED 06 November 2024

CITATION
Zhang M, Wang L, Wang Q, Yang J, Peng W, Li X, Shi M and Lu K (2024) Efficacy of disitamab vedotin in non-small cell lung cancer with *HER2* alterations: a multicenter, retrospective real-world study.
Front. Oncol. 14:1441025.
doi: 10.3389/fonc.2024.1441025

Efficacy of disitamab vedotin in non-small cell lung cancer with *HER2* alterations: a multicenter, retrospective real-world study

Meiling Zhang[1†], Li Wang[2†], Qian Wang[1†], Jiu Yang[1], Wei Peng[2], Xiaoyou Li[2], Meiqi Shi[2*] and Kaihua Lu[1*]

[1]Department of Oncology, The First Affiliated Hospital of Nanjing Medical University, Nanjing, China, [2]Department of Medical Oncology, Jiangsu Cancer Hospital & Jiangsu Institute of Cancer Research & The Affiliated Cancer Hospital of Nanjing Medical University, Nanjing, China

Background: Non-small cell lung cancer (NSCLC) with human epidermal growth factor receptor 2 (*HER2*) alterations poses a substantial treatment challenge. Current *HER2*-targeted therapies offer limited efficacy. Antibody-drug conjugates (ADCs) targeting *HER2* have emerged as a promising therapeutic strategy. This study aimed to evaluate the clinical response to a novel ADC drug Disitamab vedotin (RC48) in advanced NSCLC with *HER2* alterations.

Methods: This study conducted a retrospective review of patients harboring *HER2* alterations treated with RC48 in the real world. Clinical outcomes were evaluated in terms of objective response rate (ORR), disease control rate (DCR), and progression-free survival (PFS).

Results: Out of 22 patients, 21 (95.5%) received RC48 combination therapy, while one received RC48 monotherapy. The ORR of all patients reached 45.5%, and the DCR stood at 90.9%. The median PFS (mPFS) was 7.5 months. Among patients receiving RC48 combination therapy, the ORR was 47.7%, and the mPFS of 8.1 months. The combination of RC48 with platinum+/- bevacizumab resulted in the highest ORR of 71.4% (5 out of 7 patients), with *HER2* TKI following at a 50.0% ORR (4 out of 8 patients). First-line (1L) treatment with RC48 showed an ORR of 62.5% (5 out of 8 patients), second-line (2L) treatments had a 57.1% ORR (4 out of 7 patients), and beyond second-line (>2L) treatments exhibited a 14.3% ORR (1 out of 7 patients). Patients with 1L, 2L, or >2L treatment had a mPFS of 8.1 months, 7.2 months, and 7.4 months, respectively. Patients with *HER2* mutations or amplifications, and those with concurrent mutations and amplifications at baseline, showed mPFS of 8.1 months, 9.4 months, and 7.4 months, respectively. The mPFS was significantly longer in patients with *HER2* amplification. The most common adverse events included hand-foot syndrome (54.5%), asthenia (50.0%), decreased white blood cell count (45.5%), and liver impairment (45.5%). Grade 3 adverse events occurred in one (4.5%) patient.

Conclusion: RC48, particularly in combination regimens, demonstrates promising efficacy in advanced NSCLC with *HER2* alterations. These findings underscore the need for further research to validate RC48's application in clinical practice.

KEYWORDS

***HER2* mutation, *HER2* amplification, target, non-small cell lung cancer, RC48**

1 Introduction

Non-small cell lung cancer (NSCLC) with human epidermal growth factor receptor 2 (*HER2*) alterations mainly manifest as protein overexpression, gene amplification, or gene mutation (1–3). *HER2* mutations are found in 1-4% of NSCLC and amplifications are found in 2–5% of cases (4, 5). In comparison to other oncogenic drivers, *HER2* is a distinctive molecular with a poor prognosis (3, 6). The standard first-line treatment for advanced NSCLC with *HER2* alterations, immune checkpoint inhibitor (ICI) therapy, has shown limited clinical activity with an objective response rate (ORR) ranging from 7.4% to 27.3% and median progression-free survival (mPFS) ranging from 1.9 to 2.5 months (7). Tyrosine kinase inhibitors (TKIs) are transformative agents for the treatment of NSCLC, especially in terms of epidermal growth factor receptor (*EGFR*) and anaplastic lymphoma kinase (*ALK*). However, *HER2*-targeted TKIs such as afatinib (8, 9), poziotinib (10, 11), and pyrotinib (12) had moderate efficacy as second- or later-line therapies, with ORRs of 19–30% and mPFS 4.0-6.9 months.

Regarding *HER2*-targeted monoclonal antibodies, previous studies have mostly focused on NSCLC with *HER2* protein overexpression but they have shown limited efficacy (13–15). Antibody-drug conjugates (ADCs), consisting of a monoclonal antibody (mAb) carrying a high-activity cytotoxic drug (payload) via a chemical linker, are one of the fastest growing oncology therapeutics, and are now one of the potential options for lung cancer patients (16, 17). Currently, *HER2* ADCs such as trastuzumab deruxtecan (T-DXd) and ado-trastuzumab emtansine (T-DM1) have shown considerable clinical benefits. Both agents have been recommended as options for *HER2*-mutant NSCLC after progressing with standard treatment by the National Comprehensive Cancer Network (NCCN) guidelines (18). A phase II basket trial of T-DM1 showed an ORR of 44% and mPFS of 5 months in 18 patients with advanced *HER2*-mutant NSCLC patients (19). Another clinical trial reported a 51% ORR for T-DM1 in 49 patients with *HER2*-amplified or -mutant lung cancers (20). However, the efficacy of T-DM1 has not been validated in large-scale samples and has not been approved by the Food and Drug Administration (FDA). The pivotal DESTINY-Lung 02 trial of T-DXd reported a 49% ORR, 9.9 months mPFS, and 19.5 months median overall survival (mOS) in *HER2*-mutant NSCLC (21). Based on this data, the FDA approved 5.4mg/kg T-DXd for the treatment of *HER2*-mutant locally advanced or metastasis NSCLC in August 2022. Nevertheless, 13% of patients treated with T-DXd developed adjudicated drug-related interstitial lung disease (2.0% grade >3), and one patient developed ILD at grade 5, which limits its widespread use in NSCLC patients.

Disitamab vedotin (RC48) emerges as an innovative therapeutic agent, consisting of a humanized anti-*HER2* antibody linked to monomethyl auristatin E (MMAE) via a cleavable linker (22). The National Medical Products Administration of China (NMPA) has approved RC48 for patients with *HER2*-overexpressing metastatic gastric cancer/gastroesophageal junction (G/GEJ) adenocarcinoma after >2L of treatment, and *HER2* IHC2+/3+ metastatic urothelial carcinoma post-platinum-based therapy. To date, RC48 has demonstrated promising antitumor activity and a manageable safety profile in clinical applications.

The purpose of this study is to explore the efficacy and safety of RC48 with unresectable locally advanced or metastatic NSCLC patients harboring *HER2* mutations or amplifications.

Abbreviations: ADC, antibody-drug conjugate; *ALK*, anaplastic lymphoma kinase; CR, complete response; DCR, disease control rate; *EGFR*, epidermal growth factor receptor; FDA, Food and Drug Administration; G/GEJ, gastric cancer/gastroesophageal junction; *HER2*, human epidermal growth factor receptor 2; ICI, immune checkpoint inhibitor; mAb, monoclonal antibody; MMAE, monomethyl auristatin E; mOS, median overall survival; mPFS, median progression-free survival; NCCN, National Comprehensive Cancer Network; NMPA, National Medical Products Administration of China; NSCLC, non-small cell lung cancer; ORR, objective response rate; PR, partial response; RC48, disitamab vedotin; SD, stable disease; T-DM1, ado-trastuzumab emtansine; T-DXd, trastuzumab deruxtecan; TKIs, tyrosine kinase inhibitors.

2 Materials and methods

2.1 Study design and patient population

We conducted a retrospective observational study at The First Affiliated Hospital of Nanjing Medical University (Jiangsu Provincial People's Hospital) and Jiangsu Cancer Hospital & Jiangsu Institute of Cancer Research & The Affiliated Cancer Hospital of Nanjing Medical University, from August 2021 to

March 2023. Patients over 18, diagnosed pathologically with NSCLC of unresectable, locally advanced, or metastatic stage, and confirmed to have *HER2* mutations or amplifications via PCR or NGS, were included. Data cutoff date of July 30th, 2023. Our investigation included a comprehensive review of clinicopathological characteristics, encompassing demographic data, smoking status, ECOG-PS score, cancer stage, and histological type, along with *HER2* genomic alteration status. The specifics of the treatment combination therapies, such as the dosage, treatment cycles, and duration, were documented. Ethical approvals were obtained in Ethical Committees from both institutions.

Of the 40 patients initially screened, patients with incomplete medical records, lacking follow-up, or without documented *HER2* genomic status were excluded. Eventually 22 eligible cases were enrolled in this study.

2.2 Efficacy assessment of treatment

Anonymized data were evaluated for clinicopathologic characteristics and outcomes for RC48 treatment, focusing on ORR, disease control rate (DCR), and PFS. Objective responses were evaluated based on Response Evaluation Criteria in Solid Tumors (RECIST, v1.1), where ORR was defined as the percentage of patients achieving either a complete response (CR) or partial response (PR) to the treatment. DCR was calculated as the proportion of patients exhibiting a CR, PR, or stable disease (SD). PFS was defined as the duration from the onset of treatment to the occurrence of disease progression or death from any cause. Patients experiencing relapse within six months post-systemic anticancer therapy were subsequently classified as receiving second-line treatment for their advanced disease.

2.3 Statistical analysis

For continuous variables, medians and ranges were used to summarize the demographic and clinical characteristics of patients, whereas for categorical variables, frequencies and percentages were used to describe them. The Kaplan-Meier method was employed to analyze survival outcomes. To investigate the impact of different treatments on PFS among various patient subgroups, univariate analyses were conducted. The log-rank test was employed to assess the significance of differences in PFS, with a threshold of $P < 0.05$ for statistical significance. All analyses were performed using R software (version 3.5.1).

3 Results

3.1 Patient characteristics

A total of 22 patients with *HER2*-altered NSCLC receiving monotherapy or combination therapy with RC48 were enrolled from August 2021 and March 2023. A significant majority, representing 90.9% (20 out of 22), had adenocarcinoma histologically. Only a single patient (4.5%) was treated with RC48 as a monotherapy, whereas the remaining 21 (95.5%) received combination therapies. Detailed therapeutic regimens included 8 patients with TKIs, 7 with platinum with or without bevacizumab (3 only with platinum, 4 with platinum combined with bevacizumab), 4 with antiangiogenic drugs, 2 with PD-(L)1 inhibitor with or without bevacizumab. Further demographic and clinical characteristics of the patients are shown in Table 1. Notably, eight (36.4%) patients received RC48 as 1L treatment, while 2L or >2L treatments were received by 7 (31.8%) each. Molecular profiling performed at baseline disclosed 15 patients with *HER2* mutation, 5 with *HER2* amplifications, and 2 harboring both mutation and amplification simultaneously. Brain metastases were observed in 31.8% of the patients.

3.2 Efficacy

Of the 22 patients, 10 (45.5%) patients achieved PR, and 10 (45.5%) patients showed SD, with a confirmed investigator-assessed ORR of 45.5% (10 out of 22) and a DCR of 90.9% (20 out of 22). A waterfall plot for the best percentage change in target lesion size is shown in Figure 1. At the time of data cut-off, survival analysis was conducted on all 22 patients, with the mPFS of 7.5 months (95% CI, 6.6-8.4 months) and the estimated 6-month PFS rate and 12-month PFS rate of 77.9% and 24.4%, respectively (Figure 2A).

Of note, the efficacy of the RC48 combination treatment group showed better performance when compared with monotherapy (Table 2). The mPFS of patients who received RC48 combination therapy was 8.1 months (95% CI, 7.2-9.0 months; Figure 2B). The subgroup receiving RC48 in combination with platinum-based chemotherapy (with or without bevacizumab) achieved an impressive ORR of 71.4% (95%CI: 29.0-96.3%) and the mPFS was not reached. As shown in Table 2, the group of patients treated with RC48 plus *HER2* TKIs achieved a favorable outcome with an ORR of 50.0% (95%CI: 15.7-84.3%) and a mPFS of 7.2 months (95% CI, 3.6-10.8 months; Supplementary Figure S1). Patients receiving RC48 as a first-line treatment (n=8) showed the best efficacy, with an ORR of 62.5% (95% CI, 24.5-91.5%) and a mPFS of 8.1 months (95% CI,7.2-9.0 months). Patients undergoing second-line treatment (n=7) achieved an ORR of 57.1% (95% CI, 18.4-90.1%), and a mPFS of 7.2 months (95% CI, NA-NA). Patients in the >2L treatment group (n=7) had a mPFS of 7.4 months (95% CI, 3.4-11.4 months), although showing a lower ORR of 14.3% (0.4-57.9%), (Table 2, Figures 2C, 3).

Patients with prior anti-*HER2* therapy (n=7) responded to subsequent RC48-based anti-*HER2* treatment with an ORR of 28.6% (95% CI, 3.7-71%) and the mPFS of 7.2 months (95% CI, 3.2-11.2 months; Figure 2D). Among those previously treated with anti-PD-(L)1 inhibitors (n=7), the median treatment line was 3.5 (2-5 line), the ORR was 14.3% (95% CI, 0.4-57.9%), and the mPFS was 7.4 months (95% CI, 3.3-11.5 months; Figures 2E, 3).

10.3389/fonc.2024.1441025

TABLE 1 Patients baseline characteristics and treatment therapies.

Characteristics	N=22
Sex, n (%)	
Male	14 (63.6)
Female	8 (36.4)
Age, median (range), years	61 (45-82)
Smoking history, n (%)	
Never	8 (36.4)
Former	14 (63.6)
Histology, n (%)	
Adenocarcinoma	20 (90.9)
NSCLC-nos	2 (9.1)
Brain metastases, n (%)	
No	15 (68.2)
Yes	7 (31.8)
Stage, n (%)	
III	4 (18.2)
IV	18 (81.8)
ECOG PS score, n (%)	
0	9 (40.9)
1	13 (59.1)
***HER2* alteration status, n (%)**	
Mutation	15 (68.2)
Amplification	5 (22.7)
Concurrent amplification and mutation	2 (9.1)
***HER2* mutation, n (%)**	
Y772_A775dup (exon20)	6 (50.0)
G776delinsVC (exon20)	1 (8.3)
771insAYVM (exon20)	1 (8.3)
A775_G 776insYVMA (exon20)	1 (8.3)
V777_G778insGSP (exon20)	3 (25.0)
V659E (exon17)	1 (33.3)
p.S310Y (exon8)	1 (33.3)
p.L755S (exon19)	1 (33.3)
unknow (exon20)	2 (11.8)
HER2 Amplification, median (range), copy number gain	6.8 (3.0-9.0)
RC48 treatment line, n (%)	
1L	8 (36.4)
2L	7 (31.8)
>2L	7 (31.8)
RC48 treatment line, n (%)	
Prior anti-PD- (L)1 therapy, n (%)	7 (31.8)
Prior anti-HER2 therapy, n (%)	7 (31.8)
RC48 treatment regimen, n (%)	
RC48 alone	1 (4.6)
RC48 combination therapy	21 (95.5)
RC48+ *HER2* TKIs	8 (38.1)
RC48+ Afatinib	1 (4.8)
RC48+ Pyrotinib	7 (33.3)
RC48+ platinum +/- bevacizumab	7 (33.3)
RC48+Carboplatin	2 (9.5)
RC48+ Loroplatin	1 (4.8)
RC48+Carboplatin + bevacizumab	3 (14.3)
RC48+Loroplatin+ bevacizumab	1 (4.8)
RC48+ antiangiogenic drugs	4 (19.1)
RC48+bevacizumab	1 (4.8)
RC48+Anrotinib	3 (14.3)
RC48+ PD- (L)1 inhibitors +/- bevacizumab	2 (9.5)
RC48+PD- (L)1 inhibitors	1 (4.8)
RC48+PD- (L)1 inhibitors + bevacizumab	1 (4.8)
RC48 dosing cycle, n (%)	
2 weeks	1 (4.6)
3 weeks	10 (45.5)
4 weeks	11 (50.0)

HER2, human epidermal growth factor receptor 2; NSCLC, non-small cell lung cancer; ECOG, Eastern Cooperative Oncology Group; PS, performance status; TKI, tyrosine-kinase inhibitor; PD-1, programmed cell death-1; PD-L1, programmed cell death-ligand1; 1L, first line; 2L, second line.

In patients present with baseline brain metastases, the ORR was 28.6% (95% CI, 3.7-71.0%), the DCR was 71.4% (95% CI, 29.0-96.3%; Table 2). The mPFS was 8.1 months (95% CI, 6.9-9.3 months) for patients presenting with baseline brain metastases, compared to 7.5 months (95% CI, 7.3-7.7 months) for those without baseline brain metastases. This comparison revealed no significant difference in mPFS between the two groups (P=0.503; Figures 2F, 3).

Among NSCLC patients harboring *HER2* mutations (n=15), the RC48 treatment regimen had an ORR of 46.7% and a DCR of 86.7%. The *HER2*-amplified subgroup (n=5) showed an ORR of 60.0% and a DCR of 100.0%. In rare cases of concurrent amplification and mutation, the DCR reached 100.0% in both patients (Table 2, Figure 3). The mPFS of patients with *HER2* mutations, amplifications, and concurrent *HER2* mutation and amplification was 8.1 months (95% CI, 4.6-11.6 months), 9.4 months (95% CI,

10.3389/fonc.2024.1441025

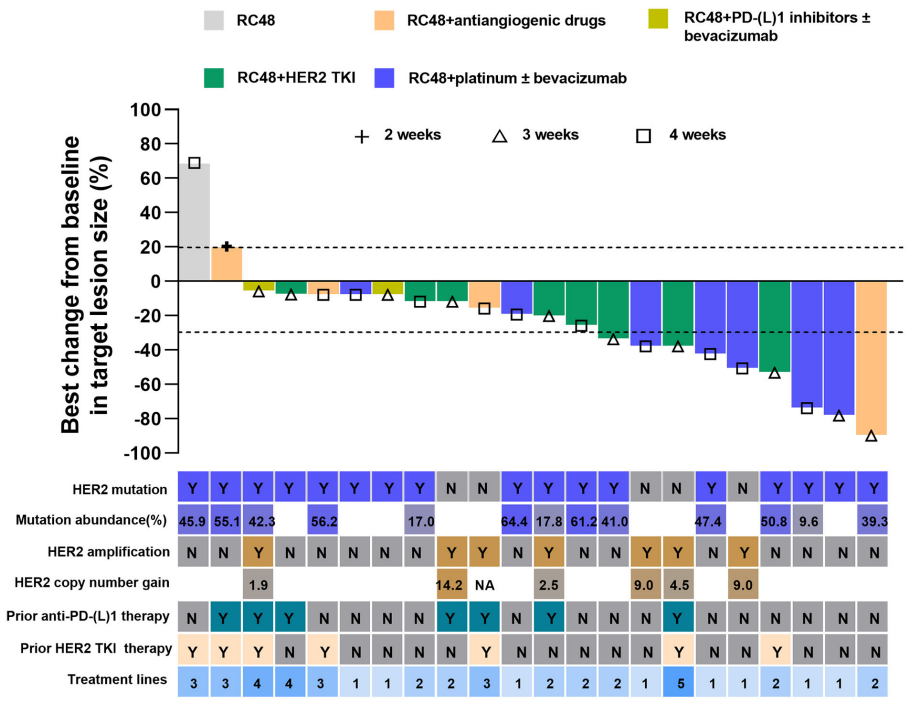

FIGURE 1
Best change from baseline in target lesion size by each patient. The line at -30% indicates a partial response. Alphabet in the *HER2* mutation row or *HER2* amplification row indicate status. Y, yes; N, no; *HER2*, human epidermal growth factor receptor 2; TKI, tyrosine kinase inhibitor; PD-1, programmed cell death-1; PD-L1, programmed cell death-ligand1; CI, Confidence interval.

NA-NA) and 7.4 months (95% CI, NA-NA), respectively (Figure 2G). Median PFS was significantly prolonged in *HER2*-amplified patients, and no significant difference in mPFS was observed (P=0.73).

3.3 Safety

The duration of RC48 treatment ranged from 2 to 19 months with a median treatment period of 5.5 months. Importantly, none of the patients were found to have reduced or discontinued their medication due to side effects during treatment. Adverse events are detailed in Table 3. All patients reported at least one AE. The most common adverse events included hand-foot syndrome (54.5%), asthenia (50.0%), decreased white blood cell count (45.5%), and liver impairment (45.5%). Grade 3 adverse events occurred in one (4.5%) patient.

4 Discussion

HER2-targeted therapeutics have shown favorable antitumor efficacy, including tyrosine kinase inhibitors (afatinib, lapatinib, neratinib, and tucatinib), monoclonal antibodies (mAbs) (trastuzumab, pertuzumab, initumumab), and bispecific antibodies (23). mAbs precisely targets tumor surface antigens. However, its clinical efficacy is often inadequate because its lethality against cancer cells is not inadequate when using mAbs alone. ADC drugs are monoclonal antibodies loaded with a small toxin molecule which specifically targeting cancer cells and then produce a potent toxic effect. ADC drugs make up for the limitations of *HER2*-targeted therapies. Moreover, the ability to exert cytotoxic activity against antigen-negative cells of ADC drugs, also called the bystander effect, allows to overcome tumor heterogeneity (24). RC48 is a novel ADC drug comprised of disitamab coupling with the cytotoxic agent MMAE via a cleavable linker. It was well tolerated and showed promising efficacy in several *HER2*-positive cancers such as breast cancer (25), gastric cancer (26), and urothelial carcinoma (27).

To our knowledge, this is the first study conducted in a real-world setting to report the efficacy and safety of RC48 combination therapy in patients with advanced *HER2*-altered NSCLC. Our findings reveal that RC48 therapy yield a favorable clinical response with an ORR of 45.5%, a DCR of 90.9%, and a mPFS of 7.5 months among *HER2*-altered NSCLC. The combination therapy, particularly, showed enhanced effectiveness with an ORR of 47.6% and a mPFS of 8.1 months, underscoring the significant clinical benefits RC48 may offer to patients with *HER2*-altered NSCLC.

In our study, we observed that the combination therapy (RC48 with platinum-based chemotherapy, with or without bevacizumab) showed an encouraging ORR of 71.4%. Chemotherapy, as cytotoxic

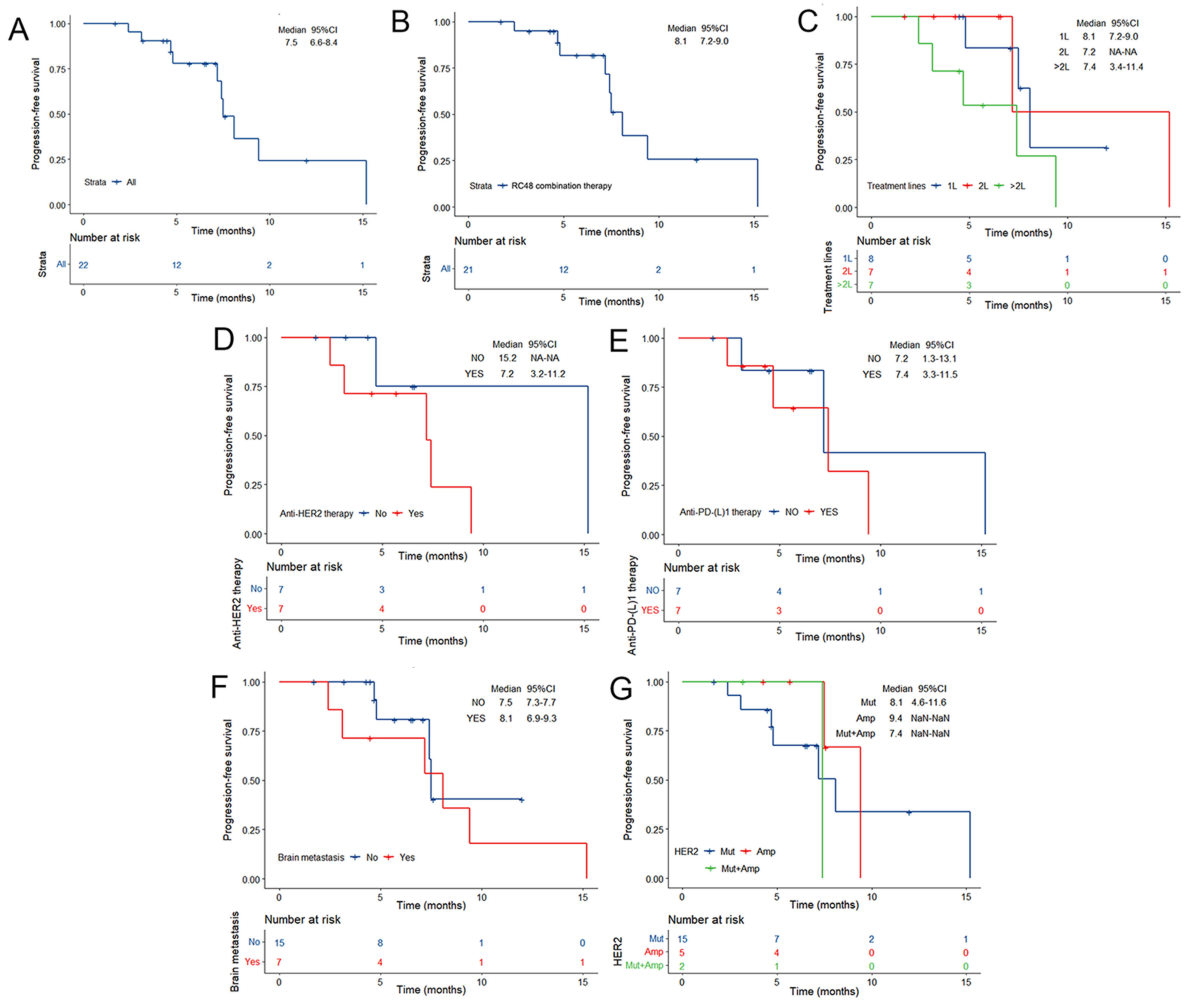

FIGURE 2
Kaplan–Meier estimates of PFS according to **(A)** the overall NSCLC population, **(B)** RC48 combination therapy, **(C)** RC48 treatment line, **(D)** prior anti-*HER2* therapy, **(E)** prior anti-PD-(L)1 therapy, **(F)** brain metastases and **(G)** *HER2* alteration status at baseline. TKI, tyrosine kinase inhibitor; PD-1, programmed cell death-1; PD-L1, programmed cell death-ligand1; CI, Confidence interval. Mut, mutation; Amp, amplification; Mut+ Amp, concurrent mutation and amplification; HER, human epidermal growth factor receptor 2; CI, Confidence interval.

partners of ADCs, can not only interfere with the cell cycle but also modulate the expression of surface antigen targeted by ADCs. Platinum agents, which cause S phase cell cycle arrest and subsequent G2/M phase accumulation, seem to have a synergistic effect with microtubule inhibitors like MMAE within RC48 (28). This combination potential has also been illustrated by carboplatin with mirvetuximb soravtansine (Folate receptor (FR)a-DM4) (29). Furthermore, the well-balanced DAR design of 4 in RC48 also demonstrated a milder toxicity, making it an appealing and flexible companion of platinum in clinical settings (28, 30). As platinum-based chemotherapy still plays a fundamental role in NSCLC treatment, ADCs have the potential to enable the development of highly potent and safe combinations by replacing cytotoxic regimens based on a better understanding of mechanisms. Moreover, antiangiogenic agents may synergistically enhance the delivery of ADCs to tumor cells by normalizing the vasculature and improving treatment sensitivity (6, 31). The combination of anetumab ravtansine with bevacizumab has shown potent effects in ovarian cancer model (32). However, as far as we know, such a combination design has not been tested in clinical trials in NSCLC. Therefore, our data provides real-world evidence for future ADC clinical trial designs of similar combination schemes with antiangiogenesis in NSCLC.

The efficacy of RC48 in combination with *HER2*-TKIs also merits attention, with an ORR of 50.0% and a mPFS of 7.2 months observed in our study. The addition of *HER2*-ADC to pan-HER irreversible inhibitor *HER2*-TKIs, predominantly pyrotinib in our study, demonstrates synergistic efficacy in terms of ORR. In previous studies, pyrotinib monotherapy was shown to have an ORR of 30% as well as an mPFS of 6.9 months in *HER2*-altered NSCLC (12, 33). Co-administration of these agents may enhance the internalization of *HER2*-ADC, eliciting robust antitumor

10.3389/fonc.2024.1441025

TABLE 2 Clinical response to RC48 in the overall *HER2* alterations NSCLC population and subgroups population.

	HER2 alteration status			Brain metastases		RC48 treatment line			Prior anti-PD-(L)1 therapy		Prior anti-*HER2* therapy		RC48 treatment regiment				Overall (N=22)
													RC48 alone	RC48 combined with			
	Mut (N=15)	Amp (N=5)	Mut + Amp (N=2)	Yes (N=7)	No (N=15)	1L (N=8)	2L (N=7)	>2L (N=7)	Yes (N=7)	No (N=7)	Yes (N=7)	No (N=7)	(N=1)	*HER2* TKIs (N=8)	Platinum +/- bevacizumab (N=7)	Antiangiogenic drugs (N=4)	PD-(L)1inhibitors +/- bevacizumab (N=2)	
ORR, n (%) [95% CI]	7(46.7) [21.3-73.4]	3(60) [14.7-94.7]	0 [0-84.2]	2(28.6) [3.7-71.0]	8(53.3) [26.6-78.7]	5(62.5) [24.5-91.5]	4(57.1) [18.4-90.1]	1(14.3) [0.4-57.9]	1(14.3) [0.4-57.9]	4(57.1) [18.4-90.1]	2(28.6) [3.7-71]	3(42.9) [9.9-81.6]	0 [0-97.5]	4(50.0) [15.7-84.3]	5(71.4) [29.0-96.3]	1(25) [0.6-80.6]	0 [0-84.2]	10(45.5%) [24.4-67.8]
CR	0	0	0	0	0	0	0	0	0	0	0	0	0	0	0	0	0	0
PR	7 (46.7)	3 (60.0)	0	2 (28.6)	8(53.3)	5(62.5)	4(57.1)	1 (14.3)	1(14.3)	9(60.0)	2(28.6)	8(53.5)	0	4(50.0)	5(71.4)	1(25.0)	0	10 (45.5)
SD	6(40.0)	2 (40.0)	2 (100.0)	3(42.8)	7(46.7)	3(37.5)	3(42.9)	4 (57.1)	5(71.4)	5(33.3)	3(42.9)	7(46.5)	0	4(50.0)	2(28.6)	2(50.0)	2(100.0)	10 (45.5)
PD	2(13.3)	0	0	2 (28.6)	0	0	0	2 (28.6)	1(14.3)	1	2(28.6)	0	1	0	0	1(25.0)	0	2 (9.1)
DCR, n (%) [95% CI]	13(86.7) [59.5-98.3]	5(100.0) [47.8-100]	2(100.0) [15.8-100]	5(71.4) [29.0-96.3]	15(100.0) [78.2-100]	8(100.0) [63.1-100]	7(100.0) [59.0-100]	5(71.4) [29.0-96.3]	6(85.7) [42.1-99.6]	6 (85.7) [42.1-99.6]	5(71.4) [29.0-96.3]	7(100.0) [59.0-100]	0 [0-97.5]	8(100.0) [63.1-100]	7(100.0) [59.0-100]	3(75.0) [19.4-99.4]	2(100.0) [15.8-100]	20(90.9) [70.8-98.9]

CR, complete response, PR, partial response, SD, stable disease, PD, progressive disease, ORR, objective response rate, DCR, disease control rate; ORR, objective response rate; ECOG, Eastern Cooperative Oncology Group; PS, performance status; *HER2*, human epidermal growth factor receptor 2; Mut, mutation; Amp, amplification; Mut+ Amp, concurrent mutation and amplification; 1L, first line; 2L, second line; TKI, tyrosine kinase inhibitor; PD-1, programmed cell death-1; PD-L1, programmed cell death-ligand1; CI, Confidence inter

activity. Sub-therapeutic doses of TKI could be adequate for enhancing ADC-dependent cell death and tumor shrinkage, thereby reducing the adverse effects associated with the daily use of these agents (20). A concern with pyrotinib is its toxicity, which limits its clinical dosage. The most common TRAE observed with a dose of 400 mg of pyrotinib was diarrhea (92.6%), and the severity was positively in line with the dosage (20, 34). In our study, seven patients received pyrotinib, which was initiated at a low dose of 240 mg, and the dose was increased to 320 mg if no adverse reactions were observed. This combined regimen showed a manageable safety profile with discrete dose management based on patient tolerance. These data also suggest that the combination of RC48 with pyrotinib may be a promising therapeutic approach for *HER2*-altered NSCLC and warrants further comprehensive clinical evaluation.

Our study also differentiated the efficacy of RC48 among various *HER2* alterations and slight differences in efficacy were observed. For *HER2*-mutant NSCLC, the combination treatments exhibited an ORR of 46.7% and a median PFS of 8.1 months, comparable to current *HER2* ADCs like T-DXd and T-DM1 (19, 21). Those data suggest that RC48 presents a potential treatment option in patients with *HER2*-mutated NSCLC. In cases of *HER2* amplification, RC48 combination strategies showed promising results, with an ORR of 60.0% and a mPFS of 9.4 months. A preclinical study suggests that T-DXd could effectively inhibit the proliferation of *HER2*-amplified cells *in vitro* and *in vivo* (35). Other anti-*HER2* therapies include *HER2*-amplified NSCLC patients, such as T-DM1, which shows an ORR of 55% in 14 *HER2*-amplified patients enrolled in a phase II basket trial and pyrotinib, which also showed an ORR of 22.2% and a mPFS of 6.3 months in 22 patients (20, 34). These results suggest that *HER2* amplification may also be a target for anti-*HER2* therapy in NSCLC. However, there still requires large sample size research to prospectively identify optimal amplification cut-off value to target patients who can benefit most from anti-*HER2* therapies.

It is important to note that there was no statistically significant differences in our results, particularly in the mPFS comparisons between patients with and without baseline brain metastases and among different *HER2* alteration subgroups. It might be because the small sample size reduces the statistical power and may not represent a broader patient population

There are several limitations in this study. First, the retrospective nature of the study makes bias inevitable, and prospective studies are needed to validate these results. Second, although this study provided a comprehensive evaluation of all available treatment options and RC48 showed excellent antitumor activity in *HER2*-altered NSCLC, the small sample size reduces the statistical power and caution should be exercised in interpreting these results. Thirdly, this study was conducted during the COVID-19 pandemic, which may also have influenced outcomes, including delays in patient's access to medical care, and delays in RC48 treatment. At last, the retrospective nature of the study may result in underreporting or recall bias in reporting AEs. Therefore, future prospective studies with more rigorous safety monitoring are

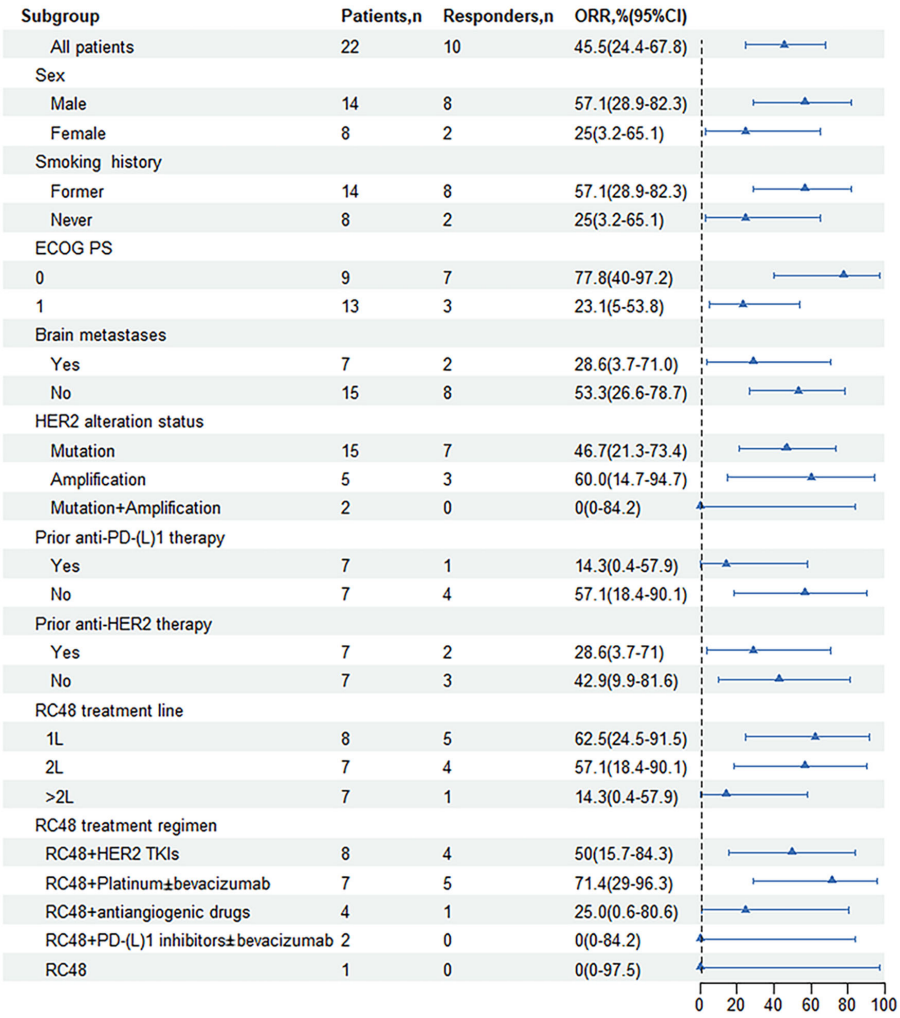

FIGURE 3
Forest plot of subgroup analysis of objective response rates by baseline demographic and disease characteristics. ORR, objective response rate; ECOG, Eastern Cooperative Oncology Group; PS, performance status; *HER2*, human epidermal growth factor receptor 2; Mutation + Amplification, concurrent mutation and amplification; 1L, first line; 2L, second line; TKI, tyrosine kinase inhibitor; PD-1, programmed cell death-1; PD-L1, programmed cell death-ligand1; CI, Confidence interval.

TABLE 3 Adverse events in the patients treated with RC48, n (%).

Event	All grades	Grade 1	Grade 2	Grade 3
Decreased WBC count	10 (45.5)	7 (31.8)	2 (9.1)	1 (4.5)
Hand-foot syndrome	12 (54.5)	12 (54.5)	0	0
Asthenia	11 (50.0)	11 (50.0)	0	0
Liver impairment	10 (45.5)	10 (45.5)	0	0
Anemia	8 (36.4)	7 (31.8)	1 (4.5)	0
Diarrhea	7 (31.8)	6 (27.3)	1 (4.5)	0
Nausea or vomiting	6 (27.3)	6 (27.3)	0	0
Anorexia	6 (27.3)	6 (27.3)	0	0
Decreased platelet count	3 (13.6)	2 (9.1)	1 (4.5)	0
Rash	2 (9.1)	2 (9.1)	0	0

AE, adverse event; WBC, white blood cell.

needed to provide a more comprehensive understanding of the safety profile of RC48.

5 Conclusion

Despite the small sample size, this investigation introduces a viable therapeutic alternative for patients with advanced *HER2*-altered NSCLC, particularly through a regimen incorporating RC48 in conjunction with platinum-based chemotherapy, with or without bevacizumab. RC48-based therapies pave the way for new treatment in the case of HER2-amplified patients. Overall, the safety profile was well tolerated, and no dose reduction or discontinuation of treatment was found due to side effects. However, further studies with larger sample sizes are needed to confirm these preliminary findings. Future research on HER2-targeted ADCs should primarily focus on combination treatment strategies with other treatment modalities, to further improve patients' outcomes.

Data availability statement

The original contributions presented in the study are included in the article/Supplementary Material. Further inquiries can be directed to the corresponding authors.

Ethics statement

The studies involving humans were approved by both the Ethics Committee of The First Affiliated Hospital of Nanjing Medical University (Jiangsu Provincial People's Hospital) and the Ethics Committee of Jiangsu Cancer Hospital & Jiangsu Institute of Cancer Research & The Affiliated Cancer Hospital of Nanjing Medical University. The studies were conducted in accordance with the local legislation and institutional requirements. The ethics committee/institutional review board waived the requirement of written informed consent for participation from the participants or the participants' legal guardians/next of kin because this retrospective study did not involve direct intervention or interaction with study participants.

Author contributions

MZ: Data curation, Formal analysis, Investigation, Writing – original draft. LW: Data curation, Formal analysis, Investigation, Writing – original draft. QW: Data curation, Formal analysis, Investigation, Writing – original draft. JY: Methodology, Supervision, Visualization, Writing – review & editing. WP: Methodology, Supervision, Visualization, Writing – review & editing. XL: Writing – review & editing, Resources. MS: Conceptualization, Methodology, Writing – review & editing, Funding acquisition. KL: Conceptualization, Methodology, Writing – review & editing, Funding acquisition.

Funding

The author(s) declare financial support was received for the research, authorship, and/or publication of this article. This work was supported by the National Natural Science Foundation of China (Grant No. 82172708).

Acknowledgments

The authors would like to thank the patients and their families, clinical researchers, and their teams and hospitals that have participated in this study.

Conflict of interest

The authors declare that the research was conducted in the absence of any commercial or financial relationships that could be construed as a potential conflict of interest.

Publisher's note

Supplementary material

The Supplementary Material for this article can be found online at: https://www.frontiersin.org/articles/10.3389/fonc.2024.1441025/full#supplementary-material

References

1. Passaro A, Jänne PA, Peters S. Antibody-drug conjugates in lung cancer: Recent advances and implementing strategies. *J Clin Oncol.* (2023) 41:3747–61. doi: 10.1200/jco.23.00013

2. Song Z, Yu X, Shi Z, Zhao J, Zhang Y. HER2 mutations in Chinese patients with non-small cell lung cancer. *Oncotarget.* (2016) 7:78152–8. doi: 10.18632/oncotarget.11313

3. Zhang S, Wang W, Xu C, Zhang Y, Cai X, Wang Q, et al. Chinese expert consensus on the diagnosis and treatment of HER2-altered non–small cell lung cancer. *Thorac Cancer.* (2022) 14:91–104. doi: 10.1111/1759-7714.14743

4. Nützinger J, Bum Lee J, Li Low J, Ling Chia P, Talisa Wijaya S, Chul Cho B, et al. Management of HER2 alterations in non-small cell lung cancer - the past, present, and future. *Lung Cancer.* (2023) 186:107385. doi: 10.1016/j.lungcan.2023.107385

5. Jebbink M, de Langen AJ, Boelens MC, Monkhorst K, Smit EF. The force of HER2 - a druggable target in NSCLC? *Cancer Treat Rev.* (2020) 86:101996. doi: 10.1016/j.ctrv.2020.101996

6. Chen J, Xu C, Wang Q, Lv J, Lu W, Zhang Y, et al. Exploration on the first-line treatment of ERBB2-altered advanced non-small cell lung cancer: A multicenter retrospective study. *Lung Cancer.* (2023) 183:107315. doi: 10.1016/j.lungcan.2023.107315

7. Vokes NI, Pan K, Le X. Efficacy of immunotherapy in oncogene-driven non-small-cell lung cancer. *Ther Adv Med Oncol.* (2023) 15:17588359231161409. doi: 10.1177/17588359231161409

8. Peters S, Curioni-Fontecedro A, Nechushtan H, Shih JY, Liao WY, Gautschi O, et al. Activity of afatinib in heavily pretreated patients with ERBB2 mutation-positive advanced NSCLC: Findings from a global named patient use program. *J Thorac Oncol.* (2018) 13:1897–905. doi: 10.1016/j.jtho.2018.07.093

9. Dziadziuszko R, Smit EF, Dafni U, Wolf J, Wasąg B, Biernat W, et al. Afatinib in NSCLC with HER2 mutations: Results of the prospective, open-label phase ii niche trial of european thoracic oncology platform (ETOP). *J Thorac Oncol.* (2019) 14:1086–94. doi: 10.1016/j.jtho.2019.02.017

10. Le X, Cornelissen R, Garassino M, Clarke JM, Tchekmedyian N, Goldman JW, et al. Poziotinib in non-small-cell lung cancer harboring HER2 exon 20 insertion mutations after prior therapies: Zenith20-2 trial. *J Clin Oncol.* (2022) 40:710–8. doi: 10.1200/jco.21.01323

11. Elamin YY, Robichaux JP, Carter BW, Altan M, Gibbons DL, Fossella FV, et al. Poziotinib for patients with HER2 exon 20 mutant non-small-cell lung cancer: Results from a phase II trial. *J Clin Oncol.* (2022) 40:702–9. doi: 10.1200/jco.21.01113

12. Zhou C, Li X, Wang Q, Gao G, Zhang Y, Chen J, et al. Pyrotinib in HER2-mutant advanced lung adenocarcinoma after platinum-based chemotherapy: A multicenter,

open-label, single-arm, phase ii study. *J Clin Oncol*. (2020) 38:2753–61. doi: 10.1200/jco.20.00297

13. Kinoshita TG I, Watanabe K, Maemondo M, Oizumi S, Amano T, Hatanaka Y, et al. A phase II study of trastuzumab monotherapy in pretreated patients with non-small cell lung cancers (NSCLCs) harboring HER2 alterations: HOT1303-B trial. *Ann Oncol* (2018). doi: 10.1093/annonc/mdy292.112

14. Lara PN Jr., Laptalo L, Longmate J, Lau DH, Gandour-Edwards R, Gumerlock PH, et al. Trastuzumab plus docetaxel in HER2/neu-positive non-small-cell lung cancer: A california cancer consortium screening and phase II trial. *Clin Lung Cancer*. (2004) 5:231–6. doi: 10.3816/clc.2004.n.004

15. Langer CJ, Stephenson P, Thor A, Vangel M, Johnson DH. Trastuzumab in the treatment of advanced non-small-cell lung cancer: Is there a role? Focus on eastern cooperative oncology group study 2598. *J Clin Oncol*. (2004) 22:1180–7. doi: 10.1200/jco.2004.04.105

16. Chau CH, Steeg PS, Figg WD. Antibody-drug conjugates for cancer. *Lancet*. (2019) 394:793–804. doi: 10.1016/s0140-6736(19)31774-x

17. Coleman N, Yap TA, Heymach JV, Meric-Bernstam F, Le X. Antibody-drug conjugates in lung cancer: Dawn of a new era? *NPJ Precis Oncol*. (2023) 7:5. doi: 10.1038/s41698-022-00338-9

18. NCCN clinical practice guidelines in oncology (NCCN guidelines®)non-small cell lung cancer. (Version 1.2024).

19. Li BT, Shen R, Buonocore D, Olah ZT, Ni A, Ginsberg MS, et al. Ado-trastuzumab emtansine for patients with HER2-mutant lung cancers: Results from a phase ii basket trial. *J Clin Oncol*. (2018) 36:2532–7. doi: 10.1200/jco.2018.77.9777

20. Li BT, Michelini F, Misale S, Cocco E, Baldino L, Cai Y, et al. HER2-mediated internalization of cytotoxic agents in ERBB2 amplified or mutant lung cancers. *Cancer Discovery*. (2020) 10:674–87. doi: 10.1158/2159-8290.Cd-20-0215

21. Goto K, Goto Y, Kubo T, Ninomiya K, Kim SW, Planchard D, et al. Trastuzumab deruxtecan in patients with HER2-mutant metastatic non-small-cell lung cancer: Primary results from the randomized, phase II destiny-lung02 trial. *J Clin Oncol*. (2023) 41:4852–63. doi: 10.1200/jco.23.01361

22. Li H, Yu C, Jiang J, Huang C, Yao X, Xu Q, et al. An anti-HER2 antibody conjugated with monomethyl auristatin e is highly effective in HER2-positive human gastric cancer. *Cancer Biol Ther*. (2016) 17:346–54. doi: 10.1080/15384047.2016.1139248

23. Oh DY, Bang YJ. HER2-targeted therapies - a role beyond breast cancer. *Nat Rev Clin Oncol*. (2020) 17:33–48. doi: 10.1038/s41571-019-0268-3

24. Wu JM, Lin MT. Effects of specific nutrients on immune modulation in patients with gastrectomy. *Ann Gastroenterol Surg*. (2020) 4:14–20. doi: 10.1002/ags3.12299

25. Li C, Sun L, Liu Z, Sun H, Wang X, Yu Q, et al. Efficacy and safety of disitamab vedotin after trastuzumab for HER2 positive breast cancer: A real-world data of retrospective study. *Am J Cancer Res*. (2024) 14:869–79. doi: 10.62347/emik7909

26. Nie C, Xu W, Guo Y, Gao X, Lv H, Chen B, et al. Immune checkpoint inhibitors enhanced the antitumor efficacy of disitamab vedotin for patients with HER2-positive or HER2-low advanced or metastatic gastric cancer: A multicenter real-world study. *BMC Cancer*. (2023) 23:1239. doi: 10.1186/s12885-023-11735-z

27. Chen M, Yao K, Cao M, Liu H, Xue C, Qin T, et al. HER2-targeting antibody-drug conjugate rc48 alone or in combination with immunotherapy for locally advanced or metastatic urothelial carcinoma: A multicenter, real-world study. *Cancer Immunol Immunother*. (2023) 72:2309–18. doi: 10.1007/s00262-023-03419-1

28. Fuentes-Antrás J, Genta S, Vijenthira A, Siu LL. Antibody-drug conjugates: In search of partners of choice. *Trends Cancer*. (2023) 9:339–54. doi: 10.1016/j.trecan.2023.01.003

29. Ponte JF, Ab O, Lanieri L, Lee J, Coccia J, Bartle LM, et al. Mirvetuximab soravtansine (IMGN853), a folate receptor alpha-targeting antibody-drug conjugate, potentiates the activity of standard of care therapeutics in ovarian cancer models. *Neoplasia*. (2016) 18:775–84. doi: 10.1016/j.neo.2016.11.002

30. Shi F, Liu Y, Zhou X, Shen P, Xue R, Zhang M. Disitamab vedotin: A novel antibody-drug conjugates for cancer therapy. *Drug Delivery*. (2022) 29:1335–44. doi: 10.1080/10717544.2022.2069883

31. Jain RK. Normalizing tumor vasculature with anti-angiogenic therapy: A new paradigm for combination therapy. *Nat Med*. (2001) 7:987–9. doi: 10.1038/nm0901-987

32. Quanz M, Hagemann UB, Zitzmann-Kolbe S, Stelte-Ludwig B, Golfier S, Elbi C, et al. Anetumab ravtansine inhibits tumor growth and shows additive effect in combination with targeted agents and chemotherapy in mesothelin-expressing human ovarian cancer models. *Oncotarget*. (2018) 9:34103–21. doi: 10.18632/oncotarget.26135

33. Liu SM, Tu HY, Wei XW, Yan HH, Dong XR, Cui JW, et al. First-line pyrotinib in advanced HER2-mutant non-small-cell lung cancer: A patient-centric phase 2 trial. *Nat Med*. (2023) 29:2079–86. doi: 10.1038/s41591-023-02461-x

34. Song Z, Lv D, Chen SQ, Huang J, Li Y, Ying S, et al. Pyrotinib in patients with HER2-amplified advanced non-small cell lung cancer: A prospective, multicenter, single-arm trial. *Clin Cancer Res*. (2022) 28:461–7. doi: 10.1158/1078-0432.Ccr-21-2936

35. Odintsov I, Makarem M, Nishino M, Bachert SE, Zhang T, LoPiccolo J, et al. Prevalence and therapeutic targeting of high-level ERBB2 amplification in NSCLC. *J Thorac Oncol*. (2023) 19:732–48. doi: 10.1016/j.jtho.2023.12.019

frontiers | Frontiers in Oncology

TYPE Original Research
PUBLISHED 04 December 2024
DOI 10.3389/fonc.2024.1451589

OPEN ACCESS

EDITED BY
Sharon R. Pine,
University of Colorado, United States

REVIEWED BY
Chuanbo Xie,
Sun Yat-sen University Cancer Center (SYSUCC), China
Shigao Huang,
Air Force Medical University, China

*CORRESPONDENCE
Zilong Lu
lzllzl22@163.com
Aiqiang Xu
aqxuepi@163.com

†These authors have contributed equally to this work

RECEIVED 19 June 2024
ACCEPTED 19 November 2024
PUBLISHED 04 December 2024

CITATION
Jiang F, Fu Z, Chu J, Ren J, Xu C, Xu X, Guo X, Lu Z and Xu A (2024) Lung cancer incidence and mortality in trend and prediction between 2012-2030 in Shandong Province, using a Bayesian age-period-cohort model.
Front. Oncol. 14:1451589.
doi: 10.3389/fonc.2024.1451589

Lung cancer incidence and mortality in trend and prediction between 2012-2030 in Shandong Province, using a Bayesian age-period-cohort model

Fan Jiang[1†], Zhentao Fu[1†], Jie Chu[1], Jie Ren[1], Chunxiao Xu[1], Xiaohui Xu[1], Xiaolei Guo[1], Zilong Lu[1*] and Aiqiang Xu[2*]

[1]Department of Chronic and Non-communicable Disease Control and Prevention, Shandong Center for Disease Control and Prevention, Jinan, China, [2]Institute of Preventive Medicine in Shandong University, Shandong Academy of Preventive Medicine, Jinan, China

Objectives: Lung cancer is one of the most common cancers in Shandong Province, China. Projecting future cancer trend is crucial for planning cancer control. We aimed to examine the trend of lung cancer incidence and mortality from 2012 to 2023, and predict the lung cancer burden to 2030 in Shandong.

Methods: Data of lung cancer incidence and mortality from 2012 to 2023 were obtained from the Shandong Cancer Registries. The average annual percentage change (AAPC) was used to quantify the trend of the lung cancer age-standardised rate using Joinpoint software. Bayesian age-period-cohort model was used to predict lung cancer incidence and mortality from 2024 to 2030.

Results: The age-standardised incidence rate (ASIR) remained stable from 2012 to 2023. The ASIR in males decreased with an AAPC of -1.350%, while the ASIR in females increased with an AAPC of 2.429%. The age-standardised mortality rate (ASMR) decreased with an AAPC of -2.911%. This trend was also observed in males (AAPC=-2.513%), females (AAPC=-3.632%), urban areas (AAPC=-3.267%) and rural areas (AAPC=-2.603%). For our predictions, the ASIR will increase to 49.21 per 100,000 until 2030, with an AAPC of 1.873%. This upward trend is expected for females and urban areas, with an AAPC of 4.496% and 4.176%, while it is not observed for males and rural areas. The ASMR is expected to remain stable up to 2030, and this trend will maintain both in males and females. The ASMR will exhibit an upward trend (AAPC=1.100%) in urban areas and a downward trend (AAPC=-0.915%) in rural areas.

Conclusion: The ASIR of lung cancer will increase until 2030, while the ASMR of lung cancer is expected to remain stable in Shandong. It is necessary to take further preventive measures such as strengthening tobacco control, enhancing health education and expanding screening efforts.

KEYWORDS

lung cancer, incidence, mortality, prediction, Shandong

Introduction

Lung cancer has been the most commonly cancer and the leading cause of cancer death worldwide. According to the latest global cancer statistics estimates in 2022, there have been about 2.48 million new cases of lung cancer in the world, accounting for 12.4% of the total new cases, and about 1.82 million lung cancer deaths, accounting for 18.7% of the total cancer deaths (1). In China, lung cancer has always ranked first in terms of incidence and mortality, with 1.06 million new cases of lung cancer and 0.73 million lung cancer deaths based on the Chinese cancer registry data statistics in 2022 (2).

Since the 1960s, developed countries began to implement tobacco control measures in time to control the growth of lung cancer (3). In the United States, the incidence of lung cancer in men has been decreasing since its peak in 1980s, while the incidence of lung cancer in women has been decreasing since 2005 (4). Nevertheless, in China, the incidence and mortality of lung cancer have increased rapidly in the past 30 years, with an annual increase of 3.7% and 3.3%, respectively. Until in the last decade, the age-standardised incidence rate (ASIR) reached a plateau while the age-standardised mortality rate (ASMR) showed a slight downward trend (5). As the increasing ageing world population, the disease burden of lung cancer will be likely to continue to increase in developing countries especially in China.

Shandong is the second most populous province in China, with 102 million people, accounting for 7.2% of the Chinese population. The large population base leads to large numbers of lung cancer cases and deaths, and the disease burden of lung cancer in Shandong is very heavy. According to data from the Shandong Cancer Registries (6), in 2018, the ASIR and ASMR of lung cancer in Shandong were 42.56 per 100,000 and 29.77 per 100,000 respectively, which were higher than the ASIR and ASMR in China (38.23 per 100,000 and 27.18 per 100,000) (7). In addition, Shandong is one of the provinces with the fastest growth rate in lung cancer incidence and mortality in China (8, 9), and the disease burden of lung cancer was also significantly higher than other provinces in China, such as Henan Province (10), Jiangsu Province (11), Sichuan Province (12), Gansu Province (13) and Jiangxi Province (14). Therefore, understanding and predicting the epidemic trend of lung cancer in Shandong can provide an important basis for the study of lung cancer prevention and control strategies, so as to effectively reduce the burden of lung cancer in Shandong.

Through mathematical models, future cancer burden can be predicted using past surveillance data, based on the assumption that recent incidence or mortality trends will continue to some extent in the future. In particular, Bayesian age-period-cohort model (BAPC) has demonstrated its efficacy as a tool for analysing and predicting incidence and mortality trends (15, 16). In the UK, this model was used to predict cancer incidence and mortality in the country in 2020, 2025, 2030 and 2035 (17–20). Scholars in our country have also used this model to predict the mortality of esophageal cancer and the incidence of lung cancer (21, 22). Currently, few studies were reported on predicting the burden of lung cancer based on population cancer registration data in Shandong Province and even in China. In view of this, our study aimed to provide an estimate of the burden of lung cancer through 2030, to provide the reference basis for formulating the accurate prevention and control policy of lung cancer.

Materials and methods

Data sources

The Shandong Center for Disease Control and Prevention takes on the crucial role of assembling, assessing, and examining cancer-related information from population-based registries. Data for cancer patients was comprehensively furnished by cancer registries in Shandong, which encompassed 13 urban and 22 rural registries in 2023. Lung cancer cases were defined, according to the tenth revision of the International Statistical Classification of Diseases (23), by code C33-C34. The final dataset included variables describing year, sex, age at diagnosis, death age, region (urban or rural area), diagnosis date, death date. Age was divided into 18 subgroups, including 0-4 years, 5-9 years, 10-14 years, and then in 5-year age groups up to 80-84 years, and finally 85 years or older. The population data by sex and age group came from the Census Register of Public Security and the Statistical Yearbook in Shandong. All lung cancer cases in Shandong between 2012 and 2023 were included.

Quality control

The quality of the cancer registration data was assessed according to the standards and requirements of "Guideline for Chinese Cancer Registration (2016)" and International Agency for Research on Cancer/International Association of Cancer Registries (IARC/IACR), including the validity, reliability, completeness and comparability (24, 25). The key indicators for quality control include the mortality to incidence ratio (M/I), the proportion of morphological verification (MV%), and the percentage of cases identified with death certification only (DCO%). Eligible data from cancer registries in 2023 covered 37.46 million people, accounting for 37.52% of the Shandong Province population.

Statistical analysis

Lung cancer data was summarised and analysed using SAS (version 9.4) and Excel (version 2013). We obtained statistics including incidence, age-specific incidence, mortality and age-specific mortality of lung cancer calculated by year, sex, urban and rural areas. The age-standardised rate was adjusted based on the age composition of Chinese standard population in 2000. To assess the overall trends across multiple periods comprehensively, the average annual percentage change (AAPC) was employed to measure the temporal progression of incidence and mortality rates (26). This method captured the rates from 2012 to 2023, reflecting past trends, and from 2024 to 2030, signifying future trends. The

AAPC and 95% confidence intervals (CI) were estimated by Joinpoint (version 4.8.0.1). A positive AAPC indicates an upward trend in incidence (mortality) over this time period, whereas a downward trend if the AAPC is negative (27).

Age-period-cohort model can analyse the effect of age, period and cohort on cancer incidence and mortality, and predict the incidence and mortality according to the effect value of each factor. The classical age-period-cohort model is general linear model. When only age and period factors are included in the model, it is called an age-period model. When only age and cohort factors are included in the model, it is called an age-cohort model. The Epi package in R software can build age-period-cohort model and choose the best model by comparing the deviance of different models. After identifying the factors that need to be incorporated into the model, the model can be used for predictive analysis.

This model was implemented using the Bayesian Age-Period-Cohort Modelling and Prediction package (BAMP) of R (version 4.2.3) (28). Bayesian method can use not only the information of the sample, but also other known information outside the sample, that is, the prior information. The Bayesian method provides a way to calculate the probability of a hypothesis by combining prior information about an unknown parameter with sample information according to a Bayesian formula, then the unknown parameters are inferred according to the posterior information (29). BAMP describes the effect of age, period, and cohort by random walk (RW) priors of different orders (30). The RW-1 prior assumes a constant trend over the time scale, whereas the RW-2 prior assumes a linear time trend (31, 32). The results of the iterations were used to estimate the parameter values for age, period, and cohort effects based on different RW choices through Markov chain Monte Carlo (MCMC) method iterations. The more iterations, the higher the accuracy of the model. This method can smooth the effect of age, period and cohort, and avoid the large fluctuation between the two groups, so that the estimation result is more stable and reliable (33).

In this study, we first observed the change trend of period and cohort factors of lung cancer incidence and mortality using the function of apc.fit and apc.frame in Epi package, and selected the suitable RW combination incorporating the BAMP model. MCMC simulations were run for 1,010,000 iterations with the initial 10,000 iterations used as burn-in to minimize the effect of initial values. The median iterative values and 95% CI (using 2.5% and 97.5% of the 1,000,000 iterated results, respectively) were obtained by the MCMC simulations in the models. Finally, we obtained the predictions of lung cancer incidence and mortality in 2024-2030. The posterior deviance and predictive deviance of the model were used as a measure of the goodness of fit.

Result

Lung cancer incidence and mortality in Shandong, 2012-2023

Table 1 showed the lung cancer incidence in Shandong from 2012 to 2023. The crude incidence rate of lung cancer showed a significant upward trend, increasing from 66.96 per 100,000 to 85.34 per 100,000 (AAPC=2.295%, P<0.01). The ASIR remained stable for the 12-year period. For both males and females, the crude incidence rate displayed an increasing trend, with an AAPC of 1.254% (P=0.01) in males and an AAPC of 4.078% (P<0.01) in females. The ASIR in males decreased from 58.59 per 100,000 to 51.34 per 100,000 (AAPC=-1.350%, P<0.01), while the ASIR in females increased from 28.61 per 100,000 to 35.71 100,000 (AAPC=2.429%, P<0.01). The crude incidence rate showed an increasing trend in rural areas (AAPC=3.549%, P<0.01) but no significant change in urban areas. The ASIR remained stable both in urban and rural areas.

As shown in Table 2, the crude mortality rate of lung cancer in Shandong has been stable from 2012 to 2023. After adjusting the age structure, there was an obvious declined trend exhibited both in males and females, urban and rural areas. The overall ASMR reduced by 2.911% per year (AAPC=-2.911%, P<0.01). In addition, the ASMR in males decreased from 44.75 per 100,000 to 35.09 per 100,000 (AAPC=-2.513%, P<0.01), while the ASMR in females decreased from 20.41 per 100,000 to 14.54 per 100,000 (AAPC=-3.632%, P<0.01). The ASMR in urban and rural areas reduced from 28.17 per 100,000 and 35.69 per 100,000 to 21.41 per 100,000 and 27.14 per 100,000, respectively (Urban AAPC=-3.267%, P<0.01; Rural AAPC=-2.603%, P<0.01).

Age-period-cohort analysis of the lung cancer incidence and mortality

We compared the residual deviance of different sub-models after including age, period and cohort factors, and then selected the best model to predict the future incidence and mortality of lung cancer. Tables 3, 4 showed the change in deviance in the sequential building of the models. Results showed that the deviance value of the age-period-cohort model (APC) for lung cancer incidence was 1217.01, indicating a good fit of the model compared with the age-cohort model (1817.48 for AC) and age-period model (1880.92 for AP). The APC model was also fitted to male, female, urban and rural populations. The deviance value of the APC model (827.12) for mortality was significantly better than the AC model (1084.97) and the AP model (1578.57). Therefore, our subsequent estimations were based on the APC model.

We plotted the crude incidence and mortality rates of lung cancer by age, period and cohort effects. Figures 1, 2 illustrated the observed crude rates in 1-year period and 5-year age group, excluding the age group under 30 years old because of the rare cases. The incidence rates increased with age in every period, rising substantially after aged 55 years, peaking at aged 80 years, and decreasing slightly aged 85 years (Figure 1A). During the period of 2012-2023, the incidence rates remained relatively stable among age groups under 75 years, while it decreased with the period among age groups above 75 years (Figure 1B). Cohort trends suggested that the cohort effect increased across age groups but diminished sharply within each period (Figures 1C, D). From 2012 to 2023, the mortality rates increased with age in every period, and displayed a fluctuating downward trend for each age group (Figures 2A, B).

TABLE 1 Incidence of lung cancer from 2012 to 2023 in Shandong (per 100,000).

Year	Overall		Male		Female		Urban		Rural	
	Crude Rate	ASIR	Crude Rate	ASIR	Crude Rate	ASIR	Crude Rate	ASIR	Crude Rate	ASIR
2012	66.96	43.00	86.59	58.59	46.96	28.61	65.96	41.45	67.90	44.50
2013	68.05	43.21	87.80	58.80	47.92	28.45	67.84	41.56	68.23	44.62
2014	72.60	43.86	92.95	59.23	51.82	29.52	71.21	41.34	73.75	46.01
2015	70.57	41.28	92.50	57.15	48.16	26.58	74.61	40.52	68.48	41.83
2016	75.04	41.55	97.31	57.03	52.30	27.29	78.39	40.86	72.57	42.11
2017	75.59	41.79	96.54	55.91	54.24	28.68	74.36	39.58	76.42	43.37
2018	78.15	42.56	97.55	55.24	58.43	30.83	77.74	40.83	78.49	44.22
2019	85.35	45.47	103.84	57.03	66.59	34.70	82.46	43.08	86.54	46.91
2020	89.45	46.87	108.36	58.47	70.11	36.14	88.02	45.32	90.50	48.08
2021	79.97	41.77	94.38	50.77	65.35	33.88	70.88	38.79	89.63	44.70
2022	80.75	40.55	96.83	50.01	64.4	32.26	71.53	38.00	88.36	42.47
2023	85.34	42.93	99.95	51.34	70.5	35.71	72.08	38.94	100.69	46.97
AAPC (%)	2.295	-0.003	1.254	-1.350	4.078	2.429	0.217	-0.415	3.549	0.346
95% CI (%)	(1.430~3.168)	(-0.809~0.811)	(0.370~2.145)	(-2.003~-0.662)	(2.981~5.186)	(1.150~3.723)	(-0.930~1.377)	(-1.302~0.480)	(2.743~4.362)	(-0.504~1.202)
t	5.95	-0.01	3.17	-4.36	8.41	4.26	0.37	-1.04	9.94	0.91
P	<0.01	0.99	0.01	<0.01	<0.01	<0.01	0.71	0.33	<0.01	0.39

ASIR, age-standardised incidence rate; AAPC, average annual percentage change.

10.3389/fonc.2024.1451589

TABLE 2 Mortality of lung cancer from 2012 to 2023 in Shandong (per 100,000).

Year	Overall		Male		Female		Urban		Rural	
	Crude rate	ASMR	Crude rate	ASMR	Crude rate	ASMR	Crude rate	ASMR	Crude rate	ASMR
2012	50.46	32.00	66.10	44.75	34.54	20.41	45.69	28.17	54.99	35.69
2013	55.44	34.64	72.62	48.40	37.93	22.02	53.83	32.41	56.75	36.52
2014	57.93	34.47	75.71	48.08	39.76	21.94	56.17	32.04	59.37	36.55
2015	55.85	32.00	73.86	45.24	37.44	19.93	56.72	29.81	55.40	33.34
2016	56.82	30.83	75.48	43.80	37.77	18.93	58.61	29.84	55.51	31.63
2017	57.94	31.15	77.55	44.32	37.95	18.99	55.31	28.33	59.71	33.17
2018	57.04	29.77	76.45	42.54	37.30	17.98	55.18	27.30	58.58	32.05
2019	61.02	30.79	80.67	43.10	41.08	19.37	54.98	26.82	64.32	33.28
2020	60.68	29.67	80.87	42.15	40.03	18.11	57.35	27.11	63.11	31.63
2021	51.62	24.6	69.91	36.1	33.08	14.31	43.42	21.45	60.34	27.75
2022	56.62	25.96	76.73	38.09	36.19	15.1	49.56	23.64	62.45	27.79
2023	53.27	24.22	71.39	35.09	34.87	14.54	44.12	21.41	63.87	27.14
AAPC (%)	0.207	-2.911	0.499	-2.513	-0.362	-3.632	-0.605	-3.267	1.301	-2.603
95% CI (%)	(-0.910~1.337)	(-3.932~-1.879)	(-0.586~1.596)	(-3.404~-1.614)	(-1.572~0.863)	(-4.856~-2.392)	(-3.564~2.444)	(-4.572~-1.944)	(0.653~1.952)	(-3.404~-1.796)
t	0.41	-6.23	1.02	-6.18	-0.66	-6.45	-0.39	-5.45	4.49	-7.12
P	0.69	<0.01	0.33	<0.01	0.52	<0.01	0.69	<0.01	<0.01	<0.01

ASMR: age-standardised mortality rate, AAPC: average annual percentage change.

10.3389/fonc.2024.1451589

TABLE 3 Comparison of age-period-cohort sub-models for lung cancer incidence.

Terms in model	Overall		Male		Female		Urban		Rural	
	Residual deviance	*P* value	Residual deviance	*P* value	Residual deviance	*P* value	Residual deviance	*P* value	Residual deviance	*P* value
Age	2474.99	NA	1345.45	NA	2762.91	NA	1903.13	NA	1337.31	NA
Age-drift	2426.36	<0.01	896.39	<0.01	2493.83	<0.01	1778.76	<0.01	1336.05	<0.01
Age-cohort	1817.48	<0.01	737.68	<0.01	1168.78	<0.01	1134.54	<0.01	1195.14	<0.01
Age-period-cohort	1217.01	<0.01	493.93	<0.01	738.80	<0.01	816.27	<0.01	894.09	<0.01
Age-period	1880.92	<0.01	661.76	<0.01	2121.19	<0.01	1525.88	<0.01	1041.07	<0.01

N/A, Not applicable.

The cohort effect increased across age groups and decreased sharply within each period (Figures 2C, D).

Predicted lung cancer incidence and mortality in Shandong, 2024-2030

We predicted the ASIR and ASMR from 2024 to 2030 using the BAPC model, stratified by sexes and regions. The ASIR of lung cancer will increase from 43.38 per 100,000 in 2024 to 49.21 per 100,000 in 2030 (AAPC=1.873%, *P*=0.02) (Table 5). An upward trend is expected for females and urban areas, with the AAPC of 4.496% (*P*<0.01) and 4.176% (*P*<0.01), respectively. No significant change is observed for males and rural areas (Table 5; Figure 3). The ASMR of lung cancer in the overall population, encompassing both males and females, are expected to maintain stability up to the year 2030 (Table 6). An upward trend is expected for urban areas with the AAPC of 1.100% (*P*=0.03). However, for rural areas, the ASMR showed a slightly downward trend with the AAPC of -0.915% (*P*<0.01) (Table 6; Figure 4).

Discussion

In 2023, China has launched the plan of "Healthy China Cancer Prevention and Control Action Implementation (2023-2030)". The plan states that by 2030, the rising incidence and mortality of cancer in China will be curbed, and the disease burden of patients will be effectively controlled. Only by understanding the future development trend of different cancers, we can evaluate the effect of current prevention and control measures and adjust the future prevention and control policies. Shandong is the second most populous province in China, with 102 million people. Lung cancer has the highest incidence and mortality rates of all cancers, in both China and Shandong province. Therefore, our study aimed to analyze and predict the development trend of lung cancer in Shandong, providing data reference for realizing the goal of "Healthy China 2030" to curb the incidence and mortality of lung cancer and optimizing the prevention and control strategy of lung cancer in the future.

In this study, we examined the lung cancer incidence and mortality trend from 2012 to 2023 in Shandong Province. We observed the crude incidence rate of lung cancer displayed an obvious upward trend but the crude mortality rate of lung cancer did not change significantly. However, after adjusting the age structure, the incidence rate remained stable while the mortality rate reduced by 2.911% per year during the 12-year period. These results were in consistent with the outcomes of a nationwide study (5). Other provinces have followed a similar trend. In developed Shanghai, the ASIR of lung cancer increased significantly with an APC of 5.12% from 2010 to 2016, while the ASMR decreased with an APC of 0.87% (34). From 2006 to 2015, the incidence and mortality of lung cancer in Jiangsu Province showed an obvious upward trend, with an average annual increase rate of 4.06% and 3.95% respectively. However, after adjusting the age structure, they tend to be stable (11). In Henan Province, the ASIR and ASMR of lung cancer showed a stable trend during 2010-2019 (10). These results

TABLE 4 Comparison of age-period-cohort sub-models for lung cancer mortality.

Terms in model	Overall		Male		Female		Urban		Rural	
	Residual deviance	*P* value	Residual deviance	*P* value	Residual deviance	*P* value	Residual deviance	*P* value	Residual deviance	*P* value
Age	3654.31	NA	2168.83	NA	1704.27	NA	2190.91	NA	1785.74	NA
Age-drift	1863.62	<0.01	1170.01	<0.01	899.89	<0.01	1183.34	<0.01	1026.16	<0.01
Age-cohort	1084.97	<0.01	568.34	<0.01	666.32	<0.01	760.42	<0.01	679.24	<0.01
Age-period-cohort	827.12	<0.01	466.47	<0.01	510.28	<0.01	674.01	<0.01	510.05	<0.01
Age-period	1578.57	<0.01	1052.77	<0.01	731.05	<0.01	1084.93	<0.01	848.09	<0.01

N/A, Not applicable.

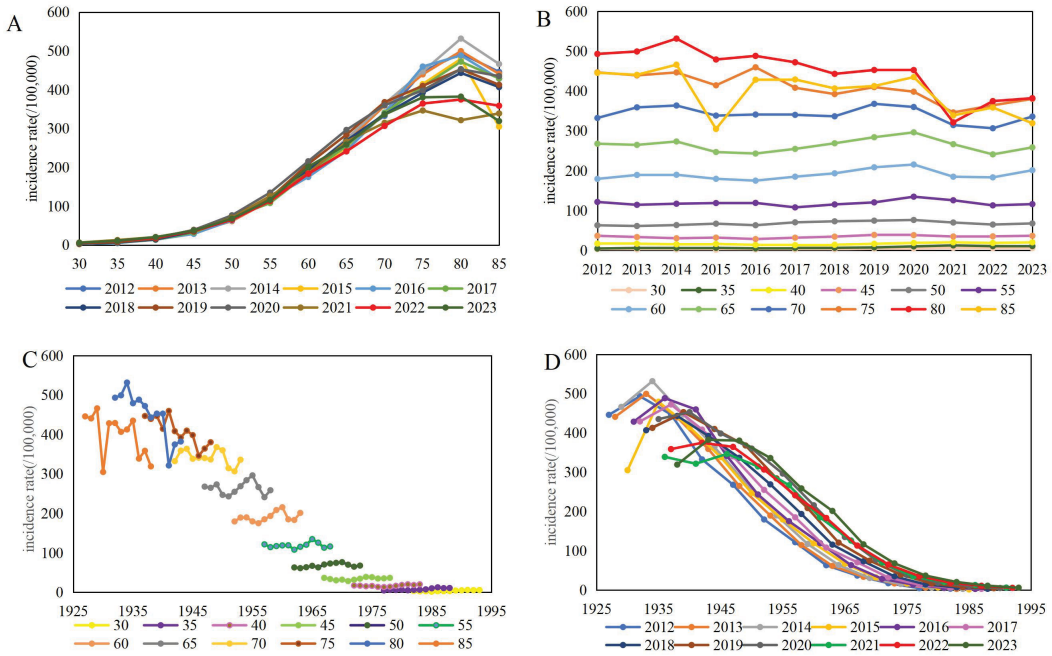

FIGURE 1
Incidence of lung cancer per 100,000 by age, period and cohort effect [**(A)** age trend by period; **(B)** period trend by age; **(C)** cohort trend by age; **(D)** cohort trend by period].

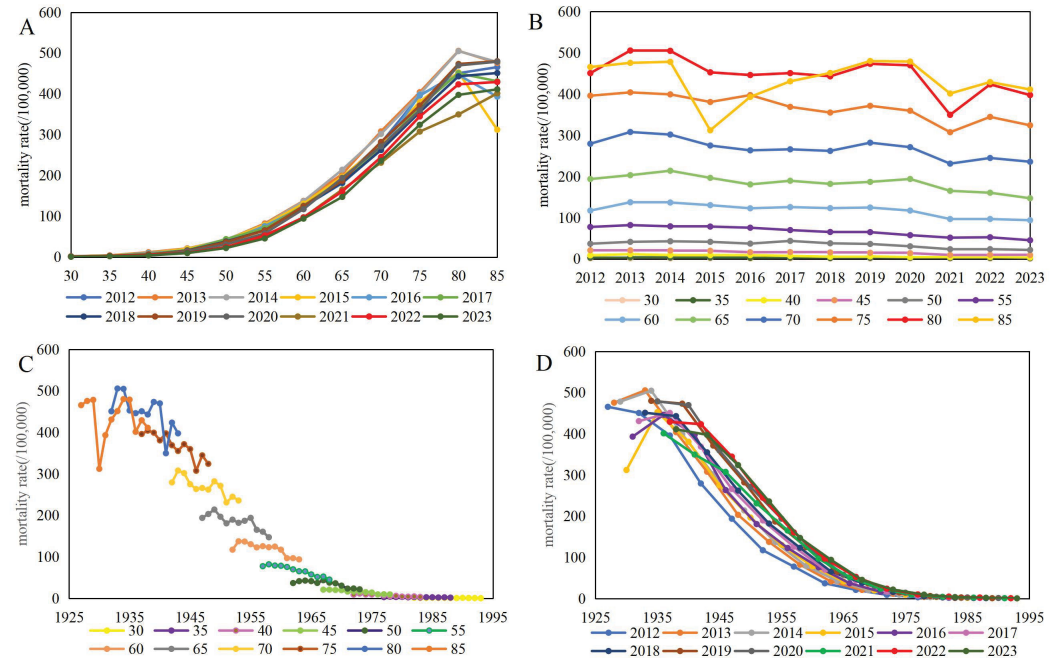

FIGURE 2
Mortality of lung cancer per 100,000 by age, period and cohort effect [**(A)** age trend by period; **(B)** period trend by age; **(C)** cohort trend by age; **(D)** cohort trend by period].

TABLE 5 Incidence of lung cancer from 2024 to 2030 in Shandong predicted by BAMP (per 100,000).

Year	Overall	Male	Female	Urban	Rural
2024	43.38 (38.95~48.34)	51.01 (46.19~56.21)	36.55 (31.04~42.45)	40.74 (35.20~47.20)	46.10 (40.89~51.79)
2025	44.70 (38.46~51.82)	50.95 (44.63~58.17)	38.31 (31.05~47.14)	43.32 (35.73~53.05)	46.14 (39.49~53.96)
2026	43.73 (36.48~52.28)	49.77 (42.50~58.54)	39.16 (30.88~49.87)	42.12 (33.64~54.12)	45.33 (37.53~54.80)
2027	43.91 (35.73~54.18)	49.22 (41.21~59.30)	39.96 (30.12~53.16)	43.18 (33.53~58.10)	44.82 (36.16~55.61)
2028	45.66 (36.32~57.82)	49.74 (40.70~60.95)	42.43 (30.46~58.35)	45.73 (34.68~63.16)	45.56 (35.89~57.57)
2029	46.95 (36.37~61.05)	49.80 (39.72~62.33)	44.86 (31.31~65.55)	49.50 (35.68~72.39)	45.86 (34.98~59.63)
2030	49.21 (37.17~65.64)	49.97 (39.19~63.70)	48.29 (32.80~74.31)	53.13 (37.07~80.77)	46.68 (35.10~62.27)
AAPC (%)	1.873	-0.385	4.496	4.176	0.109
95% CI (%)	(0.291~3.481)	(-1.013~0.247)	(3.588~5.413)	(1.560~6.859)	(-0.503~0.724)
t	2.32	-1.20	9.87	3.15	0.35
P	0.02	0.23	<0.01	<0.01	0.73

AAPC, average annual percentage change.

could be attributed to several advancements. With the implementation of anti-smoking policies and environmental pollution control, the ASIR has been effectively controlled and is gradually becoming stable. Improvements in lung cancer treatment, the establishment of early diagnosis and treatment programs, and advancements in lung cancer screening technology have likely contributed to better patient survival rates and a reduction in mortality. In 2009, lung cancer was included in the "Rural Cancer Early Diagnosis and Early Treatment Project", which initiated the screening of high-risk population of lung cancer in China (35). The urban cancer early diagnosis and treatment program, launched in 2012, also encompasses lung cancer screening initiatives (36). These programs have utilized low-dose spiral CT scans for lung cancer screen. Studies indicates that low-dose spiral CT has been effective in enhancing the early diagnosis rate of lung cancer, subsequently leading to a decrease in mortality rates (37).

Most developed countries, including the UK, the United States, Australia and Canada, male lung cancer incidence showed a stable or even continuous decline. These countries have a smoking epidemic earliest, so the incidence of lung cancer had been high for a long time.

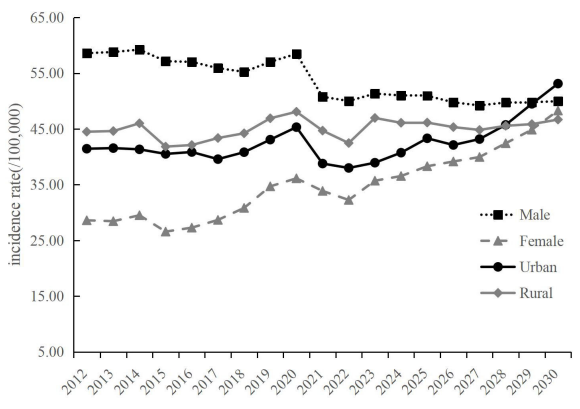

FIGURE 3
Predicted lung cancer incidence of Shandong from 2024 to 2030, by sexes and regions.

They adopted the tobacco control measures relatively early, and as smoking rates fell, so did lung cancer mortality (38). The United States is the most typical country, where smoking rates among men have fallen from 42% in 1990 to 13.7% in 2018 over the past 25 years, resulting in a 45% reduction in male lung cancer mortality (39). However, due to the increasing and aging population, the incidence of lung cancer will continue to increase in the near future, which is a major public health challenge. China is one of the countries with the fastest aging population growth in the world, therefore, lung cancer prevention in our country faces more challenges (40). The successful progress in the prevention and treatment of lung cancer in developed countries such as the United States can be used as a reference for the formulation of lung cancer prevention and treatment strategies in our country (41).

A marked gender disparity was found in the disease burden of lung cancer in Shandong, with men experiencing much higher incidence and mortality rates than female. Additionally, the ASIR in males decreased by 1.35% during the past 12 years, while the ASIR in females increased by 2.43%. The ASMR for both males and females have exhibited a decline, with women experiencing a more pronounced reduction of 3.63% compared to men at 2.51%. These findings corresponded with worldwide observations and our country's data. In global, the world-standard incidence rate of lung cancer was higher in males compared to females over the period from 1990 to 2019. However, the gender gap is progressively diminishing, with a 12.5% reduction for males and a 22.3% increase for females (42). In China, the world-standard incidence rate for lung cancer among men has remained stable or slightly decreased after 2000, while it has increased by approximately 1.0% per year for women (5). It is probable that the gender difference in smoking prevalence accounts for the higher incidence and mortality in males. The persistence of smoking over time is identified as the most influential factor in determining the risk of lung cancer for smokers (43). According to the China Smoking Hazards Report 2020, approximately 296 million are men among the 308 million smokers, while the smoking prevalence for women has consistently been lower (44). In Shandong, the smoking prevalence among men

TABLE 6 Mortality of lung cancer from 2024 to 2030 in Shandong predicted by BAMP (per 100,000).

Year	Overall	Male	Female	Urban	Rural
2024	24.38 (20.89~28.72)	35.46 (30.24~41.03)	14.82(12.26~17.92)	21.69 (17.22~27.43)	27.15 (23.87~30.95)
2025	24.82 (20.02~30.78)	35.84 (28.74~44.05)	15.06(11.61~19.67)	22.77 (16.87~31.39)	26.93 (22.70~32.12)
2026	24.21 (18.57~31.61)	35.77 (27.77~46.30)	14.47(10.58~19.79)	22.24 (15.34~33.64)	26.54 (21.72~33.02)
2027	23.94 (17.81~32.33)	35.43 (26.12~47.60)	14.51(10.1~21.03)	22.13 (14.36~35.30)	26.36 (20.97~33.64)
2028	23.94 (17.27~33.80)	35.64 (25.63~49.48)	14.47(9.82~21.98)	22.70 (14.02~37.83)	26.04 (20.19~34.19)
2029	24.07 (16.70~35.10)	35.54 (24.63~50.82)	14.79(9.44~23.09)	22.84 (13.36~40.30)	26.00 (19.55~34.92)
2030	24.34 (16.20~36.54)	35.46 (23.61~52.85)	14.94(9.31~24.23)	23.81 (13.42~44.58)	25.67 (18.94~35.47)
AAPC (%)	-0.276	-0.073	-0.043	1.100	-0.915
95% CI (%)	(-0.870~0.321)	(-0.301~0.155)	(-0.907~0.829)	(0.137~2.073)	(-1.062~-0.769)
t	-1.19	-0.82	-0.13	2.94	-15.98
P	0.29	0.45	0.90	0.03	<0.01

AAPC, average annual percentage change.

(58.07%) was obviously higher than that among women (1.53%) (45). Therefore, the decline in lung cancer rates among men is largely attributed to effective tobacco control measures. Yet, the increased incidence rate in women is associated with certain specific risk factors, including exposure to secondhand smoke and cooking oil fumes (46, 47). Moreover, advancements in early detection and treatment have intensified the decrease in lung cancer mortality, contributing to prolonged survival rates.

Our results showed that the lung cancer incidence and mortality were higher in rural areas than in urban areas after adjusting the age structure. The higher incidence rate in rural areas may be associated to the lifestyle and environmental factors, particularly the urban-rural divide in the utilization of solid fuels and domestic water resources (48). In addition, the age-standardised mortality rates were on the downward trend both in urban and rural areas in our study, which was largely due to the implementation of effective tobacco control strategies and the inclusion of lung cancer screening in early diagnosis and treatment program.

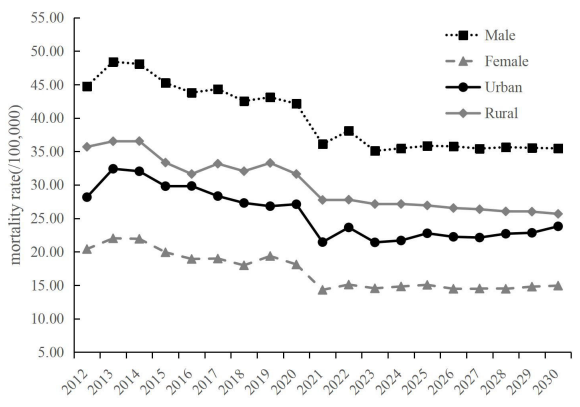

FIGURE 4
Predicted lung cancer mortality of Shandong from 2024 to 2030, by sexes and regions.

Through an age-period-cohort model, we were able to determine the effects of age, period, and cohort on cancer incidence and mortality, representing an essential initial step in understanding the disease's causal mechanisms. The extent of exposure to the vast majority of risk factors increases with age, so that almost all cancer incidence and mortality are positively associated with age (49). The period effect comprises a range of factors that concurrently affect all individuals during a particular time in history such as pollution or healthcare interventions (50). The cohort effect derives from a population-specific experience or exposure in a birth cohort, such as child malnutrition or changing habits during wartime (51, 52). The results showed that age was the key factor of lung cancer incidence and mortality, and the risk of lung cancer and death increased with age, this may be due to body's cumulative exposure to carcinogens and increased mutations over time (53, 54). We also found the age effect was predominantly observed in the elderly population, which could be associated with the increased aging population in China. The period effect in our study showed that the risk of death from lung cancer decreased over time in all age groups. It may be attributed to the enforcement of various cancer prevention and control policies. The cohort effect could be related to an elevated educational level and a greater awareness of the disease prevention and control within the more recent birth cohorts (55). Additionally, after the establishment of the People's Republic of China, the national economy developed steadily, the living environment of the residents improved significantly, and the medical resources continued to expand, leading to a reduction in the risks of lung cancer occurrence and mortality.

The BAPC model offered reliable and stable estimations for disease prediction (33). We predicted the incidence and mortality of lung cancer in Shandong Province from 2024 to 2030 using the BAPC model. Our results show that the ASIR of lung cancer will increase to 49.21 per 100,000 until 2030, with the AAPC of 1.873%. This upward trend is expected for females and urban areas, with the AAPC of 4.496% and 4.176%, while it is not observed for males and rural areas. The ASMR of lung cancer is expected to remain stable up to 2030, and this trend will maintain both in males and females.

For urban areas, the ASMR will exhibit an increasing trend with the AAPC of 1.100%, and in contrast, it will show a slightly decreasing trend with the AAPC of -0.915% for rural areas. With the escalation of the aging population, a steady growth in lung cancer incidence is anticipated throughout the population. It is necessary to take further preventive measures such as strengthening tobacco control, enhancing health education and expanding screening efforts. Additionally, the stabilisation of lung cancer mortality after 2024 year may be mainly influenced by the incidence and survival rate of lung cancer. An increase in incidence may lead to an increase in mortality, while an increase in survival may lead to a decrease in mortality. The results of this study predicts that it shows an upward trend in the ASIR of lung cancer after 2024 year, which may be associated with increased exposure to risk factors, whereas our previous study showed that (56), the relative survival rate of lung cancer increased from 17.6% in 2012-2014 to 24.4% in 2018-2020, mainly due to the improvement of treatment level and the implementation of early diagnosis and treatment program. Therefore, the ASMR of lung cancer tends to be stable with the increase of the ASIR and survival rate.

For the prediction of outcomes in this study we need to be aware that underreporting or diagnostic errors may occur during cancer registration, and therefore part of the results may be underestimated (57). Furthermore, as this study is based on historical data over a short period of time, estimates of future rates should not be overinterpreted. The prediction of cancer burden is the basis of many epidemiological studies, which can provide scientific guidance for cancer prevention and control. Therefore, it is urgent to carry out the research of cancer burden prediction based on the more extensive coverage, more representative data, longer and more complete historical data.

In summary, the age-standardised incidence rate of lung cancer will increase until 2030 in Shandong, while the age-standardised mortality rate of lung cancer is expected to remain stable. The findings will offer valuable insights for a comprehensive understanding of the prevailing lung cancer landscape in Shandong, supplying vital information for healthcare professionals in disease surveillance and control initiatives.

Data availability statement

The raw data supporting the conclusions of this article will be made available by the authors, without undue reservation.

Ethics statement

The studies involving humans were approved by Institutional Review Board of Shandong Center for Disease Control and Prevention. The studies were conducted in accordance with the local legislation and institutional requirements. The participants provided their written informed consent to participate in this study.

Author contributions

FJ: Conceptualization, Data curation, Formal analysis, Investigation, Resources, Software, Validation, Visualization, Writing – original draft, Writing – review & editing. ZF: Conceptualization, Data curation, Formal analysis, Writing – review & editing. JC: Data curation, Supervision, Writing – review & editing. JR: Writing – review & editing, Supervision. CX: Writing – review & editing, Supervision. XX: Writing – review & editing, Data curation. XG: Funding acquisition, Project administration, Supervision, Writing – review & editing. ZL: Project administration, Supervision, Writing – review & editing. AX: Funding acquisition, Project administration, Supervision, Writing – review & editing.

Funding

The author(s) declare financial support was received for the research, authorship, and/or publication of this article. This study was funded by the Taishan Scholar Foundation of Shandong Province (ts201511105), Key Technology Research and Development Program of Shandong Province (2016GSF201231), Medical and health science and technology development project of Shandong Province (202012051127), Medical and health science and technology development project of Shandong Province (202412051228).

Acknowledgments

The authors would like to thank all participants who participated in the study.

Conflict of interest

The authors declare that the research was conducted in the absence of any commercial or financial relationships that could be construed as a potential conflict of interest.

Publisher's note

References

1. World Health Organization. *Global cancer burden growing, amidst mounting need for services* (2024). Available online at: https://www.who.int/news/item/01-02-2024-global-cancer-burden-growing–amidst-mounting-need-for-services (accessed February 1, 2024).

2. Wang SM, Zheng RS, Han BF, Li L, Chen R, Sun KX, et al. Age distribution of cancer incidence and mortality in China in 2022. *China Cancer*. (2024) 33:165–74. doi: 10.11735/j.issn.1004-0242.2024.03.A001

3. GBD 2015 Tobacco Collaborators. Smoking prevalence and attributable disease burden in 195 countries and territories, 1990-2015: A systematic analysis from the Global Burden of Disease Study 2015. *Lancet*. (2017) 389:1885–906. doi: 10.1016/S0140-6736(17)30819-X

4. Siegel RL, Miller KD, Fuchs HE, Jemal A. Cancer statistics, 2022. *CA Cancer J Clin*. (2022) 72:7–33. doi: 10.3322/caac.21708

5. Li X, Gao S. Trend analysis of the incidence, morbidity and mortality of lung cancer in China from 1990 to 2019. *Chin J Prev Contr Chron Dis*. (2021) 29:821–6. doi: 10.16386/j.cjpccd.issn.1004-6194.2021.11.005

6. Ma JX, Guo XL, Fu ZT. Shandong cancer registry annual report 2021. *Shandong Sci Technol Press*. (2022), 34–42.

7. National Cancer Center. *China Cancer Registry Annual Report 2021*. Beijing: People's Medical Publishing House (2023). p. 84–6.

8. National Center for Chronic and Non-communicable Disease Control and Prevention and Chinese Center for Disease Control and Prevention. *The atlases for the main causes of death of Chinese population*. Beijing: China Cartographic Publishing House (2016) p. 89–91.

9. National Office for Cancer Prevention and Control, National Central for Cancer Registry, Disease Prevention and control Bureau and Ministry of Health China. *Chinese cancer mortality report, the third national retrospective survey of death by cause*. Beijing: People' s Medical Publishing House (2010) p. 24–36.

10. Guo XL, Chen Q, Xu HF, Liu Y, Wang XY, Kang RH, et al. Epidemiological characteristics of lung cancer in Henan province in 2019 and its trend from 2010 to 2019. *China Cancer*. (2024) 33:358–65. doi: 10.11735/j.issn.1004-0242.2024.05.A004

11. Wang LC, Zhou JY, Han RQ, Lu Y, Luo PF, Miao WG, et al. Incidence and mortality of lung cancer in Jiangsu province in 2015 and the trend of changes during 2006-2015. *China Cancer*. (2020) 29:579–85. doi: 10.11735/j.issn.1004-0242.2020.08.A004

12. Hu F, Ma Y, Kang H. Death trends and age-period-cohort model analyses of lung cancer, Sichuan, 2007-2021. *Modern Prev Med*. (2024) 51:1370–6. doi: 10.20043/j.cnki.MPM.202401393

13. Lu CX, Ma JX, Ma JH, Zhou H, Xue JJ, Ding GH, et al. Epidemiological characteristics of lung cancer incidence in the tumor registration area of Gansu Province from 2010 to 2019. *Chin J Lung Cancer*. (2024) 27:88–95. doi: 10.3779/j.issn.1009-3419.2024.102.05

14. Liu J, Li ZJ, Yan W, Xu Y, Chen XN. Time trend analysis of lung cancer prevalence and disease burden in cancer registration areas in Jiangxi province. *Chin J Health Statistics*. (2023) 40:730–7. doi: 10.11783/j.issn.1002-3674.2023.05.022

15. Liu ZQ, Jiang YF, Fang QW, Yuan HB, Cai N, Suo C, et al. Future of cancer incidence in Shanghai, China: Predicting the burden upon the ageing population. *Cancer Epidemiol*. (2019) 60:8–15. doi: 10.1016/j.canep.2019.03.004

16. Lin X, Bloom MS, Du ZC, Hao YT. Trends in disability-adjusted life years of lung cancer among women from 2004 to 2030 in Guangzhou, China: A population-based study. *Cancer Epidemiol*. (2019) 63:101586. doi: 10.1016/j.canep.2019.101586

17. Moller H, Fairley L, Coupland V, Okello C, Green M, Forman D, et al. The future burden of cancer in England: incidence and numbers of new patients in 2020. *Br J Cancer*. (2007) 96:1484–8. doi: 10.1038/sj.bjc.6603746

18. Oisen AH, Parkin DM, Sasieni P. Cancer mortality in the United Kingdom: projections to the year 2025. *Br J Cancer*. (2008) 99:1549–54. doi: 10.1038/sj.bjc.6604710

19. Pesola F, Ferlay J, Sasieni P. Cancer incidence in English children, adolescents and young people: past trends and projections to 2030. *Br J Cancer*. (2017) 117:1865–73. doi: 10.1038/bjc.2017.341

20. Smittenaar CR, Petersen KA, Stewart K, Moitt N. Cancer incidence and mortality projections in the UK until 2035. *Br J Cancer*. (2016) 115:1147–55. doi: 10.1038/bjc.2016.304

21. Liu SZ, Zhang F, Quan PL, Lu JB, Liu ZC, Sun XB. Time trends of esophageal cancer mortality in Linzhou city during the period 1988-2010 and a Bayesian approach projection for 2020. *Asian Pac J Cancer Prev*. (2012) 13:4501–4. doi: 10.7314/apjcp.2012.13.9.4501

22. Chen WQ, Zheng RS, Zeng HM. Bayesian age-period-cohort prediction of lung cancer incidence in China. *Thorac Cancer*. (2011) 2:149–55. doi: 10.1111/j.1759-7714.2011.00062.x

23. World Health Organization. *International statistical classification of diseases and related health problems 10th version* (2019). Available online at: https://icd.who.int/browse10/2019/en.

24. National Cancer Center. *Guideline for Chinese Cancer Registration* Vol. 2016. Beijing: People's Medical Publishing House (2016). p. 147–62.

25. Bray F, Parkin DM. Evaluation of data quality in the cancer registry: principles and methods part I: comparability, validity and timeliness. *Eur J Cancer*. (2009) 45:747755. doi: 10.1016/j.ejca.2008.11.032

26. Krishnamoorthy Y, Rajaa S, Giriyappa DK, Bharathi A, Velmurugan B, Ganesh K. Worldwide trends in breast cancer incidence from 1993 to 2012: Age-period-cohort analysis and joinpoint regression. *J Res Med Sci*. (2020) 25:98. doi: 10.4103/jrms.JRMS_708_19

27. Ilic M, Ilic I. Cancer mortality in Serbia, 1991-2015: an age-period cohort and joinpoint regression analysis. *Cancer Commun (Lond)*. (2018) 38:10. doi: 10.1186/s40880-018-0282-3

28. Schmid VJ, Held L. Bayesian age-period-cohort modeling and prediction-BAMP. *J Stat Software*. (2007) 21:1–15. doi: 10.18637/jss.v021.i08

29. Zhu GQ, Liu QO. Mathematical statistics of medicine. *Beijing: Higher Educ Press*. (2006).

30. Berzuini C, Clayton D. Bayesian analysis of survival on multiple time scales. *Stat Med*. (1994) 13:823–38. doi: 10.1002/sim.4780130804

31. Yao Y, Stephan KE. Markov chain Monte Carlo methods for hierarchical clustering of dynamic causal models. *Hum Brain Mapp*. (2021) 42:2973–89. doi: 10.1002/hbm.25431

32. Harrington SM, Wishingrad V, Thomson RC. Properties of markov chain monte carlo performance across many empirical alignments. *Mol Biol Evol*. (2021) 38:1627–40. doi: 10.1093/molbev/msaa295

33. Bray F, Møller B. Predicting the future burden of cancer. *Nat Rev Cancer*. (2006) 6:63–74. doi: 10.1038/nrc1781

34. Dou JM, Wu CX, Pang Y, Bao PP, Wang CF, Gong YM, et al. The incidence and mortality of lung cancer in 2016 and their trends from 2002 to 2016 in Shanghai. *Tumor*. (2023) 43:266–76. doi: 10.3781/j.issn.1000-7431.2023.2206-0436

35. Zhou QH, Fan YG, Wu N, Huang WC, Wang Y, Li L, et al. Demonstration program of population based lung cancer screening in China: Rationale and study design. *Thorac Cancer*. (2014) 5:197–203. doi: 10.1111/1759-7714.12078

36. Dai M, Shi JF, Li N. Project design and target of early diagnosis and treatment of urban cancer in China. *Chin J Prev Med*. (2013) 47:179–82. doi: 10.3760/cma.j.issn.0253-9624.2013.02.018

37. Wei M, Qiao Y. Progress of lung cancer screening with low dose helical computed tomography. *Chin J Lung Cancer*. (2020) 23:875–82. doi: 10.3779/j.issn.1009-3419.2020.101.40

38. Xiao JL, Zheng Y. The global prevalence and prevention progress of lung cancer. *China Oncol*. (2020) 30:721–5. doi: 10.19401/j.cnki.1007-3639.2020.10.001

39. Creamer MR, Wang TW, Babb S, Cullen KA, Day H, Willis G, et al. Tobacco product use and cessation indicators among adults-United States, 2018. *MMWR Morb Mortal Wkly Rep*. (2019) 68:1013–9. doi: 10.15585/mmwr.mm6845a2

40. Xia C, Dong X, Li H, Cao MM, Sun DQ, He SY, et al. Cancer statistics in China and United States, 2022: profiles, trends, and determinants. *Chin Med J (Engl)*. (2022) 135:584–90. doi: 10.1097/CM9.0000000000002108

41. Schilsky RL, Nass S, Le Beau MM, Benz EJ Jr. Progress in cancer research, prevention, and care. *N Engl J Med*. (2020) 383:897–900. doi: 10.1056/NEJMp2007839

42. GBD 2019 Respiratory Tract Cancers Collaborators. Global, regional, and national burden of respiratory tract cancers and associated risk factors from 1990 to 2019: a systematic analysis for the Global Burden of Disease Study 2019. *Lancet Respir Med*. (2021) 9:1030–49. doi: 10.1016/S2213-2600(21)00164-8

43. Doll R, Peto R, Boreham J, Sutherland I. Mortality in relation to smoking: 50 years' observations on male British doctors. *BMJ*. (2004) 328:1519. doi: 10.1136/bmj.38142.554479.AE

44. National Health Commission of the People's Republic of China. *The National Health Commission released "Report on health hazards of smoking in China, 2020"*. Available online at: https://www.gov.cn/xinwen/2021-05/30/content_5613994.htm (accessed May 30, 2021).

45. Li JL, Qiao YJ, Deng LP, Dong HL, Wu BY. Status of smoking, secondhand smoke exposure and cognition of tobacco harm in patients with chronic diseases in Shandong province. *Med J Chin People's Health*. (2018) 30:89–91. doi: 10.3969/j.issn.1672-0369.2018.07.040

46. Jiang DM, Zhang LJ, Liu WB, Ding YB, Yin JH, Ren RB, et al. Trends in cancer mortality in China from 2004 to 2018: A nationwide longitudinal study. *Cancer Commun (Lond)*. (2021) 41:1024–36. doi: 10.1002/cac2.12195

47. Qiu AY, Leng SG, McCormack M, Peden DB, Sood A. Lung effects of household air pollution. *J Allergy Clin Immunol Pract*. (2022) 10:2807–19. doi: 10.1016/j.jaip.2022.08.031

48. Yu K, Qiu GK, Chan KH, Lam KB, Kurmi OP, Bennett DA, et al. Association of solid fuel use with risk of cardiovascular and all-cause mortality in rural China. *JAMA*. (2018) 319:1351–61. doi: 10.1001/jama.2018.2151

49. Wong IOL, Schooling CM, Cowling BJ, Leung GM. Breast cancer incidence and mortality in a transitioning Chinese population: current and future trends. *Br J Cancer*. (2015) 112:167–70. doi: 10.1038/bjc.2014.532

50. Nasreen S, Wilk P, Mullowney T, Karp I. Age, period, and cohort effects on asthma prevalence in Canadian adults, 1994–2011. *Ann Epidemiol*. (2020) 41:49–55. doi: 10.1016/j.annepidem.2019.11.005

51. O'Brien RM. Mixed models, linear dependency, and identification in age-period-cohort models. *Stat Med*. (2017) 36:2590–600. doi: 10.1002/sim.7305

52. Rutherford MJ, Lambert PC, Thompson JR. Age-period-cohort modeling. *Stata J*. (2010) 10:606–27. doi: 10.1177/1536867X1101000405

53. Peto R, Parish SE, Gray RG. There is no such thing as ageing, and cancer is not related to it. *IARC Sci Publ*. (1985) 58):43–53.

54. Campisi J, d'Adda di Fagagna F. Cellular senescence: when bad things happen to good cells. *Nat Rev Mol Cell Biol*. (2007) 8:729–40. doi: 10.1038/nrm2233

55. Rees PH. Education's role in China's demographic future. *Proc Natl Acad Sci USA*. (2021) 118:e2115618118. doi: 10.1073/pnas.2115618118

56. Jiang F, Fu ZT, Lu ZL, Chu J, Guo XL, Xu AQ. Cancer survival during 2012-2018 in cancer registries of Shandong Province. *Chin J Prev Med*. (2022) 56:806–14. doi: 10.3760/cma.j.cn112150-20210910-00882

57. Wei WQ, Zeng HM, Zheng RS, Zhang SW, An L, Chen R, et al. Cancer registration in China and its role in cancer prevention and control. *Lancet Oncol*. (2020) 21:e342–9. doi: 10.1016/S1470-2045(20)30073-5

frontiers | Frontiers in Medicine

TYPE Original Research
PUBLISHED 07 January 2025
DOI 10.3389/fmed.2024.1491337

OPEN ACCESS

EDITED BY
Alessandro Leonetti,
University Hospital of Parma, Italy

REVIEWED BY
Wencai Liu,
Shanghai Jiao Tong University, China
Niu Jinliang,
Second Hospital of Shanxi Medical University, China

*CORRESPONDENCE
Yuanyuan Cai
✉ caiyy830819@126.com

RECEIVED 04 September 2024
ACCEPTED 16 December 2024
PUBLISHED 07 January 2025

CITATION
Meng X, Wang P, Liu J, Sun D, Ju Z and Cai Y (2025) Dynamic assessment of long-term survival in survivors with stage III non-small cell lung cancer: a novel conditional survival model with a web-based calculator.
Front. Med. 11:1491337.
doi: 10.3389/fmed.2024.1491337

Dynamic assessment of long-term survival in survivors with stage III non-small cell lung cancer: a novel conditional survival model with a web-based calculator

Xiangdi Meng[1,2], Peihe Wang[1], Jie Liu[1], Daqing Sun[1], Zhuojun Ju[2] and Yuanyuan Cai[1]*

[1]Department of Radiation Oncology, Weifang People's Hospital, Weifang, China, [2]Department of Radiation Oncology, Gunma University Graduate School of Medicine, Maebashi, Japan

Background: Conditional survival (CS) analysis can estimate further survival probabilities based on the time already survived, providing dynamic updates for prognostic information. This study aimed to develop a CS-nomogram to promote individualized disease management for stage III non-small cell lung cancer (NSCLC).

Methods: This study included patients diagnosed with stage III NSCLC in the Surveillance, Epidemiology, and End Results database from 2010 to 2017 (N = 3,512). The CS was calculated as $CS(y|x) = OS(y + x)/OS(x)$, where $OS(y + x)$ and $OS(x)$ were the overall survival (OS) in the year $(y + x)$ and year x, respectively, calculated by the Kaplan–Meier method. We used the least absolute shrinkage and selection operator (LASSO) regression to identify predictors and developed the CS-nomogram based on these predictors and the CS formula.

Results: The CS analysis provided real-time updates on survival, with 5-year OS improving dynamically from 14.4 to 29.9%, 47.9, 66.0, and 80.8% (after 1–4 years of survival). Six independent predictors (age, tumor size, N status, surgery, radiotherapy and chemotherapy) were identified for the development of the CS-nomogram and its web version (https://dynapp.shinyapps.io/NSCLC/). The model performed with an excellent concordance index (C-index) of 0.71 (95% CI: 0.70–0.72), and a median time-dependent AUC of 0.71–0.73 from 200 iterations 5-fold cross-validation.

Conclusion: The study demonstrated the improvement in real-time OS over time in stage III NSCLC survivors and developed the novel CS-nomogram to provide patients with updated survival data. It provided novel insights into clinical decisions in follow-up and treatment for survivors, offering a convenient tool for optimize resource allocation.

KEYWORDS

conditional survival, non-small cell lung cancer, nomogram, overall survival, prognostic factor

1 Introduction

Non-small cell lung cancer (NSCLC) accounts for approximately 85–90% of all lung cancers (1–6), with 20–30% of cases diagnosed at stage III, a group characterized by substantial heterogeneity (3–7). This heterogeneity poses significant challenges for both treatment and follow-up. Although various treatment strategies, such as surgery, radiotherapy, targeted and immunotherapy, have been used to manage the disease, the prognosis for stage III patients remains unfavorable and individual survival rates vary widely (4, 7–9). Previous studies have confirmed that the real-time prognosis of cancer survivors improved dynamically over time, indicating that initial prognostic assessments at diagnosis may underestimate a patient's current prognosis (10–12). Unfortunately, the lack of personalized assessment tools has prevented survivors from receiving an up-to-date, personalized prognosis. In addition, traditional survival estimates provide only static data tied to the initial diagnosis, underscoring the need for a dynamic monitoring system that can continuously update individualized survival information throughout follow-up.

Conditional survival (CS) analysis predicts future survival using the time survived (13). Compared with traditional survival analysis, CS analysis provided a relatively accurate estimate of the change in patient prognosis over time and allowed real-time updating of survival data (13–15). CS analysis has been widely used in various cancers to optimize clinical decision-making and reduce psychological distress in survivors (16–19). Additionally, several clinicopathological factors, such as age, tumor stage, and treatment strategy, have been demonstrated to impact the individualized prognosis of NSCLC patients (20). The CS nomogram is a tool based on CS analysis and statistical modeling methods that integrated individualized information and considered survival time, allowing real-time updating of survival data for patients at different follow-up time points (15). However, these methods have never been applied to stage III NSCLC.

This study aimed to elucidate changes in survival over time in patients with stage III NSCLC and to develop an easy-to-use CS nomogram and host it on a website to provide individualized, real-time prognostic information to inform patients of their latest survival data and guide optimal clinical decision making.

2 Materials and methods

2.1 Patients and variables selection

After obtaining access to the Surveillance, Epidemiology, and End Results (SEER) database, we collected NSCLC patients aged 18 years or older between 2010 and 2017 according to the International Classification of Diseases for Oncology (ICD-O-3) (site code C34 "Lung and bronchus" and morphology code 8046/3 "non-small cell carcinoma"). In addition, we excluded the following patients: (1) not stage III (American Joint Committee on Cancer 7th edition, AJCC 7th); (2) not confirmed by histopathology; (3) not the first primary tumor; (4) survival time less than 1 month; (5) necessary variables (age, race, marriage, gender, staging, surgery) were unknown. For the continuous variable (age), grouping was performed using a restricted cubic spline (RCS) with a cut-off point of 70 years before analysis. Tumor size was divided into groups for every 10 mm, and 70 mm or more was grouped as a separate group. Given the difficulty in determining the number of specific positive lymph node metastases in unoperated patients, lymph node metastases were grouped according to the AJCC 7th N stage. The primary clinical endpoint was overall survival (OS), defined as the time from patient diagnosis to death.

2.2 Statistical analysis

Means and standard deviations (SDs) were reported for continuous variables that followed a normal distribution. Otherwise, medians and interquartile ranges (IQRs) were reported. In addition, categorical variables were presented as numbers and percentages of cases. The Kaplan–Meier method was used to estimate overall survival (OS) in patients with stage III NSCLC.

The CS was calculated using the formula $CS(y|x) = OS(y + x)/OS(x)$, where x and y represented the survived time after diagnosis and the expected further survival time, respectively (13). For example, to calculate the real-time survival rate for patients who have survived 2 years after diagnosis for another 3 years would be $CS(3|2) = OS(3 + 2)/OS$ (2), which was 5-year OS divided by 3-year OS. In addition, the study used annual hazard rates to show the annual risk of death after the patient's diagnosis.

We used the least absolute shrinkage and selection operator (LASSO) regression to screen predictors to improve the underfitting or overfitting of the model and multivariate Cox regression to show the effect of predictors on survival. A nomogram was developed using the screened predictors to estimate individualized survival, and real-time OS was further accurately calculated based on the CS formula to develop a CS-nomogram. After entering the patient's individualized parameters, the model quantified the predictors as risk scores and calculated the total risk score, which corresponded to the individualized OS and informed the patient of the real-time OS after several years of survival. For ease of use, we deployed its web version, which provided survival predictions accurate to the month. Finally, we evaluated the performance of the CS-nomogram by reporting concordance index (C-index), time-dependent receiver operating characteristic (ROC) curves, calibration plots, decision curve analysis (DCA) curves and 200 times of 5-fold cross-internal validation.

3 Results

A total of 3,512 patients with locally advanced (stage III) NSCLC were included in the study (Figure 1), with a median age of 69 years (SD = 10.9 years). The majority of patients were of white with 79.9% (2,806/3,512), followed by black with 13.9%. In the whole cohort, 45.4 and 54.6% of patients were classified as stage IIIA and IIIB, respectively. The majority of patients underwent surgery (93%, 3,266/3,512). In addition, 63.0% (2,214/3,512) and 64.5% (2,265/3,512) of patients received radiotherapy and chemotherapy, respectively (Table 1).

The median follow-up of the study was 12 months (IQR: 5 months, 29 months), with 1-, 3-, and 5-year OS of 48.1% [95% confidence interval (CI): 46.5–49.8%], 21.8% (95% CI: 20.5–23.2%), and 14.4% (95% CI: 13.2–15.7%), respectively (Figure 2A). CS analysis showed that the real-time survival estimates of patients after diagnosis gradually improved over time, with 5-year OS increasing from an initial 14.4 to 29.9%, 47.9, 66.0, and 80.8% each year (Figure 2B). In addition, the annual hazard rate curve showed that the all-cause mortality rate for patients with stage III NSCLC decreased each year and remained relatively stable after the fourth year (Figure 2B).

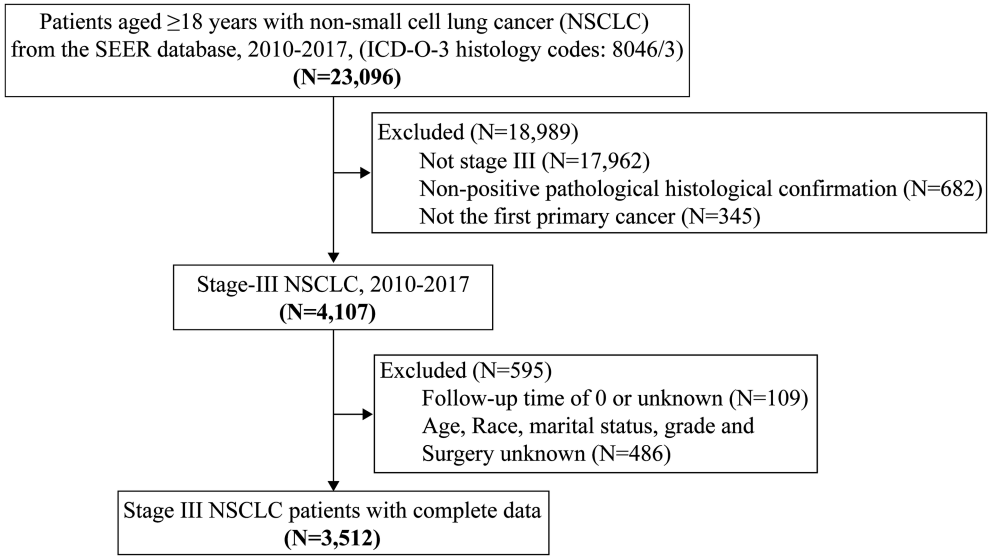

FIGURE 1
Flow chart for screening patients with Stage III non-small cell lung cancer.

TABLE 1 Clinicopathological characteristics of stage III non-small cell lung cancer patients (*N* = 3,512).

Characteristics	Whole cohort
	N = 3,512 (%)
Age at diagnosis (mean ± SD)	69.0 ± 10.9
≤70	1,899 (54.1)
>70	1,613 (45.9)
Race	
White	2,805 (79.9)
Black	489 (13.9)
Other	218 (6.2)
Marital status	
Unmarried	1,696 (48.3)
Married	1,816 (51.7)
Gender	
Male	1,968 (56.0)
Female	1,544 (44.0)
Tumor size (mm)	
≤10	120 (3.4)
11–20	443 (12.6)
21–30	530 (15.1)
31–40	518 (14.7)
41–50	486 (13.8)
51–60	387 (11.0)
61–70	349 (9.9)
>71	679 (19.3)
N status (AJCC 7th)	
N0	509 (14.5)
N1	195 (5.6)
N2	2,144 (61.0)
N3	664 (18.9)
TNM stage (AJCC 7th)	
IIIA	1,593 (45.4)
IIIB	1,919 (54.6)
Surgery	
No	3,266 (93.0)
Yes	246 (7.0)
Radiotherapy	
No	1,298 (37.0)
Yes	2,214 (63.0)
Chemotherapy	
No	1,247 (35.5)
Yes	2,265 (64.5)
Follow-up time [median (IQR)]	12 [5, 29]
Status	
Alive	463 (13.2)
Dead	3,049 (86.8)

SD, standard deviation; IQR, interquartile range; TNM, tumor-node-metastasis; AJCC, the American Joint Committee on Cancer.

The study examined the predictors using LASSO regression and found that the model constructed with age, tumor size, N status, surgery, radiotherapy and chemotherapy had a minor error (Figures 3A,B). Meanwhile, multivariate Cox regression showed a significant effect of these six predictors on OS in patients with stage III NSCLC (Figure 3C). Based on the screened predictors, we constructed a nomogram to estimate individualized 1- to 5-year OS and developed the CS-nomogram capable of predicting 5-year CS in real-time (Figure 4A). Furthermore, we deployed a web version of this model (Figure 4B, https://dynapp.shinyapps.io/NSCLC/), enabling easy real-time estimation of patient survival by entering individualized parameters and the time already survived. Notably, the model exhibited good discrimination, as evidenced by a C-index of 0.71 (95% CI: 0.70–0.72), and demonstrated stability over 5 years, with a time-dependent median area under the curve (AUC) of 0.722 across 1–5 years (Figure 5A). The calibration plots demonstrated that the

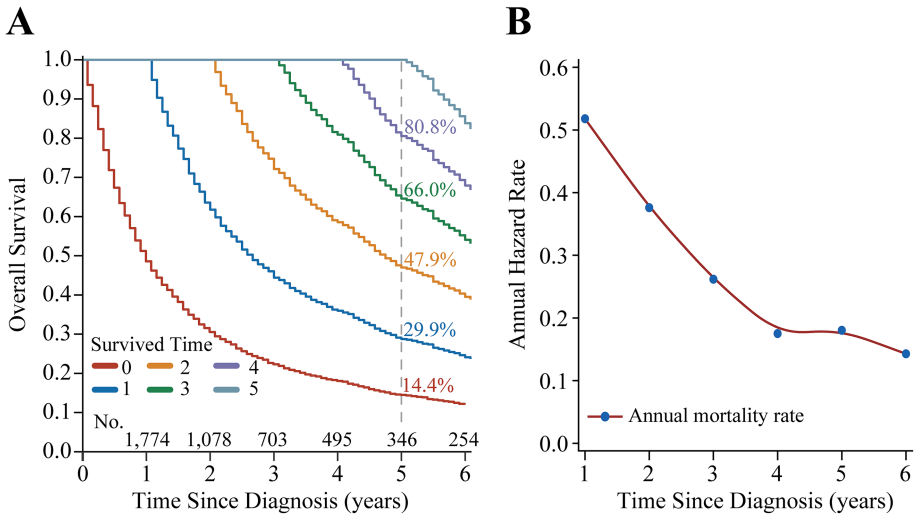

FIGURE 2
Survival analysis of patients with Stage III non-small cell lung cancer. **(A)** Kaplan–Meier curves estimating real-time survival rates after surviving for 0–5 years. **(B)** Annual hazard rate curve.

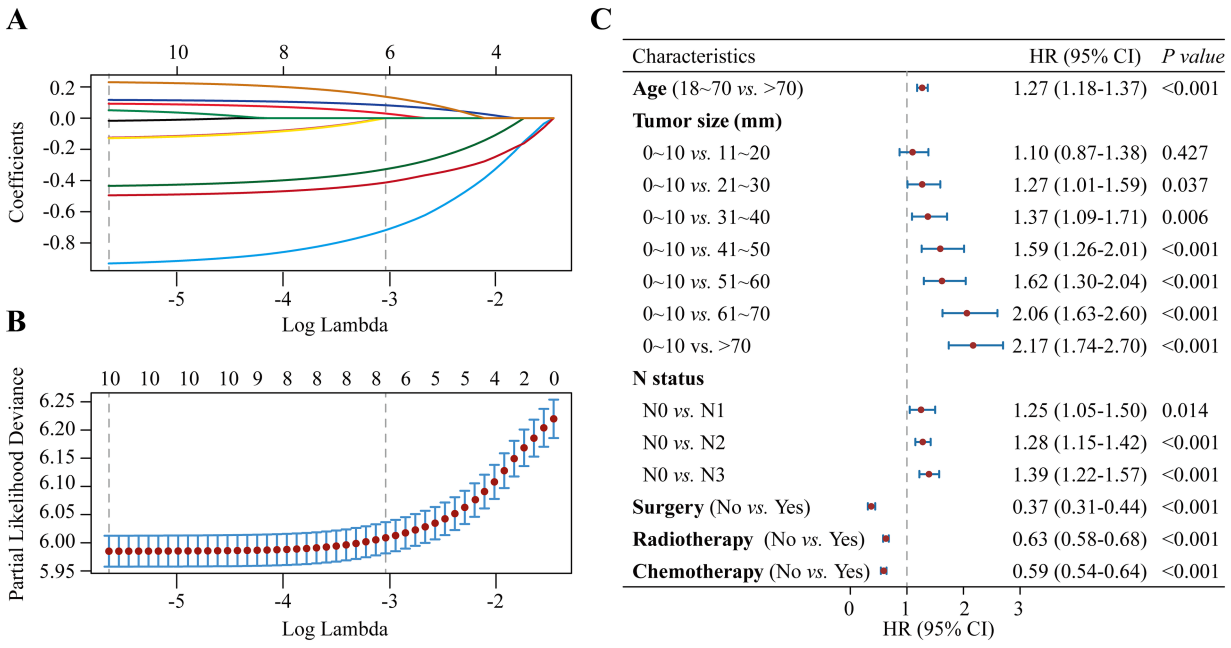

FIGURE 3
Predictor screening. **(A)** The least absolute shrinkage and selection operator (LASSO) regression with **(B)** 5-fold cross-validation, and **(C)** Multivariate Cox regression forest plot of predictors.

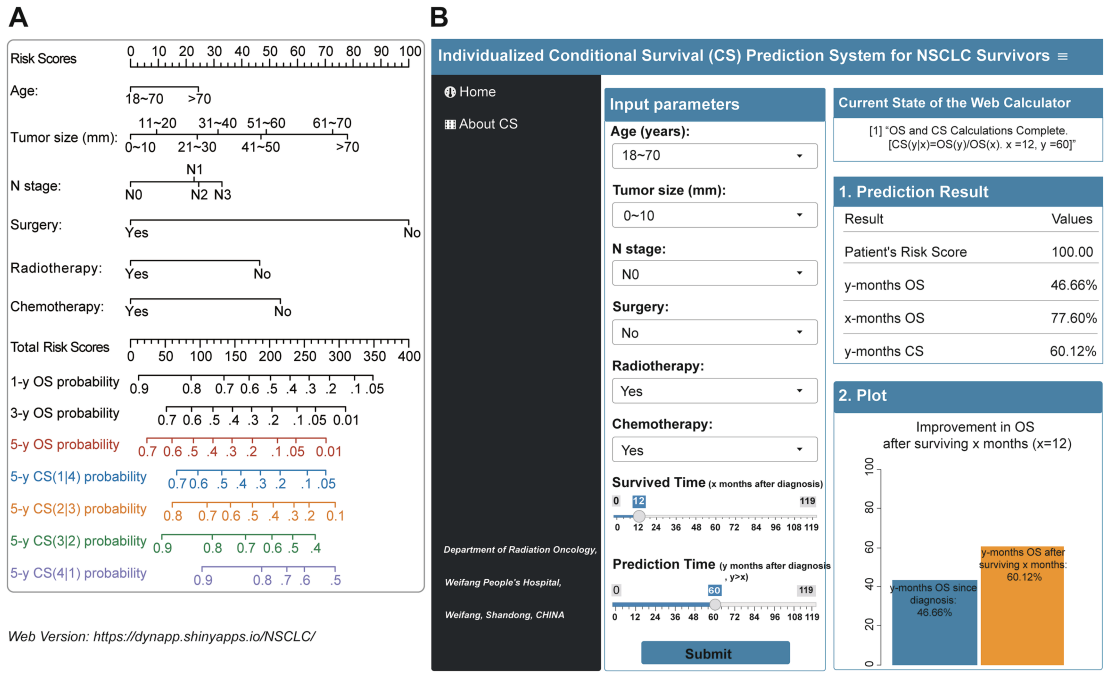

FIGURE 4
(A) Conditional survival nomogram (CS-nomogram) and **(B)** its web version for survivors with Stage III non-small cell lung cancer (https://dynapp.shinyapps.io/NSCLC/). OS, overall survival; CS, conditional survival.

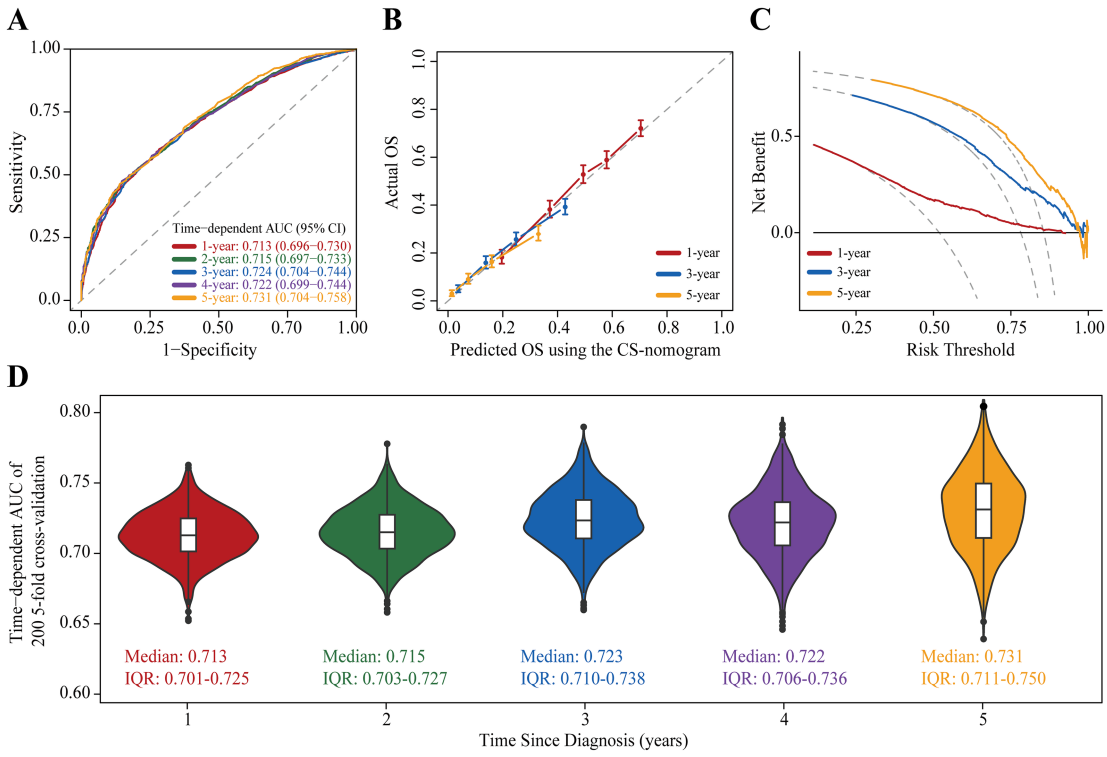

FIGURE 5
Assessment and Validation of the conditional survival nomogram (CS-nomogram). **(A)** Time-dependent area under curve (AUC); **(B)** Calibration plot and **(C)** decision curve analysis (DCA) curve for assessing the accuracy, discrimination and clinical usefulness of the conditional survival nomogram (CS-nomogram). **(D)** 200 times 5-fold cross-validation for estimating model time-dependent AUCs from 1 to 5 years. IQR, interquartile range.

model achieved high accuracy, with curves closely resembling the ideal 45° reference curve (Figure 5B). Additionally, the DCA curves highlighted the clinical utility of the CS-nomogram, showing that utilizing the model to guide clinical interventions outperformed the treat-all or treat-none strategies (Figure 5C). Lastly, the model's performance exhibited high stability through 200 iterations of 5-fold cross-validation, yielding median values of 0.713 (IQR: 0.701, 0.725), 0.715 (IQR: 0.703, 0.727), 0.723 (0.710, 0.738), 0.722 (0.706, 0.736), and 0.731 (IQR: 0.711, 0.750) for the time-dependent AUC (1–5 years after diagnosis) (Figure 5D).

4 Discussion

Stage III NSCLC is notably heterogeneous, and the lack of reliable individualized prognostic estimates poses a significant challenge for disease management. In this study, we applied a novel CS analysis method specifically to stage III NSCLC. Our observations revealed that the OS of patients gradually improved over time. Importantly, the study culminated in the successful development of a CS-nomogram, which has been deployed on a dedicated website to provide personalized, real-time updates on survival data.

NSCLC accounts for 80–85% of all lung cancer cases, with approximately one-third being initially diagnosed at locally advanced stages (6). Stage III NSCLC encompasses a spectrum of different clinical conditions, exhibits significant heterogeneity, and requires a multidisciplinary treatment approach with various therapies (3, 6, 7). Additionally, considerable variability in patient survival rates was observed (9). Our study found the median survival of patients to be only 12 months (95% CI: 12–13 months), corroborating the findings of Flores et al. (8). Advanced age, smoking, and late staging emerged as unfavorable prognostic factors for patients (1, 20–22). To establish an appropriate age stratification cut-off, we conducted an RCS analysis with the objective of achieving a significant difference in OS between the two patient groups, thus enhancing the model's utility. It was important to note that the SEER database's incomplete description of T status compounded the challenges of staging conversion between AJCC versions 7 and 8. Consequently, rather than incorporating T status directly into our model, we utilized tumor size as a surrogate marker. Although this method may sacrifice some details, such as the extent of invasion and depth of infiltration, the choice of tumor size as a variable offers greater accessibility, thereby improving our model's generalizability. To enhance survival outcomes in locally advanced NSCLC, previous research has suggested various treatments, including surgical intervention, concurrent radiotherapy, adjuvant radiotherapy, or chemotherapy for patients with stage III disease. In our model, the absence of surgery corresponded to a quantitative risk score of 100, while the inclusion of radiotherapy and chemotherapy lowered the risk scores by 46.4 and 53.9, respectively. This implied that in cases where surgery was not an option, a combination of radiotherapy and chemotherapy could offer a comparable survival advantage. The heterogeneity of clinicopathologic characteristics and treatments in current cancer research presents a substantial challenge in the implementation of individualized survival estimates (23, 24). Crucially, the lack of a reliable tool for personalized survival estimation had previously placed a significant psychological burden on survivors, leaving them uncertain about their life expectancy. Furthermore, the inability to stratify survivors accurately based on risk led to the need for indiscriminate follow-up of all patients, thereby adding to the strain on healthcare systems. The CS-nomogram developed in this study emerges as a vital tool to alleviate these concerns.

Contrasting with traditional survival estimation methods, CS analysis considers not only the baseline characteristics of patients at diagnosis but also the duration already survived (14). This model offered a more dynamic and individualized approach to survival estimation, enabling physicians to more accurately assess patient prognosis and make informed clinical decisions (25). In our study, we noted a consistent and progressive improvement in real-time survival among patients with stage III NSCLC. Similar trends have been observed in breast (26), esophageal (17, 27), colorectal (14) and lymphoma cancers (28, 29), underlining its significance as a crucial indicator for follow-up. Previous research suggested that this improvement was attributable to a natural selection effect: the occurrence of death among high-risk stage III NSCLC patients led to an increase in the average survival of low-risk individuals, thereby contributing to the ongoing enhancement in real-time survival rates (14).

The CS-nomogram presents the significant advantage of providing real-time updates on individual survival data for survivors during follow-up, marking a substantial improvement over previous method (29). Traditional nomograms are based on the patient's condition at the time of initial diagnosis, and their 5-year OS does not change with the duration of survival after diagnosis, making them a static prediction tool. In current clinical consultations, patients are increasingly interested in knowing their prognosis after surviving for a certain period of time. This is a common question during routine follow-up. The introduction of the CS model has greatly simplified this issue. For instance, inputting a patient's clinical parameters and the duration already survived (e.g., 2 years) into the model yields a risk score of 121.17 points, initially corresponding to a 5-year OS of 36.85% at diagnosis. Notably, since the patient has survived for 2 years, the CS model can update the 5-year OS to 66.92% [5-year CS (3|2)]. This updated information significantly boosts patients' confidence in combating the disease and alleviates their anxiety. Moreover, the clinicopathologic features utilized in the monitoring system have been demonstrated in prior studies to be pertinent in stage III NSCLC, while also being convenient and user-friendly. For clinicians, the CS-nomogram aids in the individualized assessment of patient survival and allows for more targeted follow-up strategies for high-risk patients or those who are potential clinical trial candidates. This undoubtedly enhances patient management and the efficient use of medical resources.

The current study has many limitations to report. First, retrospective bias was inevitable; second, some essential variables, such as smoking history and physical status, were missing from the SEER database, which may have limited some of our analyzes. Third, patient survival will continue to improve with the advent of new therapies, such as targeted agents and immunotherapies, and patient survival may be underestimated. Fourth, although the model was internally evaluated and validated to demonstrate superior performance, external validation is also necessary. Therefore, in future research, we will introduce more useful variables to the existing methods to ensure the performance and generalizability of the model.

5 Conclusion

In this study, we demonstrated that real-time OS in stage III NSCLC survivors improved over time. We developed a CS-nomogram and its web-based version to inform patients of their updated survival data, which is expected to bring new guidance to disease management.

Data availability statement

The raw data supporting the conclusions of this article will be made available by the authors, without undue reservation.

Ethics statement

The requirement of ethical approval was waived by Weifang People's Hospital Ethics Committee for the studies involving humans because this was a retrospective study. The studies were conducted in accordance with the local legislation and institutional requirements. The ethics committee/institutional review board also waived the requirement of written informed consent for participation from the participants or the participants' legal guardians/next of kin because this was a retrospective study and all patients were anonymized.

Author contributions

XM: Conceptualization, Project administration, Writing – original draft, Writing – review & editing, Methodology, Resources, Software, Validation, Visualization. PW: Software, Validation, Writing – original draft, Writing – review & editing, Data curation, Investigation. JL: Validation, Writing – original draft, Writing – review & editing, Formal analysis, Funding acquisition, Project administration, Visualization. DS: Validation, Visualization, Writing – original draft, Writing – review & editing, Conceptualization, Methodology, Software. ZJ: Validation, Visualization, Writing – original draft, Writing – review & editing. YC: Writing – original draft, Writing – review & editing, Conceptualization, Data curation, Formal analysis, Funding acquisition, Investigation, Project administration.

Funding

The author(s) declare that no financial support was received for the research, authorship, and/or publication of this article.

Conflict of interest

The authors declare that the research was conducted in the absence of any commercial or financial relationships that could be construed as a potential conflict of interest.

Publisher's note

References

1. Liang W, He J, Shen Y, Shen J, He Q, Zhang J, et al. Impact of examined lymph node count on precise staging and long-term survival of resected non-small-cell lung Cancer: a population study of the us Seer database and a Chinese multi-institutional registry. *J Clin Oncol*. (2017) 35:1162–70. doi: 10.1200/jco.2016.67.5140

2. Jemal A, Center MM, DeSantis C, Ward EM. Global patterns of Cancer incidence and mortality rates and trends. *Cancer Epidemiol Biomarkers Prev*. (2010) 19:1893–907. doi: 10.1158/1055-9965.Epi-10-0437

3. Shang S, Wang R, Wang F, Wu M, Chen D, Yu J. Treatment patterns for patients with Unresected stage iii Nsclc: analysis of the surveillance, epidemiology, and end results (Seer) database. *Front Oncol*. (2022) 12:874022. doi: 10.3389/fonc.2022.874022

4. Hansen RN, Zhang Y, Seal B, Ryan K, Yong C, Darilay A, et al. Long-term survival trends in patients with Unresectable stage iii non-small cell lung Cancer receiving chemotherapy and radiation therapy: a Seer Cancer registry analysis. *BMC Cancer*. (2020) 20:276. doi: 10.1186/s12885-020-06734-3

5. Jazieh AR, Onal HC, Tan DSW, Soo RA, Prabhash K, Kumar A, et al. Real-world treatment patterns and clinical outcomes in patients with stage iii Nsclc: results of kindle, a multicountry observational study. *J Thorac Oncol*. (2021) 16:1733–44. doi: 10.1016/j.jtho.2021.05.003

6. Juretic A, Sobat H, Samija M. Combined modality therapy of non-small cell lung cancers. *Ann Oncol*. (1999) 10:93–8.

7. Sigel K, Lurslurchachai L, Bonomi M, Mhango G, Bergamo C, Kale M, et al. Effectiveness of radiation therapy alone for elderly patients with Unresected stage iii non-small cell lung Cancer. *Lung Cancer (Amsterdam, Netherlands)*. (2013) 82:266–70. doi: 10.1016/j.lungcan.2013.06.011

8. Flores R, Patel P, Alpert N, Pyenson B, Taioli E. Association of Stage Shift and Population Mortality among patients with non-small cell lung Cancer. *JAMA Netw Open*. (2021) 4:e2137508. doi: 10.1001/jamanetworkopen.2021.37508

9. Evison M. The current treatment landscape in the Uk for stage iii Nsclc. *Br J Cancer*. (2020) 123:3–9. doi: 10.1038/s41416-020-01069-z

10. Jung SH, Lee HY, Chow SC. Statistical methods for conditional survival analysis. *J Biopharm Stat*. (2018) 28:927–38. doi: 10.1080/10543406.2017.1405012

11. Eloranta S, Smedby KE, Dickman PW, Andersson TM. Cancer survival statistics for patients and healthcare professionals - a tutorial of real-world data analysis. *J Intern Med*. (2021) 289:12–28. doi: 10.1111/joim.13139

12. Hieke S, Kleber M, König C, Engelhardt M, Schumacher M. Conditional survival: a useful concept to provide information on how prognosis evolves over time. *Clin Cancer Res*. (2015) 21:1530–6. doi: 10.1158/1078-0432.Ccr-14-2154

13. Zabor EC, Gonen M, Chapman PB, Panageas KS. Dynamic prognostication using conditional survival estimates. *Cancer*. (2013) 119:3589–92. doi: 10.1002/cncr.28273

14. Zamboni BA, Yothers G, Choi M, Fuller CD, Dignam JJ, Raich PC, et al. Conditional survival and the choice of conditioning set for patients with Colon Cancer: an analysis of Nsabp trials C-03 through C-07. *J Clin Oncol*. (2010) 28:2544–8. doi: 10.1200/jco.2009.23.0573

15. Meng X, Hao F, Ju Z, Chang X, Guo Y. Conditional survival nomogram predicting real-time prognosis of locally advanced breast Cancer: analysis of population-based cohort with external validation. *Front Public Health*. (2022) 10:953992. doi: 10.3389/fpubh.2022.953992

16. Latenstein AEJ, van Roessel S, van der Geest LGM, Bonsing BA, Dejong CHC, Groot Koerkamp B, et al. Conditional survival after resection for pancreatic Cancer: a population-based study and prediction model. *Ann Surg Oncol*. (2020) 27:2516–24. doi: 10.1245/s10434-020-08235-w

17. Shin DW, Kim HK, Cho J, Lee G, Cho J, Yoo JE, et al. Conditional survival of patients who underwent curative resection for esophageal squamous cell carcinoma. *Ann Surg*. (2020) 276:e86–92. doi: 10.1097/sla.0000000000004473

18. Zheng Z, Wang X, Liu Z, Lu X, Huang Y, Chi P. Individualized conditional survival nomograms for patients with locally advanced rectal Cancer treated with neoadjuvant Chemoradiotherapy and radical surgery. *Eur J Surg Oncol*. (2021) 47:3175–81. doi: 10.1016/j.ejso.2021.06.010

19. Yoo JE, Han K, Shin DW, Park SH, Cho IY, Yoon DW, et al. Conditional relative survival and competing mortality in patients who underwent surgery for lung Cancer: a Nationwide cohort study. *Int J Cancer*. (2021) 148:626–36. doi: 10.1002/ijc.33239

20. Daly ME, Singh N, Ismaila N, Antonoff MB, Arenberg DA, Bradley J, et al. Management of Stage iii non-Small-Cell Lung Cancer: Asco guideline. *J Clin Oncol*. (2022) 40:1356–84. doi: 10.1200/jco.21.02528

21. Morgensztern D, Waqar S, Subramanian J, Gao F, Trinkaus K, Govindan R. Prognostic significance of tumor size in patients with stage iii non-small-cell lung Cancer: a surveillance, epidemiology, and end results (Seer) survey from 1998 to 2003. *J Thorac Oncol*. (2012) 7:1479–84. doi: 10.1097/JTO.0b013e318267d032

22. Zhang Q, Dai Y, Liu H, Sun W, Huang Y, Gong Z, et al. Causes of death and conditional survival estimates of long-term lung Cancer survivors. *Front Immunol*. (2022) 13:1012247. doi: 10.3389/fimmu.2022.1012247

23. Duma N, Santana-Davila R, Molina JR. Non-small cell lung Cancer: epidemiology, screening, diagnosis, and treatment. *Mayo Clin Proc*. (2019) 94:1623–40. doi: 10.1016/j.mayocp.2019.01.013

24. Miller M, Hanna N. Advances in systemic therapy for non-small cell lung Cancer. *BMJ (Clinical Research Ed)*. (2021) 375:n2363. doi: 10.1136/bmj.n2363

25. Miura JT, Lindner H, Karakousis GC, Sharon CE, Gimotty PA. Conditional survival estimates for Merkel cell carcinoma reveal the dynamic nature of prognostication. *J Surg Oncol*. (2022) 126:348–55. doi: 10.1002/jso.26861

26. Meng X, Cai Y, Chang X, Guo Y. A novel conditional survival nomogram for monitoring real-time prognosis of non-metastatic triple-negative breast Cancer. *Front Endocrinol*. (2023) 14:1119105. doi: 10.3389/fendo.2023.1119105

27. Hagens ERC, Feenstra ML, Eshuis WJ, Hulshof M, van Laarhoven HWM, van Berge Henegouwen MI, et al. Conditional survival after neoadjuvant Chemoradiotherapy and surgery for Oesophageal Cancer. *Br J Surg*. (2020) 107:1053–61. doi: 10.1002/bjs.11476

28. Gao H, Ji X, Liu X, Mi L, Liu W, Wang X, et al. Conditional survival and hazards of death for peripheral T-cell lymphomas. *Aging*. (2021) 13:10225–39. doi: 10.18632/aging.202782

29. Liu X, Wu T, Zhu SY, Shi M, Su H, Wang Y, et al. Risk-dependent conditional survival and failure Hazard after radiotherapy for early-stage Extranodal natural killer/T-cell lymphoma. *JAMA Netw Open*. (2019) 2:e190194. doi: 10.1001/jamanetworkopen.2019.0194

frontiers | Frontiers in Medicine

TYPE Original Research
PUBLISHED 13 January 2025
DOI 10.3389/fmed.2024.1506254

OPEN ACCESS

EDITED BY
Vincenzo Pio Di Noia,
IRCCS Istituto Nazionale Tumori Regina Elena, Italy

REVIEWED BY
Yener Aydin,
Atatürk University, Türkiye
Mehmet Ali Bedirhan,
Yedikule Teaching Hospital, Türkiye

*CORRESPONDENCE
Mingdong Wang
✉ wmd_smmu2013@163.com
Xuewei Zhao
✉ xuewei-zhao@hotmail.com

†These authors have contributed equally to this work

RECEIVED 04 October 2024
ACCEPTED 17 December 2024
PUBLISHED 13 January 2025

CITATION
Wang Y, Yue Z, Shi X, Xia G, Qin L, Sun Q, Huang Y, Chen R, Zhao X and Wang M (2025) Comparison of safety and effectiveness of medical adhesive and metal spring coil in preoperative localization of peripheral pulmonary nodules.
Front. Med. 11:1506254.
doi: 10.3389/fmed.2024.1506254

Comparison of safety and effectiveness of medical adhesive and metal spring coil in preoperative localization of peripheral pulmonary nodules

Yifei Wang[1†], Zhenhua Yue[1†], Xiaoqian Shi[2†], Guozhan Xia[1], Linlin Qin[1], Qi Sun[1], Yiling Huang[3], Rong Chen[3], Xuewei Zhao[1*] and Mingdong Wang[1*]

[1]Department of Thoracic Surgery, Shanghai Fourth People's Hospital, School of Medicine, Tongji University, Shanghai, China, [2]Department of Pulmonary and Critical Care Medicine, Shanghai Fourth People's Hospital, School of Medicine, Tongji University, Shanghai, China, [3]Department of Nursing, Shanghai Fourth People's Hospital, School of Medicine, Tongji University, Shanghai, China

Background: Accurate preoperative positioning is the key to the success of thoracoscopic surgery for small pulmonary nodules. There are many methods for locating pulmonary nodules in clinical practice, but there are currently few research reports on the value of medical adhesive localization.

Objective: To compare the clinical value of two positioning methods, medical adhesive and metal spring coil, in the preoperative application of VATS through retrospective analysis.

Methods: A total of 288 patients who underwent thoracoscopic surgery in our hospital from January 2021 to June 2024 due to the discovery of solitary pulmonary nodules during chest CT examination were included in this study. Preoperative patients were randomly divided into two groups, with 205 patients undergoing preoperative medical adhesive positioning (Group A) and 83 patients undergoing metal spring coil positioning (Group B). After the positioning was completed, record the positioning time of each group of patients and the immediate pain score 15 min after the positioning was completed, the complications located in each group of patients, and whether there was positioning failure or not.

Results: The localization success rate of the medicine adhesive positioning group [99.5% (204/205)] was higher than that of the metal spring coil positioning group [91.6% (76/83)] ($P = 0.001$). The positioning time of the medical adhesive positioning group was 12.00 (10.00, 14.00) min, which was shorter than the 13.00 (11.00, 16.00) min of the micro coil group ($P = 0.001$). The immediate pain score (2.32 ± 0.79) of the medical adhesive positioning group 15 min after positioning was significantly lower than that of the metal spring coil positioning group (3.97 ± 0.54) ($P < 0.001$). The incidence of complications such as pneumothorax [15.7% (13/83) vs 5.4% (11/205), $P = 0.004$], pulmonary hemorrhage/hemoptysis [20.5% (17/83) vs 4.9 (10/205), $P < 0.001$] was significantly higher in the metal coil positioning group than in the medical adhesive positioning group.

Conclusion: Preoperative medical adhesive positioning for pulmonary nodules is safe, reliable, and effective. Compared with metal spring coil positioning, it has shorter positioning time, milder pain after positioning, lower incidence of positioning related complications, and more flexible arrangement of surgical timing after positioning. It has high clinical application value.

KEYWORDS

medical adhesive, metal spring coil, localization, pulmonary nodules, video-assisted thoracoscopic surgery (VATS)

1 Introduction

With the gradual popularization of low-dose thin-layer CT in early lung cancer screening, the detection rate of pulmonary nodules is gradually increasing (1). For small pulmonary nodules, if early lung cancer is highly suspected, video-assisted thoracoscopic surgery (VATS) should be the first choice for resection to clarify the diagnosis and achieve treatment goals (2, 3). However, for small pulmonary nodules with small diameter, insufficient solid components, or not close to the pleura, it is often difficult to accurately locate them during surgery, which may lead to prolonged surgery time, conversion to thoracotomy, and even surgical failure. Especially for smaller pure ground glass nodules, intraoperative localization is more difficult due to the lack of solid components. Therefore, accurate preoperative positioning is the key to surgical success (4, 5). Whether it can be accurately positioned is related to the success rate of surgery and patient efficacy. To ensure surgical effectiveness and patient safety, and to enable clinical physicians to quickly and accurately locate lung nodules during thoracoscopic surgery, it is particularly important to choose the correct and reasonable positioning method before surgery. Adopting a technique that can accurately locate pulmonary nodules before surgery can avoid unnecessary removal of normal lung tissue in patients with pulmonary nodules, which will be beneficial for their recovery (6).

At present, there are many methods for locating pulmonary nodules in clinical practice (7), such as traditional hook-wire positioning, metal spring coil positioning, as well as emerging medical adhesive positioning, metal anchoring needle positioning, and so on. Although there have been research reports on preoperative localization of pulmonary nodules, it is not yet clear which method is more advantageous. Previous study have shown that CT-guided percutaneous localization with medical adhesive can label small pGGNs and mGGNs prior to VATS, with high success and low complication rates (8). There is also study indicating that, for pulmonary nodules that are difficult to locate in VATS, CT guided coil positioning can help doctors accurately locate these nodules and make it easier and faster to remove them (9). However, there are currently few research reports on the positioning value of medical adhesives. Our study aims to compare the clinical value of two positioning methods, medical adhesive and metal spring coil, in the preoperative application of VATS through retrospective analysis. Hook-wire positioning was excluded from our study due to its sharp tip and severe post positioning pain, and metal anchoring needle positioning were also excluded from our study because their use was limited by that the positioning needle must be resected during surgery after positioning.

2 Materials and methods

2.1 Clinical data and grouping

A total of 288 patients who underwent thoracoscopic surgery in our hospital from January 2021 to June 2024 due to the discovery of solitary pulmonary nodules during chest CT examination were included in this study. Preoperative patients were randomly divided into two groups, with 205 patients undergoing preoperative medical adhesive positioning (Group A) and 83 patients undergoing metal spring coil positioning (Group B). There were 66 males and 139 females in the adhesive localization group, aged 21–82 years, with an average of 57.43 ± 12.70 years; the target nodules were located in the upper lobe of the right lung in 52 cases, the middle lobe of the right lung in 7 cases, the lower lobe of the right lung in 44 cases, the upper lobe of the left lung in 57 cases, and the lower lobe of the left lung in 45 cases. In the metal spring coil positioning group, there were 29 males and 54 females with ages ranging from 27 to 81 years, with an average of 54.77 ± 12.19 years; the target nodules were located in the upper lobe of the right lung in 20 cases, the middle lobe of the right lung in 7 cases, the lower lobe of the right lung in 24 cases, the upper lobe of the left lung in 17 cases, and the lower lobe of the left lung in 15 cases. All patients had no perioperative deaths.

2.2 Inclusion and exclusion criteria

Inclusion criteria were the following: (1) conventional thoracoscopic surgery; (2) preoperative CT scan confirmed the presence of isolated peripheral pulmonary nodules, and malignancy cannot be ruled out; (3) The distance between the pulmonary nodule and the pleural surface is greater than 5 mm, and precise positioning may not be possible through touch during surgery. Exclusion criteria were: (1) those who underwent thoracic surgery for more than one time on the same side; (2) patients with obvious abnormalities in blood biochemical examination within 7 days before surgery (e.g., liver function damage, renal function damage, et al.); (3) severe cardiac insufficiency (NYHA grade III IV), poor blood pressure control in hypertensive patients

or poor blood glucose control in diabetic patients; (4) those with adhesion in the pleural cavity; (5) patients with pulmonary bullae, chronic obstructive pulmonary disease, and other diseases are prone to pneumothorax due to puncture positioning; (6) those whom researchers evaluated as not suitable for inclusion, i.e., patients with poor compliance, hearing impairment or communication impairment, or lost to follow-up.

2.3 Instruments and equipment

The CT equipment used is Lianying high-resolution 64 slice spiral CT scanner. The medical adhesive used for positioning were Kangpaite medical adhesive (0.5 ml/tube) and the matched puncture needle (specification: 21G, length: 80 mm) produced by Beijing Kangpaite Medical Equipment Co., Ltd. The metal spring coil positioning used for positioning was German SOMATEX disposable breast positioning wire and its guide pin (length: 100 mm, specification: 20G, diameter: 0.95 mm) produced by Shanghai Songke Medical Equipment Co., Ltd.

2.4 Methods

All patients underwent pulmonary nodule localization within 8 h prior to VATS surgery, which was performed by the same respiratory physician with over 15 years of work experience. Firstly, based on preoperative CT examination to clarify the spatial relationship of pulmonary nodules, the optimal puncture path is planned and selected, and the optimal puncture position (left/right lateral position, supine position, prone position) is determined. Then, a local thin-layer CT scan (layer thickness: 1.00 mm) is performed to determine the puncture point, angle, and depth. Disinfect and drape the area of 15 square centimeters near the puncture site, and use 5 ml of 2% lidocaine to infiltrate and anesthetize the chest wall and pleura at the puncture site. Instruct the patient to breathe as calmly as possible.

Medical adhesive positioning group (Group A): Insert the needle according to the predetermined angle and depth, instruct the patient to hold their breath after inhalation, and insert the puncture needle based on the measured optimal depth. Then perform a local CT thin-layer scan to observe the position relationship between the puncture needle and the lesion. After the puncture needle reaches 5–10 mm around the lesion and 10–25 mm deep into the lungs, remove the needle core, and after confirming that there is no blood return, quickly inject 0.15 ml of medical gel that has been extracted into the lungs through the trocar, so that the medical gel was injected into the lung tissue and quickly solidifies to form a hard knot. Then, remove the trocar to complete the positioning. Cover the wound with a band aid or medical dressing. After the positioning was completed, according to the surgical schedule, the patient was sent back to the ward to wait for the surgery.

Metal spring coil positioning group (Group B): Insert the needle according to the predetermined angle and depth, instruct the patient to hold their breath after inhalation, and insert the puncture needle based on the measured optimal depth. Then perform a local CT thin-layer scan to observe the position relationship between the puncture needle and the lesion. After the puncture needle reaches 5–10 mm around the lesion and 10–25 mm deep into the lungs, gradually release the guide wire until it cannot be pushed, and be careful to avoid the guide needle moving backwards. Slowly remove the guide needle, taking care to avoid the guide needle moving backwards. Apply and fix locally to prevent the guide wire from shifting.

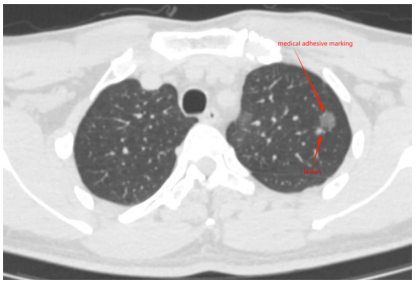

FIGURE 1
Medical adhesive marking located near the lesion.

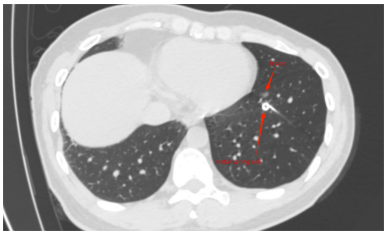

FIGURE 2
Metal spring coil located near the lesion.

Immediately perform another local thin-layer CT scan after localization to confirm the location of medical adhesive nodules (Figure 1) or metal spring coils (Figure 2), as well as the presence of complications such as pneumothorax, pulmonary bleeding, or hemoptysis, and promptly report the localization effect to the thoracic surgeon. Instruct the patient to sit quietly and observe for 15 min, avoid vigorous exercise, and return to the ward to wait for surgery after no abnormalities are found.

Under general anesthesia with double lumen endotracheal intubation, take a lateral position with the affected side facing upwards. Routine disinfection and cloth laying were performed, and all patients underwent thoracoscopic surgery using the two hole method. A 1.0 cm incision was made at the midline of the 7th rib axilla, and thoracoscopy was inserted; Make a 3 cm operating hole in the fourth intercostal space of the axillary line to explore and determine the depth of medical adhesive or metal spring coil positioning and the location of the lesion. According to the positioning, perform wedge resection or segmentectomy of the lung, and simultaneously remove the medical adhesive or metal spring coil used for positioning during the operation.

2.5 Record observation indicators

(1) After the positioning was completed, promptly record the positioning time of each group of patients and the immediate pain

score 15 min after the positioning is completed. The positioning time started from the CT scan that determines the puncture path and ended after the positioning was completed, accurate to min. After the positioning was completed, the nurse assisting in the positioning was responsible for calculating the positioning time and recording it. The immediate pain score 15 min after positioning was recorded using a VAS pain scale combined with the digital score scale (accurate to 0.1).

(2) Record the complications located in each group of patients (such as pneumothorax, pulmonary hemorrhage or hemoptysis, pleural reaction, etc.), and analyze the influencing factors of the complications.

(3) Intraoperative records of VATS: Surgical date, surgical method (wedge resection or segmentectomy), presence or absence of intrathoracic hemorrhage; is there any medical adhesive detachment/coil displacement or dislodgement that causes the inability to locate the target nodule during surgery (positioning failure).

(4) Postoperative records of VATS: Pathological results and pathological size of every localized nodules.

2.6 Statistical analysis

IBM SPSS Statistics 21.0 software was used for statistical analysis. Firstly, use the Kolmogorov-Smirnov method to verify whether the metric data conforms to a normal distribution. The measurement data which has undergone normality testing conformed to normal distribution were represented by mean ± standard deviation. Independent sample t-test was used for inter group comparison. Data that do not follow normal distribution were represented by the median (quartiles), and comparisons between groups were conducted using the Mann-Whitney U test. The categorical count data were represented by the number of cases (%), and the comparison between groups was performed using the χ^2 test or Fisher's exact probability test. The inspection level was all $P < 0.05$, indicating that the difference was statistically significant.

2.7 Ethical approval

Ethics committee of Shanghai Fourth People's Hospital and Internal Review Board of Shanghai Fourth People's Hospital have approved this study. Each patient signed an informed consent form before positioning. Declaration of Helsinki and International Ethical Guidelines for Health-related Research Involving Humans are followed. The patients have provided consent for participating the study and publication of the data on any journal.

3 Results

3.1 Comparison of general patient information

The comparison of general clinical data between two groups of patients is shown in Table 1. The difference in gender composition, location of nodules, surgical approach, and proportion of postoperative pathological types between the two groups of patients was not statistically significant ($P > 0.05$) according to the results of the χ^2 test. In addition, independent sample t-test results showed no statistically significant differences in age and pathological size of nodules between the two groups of patients ($P > 0.05$).

3.2 Comparison of positioning time and immediate pain scores 15 min after positioning between two groups of patients

The comparison of the positioning time and immediate pain scores 15 min after positioning between the two groups of patients is shown in Table 2. The Mann-Whitney U test results showed that the positioning time of Group A was significantly lower than that of Group B, and the difference was statistically significant ($P < 0.05$). The independent sample t-test results showed that the immediate pain scores 15 min after positioning of Group A was significantly lower than that of Group B, and the difference was statistically significant ($P < 0.05$).

3.3 Comparison of location related complications and positioning failure rate between two groups of patients

The comparison of location related complications between the two groups of patients is shown in Table 3. Both groups of patients did not experience any intrathoracic bleeding. The results of the χ^2 test showed that the proportion of pneumothorax, intrapulmonary bleeding/hemoptysis, medical adhesive detachment/coil displacement or dislodgement (positioning failure) in Group B was significantly higher than that in Group A, and the difference was statistically significant ($P < 0.05$). The Fisher's exact probability test results showed that there was no statistically significant difference in the proportion of pleural reactions between the two groups of patients ($P > 0.05$).

4 Discussion

The screening of lung cancer has led to an increase in the detection rate of solitary pulmonary nodules, and more than half of the postoperative pathological confirmation of solitary pulmonary nodules is malignant tumors. The diagnosis and treatment of pulmonary nodules have become an increasingly serious clinical problem (10, 11). The presence of nodules puts immense psychological pressure on patients, and long-term follow-up may also lead to disease progression. Therefore, surgeons often advocate taking active diagnostic and treatment measures, clarifying benign and malignant conditions, and implementing standardized treatment to reduce the mortality rate associated with lung cancer (12). Minimally invasive thoracoscopic surgery has become the preferred method for diagnosing and treating uncertain isolated pulmonary nodules due to its small trauma and fast

TABLE 1 Demographic and clinical characteristics of the 288 patients in the study.

	Group A (n = 205)	Group B (n = 83)	χ^2/t	P
Age, mean ± SD, y	57.43 ± 12.70	54.77 ± 12.19	1.631	0.104
Gender, No. (%)				
Male	66(32.2)	29(34.9)	0.201	0.654
Female	139(67.8)	54(65.1)		
Location of nodules, No. (%)				
Right upper lobe	52(25.4)	20(24.1)	6.149	0.188
Right middle lobe	7(3.4)	7(8.4)		
Right lower lobe	44(21.5)	24(28.9)		
Left upper lobe	57(27.8)	17(20.5)		
Left lower lobe	45(21.9)	15(18.1)		
Pathological size of nodules, mean ± SD, mm	5.01 ± 2.57	5.04 ± 2.13	0.083	0.934
Surgical approach, No. (%)				
Wedge	200(97.6)	83(100.0)	0.879	0.349
Segmentectomy	5(2.4)	0(0.0)		
Postoperation pathology, No. (%)				
Benign tumor	56(27.3)	29(35.0)	1.650	0.199
Malignant tumor				
AAH	21(10.3)	4(4.8)	2.209	0.530
AIS	80(39.0)	29(35.0)		
MIA	39(19.0)	16(19.2)		
IA	9(4.4)	5(6.0)		

AAH, atypical adenomatous hyperplasia; AIS, adenocarcinoma *in situ*; MIA, minimally invasive adenocarcinoma; IA, invasive adenocarcinoma.

TABLE 2 Comparison of positioning time and immediate pain scores 15 min after positioning between two groups of patients.

	Group A	Group B	Z/t	P
Number of cases	205	83	–	–
Positioning time [min, M(P_{25},P_{75})]	12.00 (10.00, 14.00)	13.00 (11.00, 16.00)	−3.454	0.001
Immediate pain scores 15 min after positioning ($\bar{x} \pm S$)	2.32 ± 0.79	3.97 ± 0.54	20.512	<0.001

TABLE 3 Comparison of location related complications and positioning failure rate between two groups of patients [n (%)].

Complications	Group A (n = 205)	Group B (n = 83)	χ^2	P
Pneumothorax	11 (5.4)	13 (15.7)	8.200	0.004
Intrapulmonary bleeding/Hemoptysis	10 (4.9)	17 (20.5)	16.931	<0.001
Intrathoracic bleeding	0 (0.0)	0 (0.0)	–	–
Pleural reaction	0 (0.0)	1 (1.2)	–	0.288*
Medical adhesive detachment/Coil displacement or dislodgement (positioning failure)	1 (0.5)	7 (8.4)	11.027	0.001

*Fisher's exact probability test is used.

postoperative recovery (13), but the detection effect of pulmonary nodules in thoracoscopic surgery is not ideal. Previous studies (14) have shown that up to 54% of lung nodules cannot be observed in VATS or detected by palpation, and for pulmonary ground glass nodules with a diameter <10 mm and located more than 5 mm above the pleural surface, VATS is difficult to locate. Preoperative localization of pulmonary nodules is particularly crucial as it can improve surgical efficiency and accuracy.

Since Plunkett et al. (15) first reported the high efficiency of using Hook wire to locate pulmonary nodules before surgery in 1992, multiple different preoperative localization methods including hook-wire, coil, staining material, and iodine oil have been applied, each with its own unique advantages (16, 17). Preoperative localization results in a higher success rate, shorter surgical time, and faster patient recovery for thoracoscopic lung nodule surgery (18).

Various positioning methods have their own advantages and disadvantages, and the positioning methods chosen by each unit are not the same based on specific technical conditions, clinical experience, and the actual situation of the patient.

The localization success rate of the medicine adhesive positioning group in this study was 99.5% (204/205), and the localization success rate of the metal spring coil positioning group was 91.6% (76/83). It can be seen that both localization techniques can effectively complete preoperative localization, but the localization success rate of the medical adhesive positioning group was significantly higher than that of the metal spring coil positioning group, and the difference was statistically significant ($P = 0.001$). According to literature (19), the dislocation rate of spring coil positioning is reported to be 0–6.7%. The incidence of coil dislocation in this study was slightly higher than the result, at 8.4%. This may be because with the patients' respiratory movement and the passage of time, some patients may experience displacement of the spring coil, leading to dislocation.

The positioning time of the medical adhesive positioning group was 12.00 (10.00, 14.00) min, which was shorter than the 13.00 (11.00, 16.00) min of the micro coil group, and the difference was statistically significant ($P = 0.001$). This indicates that the process of medical adhesive positioning is more convenient and efficient.

The immediate pain score (2.32 ± 0.79) of the medical adhesive positioning group 15 min after positioning was significantly lower than that of the metal spring coil positioning group (3.97 ± 0.54), and the difference was statistically significant ($P < 0.001$). After the metal spring coil positioning, the head end of the coil was retained in the lung tissue, but the metal tail end needed to penetrate the chest wall and was retained outside the chest wall. Some patients even dared not breathe due to the intense pain; while during the medical adhesive positioning, the puncture needle was promptly removed and there was no residue on the chest wall, which greatly reduced the patients' pain and made the patients' movement more convenient and free after positioning.

In terms of complications related to localization, neither group of patients experienced thoracic bleeding, and the perioperative mortality rate was 0, indicating that both medical adhesive and metal spring coil are safe localization methods. There was no statistically significant difference in the incidence of pleural reactions between the two groups of patients in this study ($P > 0.05$), but the incidence of comorbidities such as pneumothorax [15.7% (13/83) vs 5.4% (11/205), $P = 0.004$], pulmonary hemorrhage/hemoptysis [20.5% (17/83) vs 4.9 (10/205), $P < 0.001$] was significantly higher in the metal coil positioning group than in the medical adhesive positioning group, and the difference was statistically significant.

Medical adhesive is considered an ideal adhesive material and has been widely used in the treatment of bleeding, fistulas, gastrointestinal diseases, and other aspects (20). The full name of medical adhesive is alpha cyanoacrylate rapid medical adhesive, which is made by adding methyl methacrylate to alpha cyanoacrylate octyl ester as the main adhesive. When medical adhesives encounter trace amounts of anionic substances (such as blood, body fluids, tissue fluids, or organic amines in the human body), they quickly polymerize at room temperature, solidify into a film, and tightly embed with the surface of the tissue in contact. They have the function of blocking blood vessel ends and promoting blood vessel contraction, which also has a positive effect on promoting blood coagulation and avoiding pneumothorax. Medical adhesive is non-toxic and harmless, with good biological safety. Medical adhesive localization is achieved by injecting it into the lungs through percutaneous puncture guided by CT, and utilizing its mechanism of action to form a hard lump near the lesion, thus playing a role in localization.

The advantages of medical adhesive positioning are as follows: (1) Simple operation: When using medical adhesive for pulmonary nodule positioning, the operation is not complicated and easy to master; (2) Accurate positioning: Medical adhesive can quickly solidify in the body, and after solidification and hardening, it can ensure accurate positioning. Moreover, medical adhesive solidifies into a hard block in the puncture site tissue, without spreading on the pleural surface and lung parenchyma; (3) Flexible surgical timing: Medical adhesive condenses into hard particles within the tissue at the puncture site, which will not spread on the pleural surface or lung parenchyma. Therefore, positioning can be performed 72 h before surgery, avoiding the defect of hook-wire positioning requiring timely surgery within 3 h. Especially for multiple patients who need preoperative positioning, there is greater room for choice in the selection of positioning dates, and this advantage is even more obvious; (4) Clear tactile sensation: Medical adhesive can quickly solidify in the body, and after solidification and hardening, it can ensure accurate positioning; (5) Reduce complications after positioning: After the medical adhesive solidifies, it produces a large adhesive strength, which can block the broken ends of blood vessels, promote blood vessel contraction and coagulation, immediately stop bleeding, and reduce complications such as puncture bleeding and air leakage; (6) Small impact after positioning: The medical adhesive will not be absorbed in a short period of time after curing, allowing patients to have more freedom of position and feel more comfortable without affecting their activities; (7) Degradable: Medical adhesive is biodegradable, and the hardened adhesive does not need to be removed together; (8) Suitable for patients with multiple nodules: When multiple nodules need to be located simultaneously, hook wire and other metal tools can easily cause pneumothorax and mutual interference. Using medical adhesive for positioning is more convenient, and adhesive hardening will not interfere with the positioning of other nodules.

In our clinical application practice, we have summarized several precautions in the positioning process of medical adhesive: (1) For the positioning of pure ground glass pulmonary nodules, it is necessary to maintain a certain positioning distance to avoid medical adhesive covering the nodules and interfering with pathological diagnosis; (2) The speed of medical adhesive injection should be fast, and the needle should be removed immediately after completion. Delaying the needle removal may cause difficulty or lung injury due to the solidification of the adhesive.

This study still has certain limitations: It is a single center retrospective clinical study, and future multi center, larger sample randomized controlled trials are needed for validation. Despite these limitations, our study provides new insights into preoperative localization techniques.

In summary, preoperative medical adhesive positioning for pulmonary nodules is safe, reliable, and effective. Compared with metal spring coil positioning, it has shorter positioning time,

milder pain after positioning, lower incidence of positioning related complications, and more flexible arrangement of surgical timing after positioning. It has high clinical application value.

Data availability statement

The raw data supporting the conclusions of this article will be made available by the authors, without undue reservation.

Ethics statement

The studies involving humans were approved by Ethics Committee of Shanghai Fourth People's Hospital. The studies were conducted in accordance with the local legislation and institutional requirements. The participants provided their written informed consent to participate in this study.

Author contributions

YW: Conceptualization, Methodology, Software, Writing – original draft, Writing – review and editing. ZY: Writing – original draft. XS: Conceptualization, Investigation, Methodology, Software, Writing – review and editing. GX: Formal analysis, Writing – review and editing. LQ: Formal analysis, Writing – review and editing. QS: Formal analysis, Writing – review and editing. YH: Data curation, Supervision, Writing – review and editing. RC: Data curation, Supervision, Writing – review and editing. XZ: Funding acquisition, Project administration, Resources, Validation, Writing – review and editing. MW: Project administration, Resources, Validation, Visualization, Writing – review and editing.

Funding

The author(s) declare that financial support was received for the research, authorship, and/or publication of this article. This work was supported by the Special Funds for Scientific Research Initiation of Shanghai Fourth People's Hospital (No. sykyqd03201).

Conflict of interest

The authors declare that the research was conducted in the absence of any commercial or financial relationships that could be construed as a potential conflict of interest.

Generative AI statement

The authors declare that no Generative AI was used in the creation of this manuscript.

Publisher's note

References

1. Silva M, Pastorino U, Sverzellati N. Lung cancer screening with low-dose CT in Europe: strength and weakness of diverse independent screening trials. *Clin Radiol.* (2017) 72:389–400. doi: 10.1016/j.crad.2016.12.021

2. Fu YF, Zhang M, Wu WB, Wang T. Coil localization-guided video-assisted thoracoscopic surgery for lung nodules. *J Laparoendosc Adv Surg Tech A.* (2018) 28:292–7. doi: 10.1089/lap.2017.0484

3. Shen C, Li P, Li J, Che G. [Advancement of common localization of solitary pulmonary nodules for video-assisted thracoscopic surgery]. *Zhongguo Fei Ai Za Zhi.* (2018) 21:628–34. doi: 10.3779/j.issn.1009-3419.2018.08.09

4. Shen C, Li P, Li J, Che G. Marking ground glass nodules with pulmonary nodules localization needle prior to video-assisted thoracoscopic surgery. *Eur Radiol.* (2022) 32:4699–706.

5. Chan EY, Gaur P, Ge Y, Kopas L, Santacruz JF, Gupta N, et al. Management of the solitary pulmonary nodule. *Arch Pathol Lab Med.* (2017) 141:927–31.

6. Su TH, Fan YF, Jin L, He W, Hu LB. CT-guided localization of small pulmonary nodules using adjacent microcoil implantation prior to video-assisted thoracoscopic surgical resection. *Eur Radiol.* (2015) 25:2627–33. doi: 10.1007/s00330-015-3676-5

7. Refai M, Andolfi M, Barbisan F, Roncon A, Guiducci GM, Xiumè F, et al. Computed tomography-guided microcoil placement for localizing small pulmonary nodules before uniportal video-assisted thoracoscopic resection. *Radiol Med.* (2020) 125:24–30. doi: 10.1007/s11547-019-01077-x

8. Tao G, Jingying Y, Tan G, Xiaotao D, Min C. A novel CT-guided technique using medical adhesive for localization of small pulmonary ground-glass nodules and mixed ground-glass nodules (</=20 mm) before video-assisted thoracoscopic surgery. *Diagn Interv Radiol.* (2018) 24:209–12. doi: 10.5152/dir.2018.17315

9. Wang ZX, Li L, Zhang Z, Wang GH, Kong DM, Wang XD, et al. High-resolution computed tomography features and CT-guided microcoil localization of subcentimeter pulmonary ground-glass opacities: radiological processing prior to video-assisted thoracoscopic surgery. *J Thorac Dis.* (2018) 10:2676–84. doi: 10.21037/jtd.2018.04.87

10. Chung JH, Richards JC, Koelsch TL, MacMahon H, Lynch DA. Screening for lung cancer: incidental pulmonary parenchymal findings. *AJR Am J Roentgenol.* (2018) 210:503–13.

11. Keating J, Singhal S. Novel methods of intraoperative localization and margin assessment of pulmonary nodules. *Semin Thorac Cardiovasc Surg.* (2016) 28:127–36. doi: 10.1053/j.semtcvs.2016.01.006

12. Nair A, Hansell DM. European and North American lung cancer screening experience and implications for pulmonary nodule management. *Eur Radiol.* (2011) 21:2445–54. doi: 10.1007/s00330-011-2219-y

13. Burdine J, Joyce LD, Plunkett MB, Inampudi S, Kaye MG, Dunn DH. Feasibility and value of video-assisted thoracoscopic surgery wedge excision of small pulmonary nodules in patients with malignancy. *Chest.* (2002) 122:1467–70.

14. Kondo R, Yoshida K, Hamanaka K, Hashizume M, Ushiyama T, Hyogotani A, et al. Intraoperative ultrasonographic localization of pulmonary ground-glass opacities. *J Thorac Cardiovasc Surg.* (2009) 138:837–42. doi: 10.1016/j.jtcvs.2009.02.002

15. Plunkett MB, Peterson MS, Landreneau RJ, Ferson PF, Posner MC. Peripheral pulmonary nodules: preoperative percutaneous needle localization with CT guidance. *Radiology*. (1992) 185:274–6.

16. Wang B, Zeng Y, Zhao Z, Wang T, Ma Z, Yu G. A safe and novel method for video-assisted thoracic surgery preoperative localization of small pulmonary nodules by using ZT medical glue (2-octyl cyanoacrylate). *Surg Oncol.* (2020) 33:164–9. doi: 10.1016/j.suronc.2020.02.001

17. Jiang T, Lin M, Zhao M, Zhan C, Li M, Feng M, et al. Preoperative computed tomography-guided localization for pulmonary nodules with glue and dye. *Thorac Cardiovasc Surg.* (2020) 68:525–32.

18. Finley RJ, Mayo JR, Grant K, Clifton JC, English J, Leo J, et al. Preoperative computed tomography-guided microcoil localization of small peripheral pulmonary nodules: a prospective randomized controlled trial. *J Thorac Cardiovasc Surg.* (2015) 149:26–31. doi: 10.1016/j.jtcvs.2014.08.055

19. Mayo JR, Clifton JC, Powell TI, English JC, Evans KG, Yee J, et al. Lung nodules: CT-guided placement of microcoils to direct video-assisted thoracoscopic surgical resection. *Radiology*. (2009) 250:576–85.

20. Tang L, Li X, Cui J, Huang L-Y. EUS-guided coil placement and cyanoacrylate glue injection for gastric variceal bleeding with obvious spontaneous portosystemic shunts. *Endosc Ultrasound*. (2023) 12:84–9. doi: 10.4103/EUS-D-22-00006

frontiers | Frontiers in Medicine

TYPE Original Research
PUBLISHED 24 January 2025
DOI 10.3389/fmed.2025.1467871

OPEN ACCESS

EDITED BY
Alessandro Leonetti,
University Hospital of Parma, Italy

REVIEWED BY
Ricardo Martinez,
Eli Lilly, United States
Kailin Chen,
Central South University, China
Yajun Li,
Central South University, China

*CORRESPONDENCE
Liangping Xia
✉ xialp@sysucc.org.cn
Yaoxiong Xia
✉ 55490850@qq.com

†These authors have contributed equally to this work

RECEIVED 21 July 2024
ACCEPTED 02 January 2025
PUBLISHED 24 January 2025

CITATION
Wang L, You Y, He W, Hou Y, Li L, Wang L, Jiang C, Yi J, Xia Y and Xia L (2025) Previous treatment decreases efficacy of pralsetinib in RET fusion-positive non-small-cell lung cancer. *Front. Med.* 12:1467871. doi: 10.3389/fmed.2025.1467871

Previous treatment decreases efficacy of pralsetinib in RET fusion-positive non-small-cell lung cancer

Lei Wang[1†], Yafei You[2†], Wenzhuo He[3], Yu Hou[1], Lan Li[1], Li Wang[1], Chang Jiang[3], Jiahong Yi[3], Yaoxiong Xia[1*] and Liangping Xia[3*]

[1]Department of Radiotherapy, The Third Affiliated Hospital of Kunming Medical University, Yunnan Cancer Hospital, Pecking University Cancer Hospital Yunnan, Kunming, Yunnan, China, [2]The Department of Clinical Oncology, The Seventh Affiliated Hospital, Sun Yat-Sen University, Shenzhen, Guangdong, China, [3]Department of VIP Region, Sun Yat-sen University Cancer Center, State Key Laboratory of Oncology in South China, Collaborative Innovation Center for Cancer Medicine, Guangzhou, Guangdong, China

Background: Pralsetinib is a selective RET inhibitor. The ARROW trial revealed that RET fusion-positive non-small-cell lung cancer (NSCLC) can benefit from pralsetinib with tolerable adverse events (AEs). However, the efficacy and safety of pralsetinib in real world has rarely been reported.

Materials and methods: This study reviewed the efficacy and safety of pralsetinib in RET fusion-positive NSCLC patients between March 2021 and December 2021. Progression-free survival (PFS) and overall survival (OS) were evaluated by a Kaplan-Meier analysis and log-rank test. A Cox regression model was performed to identify independent prognostic factors.

Results: A total of 28 patients were enrolled, and the median follow-up time was 18.1 months. The objective response rate and disease control rate of the whole cohort were 57.2% and 71.4%, respectively, and the median PFS and OS were 8.1 months [95% confidence interval (CI), 3.1–13.2] and 13.8 months (95% CI, 2.8–24.8), respectively. Baseline characteristics of the treatment naive group and pre-treated group were listed. The median PFS tended to be better in treatment naive group (18.3 vs. 8.0 months, $P = 0.067$), while the median OS were similar between the two groups (28.4 vs. 11.6 months, $P = 0.308$). Patients with Eastern Cooperative Oncology Group Performance Status (ECOG PS) score of 2 had worse median PFS comparing with those with ECOG PS score of 0–1 (3.8 vs. 12.6 months, $P = 0.004$). Besides, patients previously treated with platinum-based chemotherapy (PBC) also revealed worse median PFS comparing with those without previous PBC (8.0 vs. 18.6 months, $P = 0.023$). Furthermore, patients previously treated with anti-programmed death-1 (PD-1) antibody or multikinase inhibitors (MKIs) showed worse median OS compared with those without previous anti-PD-1 antibody (5.0 vs. 22.0 months, $P = 0.002$) or MKIs (6.2 vs. 28.4 months, $P = 0.015$). The most common AEs was increased aspartate aminotransferase (39.3%).

Conclusion: Pralsetinib was effective in RET fusion-positive NSCLC with tolerable AEs in real-world practice. Efficacy of pralsetinib was decreased in patients previously treated with PBC, immunotherapy, or MKIs.

KEYWORDS

RET fusion, non-small-cell lung cancer, pralsetinib, survival outcomes, prognostic factors

Introduction

Non-small-cell lung cancer (NSCLC) is one of the most common causes of cancer-related deaths globally (1). The treatment approaches of NSCLC include surgery, radiotherapy, chemotherapy, immunotherapy, and target therapy alone or in combination, but the effectiveness of current therapies are not ideal. Therefore, development of new treatment is necessary.

About 1%−3% NSCLC patients have rearranged during transfection (RET) fusions, resulting in RET pathway activation (2). Multikinase inhibitors (MKIs) with anti-RET activities have been used in RET fusion-positive NSCLC in clinical practice, but the effectiveness is limited with obvious off-target toxicities (3–5). Selpercatinib (LOXO-292) and pralsetinib (BLU667) are highly selective inhibitors targeted to RET alterations. LIBRETTO-001 trial reported that the median progression-free survival (PFS) in RET fusion-positive NSCLC patients treated with selpercatinib was 17 months, and the overall response rate (ORR) in untreated and pretreated patients were 64% [95% confidence interval (CI), 54%−73%] and 85% (95% CI, 70%−94%), respectively (6). Further, the ARROW trial revealed median PFS of 17.1 months in the whole cohort of RET-altered NSCLC treated with pralsetinib (7). Besides, the ARROW trial also demonstrated a response rate of 73% (95% CI, 52%−88%) in treatment-naive subgroup, and 61% (95% CI, 50%−72%) in treated subgroup (7). Thus, selpercatinib and pralsetinib are approved for the treatment of NSCLC patients with RET fusions, and pralsetinib has been approved in China in 2021 (8).

Although real-world experience of pralsetinib in RET fusion-positive NSCLC has been reported in Italy (9), the experience of pralsetinib among Chinese population has been rarely reported. Therefore, the retrospective study was conducted to provide insight for clinical practice.

Materials and methods

Patient selection

In this retrospective study, patients with locally advanced or metastatic NSCLC between March 2021 and December 2021 at Sun Yat-sen University Cancer Center were reviewed. Inclusion criteria were as follows: (1) histologically confirmed as NSCLC; (2) locally advanced or metastatic disease (stage IIIB, IIIC, or IV unresectable disease); and (3) received at least one dose of pralsetinib. The exclusion criteria were as follows: (1) combination therapy of pralsetinib with other anti-tumor drugs; (2) lack of treatment data; and (3) lost follow-up. All clinical records and image information were reviewed. The study was approved by the Medical Ethics Committee of Sun Yat-sen University Cancer Center (B2024-130-01). Key data of this study has been uploaded onto the Research Data Deposit public platform.

Statistical analysis

Tumor response was defined by the Response Evaluation Criteria in Solid Tumors version 1.1 (10). The ORR referred to the rate of complete response (CR) and partial response (PR), and the disease control rate (DCR) referred to the rate of CR, PR, and stable disease (SD). PFS was defined as the beginning of pralsetinib to disease progression or death, and overall survival (OS) was defined as the beginning of pralsetinib to death due to any cause. Adverse events (AEs) during treatment were assessed based on the Common Terminology Criteria for Adverse Events version 5.0 (11).

Continuous and categorical variables were compared by chi squared and Mann-Whitney U tests, respectively. Survival outcomes were evaluated by the Kaplan-Meier method and log-rank test. All tests were two sided and $P < 0.05$ was considered statistically significant. Statistical analyses were performed using SPSS 25.0 software.

Results

Patient characteristics

A total of 28 RET fusion-positive advanced NSCLC patients treated with pralsetinib monotherapy were identified (Table 1). The median age was 54 years (range, 28–80 years), and 13 (46.4%) patients were male. Eight (28.6%) patients were current or former smokers, and seven (25.0%) patients had an Eastern Cooperative Oncology Group Performance Status (ECOG PS) score of 2. Except for one patient of mucoepidermoidcarcinoma, another 27 patients were diagnosed with adenocarcinoma, and 8 (28.6%) patients had brain metastasis. The most common RET fusion partner was KIF5B (53.6%). More than half (19/28, 67.9%) patients were previously treated with platinum-based chemotherapy (PBC), five patients were previously treated with anti-programmed death-1 (PD-1) antibody, and nearly half (12/28, 41.9%) patients previously received multikinase inhibitors (MKIs). There were eight patients had pralsetinib as the first-line therapy, and 20 patients were pre-treated.

Treatment

All patients were initially treated with 400 mg once daily. Eight (28.6%) patients experienced dose reduction due to AEs, including one patient of hepatotoxicity, two patients of decreased platelets, one patient of increased creatinine, two patients of increased alkaline phosphatase and aspartate aminotransferase, one patient of pneumonitis, and one patient of musculoskeletal pain, respectively. Besides, three (10.7%) patients discontinued the therapy because of hepatotoxicity, pulmonary fibrosis, and financial reason, respectively. Therapies after pralsetinib were as follows: rechallenge of chemotherapy with or without bevacizumab, local therapy, and immunotherapy.

Efficacy

With a median follow-up time of 18.1 months (range, 1.8–38.2) of the whole cohort, the median PFS and OS were 8.1 months (95% CI, 3.1–13.2; Figure 1A) and 13.8 months (95% CI, 2.8–24.8; Figure 1B), respectively. The median PFS tended to be

TABLE 1 Baseline characteristics.

Characteristics	Number ($n = 28$, %)	Treatment naive ($n = 8$, %)	Pre-treated ($n = 20$, %)	*P*-value
Age (years)				
<60	21 (75.0%)	6 (75.0%)	15 (75.0%)	1.000
≥60	7 (25.0%)	2 (25.0%)	5 (25.0%)	
Gender				
Female	15 (53.6%)	3 (37.5%)	12 (60.0%)	0.381
Male	13 (46.4%)	5 (62.5%)	8 (40.0%)	
Smoking history				
Current or former	8 (28.6%)	3 (37.5%)	5 (25.0%)	0.636
Never or unknown	20 (71.4%)	5 (62.5%)	15 (75.0%)	
Histology				
Adenocarcinoma	27 (96.4%)	8 (100.0%)	19 (95.0%)	0.862
Other	1 (3.6%)	0 (0.0%)	1 (5.0%)	
ECOG PS				
0–1	21 (75.0%)	7 (87.5%)	14 (70.0%)	0.500
2	7 (25.0%)	1 (12.5%)	6 (30.0%)	
Brain metastasis				
Yes	8 (28.6%)	1 (12.5%)	7 (35.0%)	0.381
No	20 (71.4%)	7 (87.5%)	13 (65.0%)	
RET fusion partner				
KIF5B	15 (53.6%)	4 (50.0%)	11 (55.0%)	0.784
CCDC6	5 (17.9%)	2 (25.0%)	3 (15.0%)	
Other	5 (17.9%)	0 (0.0%)	5 (25.0%)	
Unknown	3 (10.7%)	2 (25.0%)	1 (5.0%)	
Lines of previous therapy				
0	8 (28.6%)	8 (100.0%)	0 (0.0%)	/
1–2	14 (50.0%)	0 (0.0%)	14 (70.0%)	
≥3	6 (21.4%)	0 (0.0%)	6 (30.0%)	
Previous therapy				
PBC	19 (67.9%)	0 (0.0%)	19 (95.0%)	/
Anti-PD-1 antibody	5 (17.9%)	0 (0.0%)	5 (25.0%)	
MKIs	12 (42.9%)	0 (0.0%)	12 (60.0%)	

ECOG PS, Eastern Cooperative Oncology Group Performance Status; PBC, Platinum-based chemotherapy; PD-1, Programmed death-1; MKIs, Multikinase inhibitors.

better in treatment naive group compared with the pre-treated group (18.3 vs. 8.0 months, $P = 0.067$, Figure 1C), while the median OS were similar between the two groups (28.4 vs. 11.6 months, $P = 0.308$, Figure 1D).

In the whole cohort, The ORR and DCR rates were 57.2 and 71.4%, respectively (Table 2). One (3.6%) patient achieved CR, 15 (53.6%) patients achieved PR, four (14.3%) patients revealed SD, six (21.5%) patients developed progressive disease, and 2 (7.1%) patients could not be evaluated. Although the best overall responses were similar between the treatment naive group and the pre-treated group ($P = 0.443$), the treatment naive group gained better median duration of response ($P = 0.050$).

Univariate and multivariate analysis

Univariate and multivariate analysis were conducted to identify independent prognostic factors (Table 3). The univariate and multivariate analysis showed that poor ECOG PS [hazard ratio (HR), 5.052; 95% CI, 1.595–16.008; $P = 0.006$] and previous PBC (HR, 4.320; 95% CI, 1.111–16.797; $P = 0.035$) were independent

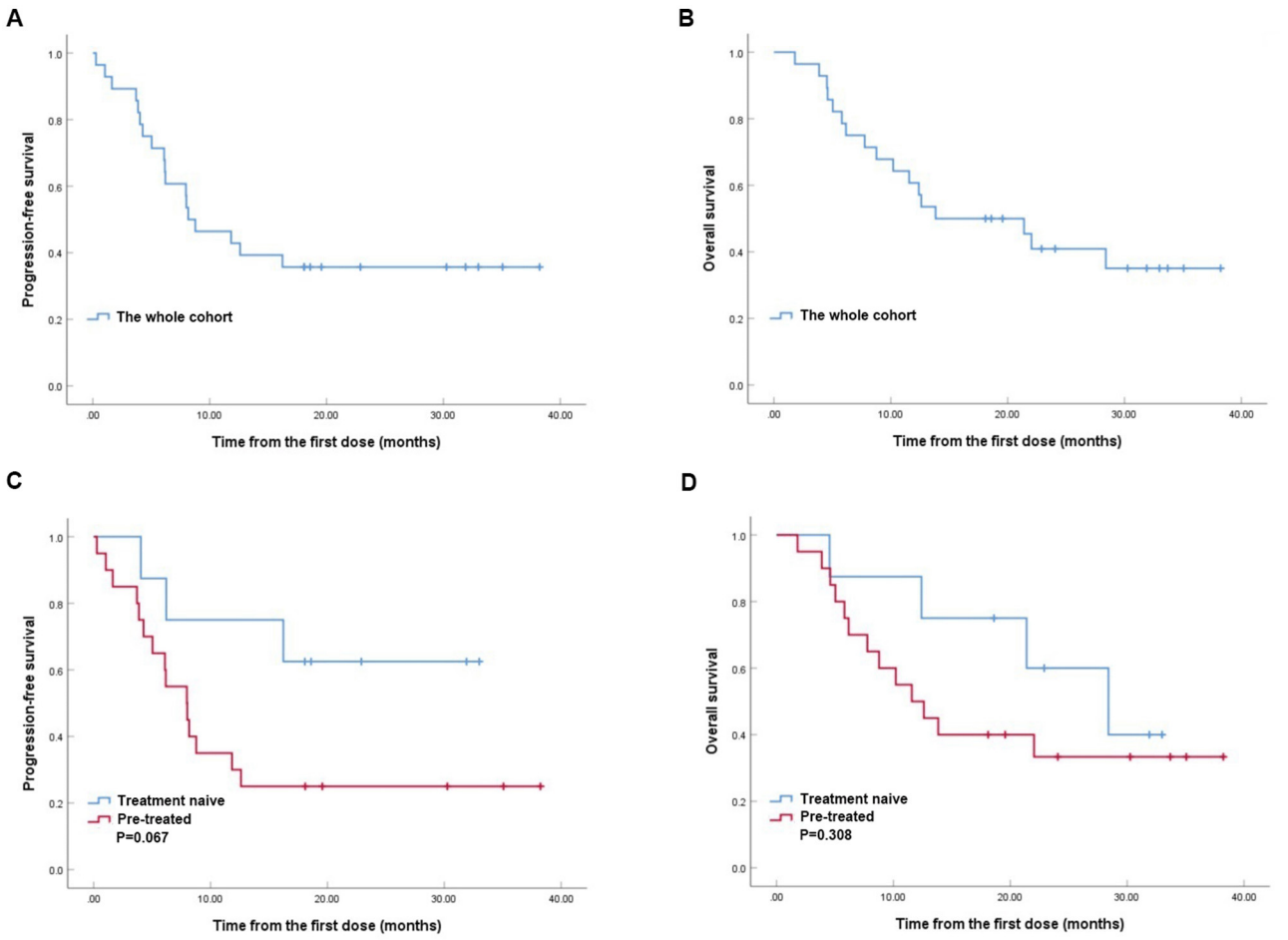

FIGURE 1
Kaplan–Meier analyses of progression-free survival (PFS) **(A)** and overall survival (OS) **(B)** in RET fusion-positive non-small-cell lung cancer patients treated with pralsetinib. Kaplan-Meier analyses of PFS **(C)** and OS **(D)** between treatment naive group and pre-treated group.

prognostic factors in PFS, while previous anti-PD-1 antibody (HR, 3.168; 95% CI, 1.010–9.941; $P = 0.048$) and previous MKIs (HR, 3.777; 95% CI, 1.284–11.111; $P = 0.016$) were independent prognostic factors in OS. Furthermore, no statistical significance of brain metastasis in PFS (HR, 0.917; 95% CI, 0.326–2.576; $P = 0.869$) and OS (HR, 0.693; 95% CI, 0.225–2.131; $P = 0.522$) were observed.

Subgroup analysis

Further analysis of PFS and OS in different subgroups were conducted (Figure 2), and the baseline characteristics between the compared groups were listed in Supplementary material (Tables 1–4). Significant better median PFS was observed in patients with ECOG PS score of 0–1 comparing with those with ECOG PS score of 2 (12.6 vs. 3.8 months, $P = 0.004$; Figure 2A), while the median OS tended to be better in ECOG PS score of 0–1 group (22.0 vs. 6.2 months, $P = 0.068$; Figure 2B). Besides, patients without previous PBC gained longer median PFS comparing with those previously treated with PBC (18.6 vs. 8.0 months, $P = 0.023$; Figure 2C), while the median OS was similar between the two groups (28.4 vs. 11.6 months, $P = 0.134$; Figure 2D). Moreover, better median PFS (12.6 vs. 5.0 months, $P = 0.029$; Figure 2E) and OS (22.0 vs. 5.0 months, $P = 0.002$; Figure 2F) were observed in patients without previous use of anti-PD-1 antibody comparing with those with previous anti-PD-1 antibody. Furthermore, although similar median PFS were observed in patients with or without previous MKIs (5.0 vs. 11.8 months, $P = 0.160$; Figure 2G), patients without previous use of MKIs revealed better median OS (28.4 vs. 6.2 months, $P = 0.015$; Figure 2H).

Safety

AEs during treatment are listed in Table 4. The most common hematological AEs were decreased hemoglobin (32.1%), decreased neutrophils (32.1%), and decreased platelets (14.3%). Increased aspartate aminotransferase (AST) and increased alanine aminotransferase (ALT) occurred in 39.3% and 25.0% patients, respectively, with 1 patient suffering from Grade 3 increased ALT. Decreased sodium affected 10.7% patients, with one patient

TABLE 2 Clinical activity endpoints in patients with measurable disease.

Variables	Number (%)	Treatment naive ($n = 8$, %)	Pre-treated ($n = 20$, %)	*P*-value
Overall response rate	16 (57.2%)	6 (75.0%)	14 (70.0%)	/
Disease control rate	20 (71.4%)	6 (75.0%)	19 (95.0%)	/
Best overall response				
Complete response	1 (3.6%)	0 (0.0%)	1 (5.0%)	0.443
Partial response	15 (53.6%)	6 (75.0%)	8 (40.0%)	
Stable disease	4 (14.3%)	0 (0.0%)	5 (25.0%)	
Progressive disease	6 (21.4%)	1 (12.5%)	5 (25.0%)	
Not evaluable	2 (7.1%)	1 (12.5%)	1 (5.0%)	
Median duration of response, months				
Rate at 6 months	71.4%	87.5%	65.0%	0.050
Rate at 12 months	42.9%	75.0%	30.0%	

experiencing ≥ Grade 3 decreased sodium. The most common general AEs were hypertension (3/28, 10.7%), vomiting (3/28, 10.7%), and pneumonitis (3/28, 10.7%), while one patient had ≥ Grade 3 hypertension and 1 patient had ≥ Grade 3 vomiting. Moreover, no patients had diarrhea or constipation during the treatment.

Discussion

RET fusions were firstly identified in lung cancer in 2012 (12), and MKIs such as cabozantinib (3), lenvatinib (4), and vandetanib (5) were available with limited responses and high rates of off-target toxicities. Pralsetinib is a highly selective RET inhibitor being developed for the treatment of various solid tumors with RET fusions (8). The phase 1/2 ARROW study enrolled 233 patients with locally advanced or metastatic solid RET fusion-positive NSCLC to treat with 400 mg once-daily oral pralsetinib (7). In the previously-treated cohort, the ORR was 57%, including 5/87 (5.7%) CR and 48/87 (55%) PR, respectively, while the ORR was 70% in the treatment-naive cohort, including 3/27 (11%) CR and 16/27 (59%) PR, respectively (7). Therefore, pralsetinib was approved for the treatment of RET fusion-positive NSCLC in the United States in 2020, and in China in 2021 (8).

In our real-world study, 28 patients with RET fusion-positive NSCLC were treated with pralsetinib monotherapy. Consistent to previous investigations demonstrating that RET fusion revealed higher frequencies in younger non-smoking female with lung adenocarcinoma (2, 13, 14), the present study showed that 75% patients had age of <60 years old, more than half patients were female, and 71.4% patients were never or unknown smokers. Besides, we observed that the most common RET fusions were KIF5B-RET (53.6%) and CCDC6-RET (17.9%), which was similar to the clinical trials (6, 7). However, the proportion of patients with ECOG PS score of 2 was 25% in the current study, which was higher than prospective studies (6, 7). Furthermore, similar to real-world data from Italy (9), only around 20% patients received pralsetinib as their first-line treatment in the current study, which was different from the analysis of the part of phase 1/2 ARROW trial in China including 31 patients in the treatment naive group and 37 patients in previous platinum-based chemotherapy group (15). Although no significant difference was observed in median OS between treatment naive group and pre-treated group (28.4 vs. 11.6 months, $P = 0.308$), treatment naive group tended to reveal longer median PFS (18.3 vs. 8.0 months, $P = 0.067$). Thus, we proposed clinicians to conduct gene test in advanced NSCLC at diagnosis, and to use pralsetinib as the first-line therapy in patients with RET fusion.

Moreover, in this retrospective study, similar ORR among the current study (57.2%), the ARROW trial (53.0%) (7), the Chinese population of the ARROW trial (66.7%) (16), and real-world investigation from Italy (66.0%) (9) were observed. However, we observed similar median PFS in the present study comparing with the real-world investigation in Italy (8.1 vs. 8.9 months) (9), but shorter median PFS comparing with the ARROW trial (8.1 vs. 17.1 months) (7) and the Chinese population analysis in ARROW trial (8.1 VS. 11.7 months) (15). These results demonstrated that the efficacy of pralsetinib in real world might be influenced by other risk factors such as previous treatments, and further investigations are warrant.

Furthermore, we observed statistical significance of previous anti-PD-1 antibody in PFS in univariate analysis (HR, 3.189; 95% CI, 1.065–9.0548; $P = 0.038$), and identified previous anti-PD-1 antibody as independent prognostic factor in OS (HR, 3.168; 95% CI, 1.010–9.941; $P = 0.048$). Besides, previous use of MKIs was identified as an independent prognostic factor in OS (HR, 3.777; 95% CI, 1.284–11.111; $P = 0.016$). These results were consistent to which reported by Meng et al. (16), indicating that patients with RET fusion NSCLC are not likely to benefit well from immunotherapy and MKIs. We also observed no statistical significance of brain metastasis in PFS (HR, 0.917; 95% CI, 0.326–2.576; $P = 0.869$) and OS (HR, 0.693; 95% CI, 0.225–2.131; $P = 0.522$) in the present study. Subbiah et al. investigated the intracranial efficacy of selpercatinib, and observed an ORR of 82% and an CR of 23% among 22 patients with

TABLE 3 Univariate and multivariate analysis of prognostic factors for 28 patients treated with pralsetinib.

Variables	PFS				OS			
	Univariate analysis		Multivariate analysis		Univariate analysis		Multivariate analysis	
	HR (95% CI)	*P*	HR (95% CI)	*P*	HR (95% CI)	*P*	HR (95% CI)	*P*
Age (years)								
<60	Ref.		–		Ref.		–	
≥60	2.076 (0.758–5.682)	0.155			1.963 (0.719–5.361)	0.188		
Gender								
Female	Ref.		–		Ref.		–	
Male	1.002 (0.394–2.549)	0.996			0.745 (0.287–1.938)	0.547		
Smoking history								
Current or former	Ref.		–		Ref.		–	
Never or unknown	1.031 (0.367–2.898)	0.954			1.490 (0.548–4.049)	0.435		
ECOG PS								
0–1	Ref.		**Ref.**		Ref.		–	
2	3.983 (1.450–10.940)	0.007	**5.052 (1.595–16.008)**	**0.006**	2.616 (0.895–7.645)	0.079		
Brain metastasis								
Yes	Ref.		–		Ref.		–	
No	0.917 (0.326–2.576)	0.869			0.693 (0.225–2.131)	0.522		
Lines of previous therapy								
0	Ref.				Ref.		–	
1–2	2.982 (0.823–10.801)	0.096			1.536 (0.472–5.000)	0.476		
≥3	3.177 (0.707–14.272)	0.131			2.955 (0.705–12.386)	0.138		
Previous PBC								
Yes	Ref.		**Ref.**		Ref.		–	
No	3.884 (1.110–13.588)	0.034	**4.320 (1.111–16.797)**	**0.035**	20320 (0.748–7.193)	0.145		
Previous anti-PD-1 antibody								
Yes	Ref.				Ref.		**Ref.**	
No	3.189 (1.065–9.548)	0.038	1.782 (0.554–5.735)	0.333	5.021 (1.634–15.426)	0.005	**3.168 (1.010–9.941)**	**0.048**
Previous MKIs								
Yes	Ref.				Ref.		**Ref.**	
No	1.924 (0.760–4.871)	0.167			3.239 (1.201–8.736)	0.020	**3.777 (1.284–11.111)**	**0.016**

HR, hazard ratio; CI, confidence interval; ECOG PS, Eastern Cooperative Oncology Group Performance Status; PBC, Platinum-based chemotherapy; PD-1, Programmed death-1; MKIs, Multikinase inhibitors. The bold values were used to highlight the statistical significance.

measurable intracranial disease, showing a robust and durable intracranial efficacy in RET fusion-positive NSCLC patients (17). Pralsetinib showed blood penetration and activity against intracranial tumors in preclinical model (18), and Passaro et al. (9) reported effectiveness of pralsetinib in intracranial disease with ORR of 66.7%. Therefore, we preferred to propose the efficacy of pralsetinib in patients with brain metastasis, and more head-to-head comparisons and large sample real-world studies are needed.

There are some differences between our study and the ARROW trial in terms of the AEs profile. Neutropenia (21%) was the most common hematological side effect in the ARROW trial (7), while decreased hemoglobin (32.1%) and neutrophils (32.1%) were the most common AEs in the current study. We preferred to attribute this difference to poor performance status (ECOG PS = 2, 25.0%) and heavy previous treatment (lines ≥3, 21.4%) before the use of pralsetinib in our study. In addition, the incidence of increased creatinine in our investigation (3.6%) was lower than which in the ARROW trial (8%) (7), while the incidences of increased AST and ALT were similar between our study and the ARROW trial. This might result from that pralsetinib is mainly metabolized by liver (8).

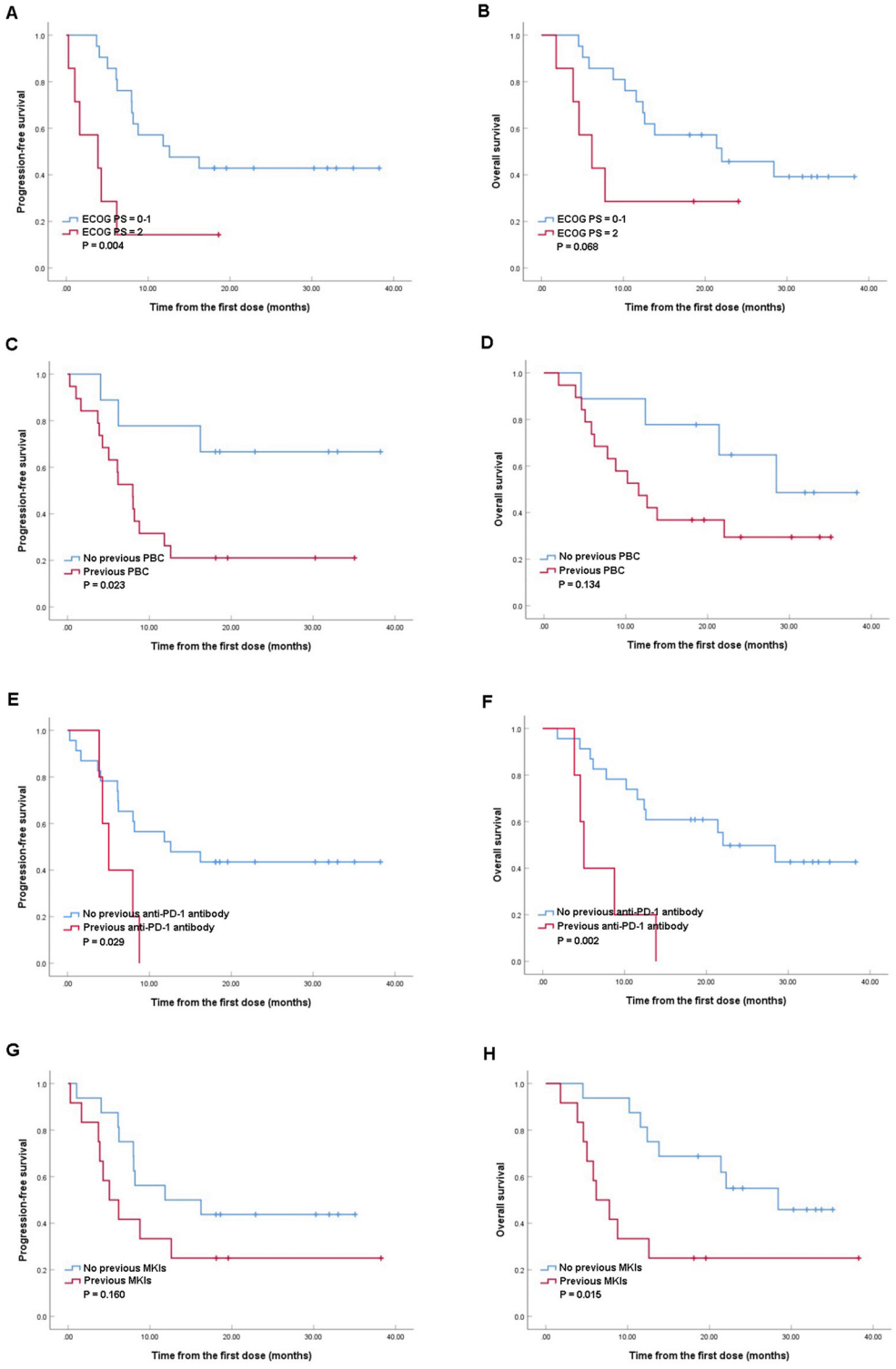

FIGURE 2
Kaplan–Meier analyses of progression-free survival and overall survival in patients with Eastern Cooperative Oncology Group Performance Status (ECOG PS) of 0–1 and ECOG PS of 2 **(A, B)**; patients with or without previous platinum-based chemotherapy (PBC) **(C, D)**, patients with or without previous anti-programmed death-1 (PD-1) antibody **(E, F)**, patients with or without previous multikinase inhibitors (MKIs) **(G, H)**.

The present study had some limitations. This was a retrospective study based on experience from a single institution with a small sample size. Although bias was unavoidable, we collected detailed data to reveal the treatment of pralsetinib in advanced NSCLC with RET fusions in real world, in order to provide clinical reference for future treatment.

TABLE 4 Treatment-related adverse events.

Adverse events	Any grade (%)	Grade 3–4 (%)
Hematology		
Decreased hemoglobin	9 (32.1%)	1 (3.6%)
Decreased lymphocytes	1 (3.6%)	0 (0.0%)
Decreased neutrophils	9 (32.1%)	1 (3.6%)
Decreased platelets	4 (14.3%)	1 (3.6%)
Chemistry		
Increased AST	11 (39.3%)	0 (0.0%)
Increased ALT	7 (25.0%)	1 (3.6%)
Increased creatinine	1 (3.6%)	0 (0.0%)
Increased alkaline phosphatase	2 (7.1%)	0 (0.0%)
Decreased calcium (corrected)	0 (0.0%)	0 (0.0%)
Decreased sodium	3 (10.7%)	1 (3.6%)
General		
Fatigue	2 (7.1%)	0 (0.0%)
Pyrexia	1 (3.6%)	0 (0.0%)
Edema	3 (10.7%)	0 (0.0%)
Musculoskeletal pain	1 (3.6%)	0 (0.0%)
Hypertension	3 (10.7%)	1 (3.6%)
Dry mouth	1 (3.6%)	0 (0.0%)
Diarrhea	0 (0.0%)	0 (0.0%)
Constipation	0 (0.0%)	0 (0.0%)
Vomiting	3 (10.7%)	1 (3.6%)
Pneumonitis	3 (10.7%)	0 (0.0%)

AST, aspartate aminotransferase; ALT, alanine aminotransferase.

Conclusions

Our study demonstrated that pralsetinib was effective in RET fusion-positive advanced NSCLC with tolerable AEs. The benefits of pralsetinib in patients previously treated with PBC, immunotherapy, or MKIs were decreased. Since this is a retrospective study from a single institution with small sample size, further large sample real-world studies worldwide are warranted.

Data availability statement

The raw data supporting the conclusions of this article are available upon request to the authors, or from the Research Data Deposit public platform (https://www.researchdata.org.cn).

Ethics statement

The studies involving humans were approved by the Medical Ethics Committee of Affiliated Hospital of Sun Yat-sen University Cancer Center with written informed consent waived (B2024-130-01). The studies were conducted in accordance with the local legislation and institutional requirements. The Ethics Committee/institutional review board waived the requirement of written informed consent for participation from the participants or the participants' legal guardians/next of kin because of the retrospective nature of the study.

Author contributions

LW: Conceptualization, Formal analysis, Funding acquisition, Project administration, Writing – original draft. YY: Conceptualization, Funding acquisition, Resources, Writing – original draft. WH: Data curation, Writing – review & editing. YH: Software, Validation, Writing – review & editing. LL: Investigation, Writing – review & editing. LW: Investigation, Methodology, Writing – review & editing. CJ: Methodology, Writing – review & editing. JY: Project administration, Resources, Writing – review & editing. YX: Conceptualization, Funding acquisition, Supervision, Writing – review & editing. LX: Conceptualization, Funding acquisition, Supervision, Writing – review & editing.

Funding

The author(s) declare financial support was received for the research, authorship, and/or publication of this article. This work was supported by the Scientific Research Fund Project of Yunnan Education Department [2023Y0662] and Yunnan Fundamental Research Projects [202401CF070001].

Conflict of interest

The authors declare that the research was conducted in the absence of any commercial or financial relationships that could be construed as a potential conflict of interest.

Publisher's note

Supplementary material

The Supplementary Material for this article can be found online at: https://www.frontiersin.org/articles/10.3389/fmed.2025.1467871/full#supplementary-material

References

1. World Health Organization. *Cancer Fact Sheet*. (2018). Available at: https://www.who.int/news-room/fact-sheets/detail/cancer

2. Zhao Z, Fu T, Gao J, Xu Y, Wu X, Chen W, et al. Identifying novel oncogenic RET mutations and characterising their sensitivity to RET-specific inhibitors. *J Med Genet.* (2020). doi: 10.1136/jmedgenet-2019-106546

3. Drilon A, Rekhtman N, Arcila M, Wang L, Ni A, Albano M, et al. Cabozantinib in patients with advanced RET-rearranged non-small-cell lung cancer: an open-label, single-centre, phase 2, single-arm trial. *Lancet Oncol.* (2016) 17:1653–60. doi: 10.1016/S1470-2045(16)30562-9

4. Hida T, Velcheti V, Reckamp KL, Nokihara H, Sachdev P, Kubota T, et al. A phase 2 study of lenvatinib in patients with RET fusion-positive lung adenocarcinoma. *Lung Cancer.* (2019) 138:124–30. doi: 10.1016/j.lungcan.2019.09.011

5. Lee SH, Lee JK, Ahn MJ, Kim DW, Sun JM, Keam B, et al. Vandetanib in pretreated patients with advanced non-small cell lung cancer-harboring RET rearrangement: a phase II clinical trial. *Ann Oncol.* (2017) 28:292–7. doi: 10.1093/annonc/mdw559

6. Drilon A, Oxnard GR, Tan DSW, Loong HHF, Johnson M, Gainor J, et al. Efficacy of selpercatinib in RET fusion-positive non-small-cell lung cancer. *N Engl J Med.* (2020) 383:813–24.

7. Gainor JF, Curigliano G, Kim DW, Lee DH, Besse B, Baik CS, et al. Pralsetinib for RET fusion-positive non-small-cell lung cancer (ARROW): a multi-cohort, open-label, phase 1/2 study. *Lancet Oncol.* (2021) 22:959–69. doi: 10.1016/S1470-2045(21)00247-3

8. Markham A. Selpercatinib: first approval. *Drugs.* (2020) 80:1119–24. doi: 10.1007/s40265-020-01343-7

9. Passaro A, Russo GL, Passiglia F, D'Arcangelo M, Sbrana A, Russano M, et al. Pralsetinib in RET fusion-positive non-small-cell lung cancer: a real-world data (RWD) analysis from the Italian expanded access program (EAP). *Lung Cancer.* (2022) 174:118–24. doi: 10.1016/j.lungcan.2022.11.005

10. Eisenhauer EA, Therasse P, Bogaerts J, Schwartz LH, Sargent D, Ford R. et al. New response evaluation criteria in solid tumors: revised RECIST guideline (version 11). *Eur J Cancer.* (2009) 45:228–47. doi: 10.1016/j.ejca.2008.10.026

11. Department of Health and Human Services and National Institutes of Health. National Cancer Institute. *Common terminology criteria for adverse events (CTCAE) v5.0 2017*. Available at: https://ctep.cancer.gov/protocoldevelopment/electronic_applications/docs/CTCAE_v5_Quick_Reference_8.5x11.pdf

12. Takamori S, Matsubara T, Haratake N, Toyokawa G, Fujishita T. Toyozawa R, et al. Targeted therapy for ret fusion lung cancer: breakthrough and unresolved issue. *Front Oncol.* (2021) 11:704084. doi: 10.3389/fonc.2021.704084

13. Yoo SS, Jin G, Jung HJ, Hong MJ, Choi JE, Jeon HS, et al. RET fusion genes in Korean non-small cell lung cancer. *J Korean Med Sci.* (2013) 28:1555–8. doi: 10.3346/jkms.2013.28.10.1555

14. Kato S, Subbiah V, Marchlik E, Elkin SK, Carter JL, Kurzrock R. RET aberrations in diverse cancers: next-generation sequencing of 4,871 patients. *Clin Cancer Res.* (2017) 23:1988–97. doi: 10.1158/1078-0432.CCR-16-1679

15. Zhou Q, Zhao J, Chang J, Wang H, Fan Y, Wang K, et al. Efficacy and safety of pralsetinib in patients with advanced RET fusion-positive non-small cell lung cancer. *Cancer.* (2023) 129:3239–51. doi: 10.1002/cncr.34897

16. Meng Y, Yang Y, Fang Y, Lin X, Xie X, Deng H, et al. The treatment status of patients in NSCLC with RET fusion under the prelude of selective RET-TKI application in China: a multicenter retrospective research. *Front Oncol.* (2022) 12:864367. doi: 10.3389/fonc.2022.864367

17. Subbiah V, Gainor JF, Oxnard GR, Tan DSW, Owen DH, Cho BC, et al. Intracranial efficacy of selpercatinib in RET fusion-positive non-small cell lung cancers on the LIBRETTO-001 trial. *Clin Cancer Res.* (2021) 27:4160–7. doi: 10.1158/1078-0432.CCR-21-0800

18. Evans E, Hu W, Cao H, Hoeflich K, Dorsch M. BLU-667 demonstrates robust activity in RET fusion-driven intracranial tumor models. *J Thorac Oncol.* (2019) 14(Supplement):S701. doi: 10.1016/j.jtho.2019.08.1491

frontiers | Frontiers in Medicine

TYPE Original Research
PUBLISHED 31 January 2025
DOI 10.3389/fmed.2025.1477275

OPEN ACCESS

EDITED BY
Alessandro Leonetti,
University Hospital of Parma, Italy

REVIEWED BY
Salvatore Annunziata,
Fondazione Policlinico Universitario A. Gemelli IRCCS, Italy
Ding Chong Yang,
Nanjing Medical University, China

*CORRESPONDENCE
Yanzhu Bian
✉ yanzhubian99@163.com

RECEIVED 07 August 2024
ACCEPTED 20 January 2025
PUBLISHED 31 January 2025

CITATION
Zheng L, Bian Y, Hu Y, Tian C, Zhang X, Li S, Yang X and Qin Y (2025) Baseline ^{18}F-FDG PET/CT parameters in predicting the efficacy of immunotherapy in non-small cell lung cancer.
Front. Med. 12:1477275.
doi: 10.3389/fmed.2025.1477275

Baseline ^{18}F-FDG PET/CT parameters in predicting the efficacy of immunotherapy in non-small cell lung cancer

Lu Zheng[1,2], Yanzhu Bian[1,2]*, Yujing Hu[1], Congna Tian[1], Xinchao Zhang[1], Shuheng Li[3], Xin Yang[1] and Yanan Qin[1]

[1]Department of Nuclear Medicine, Hebei General Hospital, Shijiazhuang, China, [2]Hebei Provincial Key Laboratory of Cerebral Networks and Cognitive Disorders, Shijiazhuang, China, [3]Department of Nuclear Medicine, Affiliated Hospital of Hebei University, Baoding, China

Objective: To analyse positron emission tomography/ computed tomography (PET/CT) imaging and clinical data from patients with non-small cell lung cancer (NSCLC), to identify characteristics of survival beneficiaries of immune checkpoint inhibitors (ICIs) treatment and to establish a survival prediction model.

Methods: A retrospective analysis was conducted on PET/CT imaging and clinical parameters of 155 NSCLC patients who underwent baseline PET/CT examination at the Department of Nuclear Medicine, Hebei General Hospital. The Kaplan–Meier curve was employed to compare progression-free survival (PFS) and overall survival (OS) between the ICIs and non-ICIs group and to assess the impact of variables on PFS and OS in the ICIs group. Multivariate Cox proportional hazards regression analysis was conducted with parameters significantly associated with survival in univariate analysis.

Results: Significant differences were observed in PFS (χ^2 = 11.910, p = 0.0006) and OS (χ^2 = 8.343, p = 0.0039). Independent predictors of PFS in the ICIs group included smoking history[hazard ratio (HR) = 2.522, 95% confidence interval (CI): 1.044 ~ 6.091, p = 0.0398], SUVmax of the primary lesion(HR = 0.2376, 95%CI: 0.1018 ~ 0.5548, p = 0.0009), MTVp (HR = 0.0755, 95%CI: 0.0284 ~ 0.2003, p < 0.001), and TLGp (HR = 0.1820, 95%CI: 0.0754 ~ 0.4395, p = 0.0002). These were also independent predictors of OS in the ICIs group[HR(95%CI) were 2.729 (1.125 ~ 6.619), 0.2636 (0.1143 ~ 0.6079), 0.0715 (0.0268 ~ 0.1907), 0.2102 (0.0885 ~ 0.4992), both p < 0.05)]. Age was an additional independent predictor of OS (HR = 0.4140, 95%CI: 0.1748 ~ 0.9801, p = 0.0449).

Conclusion: Smoking history, primary lesion SUVmax, MTVp, and TLGp were independent predictors of PFS, whilst age, smoking history, SUVmax, MTVp, and TLGp were independent predictors of OS in the ICIs group. Patients without a history of smoking and with SUVmax ≤19.2, MTVp ≤20.745cm^3, TLGp ≤158.62 g, and age ≤ 60 years benefited more from ICI treatment.

KEYWORDS

PET/CT, SUV, non-small cell lung cancer, immune checkpoint inhibitors, prognosis

1 Introduction

Lung cancer is a primary malignancy originating from the trachea, bronchial mucosa, or glands, and can be classified into small cell lung cancer (SCLC) and non-small cell lung cancer (NSCLC) based on histological heterogeneity. NSCLC accounts for approximately 80–85% of all lung cancers, with a 5-year survival rate of only 10–16% for patients with advanced NSCLC (1, 2). According to the China's latest cancer survey in 2022, lung cancer ranks first in incidence and mortality (3). Advances in medical treatment have led to an increasing number of immune checkpoint inhibitors (ICIs) being approved for lung cancer in China, and the application of immunotherapy in the treatment of NSCLC has gradually become more widespread. Preliminary studies (4, 5) have suggested that ^{18}F-fluorodeoxyglucose (^{18}F-FDG) uptake is associated with the efficacy of immunotherapy, with higher maximum standard uptake value (SUVmax) correlating with better treatment outcomes. However, higher metabolic tumour volume (MTV) and total lesion glycolysis (TLG) are associated with a higher non-response rate and worse prognosis in NSCLC patients treated with ICIs. The objective response rate to ICIs is approximately 20% with 10% of patients experiencing serious immune-related adverse events (irAEs) (6). This study aims to analyse positron emission tomography/ computed tomography (PET/CT) imaging and clinical data of NSCLC patients treated with and without ICIs, comparing differences in progression-free survival (PFS) and overall survival (OS), and identifying characteristics of patients who benefit from ICIs. A survival prediction model based on ^{18}F-FDG PET/CT parameters is developed to aid in the screening of NSCLC patients for immunotherapy.

2 Materials and methods

2.1 Patients

Clinical and imaging data of NSCLC patients who underwent baseline ^{18}F-FDG PET/CT were retrospectively reviewed at Hebei General Hospital from January 2016 to April 2023. Inclusion criteria were: patients with pathologically confirmed NSCLC, no history of other malignancies or conditions affecting imaging agent uptake, ^{18}F-FDG PET/CT performed within 1 week before treatment, and complete medical records. Exclusion criteria included patients unable to remain supine for an extended period during the examination and those who were lactating or pregnant.

A total of 174 patients' baseline clinical information was collected and 155 patients were enrolled in the study after screening. This cohort included 67 patients treated with ICIs and 88 patients who were not treated with ICIs. Collected clinical data comprised age, gender, height, weight, body mass index (BMI), smoking history and status, drinking habits, family history of cancer, pathological type, Ki-67%, stage, and various tumour markers [carcinoembryonic antigen(CEA), squamous cell carcinoma antigen(SCC), Cytokeratin 19 fragment(CYFRA21-1), neuron specific enolase(NSE)], as well as lactate dehydrogenase(LDH), white blood cells(WBC) count, neutrophilic granulocyte(NE) count, erythrocyte sedimentation rate(ESR), and C-reactive protein (CRP).

2.2 ^{18}F-FDG PET/CT examination

Before the examination, patients fasted for at least 6 h and had fasting blood glucose levels ≤11.1 mmol/L. Body mass and height were measured. The ^{18}F-FDG was provided by Hebei Andike Positron Technology Co., with a radiochemical purity of ≥95%. It was administered intravenously at a dose of 3.7–5.5 MBq/kg (0.10–0.15 mCi/kg) approximately 60 min before the PET/CT examination. Scanning was performed using the GE Discovery Elite PET/CT device, covering from the base of the skull to the middle and upper third of the thigh. CT parameters were set at 120 kV, 100 mA tube current, and 3.3 mm layer thickness. PET parameters included a 3D-TOF method for collecting PET images over 6–7 beds, with a 2-min acquisition time per bed. Images were reconstructed using full energy X-ray attenuation correction and ordered subset expectation maximisation algorithm, with a layer thickness of 3.3 mm. PET, CT and PET/CT fusion images were obtained, along with chest CT images reconstructed using a filtered back projection method with a 5 mm layer thickness and 1.25 mm thin-layer images.

2.3 Image analysis

PET/CT images were evaluated by two nuclear medicine physicians with advanced qualifications. Regions of interest (ROI) for each hypermetabolic lesion were identified on the PET/CT images, and the SUVmax was quantified. The mean standardized uptake value (SUVmean), minimum standardized uptake value (SUVmin), MTV of primary (MTVp) and TLG of primary (TLGp) were automatically extracted using a threshold of 40% of each SUVmax. The whole-body MTV(MTVwb) and whole-body TLG(TLGwb) for all lesions in each patient were calculated after determining the SUVmean and MTV for each ROI of all metastases. A circular ROI with a diameter of 1.0 cm (one in the left lobe and two in the right lobe) was delineated at normal metabolic sites in the liver, and the average SUVmax at these sites was used to calculate the tumor/liver ratio (TLR) of SUVmax (7). Lymph node and distant metastases in the PET/CT images were recorded. The characteristics of the primary lesion, including location, density, lobulation, burr, calcification, cancerous lymphangitis, and pleural effusion, were noted from the thin-slice CT images of the chest. The CT values of the primary lesion and the lengths of three radial lines were measured, with the maximum radial line length recorded as the maximum radial value.

2.4 Follow-up

Patients' outcome information was obtained from electronic medical records, imaging reports, or telephone follow-ups until November 30, 2023. The follow-up duration ranged from 7 to 89 months, with a median of 26 months. Outcomes were classified according to response evaluation criteria in solid tumor (RECIST) criteria as complete response (CR), partial response (PR), progressive disease (PD), or stable disease (SD) (8). PFS and OS were recorded. PFS was defined as the time from the pathological diagnosis of NSCLC to disease progression, death from any cause, or the follow-up cutoff time. OS was defined as the time from pathological diagnosis to death from any cause or the follow-up cutoff time (9).

2.5 Statistical analysis

SPSS 25.0 was employed for data analysis. The Shapiro–Wilk test was used to assess normality, with normally distributed measurement data expressed as mean ± standard deviation (±SD) and non-normally distributed data presented as interquartile range (IQR). Classification variables were described as frequency (percentage). The Kaplan–Meier curve was used to compare PFS and OS between the ICIs and non-ICIs groups. Continuous variables in the ICIs group were dichotomised based on the optimal cut-off value from the receiver-operating characteristics (ROC) curve. The Kaplan–Meier curve assessed factors influencing PFS and OS in the ICIs group, and the log-rank test was used to analyse differences between groups. GraphPad Prism 9 was used to plot the curves. Statistically significant parameters identified in univariate analysis were included in the Cox proportional hazards regression model for multivariate analysis to determine independent predictors of PFS and OS. The ROC curve was used to validate the diagnostic efficacy of the risk prediction model. $p < 0.05$ was considered statistically significant.

3 Results

3.1 Basic information

3.1.1 Clinical data

Clinical data for the two groups are presented in Table 1. Amongst the 155 NSCLC, there are 67 cases in ICIs group with median age 65.0 (59.0, 70.0) years. The non-ICIs group had 88 cases with a median age of 67.0 (57.0, 74.8) years. There were more males than females in both groups (60 vs. 7.55 vs. 33). The most common pathologic types in the ICIs and non-ICIs groups were squamous carcinoma in 38 cases (56.7%) and adenocarcinoma in 63 cases (71.6%), respectively. There were no CR cases in both groups after follow-up.There were 8 (11.9%) cases of PR, 34 (50.7%) cases of SD, 25 (37.3%) cases of PD, 23 (34.3%) cases of death in the ICIs group. In the non-ICIs group, there were 1 (1.1%) PR, 28 (31.8%) SD, 59 (67.0%) PD, 58 (65.9%) deaths. TNM staging was determined according to the 8th edition of the lung cancer criteria (10).

3.1.2 PET/CT morphological characteristics and metabolic parameters

The primary lung lesions were predominantly located in the upper lobes, with 49 cases(31.6%, 49/155) in the right upper lobe and 42 cases(27.1%, 42/155) in the left upper lobe. Most lesions were peripheral (109 vs. 46). The morphology of the primary lesions varied, including lobulated, burr-like, lymphangitic spread of carcinoma, calcification, and pleural effusion. The density was predominantly homogeneous and solid. The average CT value of the primary lesions in the ICI group was 30.19 ± 9.85 HU, compared to 33.43 ± 10.47 HU in the non-ICI group. The largest diameter of the lesions was 39.0 mm (27.0, 62.0) in the ICI group and 35.0 mm (26.0, 51.0) in the non-ICI group (Table 2).

The PET/CT manifestations of primary lung cancer were characterised by high metabolic activity. Lymph node metastasis was observed in 130 cases(83.9%, 130/155), whilst distant metastasis was noted in 103 cases (66.5%, 103/155). Metabolic parameters of the primary lesions, including SUVmax, SUVmean, SUVmin, TLR, MTVp, TLGp, as well as MTVwb and TLGwb of all lesions, were assessed in both the ICI and non-ICI groups (Table 3).

3.2 Kaplan–Meier survival curve analysis

The 155 NSCLC patients were divided into two groups based on their treatment with ICIs: 67 cases(43.2%, 67/155) in the ICI group and 88 cases(56.8%, 88/155) in the non-ICI group. Kaplan–Meier survival analysis curves for PFS and OS were plotted for both groups (Figure 1). The average PFS and OS in the ICI group were 46.55 months and 50.47 months, respectively, compared to 28.60 months and 36.27 months in the non-ICI group. The differences in PFS($\chi^2 = 11.910$, $p = 0.0006$) and OS($\chi^2 = 8.343$, $p = 0.0039$) between the two groups were statistically significant, with patients in the ICI group experiencing longer PFS and OS than those in the non-ICI group.

3.3 Univariate and multivariate analysis of ^{18}F-FDG PET/CT parameters and clinical features on PFS and OS in the ICIs group

3.3.1 Univariate analysis of ^{18}F-FDG PET/CT parameters and clinical features for PFS and OS

All continuous variables in the ICI group were dichotomised based on the ROC curve's cut-off value. These variables included clinical data such as age, height, weight, BMI, smoking status, Ki-67%, CEA, SCC, NSE, CYFRA21-1, LDH, WBC, NE, ESR, and CRP; PET/CT parameters such as the CT value and maximum diameter of the primary lesion, SUVmax, SUVmean, SUVmin, MTVp, TLGp, TLR, MTVwb, and TLGwb of all lesions; and various categorical variables including gender, smoking history, alcohol consumption, family history of cancer, pathological type, intralobular location of the primary lesion, and the presence or absence of lobulation, burr, cancerous lymphangitis, calcification, pleural effusion, lymph node metastasis, distant metastasis, and stage. These factors were evaluated using the Kaplan–Meier curve for survival analysis and the log-rank test for univariate analysis. The results indicated that factors influencing PFS included smoking history, CT value and maximum diameter of the primary focus, SUVmax, SUVmean, SUVmin, TLR, MTVp, TLGp, MTVwb, and TLGwb($\chi^2 = 4.224, 5.923, 13.366, 11.036, 4.984, 8.288, 8.906, 26.927, 14.35, 4.86, 13.932$, all $p < 0.05$). For OS, the influencing factors were age, smoking history, SCC, primary CT value and maximum diameter, SUVmax, SUVmean, SUVmin, TLR, MTVp, TLGp, and total lesion TLGwb($\chi^2 = 4.023, 4.931, 4.712, 7.334, 12.497, 9.780, 5.095, 6.705, 7.765, 27.787, 12.487, 12.363$, $p < 0.05$) (Table 4).

3.3.2 Multivariate analysis of ^{18}F-FDG PET/CT parameters and clinical features on PFS and OS

Statistically significant indicators from univariate analysis were included in Cox multivariate analysis. This analysis identified smoking history[hazard ratio (HR) = 2.522, 95% confidence interval (CI): 1.044 ~ 6.091. $p = 0.0398$], primary SUVmax(HR = 0.2376, 95%CI: 0.1018 ~ 0.5548, $p = 0.0009$), MTVp(HR = 0.0755, 95%CI: 0.0284 ~ 0.2003, $p < 0.001$), and TLGp(HR = 0.1820, 95%CI: 0.0754 ~ 0.4395, $p = 0.0002$) as

TABLE 1 Clinical data of NSCLC patients in the ICIs and non-ICIS groups.

Clinical data	ICIs group	Non-ICIs group
Age/years	65.0 (59.0, 70.0)	67.0(57.0, 74.8)
Sex		
Male	60 (89.6%)	55 (62.5%)
Female	7 (10.4%)	33 (37.5%)
Height/cm	170.0 (168.0, 175.0)	168.0 (160.0, 172.0)
Body mess/kg	70.0 (62.5.0, 75.0)	65.5 (60.0, 75.0)
BMI/kg·m^{-2}	24.22 (21.97, 25.95)	24.08 (21.69, 26.08)
Smoking history	31 (46.3%)	25 (28.4%)
Smoking status/pack-years	24 (0.40)	20 (0.30)
Drinking	8 (11.9%)	14 (15.9%)
Family history of cancer	14 (20.9%)	17 (19.3%)
Pathological type		
Adenocarcinoma	26 (38.8%)	63 (71.6%)
Squamous carcinoma	38 (56.7%)	17 (19.3%)
Adenosquamous carcinoma	1 (1.5%)	5 (5.7%)
Large cell carcinoma	1 (1.5%)	1 (1.1%)
No specific type	1 (1.5%)	0
Alveolar cell carcinoma	0	1 (1.1%)
Pulmonary blastoma	0	1 (1.1%)
Ki-67%	40.0 (30.0, 60.0)	30.0 (20.0, 55.0)
CEA/ng·ml^{-1}	4.88 (2.62, 7.63)	12.26 (3.81, 49.19)
SCC/ng·ml^{-1}	1.87 (1.26, 3.52)	1.52 (1.07, 2.21)
NSE/ng·ml^{-1}	13.10 (10.04, 17.83)	14.08 (11.56, 17.60)
CYFRA21-1/ng·ml^{-1}	11.10 (4.18, 18.20)	4.84 (3.43, 8.83)
LDH/U·L^{-1}	175.70 (151.83, 208.03)	189.10 (165.68, 225.78)
WBC/L^{-1}	7.18 (5.48, 8.73)	7.00 (5.90, 9.56)
NE/L^{-1}	5.18 (3.78, 7.99)	4.90 (3.74, 7.00)
ESR/mm·h^{-1}	14.00 (6.50, 37.00)	17.00 (10.00, 28.00)
CRP/mg·L^{-1}	12.11 (3.19, 73.09)	12.69 (1.21, 55.78)
TNM stage		
I	1 (1.5%)	3 (3.4%)
II	2 (3.0%)	1 (1.1%)
III	21 (31.3%)	27 (30.7%)
IV	43 (64.2%)	57 (64.8%)
Follow-up		
CR	0	0
PR	8 (11.9%)	1 (1.1%)
SD	34 (50.7%)	28 (31.8%)
PD	25 (37.3%)	59 (67.0%)
Number of deaths	23 (34.3%)	58 (65.9%)
PFS/month	19.5 (10.5, 29.0)	15.0 (7.0, 28.5)
	(1.0 ~ 73.0)	(1.0 ~ 73.0)
OS/month	22.0 (12.0, 36.8)	20.0 (11.0, 36.0)
	(4.0 ~ 81.0)	(1.0 ~ 89.0)

CEA, carcinoembryonic antigen; SCC, squamous cell carcinoma antigen; NSE, neuron specific enolase; CYFRA21-1, Cytokeratin 19 fragment; LDH, lactate dehydrogenase; WBC, white blood cells; NE, neutrophilic granulocyte; ESR, erythrocyte sedimentation rate; CRP, C-reactive protein; CR, complete response; PR, partial response; PD, progressive disease; SD, stable disease; PFS, progression-free survival; OS, overall survival.

independent predictors of PFS in the ICI group (Figure 2). These parameters were also independent predictors of OS[HR (95%CI) were 2.729 (1.125–6.619), 0.2636 (0.1143 ~ 0.6079), 0.0715 (0.0268 ~ 0.1907) and 0.2102 (0.0885 ~ 0.4992), respectively, $p < 0.05$), with age(HR = 0.4140, 95%CI: 0.1748–0.9801, $p = 0.0449$) additionally emerging as an independent predictor of OS (Figure 3).

TABLE 2 PET/CT morphological characteristics of NSCLC patients in ICIs and non-ICIs group.

Morphological features	ICIs group	Non-ICIs group
Distribution of lung lobes		
Right lung		
Superior lobe	23	26
Middle lobe	2	5
Inferior lobe	14	18
Left lung		
Superior lobe	20	22
Inferior lobe	8	17
Intra-leaf distribution		
Central type	23	23
Peripheral type	44	65
Lobulation	49	70
Burr	56	78
Lymphangitic spread of carcinoma	13	11
Calcification	14	18
Pleural effusion	19	29
Density		
Solid	36	56
Solid with voids	10	15
Solid with necrosis	13	12
Solid with cavity and necrosis	4	3
Heterogeneous reality	4	2
Mean CT value /HU	30.19 ± 9.85	33.43 ± 10.47
Largest diameter /mm	39.0(27.0, 62.0)	35.0(26.0, 51.0)

TABLE 3 Baseline PET/CT metabolic parameters of NSCLC patients in ICIs and non-ICIS groups.

Metabolic parameters	ICIs group	Non-ICIs group
SUVmax	14.5 (9.5, 21.9)	11.3 (7.9, 14.9)
SUVmean	8.2 (5.6, 11.9)	6.7 (4.6, 9.1)
SUVmin	4.9 (3.7, 7.0)	4.5 (3.2, 6.1)
TLR	5.17 (2.88, 6.72)	3.59 (2.61, 5.10)
MTVp/ cm^3	12.08 (5.05, 32.08)	10.93 (5.11, 21.91)
TLGp/g	106.48 (32.97, 306.93)	78.76 (22.40, 191.24)
MTVwb/ cm^3	70.72 (27.46, 120.60)	64.22 (28.10, 114.43)
TLGwb/g	378.11 (169.37, 923.52)	306.26 (167.28, 700.52)

SUVmax maximum standard uptake, SUVmean mean standardized uptake, SUVmin minimum standardized uptake, TLR tumor/liver ratio of SUVmax, MTVp metabolic tumour volume of primary, TLGp total lesion glycolysis of primary, MTVwb whole-body MTV, TLGwb whole-body TLG.

The findings indicated that NSCLC patients without a smoking history and with a primary SUVmax ≤19.2, MTVp ≤20.745cm^3, TLGp ≤158.62 g and age ≤ 60 experienced improved survival benefits following ICI treatment.

The sensitivities for predicting PFS were 0.556, 0.742, 0.565, and 0.692 for smoking history, primary SUVmax, MTVp, and TLGp, respectively, with corresponding specificities of 0.774, 0.667, 0.864, and 0.585. The area under curves (AUC) were 0.707, 0.674, 0.766, and 0.652, respectively (Figure 4). For OS, the sensitivities were 0.694, 0.710, 0.522, 0.692, and 0.625 for smoking history, primary SUVmax, MTVp, TLGp, and age, respectively, with specificities of 0.839, 0.556, 0.841, 0.512, and 0.895, and AUC values of 0.671, 0.613, 0.718, 0.591, and 0.683, respectively (Figure 5). A Cox proportional hazards regression model was established to predict PFS and OS in the ICI group, and an ROC curve was used to assess the model's diagnostic efficiency. The results showed that the sensitivity and specificity of the models based on smoking history, primary SUVmax, MTVp, and TLGp for predicting PFS were 77.3 and 73.9%, with an AUC of 0.692 (Figure 6). For OS, the models based on smoking history, primary SUVmax, MTVp, TLGp, and age had a sensitivity of 65.9%, specificity of 82.6%, and an AUC of 0.748 (Figure 7).

4 Discussion

NSCLC constitutes over 80% of all lung cancer cases, with most patients experiencing asymptomatic onset in the early stages. Nearly 70% of newly diagnosed NSCLC patients present at an advanced stage, with a 5-year survival rate of only 10 to 16% (2, 11). Currently, immunotherapy is being applied to some patients with advanced NSCLC. Immune checkpoint molecules are protective elements in the human immune system, normally regulating T cell differentiation and proliferation to maintain immune balance. However, overexpression of these immune checkpoint molecules in tumour tissues inhibits T cell activation and proliferation or induces T cell apoptosis, creating an immunosuppressive tumour microenvironment that allows tumour cells to evade immune surveillance and destruction. The use of ICIs, such as those targeting programmed death 1 (PD-1), programmed death-ligand 1(PD-L1) and cytotoxic T lymphocyte-associated antigen-4 (CTLA-4), blocks the interaction between tumour tissues and T cells, thereby restoring normal immune function and providing significant survival benefits to patients (12). In recent years, tumour immunotherapy has expanded treatment options for patients with advanced NSCLC, with ICIs targeting PD-1, PD-L1, and CTLA-4 becoming a clinical hotspot.

At present, the objective remission rate for NSCLC patients undergoing immunotherapy is only 20%, with notable individual variability and a higher incidence of serious irAEs (6). ^{18}F-FDG PET/CT is widely utilised in the diagnosis, efficacy evaluation, and prognosis assessment of lung cancer due to its non-invasive and comprehensive nature globally (13). This study aims to explore the predictive value of ^{18}F-FDG PET/CT parameters for ICIs treatment effects in NSCLC patients and to develop a survival prediction model. We retrospectively included 155 NSCLC patients who underwent baseline ^{18}F-FDG PET/CT at Hebei General Hospital from January 2016 to April 2023. Our findings suggest that ICIs treatment for advanced NSCLC patients provides significant survival benefits (1, 14). Compared to the non-ICIs group, the PFS and OS were significantly improved in the ICIs group, aligning with previous research results (5). Clinical data analysis revealed that elderly males, with a median age of 66 years, were the most common demographic, and adenocarcinoma was the predominant

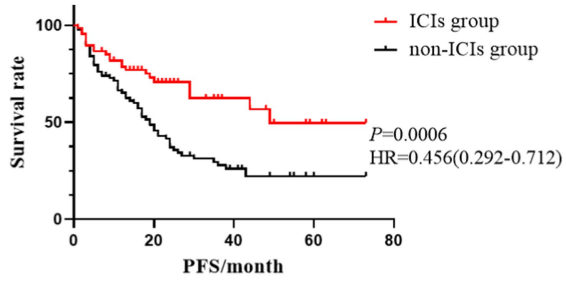

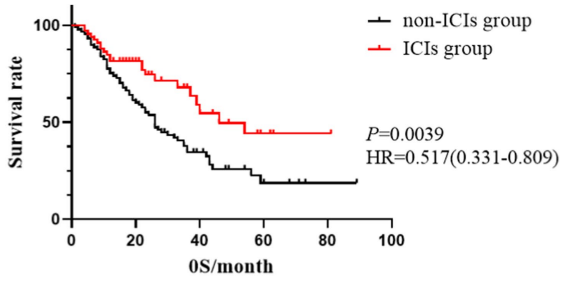

FIGURE 1
Kaplan–Meier survival curves of PFS and OS in ICIs and non-ICIS groups.

TABLE 4 Univariate analysis of ^{18}F-FDG PET/CT parameters and clinical characteristics for PFS and OS in ICIs group.

PET/CT parameters and clinical characteristics	PFS		OS	
	χ^2	p	χ^2	p
Age	3.779	0.052	4.023	0.045
Smoking history	4.224	0.040	4.931	0.026
SCC	3.487	0.062	4.712	0.030
CT value	5.923	0.015	7.334	0.007
Maximum diameter	13.366	0.000	12.497	0.000
SUVmax	11.036	0.001	9.780	0.002
SUVmean	4.984	0.026	5.095	0.024
SUVmin	8.288	0.004	6.705	0.010
TLR	8.906	0.003	7.765	0.005
MTVp	26.927	0.000	27.787	0.000
TLGp	14.350	0.000	12.487	0.000
MTVwb	4.860	0.027	3.695	0.055
TLGwb	13.932	0.000	12.363	0.000

pathological type, consistent with epidemiological data and earlier studies (15). The baseline ^{18}F-FDG PET/CT metabolic parameters in NSCLC patients are closely linked to general data and lesion morphological characteristics. Therefore, these parameters should be assessed in conjunction with other clinical and scientific data to provide a more personalised and accurate diagnosis and treatment plan.

Univariate analysis of ^{18}F-FDG PET/CT parameters and clinical characteristics in the ICIs treatment group identified several factors influencing PFS, including smoking history, CT value and maximum diameter, SUVmax, SUVmean, SUVmin, TLR, MTVp, TLGp, MTVwb, and TLGwb. For OS, the influencing factors included age, smoking history, SCC, CT value and maximum diameter, SUVmax, SUVmean, SUVmin, TLR, MTVp, TLGp, and TLGwb. Independent predictors of PFS in the ICIs group were smoking history, primary SUVmax, MTVp, and TLGp. For OS, the independent predictors included age, smoking history, primary SUVmax, MTVp, and TLGp. Smoking history is a well-known risk factor for lung cancer, with studies indicating that the earlier smoking starts, the higher the risk of developing lung cancer, increasing 14 - fold, 8 - fold, and 5 - fold for children, adolescents, and adults, respectively, along with increased mortality (16). In this study, smoking history emerged as an independent predictor of both PFS and OS in NSCLC patients. Xu et al. (17) suggested that smoking status (pack-years), smoking duration, and time to quit smoking could be effective predictors of lung cancer incidence and mortality. However, smoking quantity alone was not an independent risk factor for NSCLC survival in this study, possibly due to the small sample size or inaccuracies in patient smoking data. Ken et al. (5) found that age, primary SUVmax, MTVp, and TLGp were effective predictors of long-term prognosis in NSCLC patients receiving ICIs, aligning with our multifactorial analysis results. Their study also identified carcinomatous lymphangiopathy as an independent predictor, though this finding may vary due to difficulties in diagnosing carcinomatous lymphangiopathy, potentially complicated by other lung conditions like interstitial fibrosis or inflammation. Giulia et al. (15) showed that MTV and TLG are important prognostic factors, positively correlating with disease progression, though SUVmax showed no correlation with PFS and OS, possibly due to differences in study populations and individual disease heterogeneity. In our study, MTVp predicted PFS and OS in ICIs-treated advanced NSCLC patients with AUCs of 0.766 and 0.718, indicating high predictive efficacy. Hye et al. (7) suggested that TLR is an independent prognostic factor for disease recurrence and patient survival in stage IB and IIA NSCLC, though its prognostic value in advanced stages remains unclear and requires further investigation. Karolien et al. (18) found that survival was not related to baseline MTVwb. Similarly, in our study, neither MTVwb nor TLGwb effectively predicted therapeutic response to ICIs in NSCLC patients. The findings indicate that NSCLC patients with no smoking history and primary SUVmax $\leq$19.2, MTVp $\leq$20.745cm^3, TLGp $\leq$158.62 g and age $\leq$ 60 who received ICIs treatment experienced better survival benefits. This information could aid in the clinical screening of patients suited for ICIs treatment, improving the objective response and effective response rates and offering NSCLC patients better prognostic outcomes. Based on these results, PFS and OS prediction models for the ICIs group were established using the Cox proportional hazards regression model,

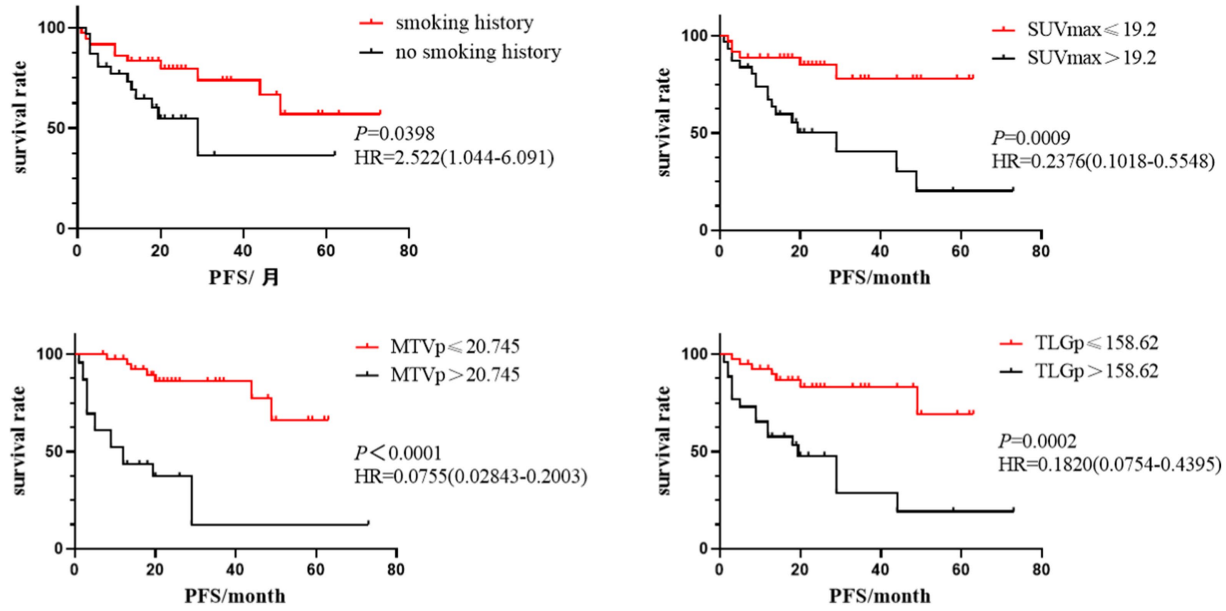

FIGURE 2
Kaplan–Meier survival analysis curves of smoking history, primary SUVmax, MTVp and TLGp on PFS in ICIs group.

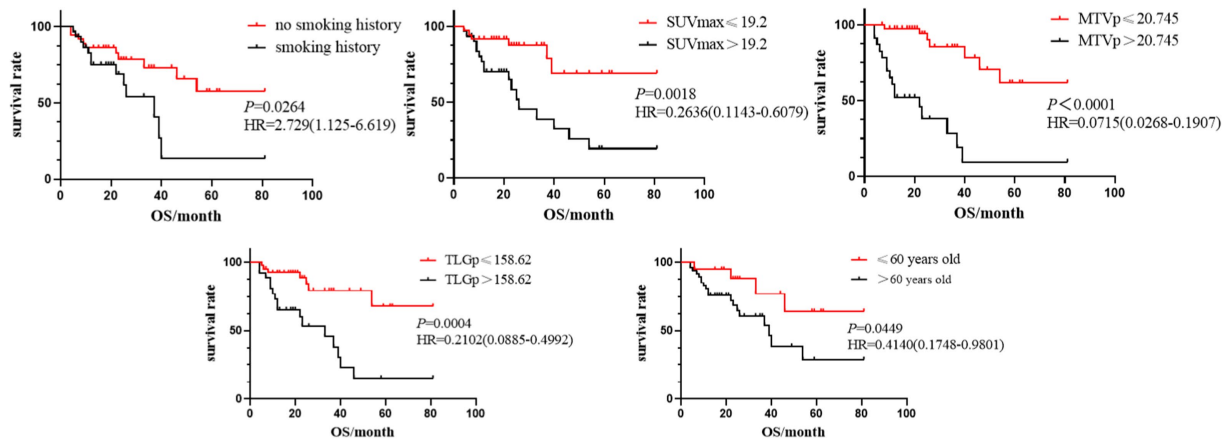

FIGURE 3
Kaplan–Meier survival analysis curves of smoking history, primary SUVmax, MTVp, TLGp and age on OS in ICIs group.

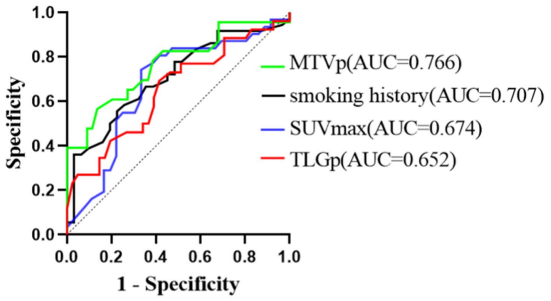

FIGURE 4
ROC curve of PFS predicted by smoking history, primary SUVmax, MTVp and TLGp in ICIs group.

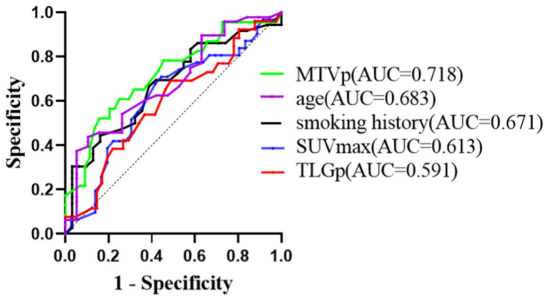

FIGURE 5
ROC curve of OS predicted by smoking history, primary SUVmax, MTVp, TLGp and age in ICIs group.

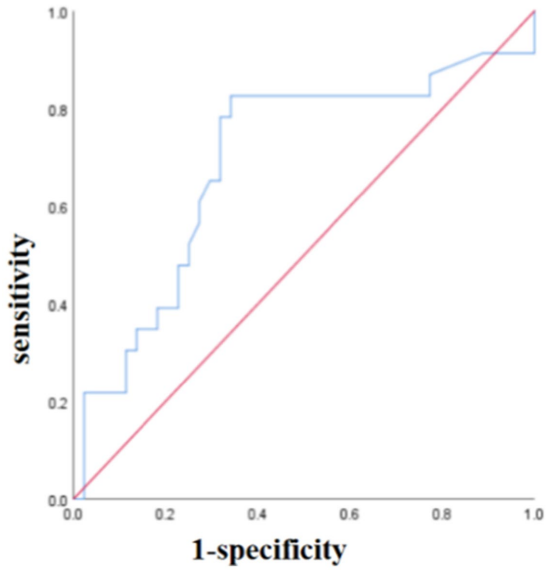

FIGURE 6
The ROC curve of PFS predicted by smoking history, primary SUVmax, MTVp and TLGp models in ICIs group.

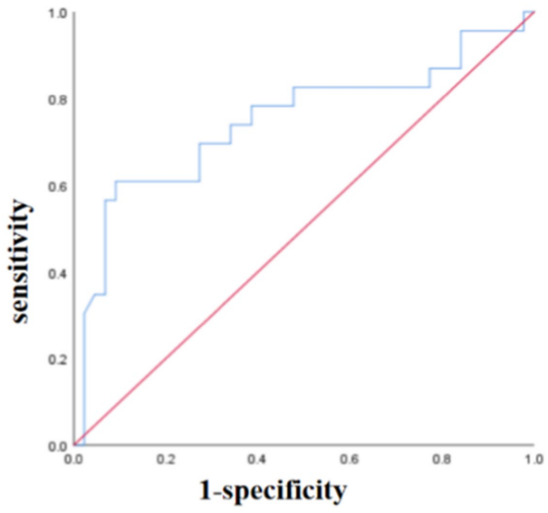

FIGURE 7
The ROC curve of OS predicted by age, smoking history, primary SUVmax, MTVp and TLGp models in ICIs group.

with ROC curve analysis showing AUCs of 0.692 and 0.748, respectively, demonstrating good predictive efficiency.

The non-ICIs group did not undergo ICIs treatment for 3 main reasons: firstly, time reasons prevented some patients from applying ICIs treatment. The 155 patients included in this paper were screened from January 2016. Whilst ICIs therapy has emerged in recent years and gradually entered the clinic for the benefit of patients. Secondly, ICIs therapy requires patients to have some clinical indications. Finally, ICIs therapy is currently expensive and requires a certain economic basis to support patients to receive a sufficient course of treatment to achieve the therapeutic purpose. These leads to some patients not being able to apply ICIs.

This study has certain limitations. Although pathological biopsy is crucial for accurately assessing tumour nature and progression, sampling quality can be affected by various factors, and practical issues arise with multiple and continuous pathological examinations. The study did not fully obtain expression data for PD-1 and other immune checkpoints through immunohistochemistry. As a retrospective study, it may be subject to selection bias. Additionally, the absence of an external validation of monocentric data with small sample size and the lack of subgroup analyses for first-line versus second-line ICIs treatment and specific medication regimens limit the generalizability of the findings. The external validation of larger samples of multicenter data is needed in the future.

5 Conclusion

(1) Compared with the non-ICIs group, ICIs treatment significantly improves survival and prolongs survival time in NSCLC patients. (2) Smoking history, primary SUVmax, MTVp, and TLGp are independent predictors of PFS in the ICIs group. Age, smoking history, primary SUVmax, MTVp, and TLGp are independent predictors of OS in the ICIs group. All these predictors exhibit good forecasting efficiency. (3) NSCLC patients without a smoking history and with a primary SUVmax $\leq$19.2, MTVp $\leq$20.745cm^3, TLGp $\leq$158.62 g and age $\leq$ 60 experience better survival benefits following ICIs treatment.

Data availability statement

The original contributions presented in the study are included in the article/supplementary material, further inquiries can be directed to the corresponding author.

Ethics statement

The studies involving humans were approved by Institutional Review Board of Hebei General Hospital. The studies were conducted in accordance with the local legislation and institutional requirements. The participants provided their written informed consent to participate in this study.

Author contributions

LZ: Data curation, Formal analysis, Investigation, Methodology, Software, Writing – original draft. YB: Conceptualization, Funding acquisition, Project administration, Supervision, Writing – review & editing. YH: Data curation, Software, Writing – review & editing. CT: Data curation, Software, Writing – review & editing. XZ: Data curation, Writing – review & editing. SL: Data curation, Writing – review & editing. XY: Data curation, Writing – review & editing. YQ: Data curation, Writing – review & editing.

Funding

The author(s) declare that financial support was received for the research, authorship, and/or publication of this article. The government funded the training project for outstanding talents in clinical medicine in 2021(2021037), Key Science and Technology Research Program of the Health Commission of Hebei Province (20241560).

Acknowledgments

We would like to thank the patient for agreeing to our reporting of her case and all the medical staff involved in the patient's diagnosis and treatment.

Conflict of interest

The authors declare that the research was conducted in the absence of any commercial or financial relationships that could be construed as a potential conflict of interest.

Publisher's note

References

1. Du Y, Fan CJ, Shen WX, Xin T. Progress in immunotherapy of non-small cell lung cancer. *J Mod Oncol.* (2021) 29:2368–71. doi: 10.3969/j.issn.1672-4992.2021.13.038

2. Jeon DS, Kim HC, Kim SH, Kim TJ, Kim HK, Moon MH, et al. Five-year overall survival and prognostic factors in patients with lung Cancer: results from the Korean Association of Lung Cancer Registry (KALC-R) 2015. *Cancer Res Treat.* (2023) 55:103–11. doi: 10.4143/crt.2022.264

3. Zheng RS, Chen R, Han BF, Wang SM, Li L, Sun KX, et al. Cancer incidence and mortality in China, 2022. *J Natl Cancer Cent.* (2024) 4:47–53. doi: 10.1016/j.jncc.2024.01.006

4. Hashimoto K, Kaira K, Yamaguchi O, Mouri A, Shiono A, Miura Y, et al. Potential of FDG-PET as prognostic significance after anti-PD-1 antibody against patients with previously treated non-small cell lung Cancer. *J Clin Med.* (2020) 9:725–5. doi: 10.3390/jcm9030725

5. Kudura K, Ritz N, Kutzker T, Hoffmann MHK, Templeton AJ, Foerster R, et al. Predictive value of baseline FDG-PET/CT for the durable response to immune checkpoint inhibition in NSCLC patients using the morphological and metabolic features of primary tumors. *Cancers.* (2022) 14:6095–5. doi: 10.3390/cancers14246095

6. Cui SH, Ge XX, Li XY. A real-world study on the incidence and outcome of immune-related adverse events in lung Cancer patients. *Zhongguo Fei Ai Za Zhi.* (2023) 26:257–64. doi: 10.3779/j.issn.1009-3419.2023.101.08

7. Park HL, Boo SH, Park SY, Moon SW, Yoo IR. Prognostic value of TLR from FDG PET/CT in patients with margin-negative stage IB and IIA non-small cell lung cancer. *Eur Radiol.* (2023) 33:7274–83. doi: 10.1007/s00330-023-09641-w

8. Singla R, Jajodia A, Agrawal RK, Rao A, Pasricha S, Batra U. Comparison of RECIST and iRECIST criteria in patients with advanced lung cancer treated with nivolumab. *J Cancer Res Ther.* (2023) 19:1212–8. doi: 10.4103/jcrt.jcrt_1456_21

9. Feng YW, Wang P, Chen YQ, Dai WL. ^{18}F-FDG PET/CT for evaluation of metastases in nonsmall cell lung cancer on the efficacy of immunotherapy. *Nucl Med Commun.* (2023) 44:900–9. doi: 10.1097/MNM.0000000000001737

10. Li H. Overview of the AJCC lung Cancer staging system, eighth edition may give us more thought: opportunities and challenges. *Zhonghua Wai Ke Za Zhi.* (2017) 55:346–50. doi: 10.3760/cma.j.issn.0529-5815.2017.05.007

11. Xu X, Li JH, Yang Y, Sang SB, Deng SM. The correlation between PD-L1 expression and metabolic parameters of ^{18}F-FDG PET/CT and the prognostic value of PD-L1 in non-small cell lung cancer. *Clin Imag.* (2022) 89:120–7. doi: 10.1016/j.clinimag.2022.06.016

12. Lin L, Xiao L, Li L, Chen C, Zhang HR, Yu CY, et al. A meta-analysis of the efficacy of programmed cell death 1/its ligand inhibitors plus cytotoxic T-lymphocyte-associated antigen 4 inhibitors in non-small cell lung cancer. *Front Pharmacol.* (2024) 15:1267763. doi: 10.3389/fphar.2024.1267763

13. Evangelista L, Cuocolo A, Pace L, Mansi L, Del Vecchio S, Miletto P, et al. Performance of FDG-PET/CT in solitary pulmonary nodule based on pre-test likelihood of malignancy: results from the ITALIAN retrospective multicenter trial. *Eur J Nucl Med Mol I.* (2018) 45:1898–907. doi: 10.1007/s00259-018-4016-1

14. Valentinuzzi D, Vrankar M, Boc N, Ahac V, Zupancic Z, Unk M, et al. ^{18}F-FDG PET immunotherapy radiomics signature (iRADIOMICS) predicts response of non-small-cell lung cancer patients treated with pembrolizumab. *Radiol Oncol.* (2020) 54:285–94. doi: 10.2478/raon-2020-0042

15. Polverari G, Ceci F, Bertaglia V, Reale ML, Rampado O, Gallio E, et al. ^{18}F-FDG pet parameters and Radiomics features analysis in advanced Nsclc treated with immunotherapy as predictors of therapy response and survival. *Cancers.* (2020) 12:1163. doi: 10.3390/cancers12051163

16. He H, He MM, Wang HX, Qiu WH, Liu L, Long L, et al. In utero and childhood/adolescence exposure to tobacco smoke, genetic risk and lung Cancer incidence and mortality in adulthood. *Am J Resp Crit Care.* (2023) 207:173–82. doi: 10.1164/rccm.202112-2758OC

17. Gao X, Huang NH, Jiang MJ, Holleczek B, Schöttker B, Huang T, et al. Mortality and morbidity risk prediction for older former smokers based on a score of smoking history: evidence from UK biobank and ESTHER cohorts. *Age Ageing.* (2022) 51:154. doi: 10.1093/ageing/afac154

18. Vekens K, Everaert H, Neyns B, Ilsen B, Decoster L. The value of ^{18}F-FDG PET/CT in predicting the response to PD-1 blocking immunotherapy in advanced NSCLC patients with high-level PD-L1 expression. *Clin Lung Cancer.* (2021) 22:432–40. doi: 10.1016/j.cllc.2021.03.001

frontiers | Frontiers in Oncology

TYPE Case Report
PUBLISHED 25 February 2025
DOI 10.3389/fonc.2025.1474997

OPEN ACCESS

EDITED BY
Vincenzo Pio Di Noia,
IRCCS Istituto Nazionale Tumori Regina Elena, Italy

REVIEWED BY
Josephina Sampson,
University of Leeds, United Kingdom
George Gourzoulidis,
Health Through Evidence, Greece

*CORRESPONDENCE
Zuoqing Song
thoracic_expert@aliyun.com

†These authors have contributed equally to this work

RECEIVED 02 August 2024
ACCEPTED 28 January 2025
PUBLISHED 25 February 2025

CITATION
Zhang H, Xia W, Zhang Y, Bao S, Zeng J, Li X, Zhang B, Wang H, Xu S and Song Z (2025) Ensartinib as a neoadjuvant therapy for stage IIIA non-small cell lung cancer patients with EML4-ALK fusion: a case report and literature review. *Front. Oncol.* 15:1474997. doi: 10.3389/fonc.2025.1474997

Ensartinib as a neoadjuvant therapy for stage IIIA non-small cell lung cancer patients with EML4-ALK fusion: a case report and literature review

Hao Zhang[1,2†], Wei Xia[1,2†], Yifan Zhang[1,2†], Shihao Bao[1,2], Jingtong Zeng[1,2], Xianjie Li[1,2], Bo Zhang[1,2], Hanqing Wang[1,2], Song Xu[1,2] and Zuoqing Song[1,2*]

[1]Department of Lung Cancer Surgery, Tianjin Medical University General Hospital, Tianjin, China, [2]Tianjin Key Laboratory of Lung Cancer Metastasis and Tumor Microenvironment, Lung Cancer, Tianjin, China

Anaplastic lymphoma kinase (ALK) inhibitors have shown efficacy in treating ALK-positive advanced non-small cell lung cancer (NSCLC) patients. However, the effectiveness of ensartinib neoadjuvant therapy remains ambiguous. Herein, we reported that preoperative systemic treatment with the ALK inhibitor ensartinib can be beneficial for treating initially inoperable tumors. In this study, we present a case of a 60-year-old female patient who was diagnosed with stage IIIA (cT2aN2aM0, ninth TNM stage) lower left lung adenocarcinoma harboring an EML4-ALK fusion. After three months of therapy, the neoadjuvant treatment with ensartinib provided a partial response, with significant tumor and lymph node shrinkage. Preoperative ensartinib neoadjuvant therapy for NSCLC is safe and effective. Nevertheless, clinical trials can be conducted in the future to validate our results. Moreover, we performed multiple immunofluorescence staining analyses on samples before and after neoadjuvant therapy, observed and compared the changes in the expression of relevant immune cells (CD8+ T cells, macrophages, PD-1, and PD-L1), and performed a simple analysis.

KEYWORDS

ensartinib, EML4-ALK fusion, neoadjuvant, non-small cell lung cancer, immune microenvironment

1 Introduction

Lung cancer is one of the most common cancers worldwide and has high morbidity and mortality rates (1). Histologically, lung cancer can be divided into small cell lung cancer (SCLC) and non-small cell lung cancer (NSCLC), of which NSCLC accounts for 85% of all lung malignancies (2). Typically, stage I or II NSCLCs are treated via surgical resection, with adjuvant

results based on pathologic treatment. Conversely, adjuvant therapies such as chemotherapy or radiotherapy and surgical intervention are utilized for managing IIIA NSCLC patients.

Soda et al. initially reported the EML4-ALK fusion gene when they amplified a 3926-bp DNA fragment encoding a 1059 amino acid protein, the fusion protein EML4-ALK, in tumor tissue from a lung adenocarcinoma patient (3). In subsequent experiments, the EML4-ALK gene induced cancerous lesions after implantation into normal lung cells, indicating its oncogenic effect (4). About 5% of NSCLC patients show an identified ALK gene alteration,with EML4-ALK rearrangement being the most common pattern (5). EML4-ALK fusion gene positivity occurs in young NSCLC patients with either no or light smoking history (6). Targeted therapies are more effective than chemotherapy in advanced ALK-mutated NSCLC patients. Compared with those treated with chemotherapy, individuals treated with ALK-targeted agents live longer, experience more significant tumor shrinkage, and display an increased period of continued symptom deterioration (7). In recent years, several breakthroughs have been made in targeted therapy technology, resulting in the introduction of various targeted therapeutic agents for EML4-ALK (8). Several ALK tyrosine kinase inhibitors (TKIs), including crizotinib, alectinib, ceritinib, ensartinib, and buxtitinib, have been approved for treating ALK-positive NSCLC patients (9). For lung cancer patients with ALK mutations, the effect of ALK inhibitor-targeted therapy seems to be far better than that of chemotherapy. Compared with that of lorlatinib, the efficacy of targeted therapy in patients with ALK mutations has significantly improved (10, 11). In an analytical study comparing the efficacy of multiple ALK-TKIs in Asian ALK-positive NSCLC patients, ensartinib emerged as an efficient first-line treatment for Asian ALK-positive NSCLC patients (12).

Ensartinib refers to an oral, highly selective, potent ALK-tyrosine kinase inhibitor (TKI). In March 2022, it was approved as a first-line treatment for patients with ALK-positive locally advanced or metastatic NSCLC by the National Medical Products Administration (NMPA). A study by Ma et al. emphasized the efficacy of ensartinib in Chinese patients with advanced ALK NSCLC and demonstrated that ensartinib showed good clinical activity and an acceptable safety profile in Chinese patients with ALK-positive NSCLC through safety, tolerability, pharmacokinetics, efficacy, and possible pharmacodynamic biomarkers which boosted the approval of ensartinib for the treatment of ALK-positive NSCLC patients in China (13). However, very few studies are available on the efficacy of ensartinib neoadjuvant therapy in NSCLC patients who have undergone EML4-ALK fusion. Here, we report a case of a stage IIIA NSCLC patient who experienced significant tumor shrinkage and successful surgery after 3 months of targeted therapy with ensartinib.We also briefly analyzed the changes in the immune microenvironment of NSCLC patients after treatment. With this study, we hope to promote the application of neoadjuvant therapy of ensartinib for ALK-positive patients with advanced NSCLC and to promote the study of the characterization of the immune microenvironment of NSCLC patients after treatment with ALK inhibitors.

2 Case report

In this case, a 60-year-old female patient without a history of smoking underwent an enhanced computed tomography (CT) scan during a medical examination in August 2023, revealing a 20-mm-diameter mass in the left lower lung and enlarged mediastinal lymph nodes (stations 7 and 10). A lung puncture biopsy verified the diagnosis of lung adenocarcinoma. Furthermore, next-generation sequencing (NGS) of a 425-gene panel (ALK, EGFR, RET, MET, KRAS, etc.) was conducted to identify the patient's mutated genes, microsatellite instability (MSI), and tumor mutational burden (TMB). An ALK fusion mutation involving EML4 exon 13 and ALK exon 20 was subsequently discovered. Since neoadjuvant therapy and surgical resection are recommended, a dose of 225 mg of ensartinib once daily was prescribed after the patient provided informed consent. The patient developed Grade 4 edema after three weeks of medication. The targeted therapy course was discontinued, and the patient was hospitalized for symptomatic treatment, including diuresis and dehydration. After one week, significant relief was observed, and ensartinib treatment was resumed.

After three months of treatment, a chest CT scan revealed 50% tumor shrinkage and partial reduction of the mediastinal lymph nodes (Figures 1, 2). After significant shrinkage of the tumor, the patient was proposed for surgery and was admitted to the hospital for preoperative investigations. Chest CT suggested that a soft tissue density nodular shadow was visible under the pleura of the lower lobe of the left lung, measuring about 14 mm×9 mm with multiple burrs at the margin.Tumor marker indices such as gastrin-releasing peptide precursor, cytokeratin 19 fragment, squamous cell carcinoma antigen and carcinoembryonic antigen were in the normal range.The patient subsequently underwent left lower lobectomy and systemic lymph node dissection without any serious perioperative complications. Final histopathological assessments revealed pT2aN2aM0 stage invasive adenocarcinoma. The tumor was solid, vesicular, and invaded the pleura, with visible spread through the air space; metastatic carcinoma was observed in Group 5 lymph nodes (1/3). No metastatic carcinoma was observed in groups 4, 7, and 9 or in the parabronchial lymph nodes. We performed a treatment response assessment in the postoperative pathological analysis, which suggested that the percentage of residual viable tumor cells was about 30% and the mesenchyme was about 70%, with no necrosis.Three days after the surgery, a follow-up chest CT showed normalization of the lungs, which was consistent with "postoperative left lung" changes.Postoperatively, the patient continued ensartinib therapy, and the dosage was changed to 125 mg once daily. Six months after surgery, the patient's chest CT was repeated, suggesting an uneventful pulmonary recovery.Meanwhile,the patient has not experienced postoperative tumor progression or any severe drug-related adverse reactions.

To investigate alterations in the tumor microenvironment (TME) before and after neoadjuvant ensartinib treatment, multiplex fluorescence staining was performed on pre-neoadjuvant and

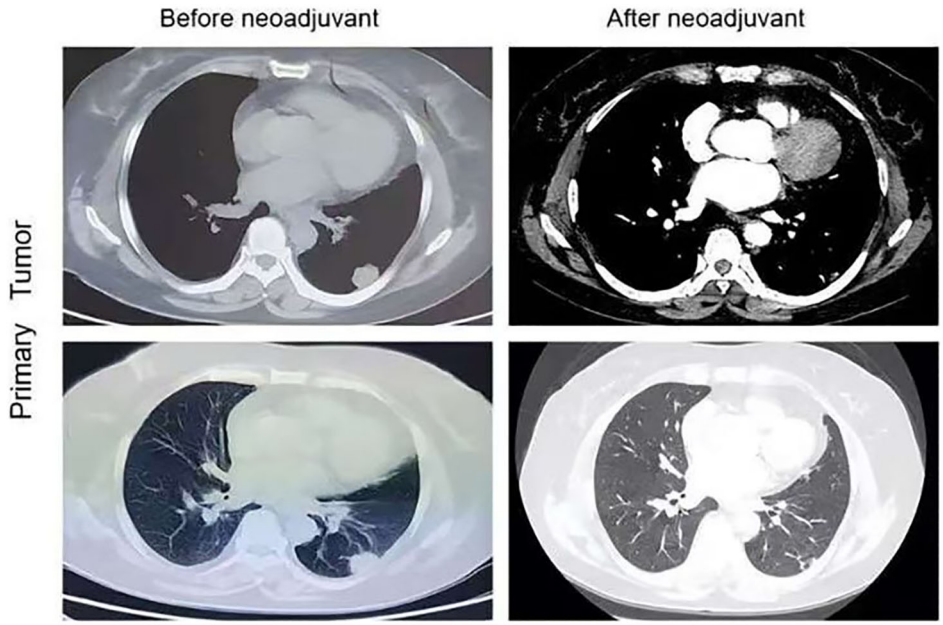

FIGURE 1
Chest CT images of left lung adenocarcinoma before and after the neoadjuvant therapy.

postoperative samples, with a focus on CD8+ T cells, macrophages, PD-1, and PD-L1 (Figure 3). We observed a significant reduction in the number of macrophages and CD8+ tumor-infiltrating lymphocytes (TILs) as well as PD-1 and PD-L1 expression. Additionally, the M1/M2 macrophage ratio also decreased (Figure 4).

3 Discussion

Neoadjuvant therapy can improve the survival rate of ALK-positive NSCLC patients. Previous studies have indicated that a majority of EML4-ALK fusion gene-positive NSCLC patients benefit significantly from molecularly targeted therapies (14–17). Herein, we report a case of ensartinib neoadjuvant treatment in an NSCLC patient with an EML4-ALK-positive mutation. Ensartinib demonstrated a significant therapeutic effect in this EML4-ALK fusion gene-positive NSCLC patient. The patient's tumor significantly decreased after ensartinib treatment, followed by successful lobectomy and systemic lymph node dissection. Postoperative pathological examination revealed metastases in the group V lymph nodes (1/3). Moreover, the patient's condition was relatively stable postoperatively, and regular follow-up was conducted.

The advent of precision medicine has improved insights into the treatment of NSCLC. The identification of driver genes and subsequent targeted therapies have expanded the treatment options for NSCLC patients (8). Nonetheless, in NSCLC patients with ALK rearrangements, single-agent ALK inhibitors are superior to chemotherapy in advanced or metastatic-stage patients (18). The clinical success of targeted therapies in advanced NSCLC patients has also played a role in their ongoing integration with neoadjuvant therapies. Several studies have suggested that neoadjuvant ALK-TKI targeted therapies are effective, thereby supporting the application of neoadjuvant ALK-directed therapies (19–21). However, the relevant guidelines have not yet advocated the use of ALK TKIs for the neoadjuvant treatment of early-stage ALK-positive NSCLC patients, and there is a lack of outcome data from large, randomized trials (22). There are two ongoing phase II trials of alectinib with neoadjuvant therapy for ALK-positive NSCLCs: the ALNEO (NCT05015010) and NAUTIKA1 (NCT04302025) trials. The ALNEO trial, aimed at examining potentially resectable stage III ALK-positive NSCLC patients, began in 2021 and is expected to be finished in 2026. The NAUTIKA-1 trial is being conducted for patients with resectable stage IB-IIIA ALK-positive NSCLC. It started in 2020 and is expected to be completed in 2029.

In a network meta-analysis, researchers included 12 RCTs involving 3169 patients with 8 treatment regimens, and compared the effects of multiple ALK inhibitors by overall survival (OS), progression-free survival (PFS), and objective remission rate (ORR). In terms of OS, alectinib ranked the highest, followed by ceritinib and ensartinib; in terms of PFS, ensartinib had a significant advantage and ranked the highest, followed by alectinib and brigatinib; in terms of ORR, alectinib ranked the highest, followed by ensartinib and lorlatinib (23). Thus, ensartinib has been evaluated in treatment-naïve ALK-positive NSCLC patients compared with other ALKIs, and has shown promising results as first-line systemic therapy, but the results remain to be confirmed by additional future studies.

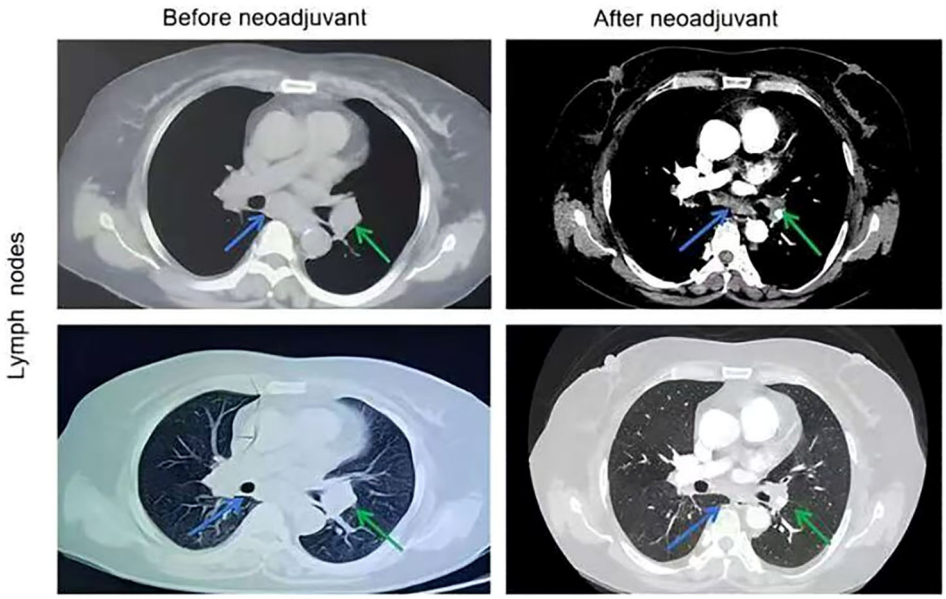

FIGURE 2
Chest CT images of lymph nodes before and after the neoadjuvant therapy. The stations 7 lymph nodes pointed by blue arrows and the stations 10 lymph nodes pointed by green arrows.

None of the available clinical trials have assessed ensartinib as a neoadjuvant therapy for ALK-positive NSCLC patients. Although there are only two studies on ensartinib in combination with neoadjuvant therapy (24, 25), they did not mention the impact of ensartinib treatment on TME. Another previous study suggested that, compared with patients with EGFR/KRAS-positive NSCLC, patients with ALK-positive NSCLC have an immunosuppressive TME (26). However, large-scale cohort studies on how the TME of ALK-positive NSCLC changes after TKI treatment are lacking. Our study revealed that after neoadjuvant therapy, ALK-positive NSCLC transitions from an immunologically "hot" tumor to a "cold" tumor with decreased infiltration of CD8+ cells and macrophages, as well

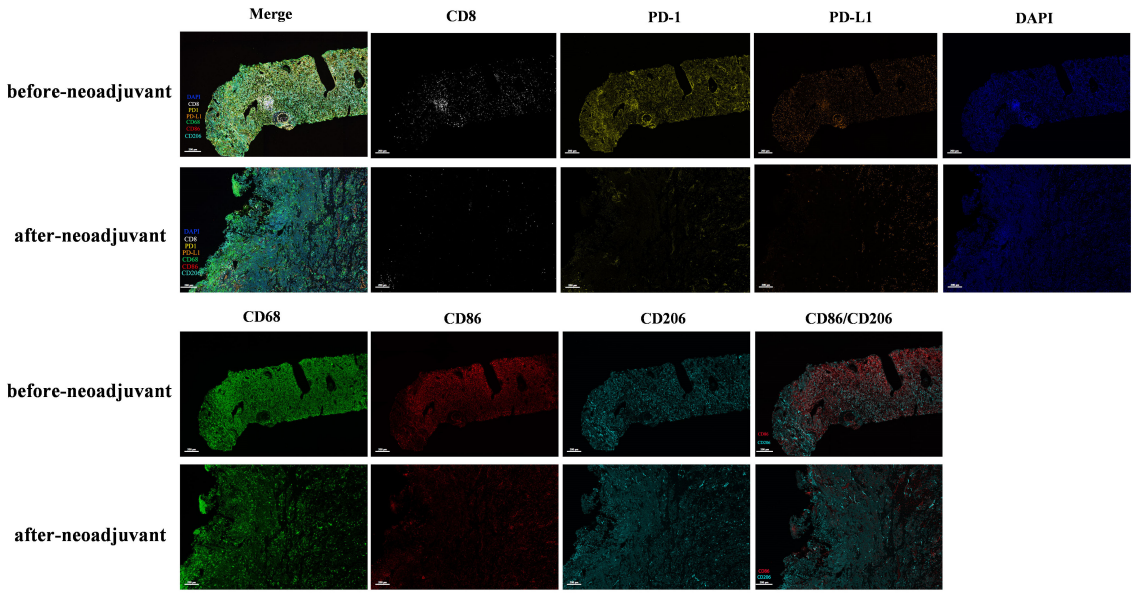

FIGURE 3
Multiplex immunofluorescence detection of immune microenvironment before and after neoadjuvant therapy.

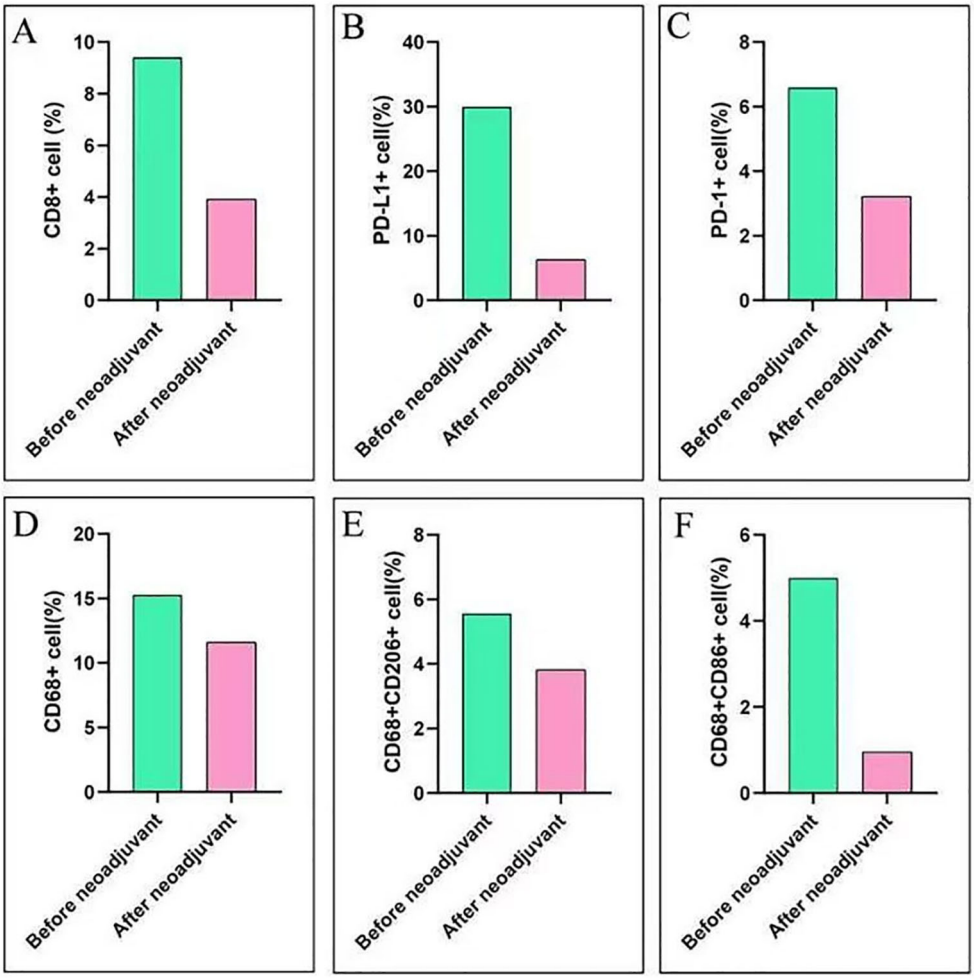

FIGURE 4
Immune score before and after neoadjuvant therapy. **(A)** Changes in CD8+ cell expression before and after neoadjuvant therapy; **(B)** Changes in PD-L1+ cell expression before and after neoadjuvant therapy; **(C)** Changes in PD-1+ cell expression before and after neoadjuvant therapy; **(D)** Changes in CD68+ cell expression before and after neoadjuvant therapy; **(E)** Changes in CD68+/CD206+ cell expression before and after neoadjuvant therapy; **(F)** Changes in CD68+/CD86+ cell expression before and after neoadjuvant therapy.

as a lower M1/M2 macrophage ratio (Figures 3, 4). Pyo K-H et al. revealed that in ceritinib-resistant ALK-positive NSCLC, the CD8+ T-cell population remained unaffected (27). Kleczko EK et al. reported that T-cell infiltration in the TME of ALK-positive NSCLC remained unaffected, whereas macrophage infiltration decreased after alectinib treatment (28).

However, many studies have proposed contrasting findings. Fang Y et al. performed RNA sequencing on 8 patients with ALK mutations and obtained immune assessment scores, which revealed no difference in the T-cell and macrophage scores of the TME before and after neoadjuvant therapy (29). In a phase IB trial of alectinib plus atezolizumab in ALK-positive patients, CD8+ T cells were estimated before treatment, and after treatment with alectinib for seven days, CD8+ T-cell infiltration increased in seven of nine patients, but the T-cell increase was not associated with the therapeutic effect of anti-PD1 therapy (30). Similarly, Cao P et al. suggested that an ALK-positive patient on alectinib had an increased tumor inflammation signature score (31). In general, the changes in the immune microenvironment after neoadjuvant therapy in ALK-positive NSCLC patients remain ambiguous. This variability might be associated with tumor heterogeneity, treatment drugs and duration, and detection methods.

4 Conclusion

We found that ensartinib neoadjuvant targeted therapy is efficient in patients with EML4-ALK fusion gene-positive NSCLC. Additionally, surgical treatment after neoadjuvant therapy is safe and feasible. Neoadjuvant ensartinib treatment might be a better therapeutic intervention than conventional radiotherapy and chemotherapy, but achieving good therapeutic effects with ensartinib therapy combined with or sequential immunotherapy may be difficult. In the future, more clinical trials are needed to evaluate the effectiveness of ensartinib in neoadjuvant therapy and patients' long-term prognosis, as well as to optimize treatment options.

Data availability statement

The original contributions presented in the study are included in the article/Supplementary Material. Further inquiries can be directed to the corresponding author.

Ethics statement

Written informed consent was obtained from the individual(s) for the publication of any potentially identifiable images or data included in this article.

Author contributions

HZ: Writing – original draft, Data curation, Methodology. WX: Writing – original draft, Data curation, Formal Analysis. YZ: Methodology, Writing – original draft, Software, Investigation. SB: Visualization, Writing – review & editing, Validation. JZ: Visualization, Supervision, Writing – review & editing. XL: Methodology, Software, Writing – review & editing. BZ: Methodology, Writing – review & editing, Investigation, Validation. HW: Conceptualization, Writing – review & editing, Investigation. SX: Funding acquisition, Validation, Writing – review & editing, Data curation. ZS: Writing – review & editing, Supervision, Writing – original draft, Funding acquisition.

Funding

The author(s) declare that financial support was received for the research, authorship, and/or publication of this article. This work was supported by the National Key R&D Program of China (2023YFC2508604), National Natural Science Foundation of China (82172776), Tianjin Key Medical Discipline (Specialty) Construction Project (TJYXZDXK-061B and TJWJ2022XK005), Diversified Input Project of Tianjin National Natural Science Foundation (21JCYBJC01770) and funding from author SX. The authors would like to thank Rupugene Technologies Co., Ltd. for their support.

Conflict of interest

The authors declare that the research was conducted in the absence of any commercial or financial relationships that could be construed as a potential conflict of interest.

The authors declare that this study received funding from Rupugene Technologies Co., Ltd. The funder covered the full cost of the immunofluorescence analysis that was performed, providing with technical and financial support.

Publisher's note

All claims expressed in this article are solely those of the authors and do not necessarily represent those of their affiliated organizations, or those of the publisher, the editors and the reviewers. Any product that may be evaluated in this article, or claim that may be made by its manufacturer, is not guaranteed or endorsed by the publisher.

Supplementary material

The Supplementary Material for this article can be found online at: https://www.frontiersin.org/articles/10.3389/fonc.2025.1474997/full#supplementary-material

References

1. Siegel RL, Miller KD, Wagle NS, Jemal A. Cancer statistics, 2023. *CA Cancer J Clin*. (2023) 73:17–48. doi: 10.3322/caac.21763

2. Miller KD, Nogueira L, Devasia T, Mariotto AB, Yabroff KR, Jemal A, et al. Cancer treatment and survivorship statistics, 2022. *CA Cancer J Clin*. (2022) 72:409–36. doi: 10.3322/caac.21731

3. Soda M, Choi YL, Enomoto M, Takada S, Yamashita Y, Ishikawa S, et al. Identification of the transforming EML4-ALK fusion gene in non-small-cell lung cancer. *Nature*. (2007) 448:561–6. doi: 10.1038/nature05945

4. Soda M, Takada S, Takeuchi K, Choi YL, Enomoto M, Ueno T, et al. A mouse model for EML4-ALK-positive lung cancer. *Proc Natl Acad Sci U S A*. (2008) 105:19893–7. doi: 10.1073/pnas.0805381105

5. Chia PL, Mitchell P, Dobrovic A, John T. Prevalence and natural history of ALK positive non-small-cell lung cancer and the clinical impact of targeted therapy with ALK inhibitors. *Clin Epidemiol*. (2014) 6:423–32. doi: 10.2147/CLEP.S69718

6. Shaw AT, Yeap BY, Mino-Kenudson M, Digumarthy SR, Costa DB, Heist RS, et al. Clinical features and outcome of patients with non-small-cell lung cancer who harbor EML4-ALK. *J Clin Oncol*. (2009) 27:4247–53. doi: 10.1200/JCO.2009.22.6993

7. Cameron LB, Hitchen N, Chandran E, Morris T, Manser R, Solomon BJ, et al. Targeted therapy for advanced anaplastic lymphoma kinase (*ALK*)-rearranged non-small cell lung cancer. *Cochrane Database Syst Rev*. (2022) 1:CD013453. doi: 10.1002/14651858.CD013453.pub2

8. Wu J, Lin Z. Non-small cell lung cancer targeted therapy: drugs and mechanisms of drug resistance. *Int J Mol Sci*. (2022) 23:15056. doi: 10.3390/ijms232315056

9. Peng L, Zhu L, Sun Y, Stebbing J, Selvaggi G, Zhang Y, et al. Targeting ALK rearrangements in NSCLC: current state of the art. *Front Oncol*. (2022) 12:863461. doi: 10.3389/fonc.2022.863461

10. Romero D. Adjuvant alectinib improves outcomes in ALK-mutant NSCLC. *Nat Rev Clin Oncol*. (2024) 21:484. doi: 10.1038/s41571-024-00899-7

11. Solomon BJ, Liu G, Felip E, Mok TSK, Soo RA, Mazieres J, et al. Lorlatinib versus crizotinib in patients with advanced ALK-positive non-small cell lung cancer: 5-year outcomes from the phase III CROWN study. *J Clin Oncol*. (2024) 42:3400–9. doi: 10.1200/JCO.24.00581

12. Wu KL, Chen HL, Tsai YM, Lee TH, Chang HM, Tsai YC, et al. First-line anaplastic lymphoma kinase (ALK) inhibitors for ALK-positive lung cancer in asian populations: systematic review and network meta-analysis. *J Clin Med*. (2021) 10:4376. doi: 10.3390/jcm10194376

13. Ma Y, Pan H, Liu Y, Zhang Y, Hong S, Huang J, et al. Ensartinib in advanced ALK-positive non-small cell lung cancer: a multicenter, open-label, two-staged, phase 1 trial. *J Thorac Dis*. (2022) 14:4751–62. doi: 10.21037/jtd-22-1606

14. Song Q, Li J, Xiong Q, Long YP, Yang B, Dong ZH, et al. Neoadjuvant immunotherapy plus chemotherapy and adjuvant targeted therapy in ALK-positive non-small-cell lung cancer. *Immunotherapy*. (2023) 15:809–17. doi: 10.2217/imt-2022-0302

15. Sentana-Lledo D, Viray H, Piper-Vallillo AJ, Widick P, Rangachari D, Wilson JL, et al. Complete pathologic response to short-course neoadjuvant alectinib in mediastinal node positive (N2) ALK rearranged lung cancer. *Lung Cancer*. (2022) 172:124–6. doi: 10.1016/j.lungcan.2022.08.014

16. Xie XH, Zhan ZJ, Qin YY, Jiang JH, Yin WQ, Zheng RH, et al. Case report: neoadjuvant and adjuvant crizotinib targeted therapy in stage IIIA-N2 ALK-positive non-small-cell lung cancer. *Front Oncol*. (2021) 11655856. doi: 10.3389/fonc.2021.655856

17. Lingling X, Maoxi C, Wei Y, Jieting Z, Yuanyuan Y, Ning X. Transformation of NSCLC to SCLC harboring EML4-ALK fusion with V1180L mutation after alectinib resistance and response to lorlatinib: A case report and literature review. *Lung Cancer*. (2023) 186:107415. doi: 10.1016/j.lungcan.2023.107415

18. Riely GJ, Wood DE, Ettinger DS, Aisner DL, Akerley W, Bauman JR, et al. Non-small cell lung cancer, version 4.2024, NCCN clinical practice guidelines in oncology. *J Natl Compr Canc Netw*. (2024) 22:249–74. doi: 10.6004/jnccn.2204.0023

19. Shi L, Gao S, Tong L, Meng Q, Zhou S, Yu D, et al. Pathological complete response to long-course neoadjuvant alectinib in lung adenocarcinoma with EML4-ALK rearrangement: report of two cases and systematic review of case reports. *Front Oncol*. (2023) 13:1120511. doi: 10.3389/fonc.2023.1120511

20. Hu Y, Ren S, Wang R, Han W, Xiao P, Wang L, et al. Case report: pathological complete response to neoadjuvant alectinib in a patient with resectable ALK-positive non-small cell lung cancer. *Front Pharmacol*. (2022) 13:816683. doi: 10.3389/fphar.2022.816683

21. Zhang C, Li SL, Nie Q, Dong S, Shao Y, Yang XN, et al. Neoadjuvant crizotinib in resectable locally advanced non-small cell lung cancer with ALK rearrangement. *J Thorac Oncol*. (2019) 14:726–31. doi: 10.1016/j.jtho.2018.10.161

22. Chen MF, Chaft JE. Early-stage anaplastic lymphoma kinase (ALK)-positive lung cancer: a narrative review. *Transl Lung Cancer Res*. (2023) 12:337–45. doi: 10.21037/tlcr-22-631

23. Peng TR, Liao PF, Wu TW. Efficacy and safety of anaplastic lymphoma kinase inhibitors for non-small cell lung cancer: A systematic review and network meta-analysis. *Thorac Cancer*. (2023) 14:929–39. doi: 10.1111/1759-7714.14824

24. Wang C, Hu Q, Sun Y, Yu F, Peng M. Complete pathological remission after neoadjuvant ensartinib in patients with locally advanced lung adenocarcinoma and with CTLC-ALK and ALK-DHX8 rearrangements. *Eur J Cancer*. (2022) 169:131–4. doi: 10.1016/j.ejca.2022.04.012

25. Wu Y, Huang L, Li W, Chai Y. Neoadjuvant target therapy with ensartinib in lung adenocarcinoma with EML4-ALK fusion variant: a case report and literature review. *Anticancer Drugs*. (2023) 34:699–706. doi: 10.1097/CAD.0000000000001432

26. Zhang B, Zeng J, Zhang H, Zhu S, Wang H, He J, et al. Characteristics of the immune microenvironment and their clinical significance in non-small cell lung cancer patients with ALK-rearranged mutation. *Front Immunol*. (2022) 13:974581. doi: 10.3389/fimmu.2022.974581

27. Pyo KH, Lim SM, Park CW, Jo HN, Kim JH, Yun MR, et al. Comprehensive analyses of immunodynamics and immunoreactivity in response to treatment in ALK-positive non-small-cell lung cancer. *J Immunother Cancer*. (2020) 8:e000970. doi: 10.1136/jitc-2020-000970

28. Kleczko EK, Hinz TK, Nguyen TT, Gurule NJ, Navarro A, Le AT, et al. Durable responses to alectinib in murine models of EML4-ALK lung cancer requires adaptive immunity. *NPJ Precis Oncol*. (2023) 7:15. doi: 10.1038/s41698-023-00355-2

29. Fang Y, Wang Y, Zeng D, Zhi S, Shu T, Huang N, et al. Comprehensive analyses reveal TKI-induced remodeling of the tumor immune microenvironment in EGFR/ALK-positive non-small-cell lung cancer. *Oncoimmunology*. (2021) 10:1951019. doi: 10.1080/2162402X.2021.1951019

30. Zheng N, Zhang Y, Zeng Y, Ma Q, Zhang R, Zhao Q, et al. Pathological response and tumor immune microenvironment remodeling upon neoadjuvant ALK-TKI treatment in ALK-rearranged non-small cell lung cancer. *Target Oncol*. (2023) 18:625–36. doi: 10.1007/s11523-023-00981-7

31. Cao P, Zhao Q, Li Y, Shi R, Zhu G, Zhang Z, et al. Case Report: ALK rearranged locally advanced lung adenocarcinoma showing inconsistent radiographic findings and pathological responses during neoadjuvant alectinib therapy. *Front Pharmacol*. (2023) 14:1140894. doi: 10.3389/fphar.2023.1140894

frontiers | Frontiers in Medicine

TYPE Original Research
PUBLISHED 03 April 2025
DOI 10.3389/fmed.2025.1491960

OPEN ACCESS

EDITED BY
Vincenzo Pio Di Noia,
IRCCS Istituto Nazionale Tumori Regina Elena, Italy

REVIEWED BY
Mark O. Wielpütz,
Heidelberg University, Germany
Jaiprakash Suresh Gurav,
Armed Forces Medical College, India

*CORRESPONDENCE
Tatjana Dell
✉ tatjana.dell@ukbonn.de

RECEIVED 05 September 2024
ACCEPTED 18 March 2025
PUBLISHED 03 April 2025

CITATION
Dell T, Feisst A, Ramig O, Layer Y, Mesropyan N, Isaak A, Pieper C, Kupczyk P, Luetkens J, Thomas D and Kuetting D (2025) MRI based volumetric lung nodule assessment - a comparison to computed tomography.
Front. Med. 12:1491960.
doi: 10.3389/fmed.2025.1491960

MRI based volumetric lung nodule assessment - a comparison to computed tomography

Tatjana Dell [1]*, Andreas Feisst[1], Olga Ramig[1], Yannik Layer[1], Narine Mesropyan[1], Alexander Isaak[1], Claus Pieper[1], Patrick Kupczyk[1], Julian Luetkens[1], Daniel Thomas[2] and Daniel Kuetting[1]

[1]Department of Diagnostic and Interventional Radiology, Quantitative Imaging Lab Bonn, University Hospital Bonn, Bonn, Germany, [2]Department of Diagnostic and Interventional Radiology, St. Vinzenz Hospital, Cologne, Germany

Purpose: Previous studies have demonstrated that nodule volumetry allows for the deduction of imaging-based biomarkers such as volume doubling time, enabling superior discrimination between benign and malignant lesions compared to 2D-based morphological characteristics. The study aimed to assess the feasibility and accuracy of *in-vivo* magnetic resonance imaging (MRI)-based volumetric assessment of lung nodules larger than 6 mm, in comparison to the current gold standard, CT.

Materials and methods: This study involved a subgroup analysis of 233 participants from a prospective, single-center lung cancer screening program using CT and MRI. Patients were included if foci ≥6 mm were detected in CT during the initial screening round, resulting in 23 participants with 47 pulmonary nodules. MRI was performed using a 1.5 Tesla unit with a transverse T2-weighted MultiVane XD imaging technique, while low-dose CT (LDCT) was performed on a 128-slice spiral CT scanner. Volumetric nodule assessment was conducted using a computer-aided diagnosis system, with images reviewed by two experienced radiologists. Statistical analysis included regression analysis, Bland-Altman analysis, and calculation of the interclass correlation coefficient (ICC) to assess correlation and reproducibility.

Results: Comparison of MRI-based volumetric assessment with LDCT as the reference standard revealed a mean nodule volume of 1.1343 ± 3.1204 cm^3 for MRI versus 1.2197 ± 3.496 cm^3 for LDCT (p = 0.203). Regression analysis demonstrated a strong linear relationship between the modalities (r^2 = 0.981, $p < 0.001$), consistently observed even for nodules <5 cm^3 (r^2 = 0.755, $p < 0.001$). Bland-Altman analysis indicated no significant systematic bias in nodule volume measurements between MRI and CT, with a mean difference of 0.12 cm^3 and narrow 95% confidence intervals (−6.852 to 6.854 cm^3). Intra-reader reproducibility for CT-based volumetry was excellent (ICC = 0.9984), while MRI-based measurements showed good reproducibility (ICC = 0.7737). Inter-reader reproducibility was high for CT (ICC = 0.995) and moderate for MRI (ICC = 0.7135).

10.3389/fmed.2025.1491960

Conclusion: This study demonstrates that MRI-based volumetry of lung nodules ≥6 mm is feasible and accurate, showing comparable precision to CT with minimal bias in volume measurements, and highlights the potential of MRI as a radiation-free alternative for lung nodule follow-up and screening.

KEYWORDS

pulmonary nodules, lung cancer screening, magnetic resonance imaging, volumetry, early detection of cancer, low-dose computed tomography, radiation protection

Introduction

Pulmonary nodules are detected in more than 1.5 million patients per year in the US and can be found in more than a third of all computed tomographic (CT) scans of the chest. These nodules frequently require follow up or other dedicated work up (1).

Volumetric lung nodule assessment is a more effective predictor of malignancy than two-dimensional (2D) evaluation based on diametric measurements. Nodule volumetry enables the deduction of imaging-based biomarkers, such as volume doubling time (VDT), leading to superior discrimination between benign and malignant lesions compared to 2D-based morphological characteristics (2).

Recent guidelines for lung nodule management recommend volumetric analysis over 2D assessment (3). This shift was largely driven by the Dutch–Belgian NELSON lung cancer screening trial, which employed volumetric analysis criteria and achieved a much lower false-positive rate than prior CT-based lung cancer screening trials (4, 5). Volumetric analysis combined with VDT analysis has emerged as an accurate predictor of malignancy (6).

While CT has been established as the gold standard for lung cancer screening, data on the potential of MRI as a radiation-free alternative are scarce (7). Although it has been shown that MRI reliably detects nodules >6 mm (8), in theory enabling MRI-based lung cancer screening, MRI based volumetric lung nodule assessment has only been evaluated *in vitro* thus far or in small human populations (9, 10). Delacoste et al. (9) conducted a pilot study demonstrating the feasibility of MR-based volumetric assessment, but the findings were limited to *in vitro* and *ex vivo* models. More recently, Darçot et al. (10) prospectively compared MRI and CT in the detection and volumetric assessment of lung nodules, reporting promising results but highlighting the need for further validation in larger cohorts. Therefore, the goal of this study was to assess the feasibility of in-vivo MRI-based lung nodule volumetry compared to CT, the reference standard for lung nodule assessment.

Abbreviations: CAD, computer-aided diagnosis system; ICC, interclass correlation coefficient; LDCT, low-dose computed tomography; MVXD, MultiVane XD; UTE, ultra-short echo time; VDT, volume doubling time.

Materials and methods

Study participants

Patients from a prospective, single center, lung cancer screening program employing both CT and MRI were used for this subgroup analysis. A total of 233 participants were recruited following the criteria employed in the German lung cancer screening trial (LUSI; 11). Study enrollment is depicted in Figure 1. In the subgroup analysis, patients were included if round foci ≥6 mm were detected in CT during the initial screening round. Of the 233 participants, 23 met the inclusion criteria with a total of 47 pulmonary round foci ≥6 mm. This study was approved by the local ethics committee, patients gave written informed consent prior to inclusion in the study.

Image acquisition

Patients underwent same-day MRI and low-dose CT (LDCT), regardless of whether pulmonary nodules were identified. LDCT was performed on a 128-slice spiral CT scanner (iCT, Philips Healthcare, Best, The Netherlands) in inspiratory breathhold with a reconstructed slice thickness of 1 mm and an increment of 0.6 mm.

MRI was performed on a 1.5 Tesla unit (Ingenia, Philips Healthcare Best, The Netherlands) in feet-first, arms-up technique using a phased array body coil. The employed MRI protocol has been previously described in detail (5). The scan protocol employs a transverse T2-weighted MultiVane XD (MVXD) imaging technique. The repetition time (TR) ranges from 950 to 1100 ms, and the echo time (TE) is set at 60 ms, with a flip angle (FA) of 90 degrees. The field of view (FOV) measures 400 mm, and the matrix size is 432 × 432 mm, providing detailed resolution. The slice thickness is maintained at 6 mm, in alignment with a previously validated protocol from our institution for two-dimensional nodule measurement (5). To enhance imaging efficiency, parallel imaging with SENSE (sensitivity-encoded) is utilized, and no partial Fourier technique is applied. Respiratory gating is employed to accommodate patient breathing, eliminating the need for breath-holding. The total acquisition time for this scan is 3 min and 18 s.

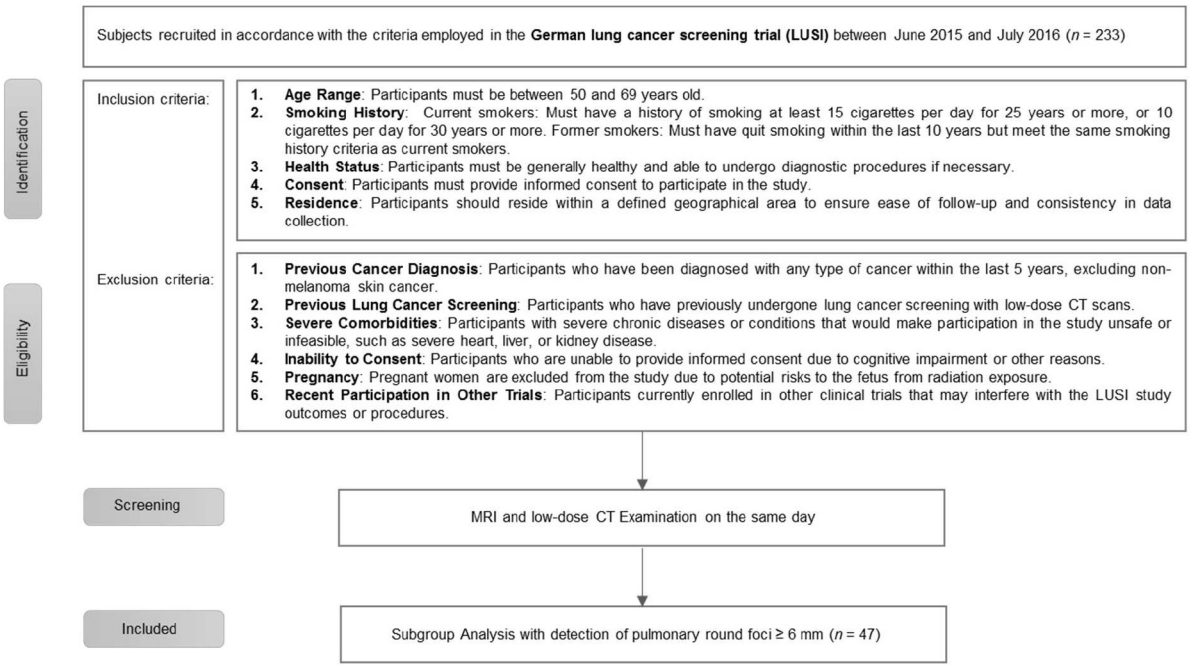

FIGURE 1
Flow diagram of study enrollment.

Data analysis

Computed tomographic and MR images were reviewed by two experienced radiologists with 9 (R1) and 10 years (R2) of experience in chest imaging, respectively. The data sets were anonymized and randomly presented to the readers preventing direct inter-modality correlation. To further avoid bias, the readers first performed nodule analysis on MR images and after an interval of 2 weeks nodule analysis was performed on CT images.

Computed tomographic and MRI volumetric nodule assessment was performed with a computer-aided diagnosis system (CAD, IntelliSpace Portal DX Server, Philips Healthcare) which allows for both automated and semiautomated nodule volumetry.

For both MRI and CT semiautomated assessment was performed; after manual identification of the various nodules the software automatically contoured the nodule edges on each slice and calculated the nodule volume (Figure 2). If the computer-generated nodule borders appeared inaccurate, manual editing of computer-generated nodule outlines was performed.

Statistical analysis

Statistical analysis was performed with SPSS 26 (IBM, Armonk, New York, USA). Subjects' demographic were summarized descriptively. Continuous variables were expressed as means ± standard deviations. Regression analysis and Bland-Altmann analysis were conducted to assess correlation and intermodality agreement, between CT and MRI based lung nodule volumetry. The interclass correlation coefficient (ICC) was calculated to determine the inter/intra-reader reproducibility.

Results

Based on LDCT as reference, mean nodule volume was 1.2197 ± 3.496 cm^3, MRI-based mean nodule volume was 1.1343 ± 3.1204 cm^3 (p = 0.203). Regression analysis revealed a linear relationship between the two modalities (r^2 = 0.981; $p < 0.001$; Figure 3A); when considering nodules ≤2.5 cm^3 (n = 44) a linear relationship was still evident (r^2 = 0.755; $p < 0.001$) (Figure 3B).

Bland Altman analysis revealed no systematic over- or underestimation of MRI in comparison to CT; mean difference: 0.12; standard deviation of differences: 3.496 (95% CI: 6.854 to −6.852) (Figure 4).

The intra-reader reproducibility assessment of CT based nodule volumetry resulted in an ICC of 0.9984 (95% CI: 0.9972 to 0.9991) for MRI based measurements ICC was 0.7737 (95% CI: 0.5142 to 0.9183). Inter-reader reproducibility revealed an ICC of 0.995 (95% CI: 0.993, 0.997) for CT and 0.7135 (95% CI: 0.4538 to 0.8581) for MRI-based measurements.

Discussion

This study demonstrates that MRI-based volumetry of lung nodules larger than 6 mm is feasible and shows comparable precision to the current reference standard, CT.

Follow-up of lung nodules, including in lung cancer screening, is often excessive due to the need to monitor even low-risk nodules, leading to frequent imaging and potential overdiagnosis. This high frequency of follow-ups can expose patients to unnecessary radiation and stress, especially when nodules are benign or slow-growing. In high risk individual nodules up to 8 mm have less than

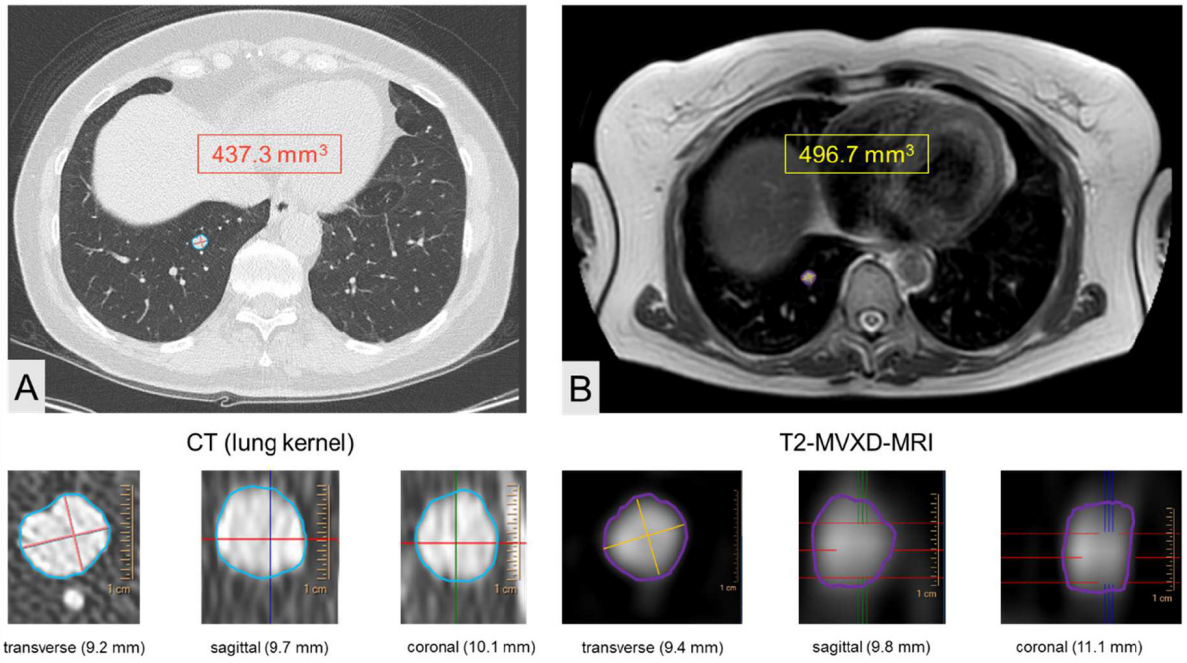

FIGURE 2
Volumetric assessment of a lung nodule in the right lower lobe using CT **(A)** and T2 weighted MVXD MRI **(B)** in a 56-year-old study patient.

1% estimated malignancy risk, and those up to 15 mm in baseline (category 4A) have a 5%–15% risk (12). In a non-risk population, nodules smaller than 1 cm have an even lower malignancy risk (13). To avoid unnecessary radiation during follow-ups, MRI could serve as an alternative.

While MRI reliably detects lung nodules larger than 4−6 mm (14, 15), limited data exists on MRI-based volumetry beyond *in vitro* and initial *in vivo* testing. Ohno et al. evaluated only 2D nodule measurement in their study with 205 participants, without assessing volumetric measurements (16). Their findings demonstrated a high detection rate for lung nodules and feasibility for Lung-RADS classification, but volumetric evaluation was not performed. Volumetric assessment is standard practice in CT, as endorsed by national guidelines and the European position statement on lung cancer screening (3, 17). In this context, the research group led by Biederer further demonstrated that, compared to diameter measurements, volumetry results in significantly smaller interobserver variability, with advanced volumetric algorithms being independent of observer experience (18).

The current results indicate only minimal bias in artificial nodule volume measurements between MRI and CT, with a discrepancy of less than 10% across the volume range. High agreement is crucial when switching modalities for follow-up. This study also identified equivalent reproducibility between MRI and CT for pulmonary nodule volumetry, ensuring consistent results across different sessions and operators.

Appropriate MRI sequence selection has been addressed in several previous studies. The current volumetric analysis was performed using a T2 TSE sequence, a choice supported by existing literature, indicating that T2 sequences yield high nodule detection rates (14, 19). Additionally, newer ultra-short echo time (UTE) based MRI sequences have also shown promising results. These UTE sequences provide high detection rates and excellent volumetric accuracy.

Notably, the employed propeller technology enables reduction of motion artifacts and thus ensures precise measurements (14). Furthermore, the additional employment of a free breathing sequence allows for inclusion of patients unable to reliably hold their breath for longer periods, as typically required during standard imaging. This aspect is of particular importance in the context of individuals with an extensive history of smoking, where comorbidities affecting lung function are frequent (20, 21).

Recently, initial results were published regarding MRI based volumetric analysis of lung nodules (10, 22). In this study evaluating the effectiveness of UTE-based MRI sequences for lung nodule detection and volumetric assessment a high correlation was found between MRI and CT for nodule volumetry. UTE MRI provided high detection rates for nodules ≥4 mm and ≥6 mm, with an excellent concordance between CT and UTE-volumetry, albeit with a slight overestimation by MRI.

The current study, employing a more conservative MRI sequence, T2 TSE Propeller, also found comparable results for MRI in comparison to CT, although only nodules >6 mm were included. Smaller nodules were not included in the current analysis due to the restricted detection rate reported in previous T2 TSE based studies (23). However, nodules smaller than 6 mm typically have a low clinical relevance, therefore follow up will only seldomly be required. In comparison to UTE, the T2 TSE Propeller technique employed in this study offers significant advantages, such as the ability to perform acquisitions during free-breathing and a superior reduction of motion artifacts. These features make the sequence particularly suitable for patients with compromised lung function, enhancing its applicability in clinical settings.

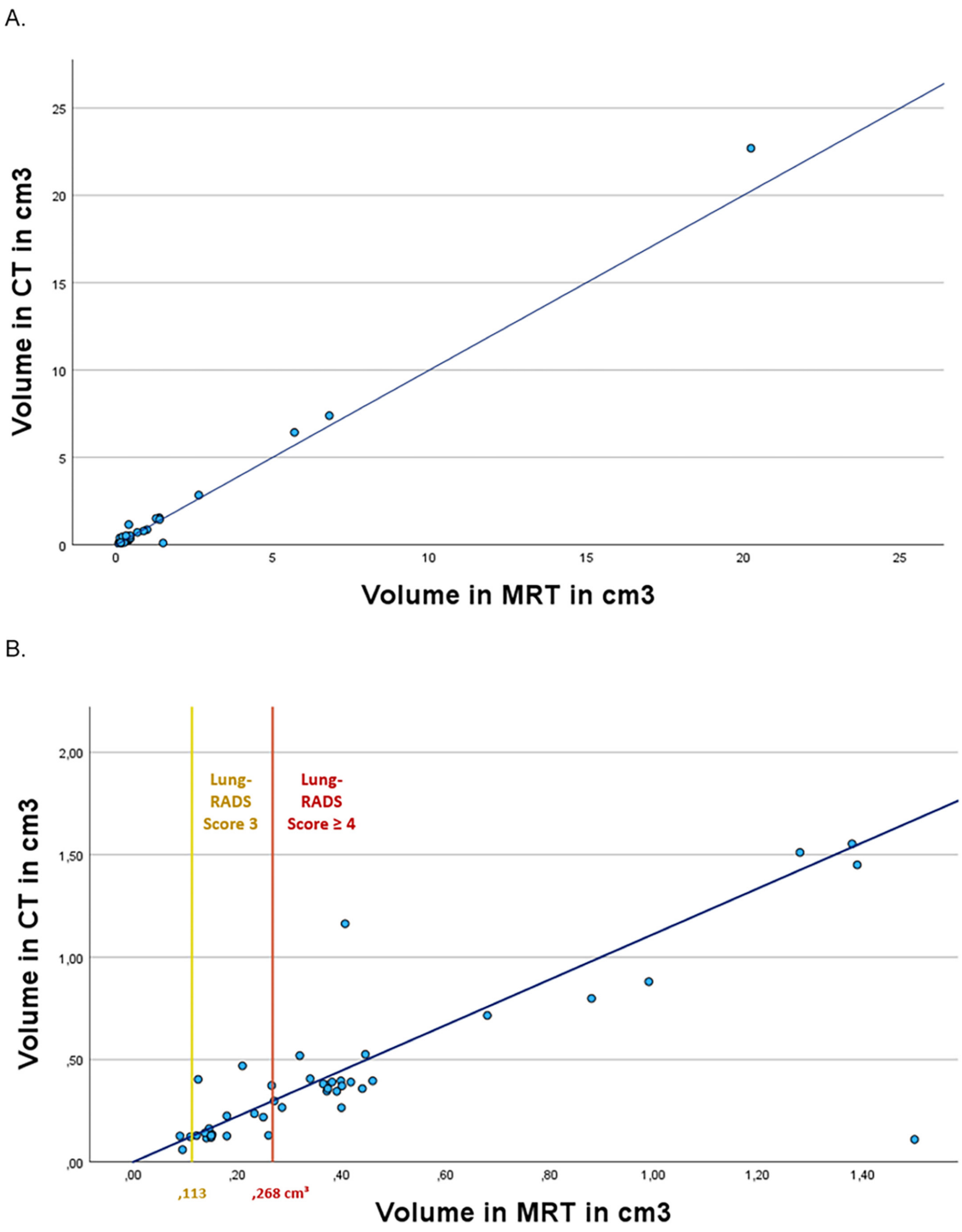

FIGURE 3
Regression analysis of CT-and MRI-based lung nodule volumetry. Correlation analysis between CT- and MRI-based lung nodule volumetric assessment for all nodules **(A)**; regression plot for nodules ≤1.5 cm^3 **(B)**. The blue regression line represents the relationship between CT and MRI measurements. Additionally, Lung-RADS-based cutoff values have been integrated: category 3 (yellow; 0.113–0.268 cm^3) and category 4 (orange; ≥0.268 cm^3).

Although MRI offers numerous potential advantages compared to the gold standard CT, it is unlikely to replace CT as the primary screening tool for lung cancer or for staging pulmonary metastasis. Nevertheless, MRI can be highly beneficial in certain scenarios, particularly for individuals sensitive to radiation exposure, such as young patients requiring frequent follow-ups. Additionally, MRI is advantageous when follow-up imaging of nodules larger than 4−6 mm is necessary and the goal is to avoid repeated CT scans.

MRI can be utilized effectively in follow-up imaging due to its ability to provide high-resolution images without the associated radiation risk of CT. This makes it an excellent choice for monitoring nodules over time, especially in patients who are at

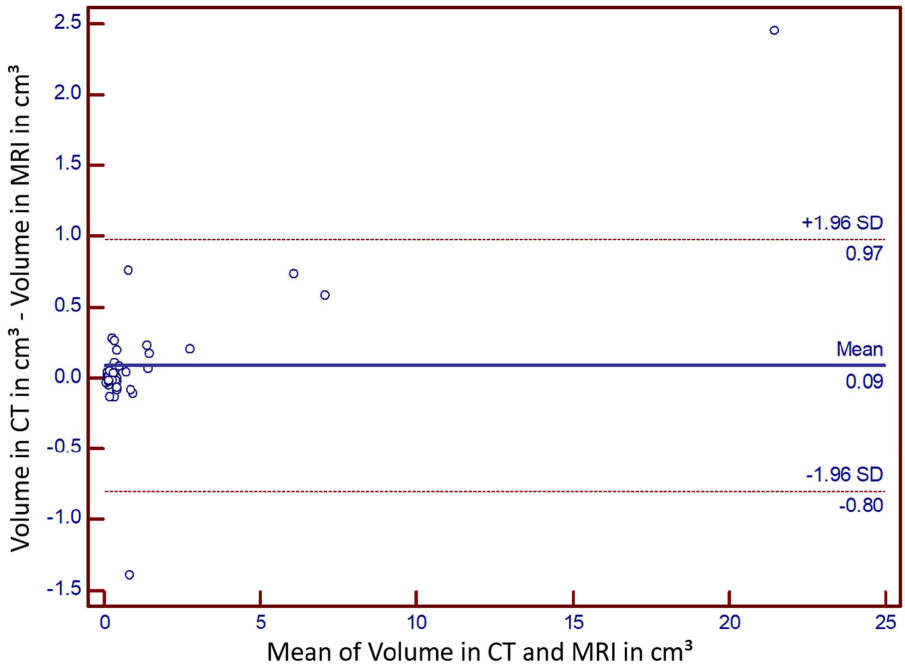

FIGURE 4
Bland-Altman analysis for intermodality comparison.

a higher risk of radiation-induced complications. For instance, young patients, who are more susceptible to the long-term effects of radiation, can benefit significantly from MRI's non-ionizing imaging technology.

This study exhibits several limitations. First and foremost, the primary limitation is the relatively small sample size of analyzed lung nodules. While the measurements were diligently carried out by two experienced radiologists, each with 9–10 years of expertise, it is prudent to question whether comparable measurement results would be obtained if less experienced examiners were involved. To enhance the generalizability and reliability of the study's findings, a larger and more diverse study population, as well as assessments by multiple readers, would be essential. Additionally, the volume measurements were executed utilizing a CAD system. It is crucial to acknowledge that different CAD systems may introduce variations in volume measurements, as evidenced by prior research (24, 25). Thus, it becomes imperative to exercise caution when extrapolating these findings to other CAD systems or methodologies, emphasizing the need for further investigation in this regard. Another noteworthy limitation lies in the absence of an exploration of inter-scan reproducibility in this *in vivo* study, which could be especially relevant for MRI scanners. The oversight of this aspect can potentially limit the reliability of the measurements over time, highlighting the need for future studies to comprehensively assess the technique's repeatability. Furthermore, the study adhered to a protocol that exclusively included nodules larger than 6 mm. This decision aligns with the known limitation of MRI in detecting smaller lesions. However, it's imperative to acknowledge that this study may not account for the full spectrum of lung nodules, particularly those with sizes below the 6 mm threshold. Additionally, subsolid nodules, which have distinct clinical significance, were not considered in the study, further narrowing the scope of its applicability.

Conclusion

In conclusion, this study demonstrates the feasibility of MRI-based volumetric analysis for lung nodules ≥6 mm, with results comparable to CT. MRI offers a radiation-free alternative for lung cancer screening and follow-up, particularly for minimizing radiation exposure.

Future research should focus on validating MRI volumetry in larger, diverse populations and exploring its potential for early lung cancer detection and nodule classification using advanced AI algorithms. Multi-center studies and long-term follow-up are essential to further assess its clinical benefits.

Data availability statement

The raw data supporting the conclusions of this article will be made available by the authors, without undue reservation.

Ethics statement

The studies involving humans were approved by Ethics Committee Bonn Application number 049/14. The studies were conducted in accordance with the local legislation and institutional requirements. The participants provided their written informed

consent to participate in this study. Written informed consent was obtained from the individual(s) for the publication of any potentially identifiable images or data included in this article.

Author contributions

TD: Data curation, Formal Analysis, Funding acquisition, Investigation, Methodology, Project administration, Resources, Software, Validation, Visualization, Writing – original draft, Writing – review and editing. AF: Data curation, Formal Analysis, Funding acquisition, Investigation, Methodology, Project administration, Software, Validation, Writing – original draft, Writing – review and editing. OR: Data curation, Funding acquisition, Project administration, Writing – original draft, Writing – review and editing. YL: Formal Analysis, Methodology, Writing – original draft, Writing – review and editing. NM: Formal Analysis, Resources, Supervision, Writing – original draft, Writing – review and editing. AI: Funding acquisition, Software, Visualization, Writing – original draft, Writing – review and editing. CP: Investigation, Supervision, Writing – original draft, Writing – review and editing. PK: Funding acquisition, Investigation, Visualization, Writing – original draft, Writing – review and editing. JL: Conceptualization, Funding acquisition, Investigation, Supervision, Writing – original draft, Writing – review and editing. DT: Conceptualization, Investigation, Writing – original draft, Writing – review and editing. DK: Conceptualization, Data curation, Formal Analysis, Funding acquisition, Investigation, Methodology, Project administration, Resources, Software, Supervision, Validation, Visualization, Writing – original draft, Writing – review and editing.

Funding

The author(s) declare that no financial support was received for the research and/or publication of this article.

Conflict of interest

The authors declare that the research was conducted in the absence of any commercial or financial relationships that could be construed as a potential conflict of interest.

Publisher's note

References

1. Mazzone PJ, Lam L. Evaluating the patient with a pulmonary nodule: a review. *JAMA*. (202) 327:264–73. doi: 10.1001/jama.2021.24287

2. Devaraj A, van Ginneken B, Nair A, Baldwin D. Use of volumetry for lung nodule management: theory and practice. *Radiology*. (2017) 284:630–44. doi: 10.1148/radiol.2017151022

3. MacMahon H, Naidich DP, Goo JM, Lee KS, Leung ANC, Mayo JR, et al. Guidelines for management of incidental pulmonary nodules detected on CT images: from the Fleischner society 2017. *Radiology*. (2017) 284:228–43. doi: 10.1148/radiol.2017161659

4. De Koning HJ, van der Aalst CM, de Jong PA, Scholten ET, Nackaerts K, Heuvelmans MA, et al. Reduced lung-cancer mortality with volume CT screening in a randomized trial. *N Eng. J Med.* (2020) 382:503–13. doi: 10.1056/NEJMoa1911793

5. National Lung Screening Trial Research Team, Aberle DR, Adams AM, Berg CD, Black WC, Clapp JD, et al. Reduced lung-cancer mortality with low-dose computed tomographic screening. *N Engl J Med.* (2011) 365:395–409. doi: 10.1056/NEJMoa1102873

6. Horeweg N, van Rosmalen J, Heuvelmans MA, van der Aalst CM, Vliegenthart R, Scholten ET, et al. Lung cancer probability in patients with CT-detected pulmonary nodules: a prespecified analysis of data from the NELSON trial of low-dose CT screening. *Lancet Oncol.* (2014) 15:1332–41. doi: 10.1016/S1470-2045(14)70389-4

7. Meier-Schroers M, Homsi R, Skowasch D, Buermann J, Zipfel M, Schild HH, et al. Lung cancer screening with MRI: results of the first screening round. *J Cancer Res Clin Oncol.* (2018) 144:117–25. doi: 10.1007/s00432-017-2521-4

8. Meier-Schroers M, Homsi R, Schild HH, Thomas D. Lung cancer screening with MRI: characterization of nodules with different non-enhanced MRI sequences. *Acta Radiol.* (2019) 60:168–76. doi: 10.1177/0284185118778870

9. Delacoste J, Dunet V, Dournes G, Lovis A, Rohner C, Elandoy C, et al. Volumetry of lung nodules: a pilot study. *Front Med.* (2019) 6:18. doi: 10.3389/fmed.2019.00018

10. Darçot E, Jreige M, Rotzinger DC, Gidoin Tuyet Van S, Casutt A, Delacoste J, et al. Comparison between magnetic resonance imaging and computed tomography in the detection and volumetric assessment of lung nodules: a prospective study. *Front Med.* (2022) 9:858731. doi: 10.3389/fmed.2022.858731

11. Becker, N, Motsch E, Trotter A, Heussel CP, Dienemann H, Schnabel PA, et al. Lung cancer mortality reduction by LDCT screening-results from the randomized German LUSI trial. *Int J Cancer.* (2020) 146:1503–13. doi: 10.1002/ijc.32486

12. Mendoza DP, Petranovic M, Som A, Wu MY, Park EY, Zhang EW, et al. Lung-RADS Category 3 and 4 nodules on lung cancer screening in clinical practice. *AJR Am J Roentgenol.* (2022) 219:55–65. doi: 10.2214/AJR.21.27180

13. Van Klaveren RJ, Oudkerk M, Prokop M, Scholten ET, Nackaerts K, Vernhout R, et al. Management of lung nodules detected by volume CT scanning. *N Engl J Med.* (2009) 361:2221–9. doi: 10.1056/NEJMoa0906085

14. Feng H, Shi G, Liu H, Xu Q, Wang L, Zhang N. The application and value of 3t magnetic resonance imaging in the display of pulmonary nodules. *Front Oncol.* (2022) 12:844514. doi: 10.3389/fonc.2022.844514

15. Hinsen M, Nagel AM, May MS, Wiesmueller M, Uder M, Heiss R. Lung nodule detection with modern low-field MRI (0.55 T) in comparison to CT. *Invest Radiol.* (2024) 59:215–22. doi: 10.1097/RLI.0000000000001006

16. Ohno Y, Takenaka D, Yoshikawa T, Yui M, Koyama H, Yamamoto K, et al. Efficacy of ultrashort echo time pulmonary MRI for lung nodule detection and lung-RADS classification. *Radiology.* (2022) 302:697–706. doi: 10.1148/radiol.211254

17. Kauczor HU, Baird AM, Blum TG, Bonomo L, Bostantzoglou C, Burghuber O, et al. European society of radiology (ESR) and the european respiratory society (ERS). ESR/ERS statement paper on lung cancer screening. *Eur Respir J.* (2020) 55:1900506. doi: 10.1183/13993003.00506-2019

18. Bolte H, Jahnke T, Schäfer FK, Wenke R, Hoffmann B, Freitag-Wolf S, et al. Interobserver-variability of lung nodule volumetry considering different segmentation algorithms and observer training levels. *Eur J Radiol.* (2007) 64:285–95. doi: 10.1016/j.ejrad.2007.02.031

19. Cieszanowski A, Lisowska A, Dabrowska M, Korczynski P, Zukowska M, Grudzinski IP, et al. Imaging of pulmonary nodules: detection rate and accuracy of size

estimation in comparison to computed tomography. *PLoS One.* (2016) 11:e0156272. doi: 10.1371/journal.pone.0156272

20. Meier-Schroers M, Kukuk G, Homsi R, Skowasch D, Schild HH, Thomas D. MRI of the lung using the PROPELLER technique: artifact reduction, better image quality and improved nodule detection. *Eur J Radiol.* (2016) 85:707–13. doi: 10.1016/j.ejrad.2015.12.016

21. Vogt FM, Herborn CU, Hunold P, Lauenstein TC, Schröder T, Debatin JF, et al. HASTE MRI versus chest radiography in the detection of pulmonary nodules: comparison with MDCT. *AJR Am J Roentgenol.* (2004) 183:71–8. doi: 10.2214/ajr.183.1.1830071

22. Wielpütz MO, Lee HY, Koyama H, Yoshikawa T, Seki S, Kishida Y, et al. Morphologic characterization of pulmonary nodules with ultrashort TE MRI at 3T. *AJR Am J Roentgenol.* (2018) 210:1216–25. doi: 10.2214/AJR.17.18961

23. Sanchez F, Tyrrell PN, Cheung P, Heyn C, Graham S, Poon I, et al. Detection of solid and subsolid pulmonary nodules with lung MRI: performance of UTE, T1 gradient-echo, and single-shot T2 fast spin echo. *Cancer Imaging.* (2023) 23:17. doi: 10.1186/s40644-023-00531-4

24. Zhao YR, van Ooijen PM, Dorrius MD, Heuvelmans M, de Bock GH, Vliegenthart R, et al. Comparison of three software systems for semi-automatic volumetry of pulmonary nodules on baseline and follow-up CT examinations. *Acta Radiol.* (2014) 55:691–8. doi: 10.1007/s00330-012-2437-y

25. De Hoop B, Gietema H, van Ginneken B, Zanen P, Groenewegen G, Prokop M. A comparison of six software packages for evaluation of solid lung nodules using semi-automated volumetry: what is the minimum increase in size to detect growth in repeated CT examinations. *Eur Radiol.* (2009) 19:800–8. doi: 10.1007/s00330-008-1229-x

Frontiers in Medicine

Translating medical research and innovation into improved patient care

A multidisciplinary journal which advances our medical knowledge. It supports the translation of scientific advances into new therapies and diagnostic tools that will improve patient care.

Discover the latest Research Topics

See more →

Frontiers

Avenue du Tribunal-Fédéral 34
1005 Lausanne, Switzerland
frontiersin.org

Contact us

+41 (0)21 510 17 00
frontiersin.org/about/contact